



**Fermi National Accelerator Laboratory**

**FERMILAB-Conf-97/279**

**Proceedings of the Workshop on Fixed Target  
Physics at the Main Injector**

Gregory J. Bock and Jorge G. Morfín

*Fermi National Accelerator Laboratory  
P.O. Box 500, Batavia, Illinois 60510*

September 1997

Proceedings of the *Workshop on Fixed Target Physics at the Main Injector*, Fermilab, Batavia Illinois,  
May 1-4, 1997



# Proceedings of the Workshop on Fixed Target Physics at the Main Injector

Fermi National Accelerator Laboratory  
Batavia, Illinois  
May 1-4, 1997

## **Editors:**

Gregory J. Bock and Jorge G. Morfin  
Fermilab

## **Sponsors:**

Fermi National Accelerator Laboratory  
U.S. Department of Energy

# Contents

<b>1</b>	<b>Executive Summary</b>	<b>9</b>
1.1	Introduction . . . . .	9
1.2	The Main Injector Neutrino Facility . . . . .	10
1.2.1	The Main Injector Neutrino Oscillation Program . . . . .	11
1.2.2	A Conventional (Non-oscillation) Main Injector Neutrino Program . . . . .	14
1.3	Experiments with Neutral Kaons . . . . .	17
1.3.1	$K_L \rightarrow \pi^0 \nu \bar{\nu}$ at KaMI . . . . .	17
1.3.2	Detector requirement for $K_L \rightarrow \pi^0 \nu \bar{\nu}$ . . . . .	18
1.3.3	Other physics opportunities at KaMI . . . . .	18
1.4	CPT Tests with Kaons . . . . .	19
1.4.1	RF-Separated Kaon Beams . . . . .	20
1.5	Experiments with Charged Kaons . . . . .	20
1.6	Strong Interaction Physics at the Main Injector . . . . .	22
1.6.1	Inclusive hadron cross sections . . . . .	22
1.6.2	Antiproton energy deposition in nuclei . . . . .	22
1.6.3	Hadronic atoms . . . . .	22
1.6.4	Drell-Yan with 50-120 GeV hadrons and mesons . . . . .	22
1.6.5	Exclusive reactions at high $P_T$ . . . . .	23
1.6.6	Low energy hadron-hadron cross sections . . . . .	23
1.6.7	Summary . . . . .	23
1.7	Low Energy Antiproton Opportunities in the Main Injector Era . . . . .	23
1.8	Booster Neutrino Program . . . . .	24
1.9	Summary of the Detector Technology Sessions . . . . .	24
1.10	Main Injector and Beams . . . . .	25
<b>2</b>	<b>Summary of the Short Baseline Neutrino Oscillation Working Group</b>	<b>26</b>
2.1	Physics Motivation . . . . .	26
2.2	Status of Existing Searches . . . . .	26
2.3	Future Searches . . . . .	27
2.4	Technological Developments . . . . .	27
2.5	Assessment of Situation . . . . .	27
2.6	Cooperation . . . . .	28

### 3 Summary of the Long Baseline Neutrino Oscillation

#### Working Group I 29

3.1	Introduction . . . . .	29
3.2	New Experimental Results . . . . .	30
3.2.1	Results from Super-Kamiokande . . . . .	30
3.2.2	Results from LSND and KARMEN . . . . .	31
3.2.3	Results from CHORUS and NOMAD . . . . .	31
3.3	Theory Review . . . . .	31
3.4	Beams and Beam Design . . . . .	32
3.5	Reactor Neutrino Experiments . . . . .	32
3.5.1	Chooz . . . . .	32
3.5.2	Palo Verde . . . . .	33
3.6	High-Energy Long-Baseline Experiments . . . . .	33
3.6.1	KEK to Super-Kamiokande . . . . .	33
3.6.2	CERN to Gran Sasso . . . . .	34
3.6.3	Fermilab to Soudan . . . . .	35
3.7	High-Energy Medium-Baseline Experiments . . . . .	37
3.8	Conclusions and Implications for Fermilab NuMI Program . . . . .	38

### 4 Summary of the Long Baseline Neutrino Oscillation

#### Working Group II 39

4.1	Physics Motivations . . . . .	39
4.2	Updates from Running Experiments . . . . .	40
4.2.1	KARMEN . . . . .	40
4.3	Present and Future $\nu$ Beams at the CERN SPS . . . . .	43
4.3.1	Introduction . . . . .	43
4.3.2	Future prospects . . . . .	43
4.3.3	The WANF . . . . .	44
4.3.4	The New Neutrino Facility (NNF) . . . . .	46
4.3.5	Possible evolution of the WANF . . . . .	46
4.3.6	The physics potential of the CERN and of the NuMI facilities . . . . .	48
4.3.7	Conclusions . . . . .	49
4.4	Future Experiments . . . . .	50
4.4.1	ICARUS . . . . .	50
4.4.2	LBL-RICH . . . . .	55
4.4.3	NOE . . . . .	55
4.4.4	OPERA . . . . .	58
4.4.5	A conventional calorimeter for an oscillation search CERN-Gran Sasso . . . . .	63
4.4.6	An "Anti-tagged" $\nu_\mu \rightarrow \nu_e$ Experiment . . . . .	65

<b>5</b>	<b>Summary of the Conventional (Non-oscillation) Physics Working Group</b>	<b>80</b>
5.1	Introduction . . . . .	80
5.2	Polarized intrinsic nucleon strangeness and elastic neutrino scattering on nucleon	80
5.3	Structure Function Measurements . . . . .	81
5.4	Charm Physics . . . . .	84
5.5	Parton propagation in nuclear matter . . . . .	84
5.6	Electroweak measurements and detector development . . . . .	85
<b>6</b>	<b>Summary of the Neutral Kaon Working Group</b>	<b>86</b>
6.1	Introduction . . . . .	86
6.2	Theoretical Motivation . . . . .	86
6.3	Current Status of KTeV . . . . .	87
6.3.1	Measurement of $\epsilon'/\epsilon$ - E832 . . . . .	88
6.3.2	Rare Kaon Decays - E799 . . . . .	89
6.4	Kaon Physics at the Main Injector . . . . .	92
6.5	$K_L \rightarrow \pi^0 \nu \bar{\nu}$ at KAMI . . . . .	92
6.5.1	Detector Requirements for $K_L \rightarrow \pi^0 \nu \bar{\nu}$ . . . . .	92
6.5.2	$K_L \rightarrow \pi^0 \nu \bar{\nu}$ at KEK . . . . .	94
6.5.3	$K_L \rightarrow \pi^0 \nu \bar{\nu}$ at Brookhaven . . . . .	94
6.5.4	Future Prospects for $K_L \rightarrow \pi^0 \nu \bar{\nu}$ . . . . .	94
6.6	Other Physics Opportunities at KAMI . . . . .	94
6.6.1	$\epsilon'/\epsilon$ at KAMI . . . . .	94
6.6.2	$K_L \rightarrow \pi^0 e^+ e^-$ at KAMI . . . . .	95
6.6.3	$\pi^+ \pi^- e^+ e^-$ at KAMI . . . . .	97
6.7	KAMI Detector . . . . .	102
6.7.1	CsI Calorimeter . . . . .	102
6.7.2	Photon Veto System . . . . .	103
6.7.3	Fiber tracking . . . . .	103
6.8	Concluding Remarks . . . . .	104
<b>7</b>	<b>Summary of the CPT Tests with Kaons Working Group</b>	<b>106</b>
<b>8</b>	<b>Summary of the Experiments with Charged Kaons Working Group</b>	<b>113</b>
8.1	Introduction . . . . .	113
8.2	Working Group Talks . . . . .	114
8.3	The CKM Experiment . . . . .	116
8.4	Beam Issues . . . . .	117
8.5	Conclusions . . . . .	118

<b>9</b>	<b>Summary of the Strong Interactions Working Group</b>	<b>120</b>
9.1	Introduction . . . . .	120
9.2	Inclusive hadron cross sections . . . . .	120
9.3	Antiproton energy deposition in Nuclei . . . . .	121
9.4	Hadronic Atoms . . . . .	121
9.5	Drell-Yan with 50-120 GeV hadrons and mesons . . . . .	121
9.6	Polarized Drell-Yan . . . . .	121
9.7	Single Spin Asymmetries in D-Y . . . . .	121
9.8	Theory/Experiment Seminar . . . . .	121
9.9	Exclusive Reactions at high $P_T$ . . . . .	122
9.10	Low energy hadron-hadron cross sections . . . . .	122
9.11	Conclusion . . . . .	122
<b>10</b>	<b>Summary of the Experiments with Low Energy Antiprotons Working Group</b>	<b>123</b>
<b>11</b>	<b>Summary of the Booster Neutrino Physics Working Group</b>	<b>124</b>
11.1	Neutrino Oscillation Formalism . . . . .	125
11.2	Experimental Motivation . . . . .	126
11.3	Overview of Beam and Detector . . . . .	129
11.4	MiniBooNE Capabilities and Issues . . . . .	131
11.4.1	Non-oscillation Neutrino Physics with MiniBooNE . . . . .	133
11.5	BooNE: A Future Upgrade to Two Detectors . . . . .	133
11.6	Conclusions . . . . .	134
<b>12</b>	<b>Summary of the Detector Technology Working Group</b>	<b>135</b>
12.1	Introduction . . . . .	135
12.2	Recent Achievements of Detector Technology in Experiments or Tests . . . . .	135
12.3	New Detector Technology Developments . . . . .	136
12.4	Concluding Words of Caution . . . . .	138
<b>13</b>	<b>Summary of the Main Injector and Beams Working Group</b>	<b>144</b>

# List of Tables

4.1	<i>Summary of the atmospheric neutrino measurements.</i> . . . . .	41
4.2	<i>Expected events at the Jura and at the Gran Sasso locations with the oscillations parameters: <math>\Delta m_{1,2}^2 \approx 0.008\text{eV}^2</math>, <math>\sin^2 2\theta_{1,2} = 0.9</math> and <math>\Delta m_{2,3}^2 \approx 1.5\text{eV}^2</math>, <math>\sin^2 2\theta_{2,3} = 0.06</math> (DIS = deep inelastic events; QE = quasi-elastic events; RES = baryon resonance production)</i> . . . . .	54
4.3	. . . . .	64
4.4	. . . . .	64
6.1	Expected single event sensitivity (SES), 90% CL on the branching ratio, the measured branching ratio or the number of events for various decay modes to be studied in KTeV. . . . .	90
6.2	Beam parameters for the KTeV and KAMI beams. KAMI-near and KAMI-far are defined in the text. . . . .	93
6.3	Inefficiency requirements for various KAMI detector components. . . . .	93
6.4	Definition of the various running scenarios considered for the study of the decay $K_L \rightarrow \pi^0 e^+ e^-$ . Two beams are used, doubling the rates for KAMI-near and KAMI-far listed in Table 6.2. . . . .	95
6.5	Efficiencies for $K_L \rightarrow \pi^0 e^+ e^-$ and $e^+ e^- \gamma \gamma$ for the various beam scenarios. Efficiency in this case is the product of detector acceptance and analysis cuts. . . . .	96
6.6	Single event sensitivities and the number of $e^+ e^- \gamma \gamma$ background events from the study of $K_L \rightarrow \pi^0 e^+ e^-$ . . . . .	97
6.7	Yields of $K_L^0 \rightarrow \pi^+ \pi^- e^+ e^-$ in KAMI . . . . .	100
11.1	The characteristics of the BooNE detector. . . . .	130
11.2	The estimated numbers of quasi elastic events for both neutrino and antineutrino scattering and for both the near (500 m) and far (1000 m) detectors (see text for explanation). . . . .	134
13.1	Protons Per Hour Under Various Modes of Operation . . . . .	147

# List of Figures

4.1	90% <i>CL</i> exclusion curves and limits for $\Delta m^2 = 100 \text{ eV}^2$ , $\sin^2(2\Theta) = 1$ from <i>KARMEN</i> for $\nu_\mu \rightarrow \nu_e$ and $\bar{\nu}_\mu \rightarrow \bar{\nu}_e$ as well as the expected sensitivity for $\bar{\nu}_\mu \rightarrow \bar{\nu}_e$ after the upgrade; oscillation limits from BNL E776 and Bugey; LSND evidence is shown as shaded areas (90% <i>CL</i> and 99% <i>CL</i> areas respectively). . . . .	69
4.2	Cross section of the <i>KARMEN</i> central detector with surrounding shield counters and massive iron blockhouse, now including the additional veto system. Cosmic muons passing or stopping in the iron which produce energetic neutrons can now be tagged by the new veto scintillators. . . . .	70
4.3	<i>Two flavor neutrino oscillation sensitivity regions (90% C.L.) for <math>\nu_\mu \rightarrow \nu_e</math> oscillations.</i> . . . . .	71
4.4	<i>Two flavor neutrino oscillation sensitivity regions (90% C.L.) for <math>\nu_\mu \rightarrow \nu_\tau</math> oscillations.</i> . . . . .	71
4.5	<i>The general view of the N<sup>OE</sup> detector</i> . . . . .	71
4.6	<i>The N<sup>OE</sup> side view.</i> . . . . .	72
4.7	<i>The N<sup>OE</sup> sensitivity to long baseline <math>\nu</math> oscillations.</i> . . . . .	73
4.8	<i>The residual <math>\nu_\mu</math> CC interaction spectrum.</i> . . . . .	74
4.9	<i>The <math>\nu_\mu</math> survival probability.</i> . . . . .	75
4.10	<i>Schematic structure of the OPERA target.</i> . . . . .	76
4.11	<i>Sensitivity of OPERA in the medium and long baseline location as compared to other experiments.</i> . . . . .	76
4.12	The number of oscillated events (top left) and the measured value of $R'$ (top-right) for maximum mixing as a function of $\Delta m^2$ : the full line is for WBB while the dashed line represents NBB case. Exclusion plots with the R method for $\nu_\mu \rightarrow \nu_e$ (bottom-left) and $\nu_\mu \rightarrow \nu_\tau$ (bottom-right). . . . .	77
4.13	Discovery potential of $\nu_\mu \rightarrow \nu_e$ (a) and exclusion plot (b). $\nu_\mu \rightarrow \nu_\tau$ : discovery potential via the single pion search in the calorimeter (c); the sensitivity of an emulsion detector (d) . . . . .	78
4.14	Exclusion plot. . . . .	78
4.15	Spectra of oscillation events for some $\Delta m_{e\mu}^2$ . . . . .	79
6.1	Plan view of KTeV detector (E832 configuration) The horizontal scale has been highly compressed relative to the vertical scale. . . . .	88
6.2	Mass peak from the first observation of $K_L \rightarrow \pi^+ \pi^- e^+ e^-$ . . . . .	89
6.3	$P_t$ distribution of $K_L \rightarrow \pi^0 \nu \bar{\nu}$ candidate events using the $2\gamma$ decay mode of the $\pi^0$ during a special 1 day run in December of 1996. . . . .	91
6.4	The KAMI "Squeezed" Geometry Detector. . . . .	96



6.5	Contributing Diagrams for the decay $K_L^0 \rightarrow \pi^+\pi^-e^+e^-$ . . . . .	98
6.6	Angles in which indirect and direct CP violation asymmetries may be seen. . . . .	99
6.7	(a) The $\sin\phi\cos\phi$ angular distribution, (b) bin by bin asymmetry between $\sin\phi\cos\phi \geq 0$ and $\sin\phi\cos\phi \leq 0$ . . . . .	101
6.8	The asymmetry vs the percent error in asymmetry for the KTeV, KAMI-far and KAMI-near scenarios. . . . .	102
11.1	90% C.L. limit expected for MiniBooNE for $\nu_\mu \rightarrow \nu_e$ appearance after one year of running, including 10% systematic error, if LSND signal is not observed. Summary of results from past experiments and expectations for the future MINOS experiment are also shown. . . . .	126
11.2	If LSND signal is observed, this plot shows the number of events expected in 1 Snowmass-year of running for MiniBooNE for the low $\Delta m^2$ favored region for LSND (shaded). Lines indicate regions excluded by past experiments (see figure 2). . . . .	127
11.3	The Super Kamioka preliminary zenith angle distribution for the multi-GeV contained events. . . . .	128
11.4	Summary of results from past experiments (narrow, dashed and dotted), future approved experiments (wide, dashed) and 90% C.L. limit expected for MiniBooNE (solid) for $\nu_\mu$ disappearance after one year of running at 1 km. Solid region indicates the favored region for the atmospheric neutrino deficit from the Kamioka experiment. A result from Kamiokanda indicating no zenith angle dependence extends the favored region to higher $\Delta m^2$ as indicated by the hatched region. . . . .	129
11.5	Schematic of the proposed detector. . . . .	130

# Chapter 1

## Executive Summary

### 1.1 Introduction

When organization of this Workshop began the envisioned attendance was on the order of 100, the majority of them being members of the already established kaon and neutrino oscillation programs. In reality, the Workshop was attended by over 200 highly motivated participants spread fairly evenly across the 11 working groups (with conveners):

- **Short Baseline Neutrino Oscillation Physics** - Juan Jose Gomez (CERN) and Rudi Thun (U. Mich)
- **Long Baseline Neutrino Oscillations Physics** - Doug Michael (Caltech) and Andre Rubbia (CERN)
- **Conventional (non-oscillation) Neutrino Physics** - Jorge G. Morfin (Fermilab) and Panagiotis Spentzouris (Columbia)
- **Neutral Kaon Physics** - Katsushi Arisaka (UCLA) and Ron Ray (Fermilab)
- **CPT tests with Kaons** - Gordon Thomson (Rutgers) and Herman White (Fermilab)
- **Charged Kaon Physics** - Peter Cooper (Fermilab) and Jack Ritchie (U. Texas/Austin)
- **Strong Interactions** - Chuck Brown (Fermilab) and Don Geesaman (ANL)
- **Anti-Proton Experiments** - Stephen Pordes (Fermilab) and Mario Macri (Genoa)
- **Neutrino Oscillation Physics with the Fermilab Booster** - Janet Conrad (Columbia) and Geoffrey Mills (LANL)
- **New Detector Technology** - Alan Bross (Fermilab) and Nick Solomey (U Chicago)
- **Main Injector and Beams** - Rick Coleman (Fermilab), Phil Martin (Fermilab) and Thornton Murphy (Fermilab)

This summary is based on the Working Group reports prepared by these conveners. Further details can be found in the individual working group reports.

For the **short baseline oscillation** group the Workshop served as a meeting ground for the Fermilab COSMOS experimenters and their CERN TOSCA colleagues to discuss appropriate technologies for next decade's short baseline experiments. The **long baseline working group** used the Workshop to compare the details of upcoming proposed or considered experiments in Japan, Europe and the US. The **conventional (non-oscillation) neutrino physics group** was geared toward developing an entirely new experiment at the Main injector Neutrino Facility. With the extremely high event rates and the development of sophisticated detection techniques inexpensive enough for the relatively massive neutrino detectors, experimentalists from COSMOS, MINOS and other neutrino programs from the US, Europe and Russia considered the wide range of opportunities offered with a Main Injector neutrino beam and began to formalize an extensive program of compelling physics topics. The **strong interactions working group** emphasized the need of a careful study of particle production over wide angular acceptance with satisfactory particle identification at these energies. Such an experiment would be of extreme interest to the NuMI group for understanding the neutrino beam used in the oscillation experiments, as well as being an important study of non-perturbative QCD.

The three Kaon working groups were each organized around existing efforts. They used the Workshop as an opportunity to refine ideas already expressed in LOI's and proposals toward the goal of providing technical physics proposals later this year.

Our community has become accustomed to associate the concept of "new facility" with the attribute "higher energy". The success of this Workshop indicates that in the past, whether through lack of the necessary detector technology, inadequate beam intensities or simply our inherent lust for higher energy, an entire panoply of rich physics has been left unstudied. The Main Injector will offer us a chance to revisit this energy regime. The appropriateness of the Main Injector's high intensity and lower energy for kaon physics and neutrino oscillation studies has long been known. This Workshop has shown the Main Injector to be also ideal for another area of study which is becoming increasingly important: non-perturbative QCD. Where once we yearned for higher energies to make sure we were far away from messy non-perturbative effects, increasing energy (because of the  $\ln E$  dependence) is bringing very little additional study-potential for QCD. Now is the opportune time to tackle the difficult job of attempting to understand what is happening as the energy scale approaches the nucleon mass from above. Recent interest in diffractive scattering is an exciting first step in this direction. A dynamic fixed-target program at Main Injector energies employing current detector techniques will take us a long way further down this road.

## 1.2 The Main Injector Neutrino Facility

As currently planned, the neutrino area of the Main Injector will be a true facility. It will consist of two types of neutrino beams; a high intensity wide-band beam geared toward rapid accumulation of statistics and a narrow-band beam which will allow the experimenter to select a restricted energy range for the neutrinos in the beam. There will be two on-site experimental halls; one about 1 km from the target for a short-baseline experiment and

the other at least 250 m further downstream to house the near detector of a long-baseline experiment.

### 1.2.1 The Main Injector Neutrino Oscillation Program

The cornerstone of the Main Injector Neutrino Facility is the Neutrino Oscillation Program. This program consists of two long-established experiments both with Stage I approval. The short baseline experiment, COSMOS, would be located about 1 km from the target and had long ago finalized its choice of technology to be keyed on a large bulk emulsion target to search for  $\nu_\mu \rightarrow \nu_\tau$  oscillations. The location of the COSMOS experiment compared to the average energy of the neutrino beam ( $L/E$ ) is optimized to search for neutrinos with masses above 1 eV which is the mass range suggested by models of cosmological dark matter. The other oscillation experiment, the long-baseline experiment MINOS, has a large near detector about 1.3 km from the target and a massive (10 Ktons) far-detector located 730 km away in a mine at Soudan, MN. This experiment's far location was chosen such that  $L/E$  would be optimized to search for oscillations of  $\nu_\mu \rightarrow \nu_\tau$  suggested by anomalies in the atmospheric neutrino rates. The MINOS experiment has set this fall as the time to choose its active detector technology.

#### Short Baseline Experiments

Two CERN short-baseline experiments, CHORUS and NOMAD, are presently searching for  $\nu_\mu \rightarrow \nu_\tau$  oscillations. CHORUS uses a bulk emulsion target to identify tau leptons by observing the characteristic track decay kinks, similar to the future COSMOS experiment at Fermilab. NOMAD depends on identifying the kinematical properties of tau decays. Based on an analysis of less than 10% of the ultimately available data sample, neither experiment has observed any tau candidates. They have set limits, which are similar to those from CCFR, based on the lack of such events ( $\sin^2 2\theta > .005$  at 90% CL for  $\Delta m^2 > 20 \text{ eV}^2$ ). The NOMAD collaboration also presented an analysis of  $\nu_\mu \rightarrow \nu_e$  oscillations which had a null result after accounting for the intrinsic  $\nu_e$  content of the beam. Based on this, they set limits on the oscillation parameters for this channel which rule out all of the high  $\Delta m^2$  region of the LSND result (see the next section on medium baseline experiments).

The ultimate mixing-angle sensitivity of CHORUS and NOMAD is expected to approach the 0.007 radian level. Neither experiment is sensitive to a tau neutrino mass below 0.5 eV. For comparison, the goals of the future Fermilab experiment, COSMOS, are to extend the region of sensitivity to mixing angles of 0.002 radian and to tau neutrino masses of 0.3 eV. Since oscillation probabilities are proportional to the square of such small mixing angles, the proposed sensitivity of COSMOS to tau production is a factor of ten better than that of CHORUS or NOMAD for tau neutrino masses above 5 eV and a factor of thirty better for lower masses.

The overall situation with respect to short baseline experiments changed recently when members of both CHORUS and NOMAD submitted a letter of intent to CERN to extend their short-baseline search for neutrino oscillations by combining elements of the CHORUS and NOMAD designs into a single experiment called TOSCA. The choice of technology for TOSCA is a distributed emulsion array inside the UA1 (NOMAD) magnet. The proposed

sensitivity of TOSCA is similar to that of COSMOS, and the expected background in both experiments is at the one-event level. Both COSMOS and TOSCA propose to run from about 2001 to 2005. The deliberations of this working group concluded with the announcement that the COSMOS and TOSCA groups have agreed to maintain contact, with two meetings planned during the next year, one in Europe and one in the U.S.

## Medium Baseline Experiments

The existing medium baseline experiments LSND and KARMEN were reviewed. The LSND collaboration presented an update of their analysis on the decay at rest signal and reiterated their interpretation that it is the result of neutrino oscillations. In addition, they presented new results on pion decay-in-flight events which gives similar results for neutrino oscillation parameters. The current status is that the lower region of  $\Delta m^2$ , ( $\Delta m^2 < 2 \text{ eV}^2$ ) is still allowed and that improved experiments will be needed to fully cover this region. KARMEN showed updated results confirming that they see no sign of oscillations but that this remains marginally consistent with the LSND observations. They reported on their plans for future running which will permit complete coverage of the LSND parameters within the next 3 years. A possible future medium baseline experiment using the existing CERN neutrino beam directed toward a detector situated in the Jura mountains was discussed.

## Long Baseline Experiments

The main goal of the long-baseline working group was to provide an overview of the current status of the various efforts on the subject rather than formulate a new experimental program for the Main Injector. As mentioned, these experiments are designed to study the oscillation region suggested by the unexpected ratio of  $\nu_\mu$  to  $\nu_e$  found in experiments sensitive to atmospheric neutrinos. The most recent study of atmospheric neutrinos is underway by the Super-Kamiokande collaboration and their first analysis of atmospheric neutrinos was presented. The new results have about 2.5 times more data than the full data set from Kamiokande (in just a fraction of a year of live-time) and with much better control over any possible fiducial volume effects. The new result for the ratio of ratios of muon-like/electron-like events from the data over the same ratio from the Monte-Carlo is consistent with the previous result from Kamiokande and IMB. The new ratio of ratios is  $0.64 \pm 0.04_{\text{stat}} \pm 0.06_{\text{sys}}$ . A very-preliminary zenith distribution for the multi-GeV events was shown. The statistics are still too low to make any real conclusions

With respect to high energy long baseline experiments, a number of experiments based on different detection techniques have been developed around existing or planned facilities and beamlines at three different locations; KEK to Super-Kamiokande, CERN to Gran Sasso and Fermilab to Soudan.

- KEK to Super-Kamiokande: The very large size of the Super-Kamiokande detector and its general ability to study neutrino events over a wide energy range, combined with its distance from KEK (250 km) invite use of the facility for a long-baseline experiment. A near detector will be built at KEK which will consist of a water-Cerenkov detector, similar to Super-Kamiokande (but smaller) and a fine-grained detector using fiber tracking in water for measuring properties of the neutrino beam. The beamline will

initially make use of the 12 GeV proton-synchrotron to create a neutrino beam with mean energy about 1.5 GeV. It is expected that this neutrino beam will begin running in 1999. A future high-intensity 50 GeV proton synchrotron would provide a neutrino beam with typical energy of about 5 GeV. The date of completion of the 50 GeV machine is roughly estimated to be around 2003.

- CERN to Gran Sasso: The Gran Sasso underground laboratory is located 730 km from CERN, making it an excellent site for locating a long-baseline experiment, should a neutrino beam be built at CERN aimed in the direction of the Gran Sasso. Using a special 350 GeV cycle of the SPS, the mean neutrino energy at the Gran Sasso would be about 15 GeV. The turn-on date for the beam to the Gran Sasso is estimated to be 5 years from the time that a decision is made to build the beam. Construction of the beam depends on funding from INFN and a decision is expected before the end of this year.

Three different detectors have been officially proposed at the Gran Sasso and other designs are under consideration/development:

- ICARUS: A very-high-resolution liquid argon TPC which essentially is a fully electronic bubble chamber. The proposed mass is 1.8 kT
  - NOE: A tracking/spaghetti calorimeter with a downstream end which will have magnetized iron for measurement of muon momentum. The total mass of the detector would be 4 kT.
  - RICH: A 25 kT water ring-imaging Cerenkov detector.
- Fermilab to Soudan: Construction of the NuMI neutrino beam line using protons from the Main Injector has been approved by Fermilab and DOE. It appears that Congress will approve \$6M in FY '98 for engineering and design of the beamline.

MINOS has been approved by Fermilab and recommended for construction by the HEPAP subpanel. The standard MINOS design is based on a sampling/tracking calorimeter with magnetized iron plates. The nominal mass of the far detector is 10 kT.

## **Review of Neutrino Oscillation Phenomenology**

Discussions on neutrino oscillation phenomenology with respect to the various experimental hints of oscillations were reviewed. It was concluded that by using three-flavor oscillation models, it is (marginally) possible to fit all observed data on neutrino oscillations. In order to completely study the full complexity of the multi-flavor mixing, good sensitivity is required to both oscillation parameters and identification of event types over a large range of oscillation probability and  $L/E$ .

## **Conclusions: The Fermilab Long baseline Neutrino Oscillation Program**

The Workshop provided an excellent overview of what is happening in the field of accelerator-based neutrino oscillation searches. The experimental hints of oscillations are strong and

this has attracted a great deal of attention to the subject around the world. In addition to the Fermilab program, the Japanese are moving forward with their plans to use Super-Kamiokande for a long-baseline experiment and there are multiple proposals for experiments at CERN using the existing beamline or a new beamline to the Gran Sasso. Although it is quite unlikely that all of these experiments will materialize, there is no doubt that competition between the sites to bring a first class detector on-line as soon as possible already exists.

This implies that although the investment in the NuMI program at Fermilab is large, it must be made on an aggressive schedule in order to ensure maximum impact on this subject.

## 1.2.2 A Conventional (Non-oscillation) Main Injector Neutrino Program

The Main Injector neutrino beam is an extremely intense beam providing event rates of roughly 4000 events /kg - year at the short-baseline detector hall location (a year defined as  $3.7 \times 10^{20}$  protons on target). By combining a beam yielding high statistics with a contemporary high precision detector, a conventional neutrino program could provide answers to questions about neutrino interactions which have been either inadequately covered or completely neglected by past neutrino experiments.

The physics prospects examined were:

1. Inclusive structure function measurements with emphasis on medium to high  $x$
2. Study of Nuclear Effects
3. Polarization of the strange component of the nucleon's sea
4. Charm Physics
5. Electroweak Measurements.
6. Study of Hadron Formation Length and Parton Propagation in Nuclear Matter

### Structure Function Measurements

Up to the present time, all the statistically significant structure function measurements with  $\nu$  beams have been made using dense nuclear targets. The high event rates of the NuMI beam allow the use of both nucleon and heavy nuclear targets, while the kinematic region permits study of moderate and high- $x$  with  $Q^2$  in both the pQCD and non pQCD regimes, and low- $x$  with low  $Q^2$ . With this kinematic coverage one could study the transition from the pQCD region to the resonance region, and obtain very significant and needed measurements on the following subjects:

**High- $x$  Structure functions and parton distribution functions.** Recent investigations of the behavior of parton distributions within the nucleon have emphasized the very high energy reach of the collider data by concentrating on the very low  $x$  region. Interestingly enough, we now have much more data exploring the low ( $< 0.1$ ) to ultra-low ( $< 0.001$ )  $x$  region than we have in the high  $x$  ( $> 0.5$ ) region. Whereas we need high energies to reach

the high  $\nu$  necessary to study the low- $x$  region we need high statistics on a nucleon target to study the high- $x$  region with low statistical and systematic errors.

Our ignorance of the high  $x$  region is not limited to the "higher twist" and nuclear effects expected (but hardly studied) in this region, but extends even to the behavior of simple partons at  $x > 0.5$ . The ratio of the d-quark to u-quark -  $d(x)/u(x)$  - is expected to approach 1/5 in the framework of pQCD, however current fits are just as consistent with this ratio approaching 0 (as predicted by bag model calculations) as the expected 0.2.

A recent project of some members of the CTEQ collaboration emphasized the limited knowledge of this region when constructing a toy model which could simultaneously explain the high- $q$ , high- $x$  anomalous ZEUS events at HERA and the high- $p_t$  events of CDF at the collider. It was found that an additional quark contribution, equal to around 1 % of the integrated d-quark contribution, could be added at  $x$  near 1.0 and  $q = 2$  GeV without seriously contradicting any available data. (Through normal  $q$ -evolution of the parton distributions these evolve down to the  $x$  of the ZEUS events at the proper  $q$ .) This exercise indicated that we can adjust high  $x$  parton distributions with relative impunity with respect to the very limited and imprecise experimental data currently available.

**Higher twist Effects.** Although twist-4 phenomena is expected to follow  $Q^{-2}$  behavior, the  $x$  dependence of the matrix element is unknown. This has made a careful study of this phenomena difficult since one needs a high statistics data set with small systematic errors over a wide range in both  $q$  and  $x$ .

Currently studies of twist-4 phenomena in electro-production experiments exist which combine SLAC  $e$ - $p$  data with BCDMS  $\mu$ - $p$  data. This study indicates that the twist-4 contribution is large and positive. On the other hand, the only studies using neutrino DIS data are based on low-statistics, heavy-target Gargamelle and BEBC bubble chamber experiments. These tend to indicate that the twist-4 contribution is relatively small and negative. Current global fits of DIS results indicate no real need for a higher-twist contribution when fitting both electro-production and neutrino production data together.

## Nuclear effects

There is very little known experimentally about nuclear effects in neutrino DIS. The only existing nucleon data are from low statistics bubble chamber experiments. Nuclear corrections are needed in order to extract the parton distribution functions of the nucleon from the high precision neutrino structure function data which are obtained using nuclear targets. Currently, the corrections applied are determined from charged lepton DIS on nuclear targets. There is no reason to expect that the nuclear effects involved in neutrino scattering and charged lepton scattering should be the same. Furthermore, nuclear effects in  $x F_3$  have never been measured. The difference (if any) between nuclear effects in  $F_2$  and  $x F_3$  would allow differentiation between the behavior of valence and sea quarks in a nuclear environment.

With the Main Injector neutrino beam we could measure the "EMC effect" region ( $0.3 < x < 0.6$ ,  $\sigma_A < \sigma_D$ ) in the pQCD regime, and the shadowing region ( $x < 0.1$ ,  $\sigma_A < \sigma_D$ ) in both the pQCD (higher  $x$ ) and the lower  $Q^2$  regions. Because of the high event rates the size of the nuclear targets could be kept small ( $\leq 1$ ton). If the different targets have similar geometry and they are simultaneously exposed to the beam, the systematic uncertainty from the beam flux will cancel in a ratio measurement. The flux systematic uncertainty is one of



the most important sources of systematic error in  $\nu$  SF measurements.

### **Polarized intrinsic nucleon strangeness and elastic neutrino scattering on nucleon**

The strange quark content of the nucleon is currently of considerable experimental and theoretical interest. Results from experiments on  $\pi N$  scattering demonstrate that the contribution of strange quarks to the nucleon mass could be as high as 20 %. Other evidence comes from the polarized DIS measurements which indicate that the strange quarks in the nucleon may be polarized opposite to the proton spin. Also, the recent observation of strong violation of the OZI-rule seen recently at LEAR experiments in  $\phi$  and  $f_2'(1525)$  production could be interpreted by postulating the presence of long-lived  $s\bar{s}$  pairs in the nucleon's wave function.

Elastic neutrino scattering off nucleons is a very good tool to obtain information about the possible polarization of the strange quarks in the nucleon. The last measurement of the  $\nu p$  elastic scattering was done 10 years ago and the re-analysis of this data was inconclusive in determining the size of the spion contribution of the strange quarks,  $\Delta s$ .

### **Charm Physics**

The rates for charm production are high (0.5-5 % of the total neutrino-nucleon cross-section), and the events are characterized by relative low multiplicities and of course low energies (and decay lengths). Since the event rates with the MI beam are high, a low mass detector could be used to study charm production. By using a detector with complete event reconstruction and high quality vertexing, a unique opportunity to study charm production inclusively would be offered.

### **Parton propagation in nuclear matter**

The question of parton propagation in dense nuclear matter is rather new and not very accurately studied. The issue is that secondary hadrons produced at the interaction point would undergo strong re-scattering when traversing the nuclear matter on their way out of nucleus. However, if the hadrons or hadron constituents are not created at the interaction point, the produced object could pass some distance in nuclear matter before attaining the normal ability to interact. This distance is referred to as formation length. A nucleus target, when compared to a nucleon target, is a unique tool for studying the properties of the state which propagates within it. In this case, by studying the evolution of parton jets one could learn more about the confinement mechanism, color transparency and formation length. Important by itself, this information is also relevant for the issue of quark-gluon plasma formation in heavy-ion collisions.

The intense Main Injector neutrino beam provides an excellent opportunity to study this subject with high statistics and low systematics. The low energy of the neutrinos is an advantage since previous studies of formation length indicated that the effect is most visible with energy transfer  $\nu$  (virtual boson energy) of about 20 GeV.

## 1.3 Experiments with Neutral Kaons

After over 30 years of hard work, the source of CP violation is still unknown. All observations are currently consistent with a Standard Model formulation with a single complex phase in the CKM matrix as well as Superweak interactions which lie entirely outside the Standard Model. There continues to be a great deal of activity in experimental neutral kaon physics at CERN, BNL, KEK, DAPHNE and Fermilab. The present round of activities at these facilities promises to shed a great deal more light on this 30+ year old question. One method for probing this issue lies in collecting large quantities of neutral K decays to charged and neutral  $2\pi$  final states and extracting the quantity  $\text{Re}(\epsilon'/\epsilon)$  from the well known double ratio. Experiments are currently underway at CERN and Fermilab to carry out this measurement with unprecedented precision. Another window on this and other interesting physics lies in rare kaon decays, a number of which are expected to have significant direct CP violating amplitudes. In order to reach sensitivities which will allow sensitive tests of the standard model, large fluxes of kaons will be required. The Main Injector at Fermilab will provide a significant flux of high energy neutral kaons. How to make the best use of this new facility using the existing KTeV detector with strategic upgrades over time was the focus of the Neutral Kaon Working group.

The current status of the KTeV detector was highlighted in two general interest talks at the workshop. Since the fall the detector has provided a new limit on  $K_L \rightarrow \pi^0 \nu \bar{\nu}$ , the first measurement of the  $K_L \rightarrow \pi^+ \pi^- e^+ e^-$  branching ratio at  $2.6 \times 10^{-7}$ , a new limit on the hypothetical SUSY particle  $R_0$ , and the first observation of a rare hyperon beta decay.

The core of much of the KaMI detector is complete. The Workshop explored the next steps.

### 1.3.1 $K_L \rightarrow \pi^0 \nu \bar{\nu}$ at KaMI

The conceptual idea of doing Kaon physics with the Main Injector started even before the KTeV experiments. In the 90's, however, the Kaon physics program was developed with the Tevatron first, and successfully realized in KTeV.

The next logical step is to bring 120 GeV proton beam onto the existing KTeV target station, and utilize most of KTeV detector infrastructure as much as we can.

The KTeV experimental hall was designed and constructed to handle the 120 GeV proton beams as well. So, there are two real issues to be discussed; First, what physics we should continue, Second, to do so, what detector upgrades are required.

As far as physics goal is concerned, it has become clear that the next Kaon physics, after the precise measurement of  $\text{Re}(\epsilon'/\epsilon)$ , will be the branching ratio measurement of  $K^0 \rightarrow \pi^0 \nu \bar{\nu}$ . This is theoretically extremely clean, and gives the best opportunity to measure the magnitude of direct CP violation in the CKM matrix, given by the Eta parameter.

Thus the main focus of this workshop was concentrated on the discussion of how to achieve this goal at KaMI.

The morning session of the second day was devoted to the discussion of detector requirement at KaMI, as well as reports from the similar experiments proposed at the other laboratories; KEK and BNL.

### 1.3.2 Detector requirement for $K_L \rightarrow \pi^0 \nu \bar{\nu}$

Single event sensitivity of  $1.0 \times 10^{-13}$  / year appears possible, which yields 20-30 Standard Model signals per year.

The real question is how to handle the background level. The study has been focused on the background from  $K_L \rightarrow 2\pi^0$ . Due to its large maximum  $P_t$  of 209 MeV, once two photons are missed in the final state there is no way to distinguish this background from the signal. The extra two photons which go outside of the CsI are correlated to each other. The most serious case is where one high energy ( $\geq 1$  GeV) photon goes in the forward direction and the other low energy one ( $\leq 20$  MeV) goes to the photon veto with large opening angle. It was shown that, in order to achieve Signal/Noise ratio of unity, the following inefficiencies are required.

1. Photon Veto inefficiency (2-20 MeV)  $\leq 0.2$
2. Photon Veto inefficiency (1-3 GeV)  $\leq 1.0 \times 10^{-5}$
3. CsI calorimeter inefficiency (3-10 GeV)  $\leq 1.0 \times 10^{-5}$
4. Beam hole calorimeter inefficiency ( $\geq 10$  GeV)  $\leq 1.0 \times 10^{-2}$

This study does not include any additional kinematical constraints such as time-of-flight of  $K_L$  or direction measurement of gammas. These kinematical measurements are helpful to relax the above requirement of detector inefficiencies. Such studies are underway.

Obviously, Detector R & D to understand the feasibility of the above efficiency by conventional, inexpensive detector technology is of the highest priority.

So far, all three groups are making good progress, and no show-stopper were reported at this workshop. Since all the groups need to develop large area photon veto detector under limited budgetary constraints, there were suggestions for an international collaboration of detector R & D at the tagged photon test beam channel at INS, Japan.

### 1.3.3 Other physics opportunities at KaMI

Whether the next round of  $\text{Re}(\epsilon'/\epsilon)$  measurements is necessary strongly depends on the results from the current activities (KTeV and NA48). Assuming that it still turns out to be inconclusive, an accuracy of  $3.0 \times 10^{-5}$  is feasible in term of statistics.

While detecting  $K_L \rightarrow \pi^0 e e$  at KaMI appears to be possible, the extraction of the three standard model contributions in light of expected backgrounds looks impossible in a first round experiment at this time. Work will continue on  $K_L \rightarrow \pi^0 \mu \mu$ .

The charged asymmetry of  $K_L \rightarrow \pi \pi e e$  is expected by the indirect CP violation from  $K^0 \bar{K}^0$  - mixing. This should be first observed by KTeV at the accuracy of about 1%. With much higher kaon flux at KaMI (the expected number of events is as high as one million), the resulting asymmetry measurement would have an accuracy of  $1.0 \times 10^{-3}$  accuracy. This level is still not enough to see direct CP violation, but may well be enough to see some unexpected effects outside of the SM.

In summary, generally speaking, more than 100 times improvement in sensitivity over the current KTeV experiment could be achieved for all the decays modes as far as kaon flux

is concerned. This corresponds to a single event sensitivity of  $1.0 \times 10^{-13}$ , much lower than any current measurement of kaon decays including two body decays such as  $K_L \rightarrow \mu e$ ,  $ee$ , and  $\mu\mu$ . In fact, although there was no discussion on these modes, it is quite possible to study these modes as well, depending on how the detector is optimized.

## 1.4 CPT Tests with Kaons

The ‘‘CPT Tests with Kaons’’ working group pursued plans of an experiment to study tests of CPT symmetry conservation that will be sensitive at the Planck scale, measurements of CP violation parameters for  $K_S$  decays that have never been measured, improved measurements of CP violation parameters in  $K_L$  decays, tests of the  $\Delta S = \Delta Q$  rule, and searches for rare  $K_S$  decays. This experiment has been described previously in a Letter of Intent to Fermilab, P894.

The  $K_L/K_S$  system forms a finely balanced interferometer that can be effected by small perturbations like CP violation or CPT violation (if it exists). The experiment is designed to maximize this interference to best search for these effects. .

The working group focused on the physics of the experiment, the experimental setup, plans for the RF-separated  $K^+$  beam, possible sites for the experiment in the Meson Lab, and on existing apparatus and magnets that would be available after 1999.

The best experimental limit on CPT violation came from Fermilab experiment E773. This limit is (at 90% confidence level),

$$\frac{|M_{K^0} - M_{\bar{K}^0}|}{M_{K^0}} < 1.3 \times 10^{-18} \quad (1.1)$$

By the Planck scale is meant

$$\frac{|M_{K^0} - M_{\bar{K}^0}|}{M_{K^0}} = \frac{M_{K^0}}{M_{Planck}} = 4.1 \times 10^{-20} \quad (1.2)$$

so the E773 result stands at 31 times the Planck scale.

In KTeV an improvement of a factor of 3 to 5 is expected. Using the regeneration method will be difficult beyond the KTeV level.

After KTeV the limit will stand a factor of 6 to 10 above the Planck scale. The CPT experiment will push the limits an order of magnitude by studying interference effects from an initially pure  $K^0$  beam. This beam will be made by the charge exchange reactions from a  $K^+$  beam. To maximize the flux of  $K^+$  made from the 120 GeV/c protons from the Fermilab Main Injector we choose a  $K^+$  momentum of 25 GeV/c. We would use a hyperon magnet to define the  $K^0$  beam, similar to the one in the Proton Center beam line. A vee spectrometer and a lead glass electromagnetic calorimeter form the detector.

A monte carlo calculation of the statistical sensitivity of the experiment yields an uncertainty in  $\phi_{+-}$  of 0.02 degrees. This is 50% better than what is needed to place a 90% confidence limit on CPT symmetry violation at the Planck scale.

### 1.4.1 RF-Separated Kaon Beams

The session on the RF-separated  $K^+$  beam was held jointly by the CPT tests with kaons, the  $K^+$ , and the Beams working groups. It was attended by all of the physicists who want to use that beam (members of the CPT and CKM collaborations), by the organizers of the beams working group, and by some of the physicists who would actually build the beam. There were three talks in the session, on the optics of the beam, on building superconducting RF cavities and on the possibility of modulating the Main Injector proton beam at a subharmonic of the RF frequency used in the  $K^+$  beam.

The goals of the beam design are as follows:

- Flux of  $2 \times 10^8$   $K^+$ /spill, with  $5 \times 5$  mm<sup>2</sup> spot size (for the CPT experiment).
- Flux of  $3 \times 10^7$   $K^+$ /spill, with 50 - 100  $\mu$ rad divergence in x and y (for the CKM experiment).
- Impurity  $\leq 10\%$ .
- Simple change-over between the two experiments.
- 25 GeV/c for CPT and 22.8 GeV/c for CKM.

The beam design that was presented accomplished all these goals. The necessary superconducting RF R & D necessary to develop this beam was detailed and fits well with the expected schedule for the main injector fixed target program. This beam could be tuned for antiprotons, as well.

Investigations of several siting options in the Meson area for both the CPT experiment and the CKM experiment are underway now.

This experiment will confront several exciting physics topics. The group concluded that both the experiment and beam are feasible, and are working hard on a Proposal.

## 1.5 Experiments with Charged Kaons

The working group focused on the opportunities for high sensitivity experiments using charged kaon beams, looking in detail at the options for precision measurements and rare decay searches using the charge kaon decay in flight technique; particularly the CKM experiment letter of intent. The initial concept for the CKM experiment was a non magnetic decay in flight spectrometer with the capability to run with at least 3MHz of kaon decays. It is based upon phototube ring imaging Cerenkov counters. The major goal of CKM is the measurement of the branching ratio of  $K^+ \rightarrow \pi^+ \nu \bar{\nu}$ .

The interest in an in-flight measurement of  $K^+ \rightarrow \pi^+ \nu \bar{\nu}$  at the Main Injector is motivated by the high kaon fluxes potentially available combined with the opportunity for long fixed-target runs in parallel with Collider running. The Brookhaven experiment focusing on this mode is currently limited by kaon flux and running time. That experiment has a good chance to observe  $K^+ \rightarrow \pi^+ \nu \bar{\nu}$  for the first time, but in the best case scenario its measurement of the branching ratio is likely to be based on a handful of events. A Main Injector experiment should not be statistics limited. A sample of 100 events appears to be a plausible goal,

permitting a 10% measurement of the branching ratio and a determination of the magnitude of the CKM matrix element  $V_{td}$  at a level where experimental and theoretical uncertainties are of similar size. The main challenge in such an experiment will be to reject backgrounds to the necessary level.

The goals set forth in the 1996 CKM EOI are:

1. To be able to observe approximately 100  $K^+ \rightarrow \pi^+ \nu \bar{\nu}$  events for a  $1.0 \times 10^{-10}$  branching ratio in two years of running.
2. To reduce all background to the level of a few events.
3. To limit capital cost to less than 10M dollars.

The detector consists of two phototube ring imaging Cerenkov counters separated by a vacuum decay volume with a surrounding photon veto system. The two RICHs are each velocity spectrometers which measure the vector velocity of the kaon and pion respectively from the center and radius of each observed ring. Both counters can be blinded to the Cerenkov light from beam pions by not instrumenting the small region illuminated by beam pion rings. The intrinsic fast time response of photomultipliers gives this design very high rate capabilities. In a simple simulation the proposed CKM detector was able to maintain  $\approx 2\%$  acceptance while controlling the background from the  $K\pi 2$  mode to the level of a few events.

An important improvement in the prospects for a rare kaon decay in flight experiment has been provided by the CPT group which has designed an RF separated  $K^+$  beam.

The availability of such a beam will make it practical for CKM to place tracking detectors in the beam. Several indications point to this as a requirement, and the original detector concept has been modified to include magnetic tracking.

The most valuable portions of the workshop were the unstructured (freewheeling) discussions when details were discussed. Particular areas of concern included various scattering and interaction processes which could corrupt events and the lack of redundant measurements, the possibility of additional background sources from  $K^+$  scattering in the detector, and questions about how the experiment could be triggered.

There was discussion on other physics measurements which might be possible in the CKM apparatus. The list identified includes high statistics studies of structure dependent form factors, precision measurements of  $V_{us}$  to  $\approx 0.1\%$ , and further searches for lepton flavor violation in K decays.

The next step is to simulate the revised apparatus and start to address the background issues at a level appropriate for a proposal. The revised CKM apparatus addresses the issues of redundant measurements and control of scattering at the conceptual level. The question now is how much these additions improve the background rejections at the level of serious simulations. An expanded working group has formed to continue the work at an accelerated rate. While observing 100  $K^+ \rightarrow \pi^+ \nu \bar{\nu}$  decays with low background is a daunting task, it is a very exciting prospect. It would be a strong addition to the Main Injector fixed-target physics program.

## 1.6 Strong Interaction Physics at the Main Injector

Much discussion revolved around the need to measure and study non-perturbative QCD, particularly at main injector energies. It focused on coherent phenomena where the interactions with multiple partons are important. In the past few years there have been significant strides in identifying which such processes are calculable and lead to firm predictions for hadron and nuclear reactions.

### 1.6.1 Inclusive hadron cross sections

An experiment to measure with large acceptance the inclusive hadron yields and correlations at main injector energies. These measurements would test, among many things, a scaling law which appears to describe many of the correlations in particle distributions and would also provide a comprehensive characterization of the secondary hadron beams which is needed to understand the neutrino flux for the main injector neutrino experiments.

### 1.6.2 Antiproton energy deposition in nuclei

Antiproton beams are perhaps the most efficient way to transfer excitation energy to atomic nuclei. This results in high-temperature, relatively low density, nuclear systems which vaporize in a liquid-gas nuclear phase transition. The first evidence for this type of transition was obtained at FNAL a decade ago in proton-nucleus collisions, but 10-20 GeV antiproton beams are clearly the tool of choice to definitively establish this behavior. The detectors for these experiments exist if the beams are available.

### 1.6.3 Hadronic atoms

Stopping mesons and hyperons produced in main injector production targets form mesic and hyperonic atoms. The exquisite sensitivity and resolution of X-ray detectors makes detecting the atomic transitions of these atoms the most accurate measurements of a number of masses and spin-orbit couplings. Significant results would have impact in a number of physics areas including the limit on the muon neutrino mass.

### 1.6.4 Drell-Yan with 50-120 GeV hadrons and mesons

The main injector is an optimum environment for Drell-Yan dimuon production at high fractional parton momenta. Several experiments were described that are only possible with the lower energy and higher flux of the MI. These include precise measurements of  $u(x)$ - $d(x)$  and  $\bar{u} - \bar{d}$  at high  $x$  on the proton, nuclear dependences, and Kaon structure functions.

If the MI proton beam were to be polarized, definitive measurements of the sea antiquark and gluon polarizations would be possible with a polarized target.

### 1.6.5 Exclusive reactions at high $P_T$

Exclusive reactions provide another regime where perturbative QCD techniques should be applicable to coherent phenomena. Many of the features of QCD in these reactions are intimately related to the phenomenon of color transparency, the reduction of the interaction cross sections for the small color singlet objects that are expected to dominate the exclusive reaction mechanisms.

### 1.6.6 Low energy hadron-hadron cross sections

The operation of a hydrogen streamer chamber with an electronic readout has now been demonstrated. This could be an ideal detector for low energy hadron-nucleon scattering including such topics as the pion-nucleon sigma term and threshold proton-antiproton elastic scattering.

### 1.6.7 Summary

It was clear that the Main Injector presented many valuable new opportunities in studying the strong interactions. It appears likely that proposals would result from the first four topics as viable collaborations are formed. A letter of intent was submitted in 1995 for Polarized Drell-Yan measurements. It seems quite possible that the unpolarized Drell-Yan and single and double spin polarized Drell-Yan measurements could use a common apparatus in a coherent program. These ideas are important to our understanding of the strong interactions and indicate future possible opportunities for the FNAL experimental program.

## 1.7 Low Energy Antiproton Opportunities in the Main Injector Era

The first question addressed was the availability of antiprotons for dedicated experiments during Collider running. An analysis suggested, to the group's surprise, that given a working Recycler, the antiproton source could devote as much as 1/3 of its time to providing antiprotons for non-collider use. The Recycler has added a degree of freedom to the antiproton production system whose impact has yet to be fully exploited.

From the side of physics experiments, the three experiments which have run in the antiproton source showed that they had by no means exhausted their topics. The antiproton lifetime experiment is planning an extension and are considering running either on the antiproton accumulator or on the Recycler in the Main Injector era. The antihydrogen experiment is submitting a proposal to measure the lamb-shift in antihydrogen using a technique based on the Stark effect induced as the  $\bar{H}$  passes through magnetic fields.

The charmonium experiment will not finish its program this run and one could envisage an apparatus with better sensitivity to low energy photons to complete the study of charmonium states that decay to two photons.

A new deceleration ring could also provide very low energy antiprotons that would allow investigations of such questions as whether antimatter falls up or down. The group pointed



out that the Fermilab source produces antiprotons at more than 20 times the rate at CERN.

## 1.8 Booster Neutrino Program

Although a Booster neutrino program has little to do with the Main Injector, it was decided to include this topic to get a complete picture of Fermilab's potential in the field of neutrino oscillations.

The purpose of the Booster Neutrino Physics working group was to develop ideas for a Booster-based neutrino oscillation experiment. This experiment would be motivated by the LSND observation, which has been interpreted as  $\bar{\nu}_\mu \rightarrow \bar{\nu}_e$ , and by the atmospheric neutrino deficit which may result from  $\nu_\mu$  oscillations. The BooNE (Booster Neutrino Experiment) program would have two phases. The first phase, MiniBooNE, is a single detector experiment designed to study  $\nu_\mu$  oscillations either through a disappearance signal or via an abnormally high rate of  $\nu_e$  events in the beam. A direct application of the experimental results would be a check of the LSND claim of observing a signal for neutrino oscillations. A subsequent phase of the experiment would introduce a second detector, with the goals of accurately measuring the  $\Delta m^2$  and  $\sin^2 2\theta$  parameters of any observed oscillations.

The MiniBooNE experiment (phase 1) could begin taking data in 2001. The detector would consist of a double-wall cylindrical tank with a 400 t fiducial volume. It would be situated 1000 m from a neutrino source.

The neutrino beam constructed using the 8 GeV proton Booster at FNAL would consist of a target followed by a focusing system and a  $\sim 30$  m long pion decay volume. The low energy, high intensity and 1  $\mu$ s time-structure of a neutrino beam produced from the booster beam are ideal for this experiment.

## 1.9 Summary of the Detector Technology Sessions

The detector technology sessions at the Workshop were of two types, one session dedicated to new developments and advances in detectors and two sessions in parallel with the Kaon and Neutrino groups, where the emphasis was more on the specific needs of future experiments along with performance reports of running experiments.

Contributions included discussion of:

1. New plastic scintillator.
2. Development of a 5 inch Hybrid Photon Detector.
3. Development of the KTeV TRD system.
4. Development of a Gas Electron Multiplier.
5. Silicon Microstrip Detectors.
6. Pixel Detector R & D at Fermilab.
7. Development of the D0 Fiber Tracker.

8. A Long Baseline RICH.

9. Icarus Liquid TPC Detector.

From the many detector limitations discussed by the physics working groups, it was obvious that several developments are needed. Detector issues of most importance include higher rate tracking, high-resolution tracking, hermetic photon veto capability, and affordable extremely-large-volume detectors for neutrino experiments.

Developing a new technology or advancing an existing one into a real research tool will take time and money, but future experiments can benefit greatly from this effort.

## 1.10 Main Injector and Beams

The key features of the new Fermilab Main Injector for fixed target physics are its high intensity, relatively high proton energy, and its ability to deliver protons to a fixed target program **simultaneously** with the production of antiprotons for the collider program. This group presented to the users options available beginning in 2000 for 120 GeV extracted beams into the Switchyard and met closely with experimenters to discuss their needs during that era. While most of the discussions centered on primary beams, the R & D plans for the superconducting RF separated kaon beams were also discussed in a joint session with the kaon groups.

The beams planned for the year 2000 and beyond include fast extracted 120GeV beam to the NuMI area as well as slow extracted (1 sec flattop) beams to the Meson area (3 primary proton beams) and a slow extracted beam to the KTeV/KAMI experiment in the Neutrino area. The capability of extracting 800 GeV to the Proton Area will be maintained, but of course it will not run during Collider operations.

Conceptual design of the changes and additions to convert the existing 800GeV switchyard to 120 GeV is nearly complete. A small working group in the Beams Division is actively studying the optics of the entire Switchyard to ascertain what changes are necessary. The important overall goal is to have the 120 GeV beams tested and ready for use during the Collider run of 2000.

The sum of intensity requests for all the developing ideas for fixed target experiments is beginning to stretch the initial design parameters. Problems of proton economics were discussed, and the issue of whether it is feasible to extract to both NUMI and Switchyard on the same Main Injector cycle was explored.

During talks on factors which limited the Main INjector initial intensity to  $3 \times 10^{13}$  the plans to explore increasing the machine intensity to  $6 \times 10^{13}$  over the course of several years were laid out. These can be accomplished without major investments in new hardware.

Members of the group then explored various scenarios for "mixed" and "interleaved" Main Injector cycles and the impact of each scenario on the protons/hour delivered to antiproton production, fast spill, and slow spill.

One conclusion of this group is that raising the intensity of the MI to 5 or  $6 \times 10^{13}$  per cycle is a very worthwhile goal.

# Chapter 2

## Summary of the Short Baseline Neutrino Oscillation Working Group

Reported by J. J. Gomez Cadenas, CERN and R. Thun, Univ. of Michigan

### 2.1 Physics Motivation

The strong evidence for cosmological dark matter and for galaxy clustering at very large scales, combined with the probable existence of a dense, primordial sea of cosmic background neutrinos, makes a search for neutrinos with masses above 1 eV a compelling research objective. The so-called "see-saw" mechanism provides motivation to focus the search on muon-neutrino to tau-neutrino oscillations. The "see-saw" mechanism gives a natural explanation for small, non-zero neutrino masses and, when embedded in a scenario of quark and lepton families, predicts a hierarchy of neutrino masses with the tau neutrino at the top.

So far, none of the present experimental indications for neutrino oscillations contradicts the possible existence of tau neutrinos with mass above 1 eV. While cosmological arguments set the mass scale of interest for this kind of search (and hence the E/L parameters of suitable experiments), they do not provide guidance on the magnitude of the relevant mixing angles. The goal of any future short-baseline ( $L \leq 1$  km) neutrino oscillation search should therefore stress the achievement of maximal sensitivity consistent with available resources.

### 2.2 Status of Existing Searches

Two CERN experiments, CHORUS and NOMAD, are presently searching for muon-neutrino to tau-neutrino oscillations. CHORUS uses an emulsion target to identify tau leptons by observing the characteristic track decay kinks. NOMAD depends instead on identifying the unique kinematical properties of tau decays. Based on an analysis of less than 10 observed any tau candidates. The corresponding limit on the mixing angle is about 0.03 to 0.04 radian. The ultimate mixing-angle sensitivity of CHORUS and NOMAD is expected to approach the 0.007 radian level. Neither experiment is sensitive to a tau neutrino mass below 0.5 eV. (Note: in the discussion of parameter limits, we assume that the tau neutrino is much more massive than the muon neutrino and that tau neutrinos mix predominantly with muon neutrinos, not electron neutrinos.)

## 2.3 Future Searches

Several years ago, Fermilab approved the short-baseline experiment E803/COSMOS as part of the NuMI program of neutrino oscillation experiments. COSMOS combines an emulsion target with a precision spectrometer to allow detailed measurements of tau decay kinks and kinematics. The goals of COSMOS are to extend the region of sensitivity to mixing angles as low as 0.002 radian and to tau neutrino masses as low as 0.3 eV. Since oscillation probabilities are proportional to the square of such small mixing angles, the proposed sensitivity of COSMOS to tau production is a factor of ten better than that of CHORUS or NOMAD for tau neutrino masses above 5 eV and a factor of thirty better for lower masses.

Very recently, members of both CHORUS and NOMAD have submitted a letter of intent to CERN to extend their short-baseline search for neutrino oscillations by combining elements of the CHORUS and NOMAD designs into a single experiment called TOSCA. The main feature of TOSCA is a distributed emulsion array inside the UA1 (NOMAD) magnet. The proposed sensitivity of TOSCA is almost identical to that of COSMOS. The expected background in both experiments is at the one-event level. COSMOS and TOSCA propose to run during a period extending from about 2001 to 2005.

## 2.4 Technological Developments

Two important technical advances in tau detection were discussed at the workshop. Emulsion groups working on CHORUS have improved the capability and speed of automatic scanning stations by an order of magnitude. One can contemplate for the first time experiments in which all neutrino events are scanned in the emulsion, avoiding the necessity of inefficient event selection criteria.

In the area of electronic vertex detection, the NOMAD group reported the construction of a prototype silicon strip detector with serially ganged ladders that span 72 cm. Such silicon arrays can measure impact parameters with sufficient accuracy to identify tau decays. Costs for this technology are claimed to be about \$ 10 per cm<sup>2</sup> of array.

## 2.5 Assessment of Situation

In principle, pursuing an interesting but difficult search with two independent experiments such as COSMOS and TOSCA is preferable. A positive result would have such enormous implications that confirmation would be demanded by the physics community. On the other hand, world resources dedicated to particle research are severely strained, raising the question of whether collaboration rather than competition might not be more appropriate under the circumstances.

Both COSMOS and TOSCA still face various hurdles. COSMOS is part of a NuMI project that has not yet received Congressional approval for construction, although it is hoped that such approval will be forthcoming during the next year. The prospects for TOSCA are clouded by a lack of funding at CERN and uncertainties in the overall CERN plan for future neutrino experiments, especially vis-a-vis long baseline experiments.

The communities involved in pursuing short-baseline neutrino oscillations would be wise to act in such a way as to ensure that at least one (and preferably both) experiments will succeed.

## **2.6 Cooperation**

Keeping the above assessment in mind, the COSMOS and TOSCA groups have agreed to maintain contact, with two meetings planned during the next year, one in Europe and one in the U.S. Contact persons are N. Reay for COSMOS and A. Eridatato for TOSCA.

# Chapter 3

## Summary of the Long Baseline Neutrino Oscillation Working Group I

Reported by D. Michael, Caltech

### 3.1 Introduction

The long-baseline sessions of the Main Injector Workshop were *very* well attended with *many* presentations of results and plans. The attendance, presentations and discussion reflected the broad international interest and excitement on this subject. This is a very brief summary of some of the highlights of the presentations.

Unlike some of the sessions, the main goal of the long-baseline sessions was to provide an overview of the current status of the various efforts on the subject rather than formulate a new experimental program for the Main Injector (NuMI already being an approved program and MINOS an approved experiment).

Although it has always been an arbitrary distinction, the term “long-baseline” neutrino oscillation experiment has grown even less well-defined as more new proposals are suggested. The key factor in defining the “baseline” is  $L/E$ , the ratio of the distance between the source of neutrinos and the experiments and the typical neutrino energy involved. As  $L/E$  becomes larger, the sensitivity to oscillations due to small  $\Delta m^2$  becomes better. A rough categorization of experiments is as follows:

- Short-baseline:  $L/E \approx 0.1$  km/GeV; sensitive to neutrino masses of significance for cosmic dark matter (assuming non-degenerate neutrino masses).
- Medium-baseline:  $L/E \approx 1$  km/GeV; sensitive to the full  $\Delta m^2$  range of the LSND effect.
- Long-baseline:  $L/E \approx 10 - 100$  km/GeV; sensitive to the full  $\Delta m^2$  range suggested by the atmospheric neutrino problem.

To date, there are no seriously proposed experiments using terrestrial neutrino sources which can address the very small  $\Delta m^2$  suggested by the solar neutrino problem. The above classifications are rough. All experiments provide some sensitivity to a range of  $\Delta m^2$  and some overlap in sensitivity to the different suggestions of neutrino oscillations. Generally however,

there is a tradeoff between sensitivity in  $\Delta m^2$  and  $\sin^2 2\theta$  since neutrino fluxes fall as  $1/L^2$  from the source. The flux of neutrinos at a particular  $L/E$  determines the necessary size of an experiment and hence the experiments tend to become bigger and relatively coarser as  $L/E$  increases. On the other hand, the more distant experiments need less capability in background rejection in order to balance systematic and statistical errors.

Within the rough guidelines described above, a rich palette of experimental proposals has been made and were described at this workshop. The various proposals are at a variety of stages of development and almost certainly not all of them will actually be realized. However, the ideas are strong and in the same way as most fixed target and collider detectors have more than one component for measurement of different features of events, it is likely that future experiments (or programs) will make use of more than one of the techniques for measuring neutrino oscillations discussed here.

## 3.2 New Experimental Results

The importance of the discussions at the workshop were heightened by the presentation of several new experimental results on neutrino oscillations:

- First results on atmospheric neutrinos from Super-Kamiokande and an update on their solar neutrino results.
- An update on the results from Soudan 2 on atmospheric neutrinos. The data are now even more consistent with those from water Cerenkov detectors with the “ratio of ratios” being  $0.61 \pm 0.18_{\text{stat}} \pm 0.04_{\text{sys}}$
- Presentation of further analysis on the LSND decay-at-rest results and presentation of their new results on decay-in-flight.
- Presentation of an updated analysis from the KARMEN collaboration.
- Presentation of a first limit on  $\nu_\mu \rightarrow \nu_\tau$  oscillations from both CHORUS and NOMAD.
- Presentation of a new limit on  $\nu_\mu \rightarrow \nu_e$  oscillations from NOMAD which rules out the high  $\Delta m^2$  region of the allowed LSND oscillation parameters.

### 3.2.1 Results from Super-Kamiokande

Probably one of the most exciting results presented was the first analysis of atmospheric neutrinos from Super-Kamiokande. The new results have about 2.5 times more data than the full data set from Kamiokande (in just a fraction of a year of live-time) and with much better control over any possible fiducial volume effects. The bottom line is that the new result for the ratio of ratios of muon-like/electron-like events from the data over the same ratio from the Monte-Carlo is consistent with the previous result from Kamiokande and IMB. The new ratio of ratios is  $0.64 \pm 0.04_{\text{stat}} \pm 0.06_{\text{sys}}$ . The zenith distribution for the sub-GeV data was shown and it is consistent with being flat but perhaps with a new hint of zenith dependence (this requires more study and statistics). A very-preliminary zenith distribution

for the multi-GeV events was shown. The statistics are still too low to make any real conclusions other than “they are working on it”. By eye, the distribution is either consistent with flat or perhaps slightly more consistent with the oscillation parameters suggested by the contained results. Further work on understanding all of the systematics associated with these data (and more data) are needed before they will make any quantitative statement about this distribution.

### 3.2.2 Results from LSND and KARMEN

The LSND collaboration presented an update of their analysis on the decay at rest (DAR) signal. They stand by the interpretation that it is the result of neutrino oscillations and show the shape of the energy spectrum is consistent with that expected from oscillations. In addition, they presented new results on pion decay-in-flight (DIF) which gives similar results for neutrino oscillation parameters. The current status is that the lower  $\Delta m^2$  “banana” ( $\Delta m^2 < 2 \text{ eV}^2$ ) is where the action lies if this is neutrino oscillations and that improved experiments will be needed to fully cover this region. KARMEN showed updated results confirming that they see no sign of oscillations but that this remains marginally consistent with the LSND observations. They reported on their plans for future running which will permit complete coverage of the LSND parameters within the next 3 years.

### 3.2.3 Results from CHORUS and NOMAD

CHORUS and NOMAD both presented first results on their search for  $\nu_\mu \rightarrow \nu_\tau$  oscillations. Neither experiment has observed any events consistent with a  $\nu_\tau$  CC event. They have set limits which are similar to those from CCFR based on the lack of such events ( $\sin^2 2\theta > .005$  at 90% CL for  $\Delta m^2 > 20 \text{ eV}^2$ ). They are continuing with data acquisition and analysis. The NOMAD collaboration also presented an analysis of  $\nu_\mu \rightarrow \nu_e$  oscillations which had a null result after accounting for the intrinsic  $\nu_e$  content of the beam. Based on this, they set limits on the oscillation parameters for this channel which rule out all of the high  $\Delta m^2$  region of the LSND result.

## 3.3 Theory Review

Discussions on neutrino oscillation phenomenology versus the various experimental hints of oscillations were given by Fogli and Pakvasa. Both speakers conclude that using three-flavor oscillation models that it is (marginally) possible to fit all observed data on neutrino oscillations. Doing so requires stretching errors to their limits, etc. However, one could just as easily assume that one or more of the experiments are wrong which very much releases constraints on expectation of oscillation parameters. The bottom line is that all of the hints for oscillations could be correct (or at least almost correct) and that a very rich set of possible oscillation phenomena could exist in the parameter space where long and medium-baseline experiments will yield data. In order to completely study the full complexity of the multi-flavor mixing, good sensitivity is required to both oscillation parameters and identification of event types over a large range of oscillation probability and L/E.



## 3.4 Beams and Beam Design

Several presentations were made on new ideas and advances in design for neutrino beams for long-baseline experiments. Some of the highlights were:

- Improvements in flux due to better horn design and optimized optics using horns.
- Reduction in near-far systematic uncertainties using an idea called the “hadron hose”. The idea is to put a thin (1mm) aluminum wire down the middle of the decay pipe and run about 1 kA of current through it. This causes the hadrons to orbit around the center of the beam-pipe, spreading the angles of the decay neutrinos. This helps to make the energy distribution at the far detector look more like that at the near detector with little change in the total flux.
- Improvements in reduction of the low-energy tail in narrow-band beams by improved optics arrangement and masking using collimators. This is important for identification of  $\nu_\tau$  CC events.
- Improved understanding of systematics associated with target production spectra with new data from the SPY collaboration.
- Improved understanding of technical requirements for focussing elements, including horn design criteria, lithium lens design criteria and positioning demands on such devices.
- Improved understanding of beam monitoring using muons.

The work represented in these talks is essential to making the best use of the beams to be used in long-baseline experiments.

## 3.5 Reactor Neutrino Experiments

Reactor neutrino experiments achieve long-baseline status by making use of low-energy reactor neutrinos (typical energy about 5 MeV) with baselines of about 1 km. The experiments have sensitivity only to  $\nu_e$  disappearance. With fiducial masses of about 5-10 T of scintillator, the current experiments will be sensitive to oscillations in the range of the atmospheric neutrino problem ( $\Delta m^2 \approx .01 \text{ eV}^2$ ) and down to  $\sin^2 2\theta \approx 0.1$ ). If the atmospheric neutrino problem is dominated by  $\nu_\mu \rightarrow \nu_e$  oscillations, these experiments will be the first to observe the clear oscillation signature.

### 3.5.1 Chooz

The Chooz experiment has been built in an existing underground hall near two new reactors in Chooz, France. It consists of a single volume of gadolinium-loaded scintillator in an acrylic vessel surrounded by an outer volume which acts as a passive absorber for neutrons. An array of phototubes around the edges of the outer volume observe light from neutrino interactions in the core. A cosmic-ray veto volume surrounds this inner detector and is optically isolated

from it. Anti-electron neutrinos from the reactor are observed by a coincidence between an initial prompt multi-MeV signal from the  $e^+$  followed several to tens of  $\mu\text{s}$  later by an 8 MeV photon resulting from neutron capture on the gadolinium. The detector is completed and currently taking data. Reactor-off data were accumulated since last fall and this spring the reactors have begun to turn on. At the time of the workshop, one of the reactors had reached 80% power and a clear signal of neutrinos has been observed. No limits (or observations!) have yet been made on neutrino oscillations. We can expect first results within about a year with complete results within about two years.

### 3.5.2 Palo Verde

The Palo Verde experiment is currently under construction at the Palo Verde nuclear power station in Arizona. The experiment is being built in an underground laboratory specially built for this purpose and located about 700m from the three reactors. The reactors at Palo Verde have been running for several years already. "Reactor off" data will be accumulated when one of the reactors is turned off for refueling. This increases the time required to get enough data for background subtraction compared to the situation at Chooz. The experiment consists of an array of 8 m long gadolinium-loaded scintillator counters surrounded by a passive water shield (for neutrons) and an active scintillator shield (for cosmic-ray muons). This experiment is shallower than Chooz and requires a higher level of coincidence in order to reject cosmic-ray-associated background. The signature for neutrino interactions will be a four-fold coincidence in at least three different interior scintillator counters; a few MeV hit from the initial  $e^+$  in prompt coincidence with hits in the 50-500 keV range in two neighboring counters from Compton scattering of the two annihilation gammas and finally an 8 MeV gamma resulting from neutron capture on the gadolinium. This experiment is scheduled to begin taking data in the autumn of 1997 and should be complete about two years from that time.

## 3.6 High-Energy Long-Baseline Experiments

Over the last few years, a number of different experiments and detection techniques have been developed around existing or planned facilities and beamlines at three different locations; KEK to Super-Kamiokande, CERN to Gran Sasso and Fermilab to Soudan.

### 3.6.1 KEK to Super-Kamiokande

Although not custom-designed for a long-baseline neutrino oscillation experiment, the very large size of the Super-Kamiokande detector and its general ability to study neutrino events over a wide energy range, combined with its distance from KEK (250 km) makes for an interesting possibility for a long-baseline experiment. The beamline aiming towards Kamiokande is currently under construction at KEK and will initially make use of the 12 GeV proton-synchrotron to create a neutrino beam with mean energy about 1.5 GeV. It is expected that this neutrino beam will begin running in 1999. A high-intensity 50 GeV proton synchrotron is being planned (for several applications) which could provide a typical neutrino energy of

about 5 GeV (just) allowing CC  $\nu_\tau$  interactions should  $\nu_\mu \rightarrow \nu_\tau$  oscillations exist with the appropriate parameters. The date of completion of the 50 GeV machine is not certain but a “common estimate” is 2003.

The far detector for the K2K (KEK to Super-Kamiokande) will of course be the Super-Kamiokande detector. A near detector will be built at KEK which will consist of a water-Cerenkov detector, similar to Super-Kamiokande (but smaller) and a fine-grained detector using fiber tracking in water for measuring properties of the neutrino beam. In the low-energy beam (the initial running) the signature for neutrino oscillations will be a deficit of  $\nu_\mu$  CC events in the far detector compared to the near detector, a variation in the energy distribution of CC events in the far and near detectors, appearance of  $\nu_e$  CC interactions (if the atmospheric anomaly is dominated by  $\nu_\mu \rightarrow \nu_e$  oscillations) and a “NC/CC” ratio by comparing the number of events with muons to the number of events with only single  $\pi^0$ 's in the final state. With two years of running it is expected that the far detector should observe about 400 CC  $\nu_\mu$  events in the absence of oscillations permitting clear signatures to be observed should the atmospheric anomaly be the result of neutrino oscillations.

### 3.6.2 CERN to Gran Sasso

The Gran Sasso underground laboratory is located 730 km from CERN, making it an excellent site for locating a long-baseline experiment, should a neutrino beam be built at CERN aimed in the direction of the Gran Sasso. The planned beamline will make use of protons from the SPS with a “front-porch” extraction at about 350 GeV with a second special 350 GeV cycle just for the neutrino beam in order to give more total protons on target. The plan is for a horn-focussed, wide-band beam with a 1 km decay pipe and a near detector site near the Geneva airport. The mean neutrino energy at the Gran Sasso in this case would be about 15 GeV. The turn-on date for the beam to the Gran Sasso is estimated to be 5 years from the time that a decision is made to build the beam. Construction of the beam depends on funding from INFN and a decision is expected before the end of this year.

Three different detectors have been officially proposed at the Gran Sasso and other designs are under consideration/development:

- ICARUS is already approved for a 600 T module to be placed in Hall C at the Gran Sasso. They propose 1800 T (three modules) for the long-baseline experiment which could be located in Hall B. ICARUS is a very-high-resolution liquid argon TPC which essentially is a fully electronic bubble chamber. The first module is now under construction and is planned to be finished by 1999. The construction uses a honey-comb insulating dewer lined with stainless-steel to contain the ultra-pure argon necessary for long drift lengths. Electrons produced by particles traversing the argon are drifted to wire planes for readout with time-stamping in order to permit a full 3D reconstruction of the event. At low energies, particle ID is provided via  $dE/dx$ . The excellent imaging of ICARUS permits a strong ability to identify certain classes of neutrino interactions:
  - $\nu_e$  CC interactions: Probably the best capability that ICARUS provides is the ability to distinguish between EM showers produced by  $\pi^0$ 's and those from electrons. ICARUS can image these showers in great detail and distinguish the conversion points of the two photons from  $\pi^0$  decay. The sensitivity for  $\nu_\mu \rightarrow \nu_e$

oscillations in ICARUS will certainly be limited by the intrinsic  $\nu_e$ 's in the beam itself and this will permit oscillation sensitivity down to the level of  $10^{-3}$  in oscillation probability or lower.

- CC/NC ratio
- $\nu_\tau$  CC signature via missing transverse momentum in  $\tau \rightarrow e\nu\nu$  quasi-elastic events. The sensitivity to oscillations will be at about the 5% oscillation probability.

Other possibilities of specific event topologies are under study.

- NOE: The proposed NOE detector is a tracking/spaghetti calorimeter. The design makes use of iron-oxide absorbers filled with scintillating fibers for calorimetry and streamer-tube or RPC layers for tracking and event topology measurement. The downstream end of the detector will have magnetized iron for measurement of muon momentum in those events where the muon does not range out upstream and have not escaped from the sides of the detector. The total mass of the detector will be 4 kT. The oscillation signatures will be based on NC/CC ratio, the energy distribution of CC events, identification of events with electrons and statistical identification of events with  $\tau$ 's by missing transverse momentum in  $\tau \rightarrow e\nu\nu$  events and  $\tau \rightarrow \pi\nu$ . The sensitivity to oscillation will be at about the 1-2% oscillation probability level.
- RICH: A 25 kT water ring-imaging Cerenkov detector has been proposed by Ypsilantis. The detector will use mirrors at the downstream end to focus the Cerenkov light onto an array of pixel photodetectors (HPD's) to image rings produced by leptons and hadrons in the final state of neutrino interactions in the water. Because of the challenge in pattern recognition, events with relatively simple final-states and where the hadrons don't shower very much will be of the greatest interest. Total shower energy is measured simply by the total charge readout from the photodetectors. Particle identification is provided by measurement of both velocity (ring size) and momentum (from multiple scattering causing rings to be fuzzy). Electrons can be further identified by their wide "shower rings". By focussing on relatively clean final states, appearance oscillation signatures for both  $\nu_e$  CC and  $\nu_\tau$  CC events are possible by electron ID and missing transverse momentum. The very large mass of the detector should permit sensitivity extending down to the  $10^{-3}$  level for  $\nu_\mu \rightarrow \nu_e$  oscillations and below the  $10^{-2}$  level for  $\nu_\mu \rightarrow \nu_\tau$  oscillations. The pattern recognition issues in this detector are considerable and work is being done now to understand how to do this task.

In addition to these officially proposed (letters of intent), thoughts are going towards construction of more-conventional sampling calorimeter-based experiments and towards using emulsion for explicit  $\tau$  identification.

### 3.6.3 Fermilab to Soudan

Construction of the NuMI neutrino beam line using protons from the Main Injector has been approved by Fermilab and DOE and Congress appears to be poised to approve \$6M in FY

'98 for engineering and design of the beamline. The high-cycle rate and current of the Main Injector will provide a very intense beam with mean neutrino energy about 10 GeV. The total number of CC events (without oscillations) in a far detector at Soudan will be about 3500/year/kT using the horn-focussed wide-band beam. A narrow-band beam design is also being developed. The decay pipe will be 800 m in length and an underground hall will house both the MINOS near detector and the COSMOS, short-baseline oscillation experiment. The beam is scheduled to be commissioned in mid-2001. At the Main Injector workshop, John Peoples re-endorsed the high priority of the NuMI project in the Fermilab program.

MINOS has been approved by Fermilab and recommended for construction by the HEPAP subpanel. The standard MINOS design is based on a sampling/tracking calorimeter with magnetized iron plates. The nominal mass of the detector is 10 kT. The thickness of the iron plates will be 2-4 cm and is under active study based on cost, schedule and physics capabilities. The active detector layers will be either gas proportional tubes or scintillator. The gas detectors would have x and y views in each plane with 2 cm effective pitch wire and strip readout. The scintillator detectors would have 2-4 cm transverse pitch strips with readout via wavelength-shifting fiber. If the iron thickness is 2 cm then x and y views would be located in every other plane. For 4 cm iron, two scintillator planes could be inserted for both x and y view in each sampling layer. R&D work on all detector technology has been quite successful. We now expect that the gas detectors can deliver better energy resolution than standard streamer tube designs, 2 cm iron looks like a feasible choice and the better calorimeter offered by scintillator looks like a real possibility.

As demonstrated at the time of the proposal, the MINOS sensitivity to neutrino oscillations covers the full region of the atmospheric neutrinos, extending down to mixing probability of about 1% or lower, depending on the signature. The standard oscillation signatures include:

- NC/CC ratio (overall oscillation probability)
- Number of  $\nu_\mu$  CC events in far versus near detectors (slightly different measurement of oscillation probability)
- Total energy distribution of CC events (measures  $\Delta m^2$ )
- Statistical identification of events containing electrons (identifies flavor component of oscillations plus extends oscillation sensitivity for  $\nu_\mu \rightarrow \nu_e$ )
- Statistical identification of  $\nu_\tau$  CC events by missing energy and other kinematics in the narrow-band beam or by  $\tau \rightarrow \pi\nu$  in the wide-band beam (identifies flavor component of oscillations)

New work on electron identification using a scintillator-based detector with 2 cm Fe absorbers has suggested that sensitivity to  $\nu_\mu \rightarrow \nu_e$  oscillations could extend significantly lower, perhaps approaching oscillation probability of  $10^{-3}$  for  $\Delta m^2 > .01 \text{ eV}^2$  where the sensitivity would be limited not by pattern recognition ability but by intrinsic  $\nu_e$ 's in the beam. Identification of  $\nu_\tau$  CC events is done either by looking for events with a muon in the final state with anomalously low total energy in the narrow-band beam or using a signature which has recently been studied for the wide-band beam. The new signature relies on the fact that the

probability that a single charged pion is produced with energy around 10 GeV is much higher in  $\nu_\tau$  CC events with the  $\tau$  decaying to a charged pion than in NC events. Events where the single pion passes through several planes of iron prior to interacting can be identified and the energy of the pion is measured by calorimetry. Using this signature, a sensitivity to oscillation at the level of about 5-10% oscillation probability will be possible.

Clear signatures of  $\nu_\tau$  CC events is a challenging proposition. The Nagoya group has suggested that using emulsion sandwiched with thin iron sheets could provide clear  $\tau$  signatures by measurement of impact parameters or kinked tracks. It is estimated that a 1 kT detector of this construction could provide  $\tau$  appearance sensitivity below  $10^{-2}$  oscillation probability. This technique would be quite complimentary to the measurements in MINOS and would provide additional assurance of being able to cover any possible oscillation scenario relevant to the atmospheric neutrinos (including three-flavor mixing where  $\nu_\mu \rightarrow \nu_\tau$  is only a few percent). Although the MINOS collaboration remains convinced that the standard detector which is proposed represents a strong capability for doing oscillation physics using a design which is *sure to work*, the collaboration remains open to study of this interesting option. It is almost certainly easy to plan on building a small amount of this type of detector to start and then continue to build more as we are convinced of its abilities and of the need for those abilities. The collaboration is actively discussing the possibility for doing this with groups interested in this technique.

### 3.7 High-Energy Medium-Baseline Experiments

The mountains surrounding CERN provide an interesting capability for medium-baseline experiments built in the Jura Mountains and using the existing West-Area neutrino beam. This beam passes through the mountains and exits at a point about 18 km from CERN. The fact that the beamline already exists is a big bonus for being able to mount new experiments on a short time scale. Two experiments have been proposed to study neutrino oscillations at this site:

- ICARUS in the Jura: This would use the same design as the detector planned for the Gran Sasso, just placing it in the Jura. The background rejection capabilities and neutrino oscillation signatures would all be similar. By being placed at this location, this detector would provide complete sensitivity to the LSND oscillations as well as partial sensitivity to the region of the atmospheric anomaly. Construction of this detector could be considered part of a phased oscillation program using ICARUS first at this site and then later at the Gran Sasso. It has been suggested that running could begin at the Jura site in 1999 and at the Gran Sasso in 2003. It is not yet clear whether this proposal would be instead of a first module of ICARUS in the Gran Sasso in 1999 or in addition to that module... its only money.
- OPERA: The OPERA detector would make use of emulsion interleaved with thin iron sheets to give more total mass. The mass of the detector proposed for the Jura is 10 T. The experiment could provide sensitivity to  $\nu_\mu \rightarrow \nu_\tau$  oscillations to lower  $\Delta m^2$  than CHORUS and NOMAD and can partially cover the region of the atmospheric neutrino anomaly. Identification of  $\nu_\tau$  CC events is done by looking for events where the  $\tau$  has

decayed in an air-gap between successive emulsion layers. This will provide a track with a kink with the characteristic path-length of the  $\tau$ .

### 3.8 Conclusions and Implications for Fermilab NuMI Program

This workshop provided an excellent overview of what is happening in the field of accelerator-based neutrino oscillation searches. The experimental hints of oscillations are strong and this has attracted a great deal of attention on the subject around the world. Reactor neutrino experiments are coming on line now or in the near future. The Japanese are moving forward with their plans to use Super-Kamiokande for a long-baseline experiment. There are a dazzling array of proposals for experiments at CERN using the existing beamline or a new beamline to the Gran Sasso. It is unlikely that all of these experiments will materialize but there is a good chance that at least some of them will be done. The idea of using emulsions in long-baseline experiments has brought a new capability which will likely make sense to incorporate at some level in any beam where the neutrinos are of high enough energy to be above  $\nu_\tau$  CC threshold.

The implications of all of this excitement around the world for the Fermilab program on neutrino oscillation are clear. This is important physics and it is generating strong competition as is frequently the case when such physics is "near". The investment in the NuMI program at Fermilab is large but must be made on an aggressive schedule in order to ensure maximum impact on this subject. We expect that in this case that neutrino oscillations will play an exciting role in the next decade of physics at Fermilab and around the world.

# Chapter 4

## Summary of the Long Baseline Neutrino Oscillation Working Group II

Reported by A. Rubbia, CERN

### 4.1 Physics Motivations

The central issue of neutrino physics is the determination of masses through neutrino oscillations. The necessity of the oscillation phenomenon initially stemmed from the results of the solar neutrino experiments[25] which all indicated a deficit of about a factor 2 with respect to the Standard Solar Models. Though the solar models are not without problems, it would seem that the most reasonable explanation is to assume that the depletion of  $\nu_e$  neutrinos is due to lepton flavor mixing  $\nu_e \rightarrow \nu_x$  occurring along the path between the Sun and the Earth. The originally preferred solution was the one of a small mass difference  $\Delta m^2 \approx 10^{-5} eV^2$  and a relatively small mixing angle between the neutrinos, coupled with a 'mass enhancement' phenomenon (MSW effect[26]). If the Sun has such a specific mechanism, then one would not expect that other experiments with more conventional sources of neutrinos would give no major depletion in flux other than the one associated to the existence of much heavier mass difference presumably connected to the mass of the tau neutrino. However, results from atmospheric neutrino experiments[27], though with significant uncertainties, also claimed a depletion factor of the same order as solar neutrino experiments but seem to indicate a mass difference of the order  $\Delta m^2 \approx 10^{-2} eV^2$ . In 1995, the LSND Collaboration[28] has reported observation of excess of events which can be interpreted as evidence for  $\bar{\nu}_\mu \rightarrow \bar{\nu}_e$  oscillations with mass difference  $\Delta m^2 \approx 1 eV^2$ . There have been many attempts to reconcile all existing neutrino experimental data in a coherent picture. It seems difficult to satisfy all the constraints with only two oscillations  $\nu_\mu \rightarrow \nu_e$  or  $\nu_\mu \rightarrow \nu_\tau$  and two mass-squared differences, say  $\Delta m^2$  and  $\Delta M^2$ . So one of the task of future neutrino experiments will be to disentangle the present experimental hints, in other words:

- Solar neutrinos deficit (MSW  $\Delta m^2 \approx 10^{-5} eV^2$ ) ?
- Atmospheric neutrinos anomaly ( $\Delta m^2 \approx 10^{-2} eV^2$ ) ?
- LSND excess ( $\Delta m^2 \approx 1 eV^2$ ) ?



An attractive and interesting possibility to increase the sensitivity of accelerator neutrino oscillations experiments down to the regions indicated by the atmospheric and LSND data, is to extend the baseline between the accelerator and the detector. Thus, the medium/long baseline experiments represent a complementary approach to the present and future short baseline experiments which are studying small mixing angles at relatively larger mass regions. The terms medium and long baseline experiments are understood as experiments that attempt to search for neutrino oscillations in the mass regions of, respectively,  $\Delta m^2 \approx 1eV^2$  and  $\Delta m^2 \approx 10^{-3} - 10^{-2}eV^2$ .

## 4.2 Updates from Running Experiments

Experiments presently in progress will be able to establish on a firmer ground the likelihood of observing neutrino oscillations in future neutrino experiments.

New experimental results presented at this workshop seem to consolidate the need for future neutrino experiments that are able to probe the  $\Delta m^2 \approx 10^{-2}eV^2$  and  $\Delta m^2 \approx 1eV^2$  mass regions (see table 4.1):

- the Soudan-II collaboration presented an updated result[29] on atmospheric neutrino based on a larger statistics of 2.63 kt-yr which yields the result  $R = 0.67 \pm 0.15_{-0.06}^{+0.04}$ , consistent with Kamiokande[27];
- the SuperKamiokande atmospheric results[30] on the double ratio are in agreement with the Kamiokande result; the results are  $R = 0.64 \pm 0.04 \pm 0.06$  in the subGeV sample and  $R = 0.52 \pm 0.09 \pm 0.08$  in the multiGeV sample. The analysis of the azimuthal angle distribution is however not finalized to allow further conclusions;
- the LSND claim was strengthened by their confirmation in the decay-in-flight (DIF)  $\nu_\mu \rightarrow \nu_e$  mode[31];
- no evidence for oscillations were so far found by NOMAD[32] ( $\nu_\mu \rightarrow \nu_e$  and  $\nu_\mu \rightarrow \nu_\tau$ ) and by CHORUS[33] ( $\nu_\mu \rightarrow \nu_\tau$ ). The data analyses are in progress and will soon explore mixing angle regions beyond the E531 result, so surprises are not impossible.

The future reactor experiments CHOOZ[34] and Palo Verde[35] which observe  $\nu_e$  survival probability and will be sensitive down to  $\Delta m^2 \approx 10^{-3}eV^2$  should soon see a large effect  $P(\nu_e \rightarrow \nu_e) \approx 0.5$  if the atmospheric anomaly is due to  $\nu_\mu \leftrightarrow \nu_e$  oscillations, thus confirming the interest in long baseline experiments.

### 4.2.1 KARMEN

Report by Klaus Eitel, for the KARMEN Collaboration, *Forschungszentrum Karlsruhe, Institut für Kernphysik I, D-76021 Karlsruhe, Postfach 3640, Germany, E-mail: klaus@ik1.fzk.de*

	$R = N(\mu/e)_{data}/R(\mu/e)_{MC}$	exposure (kt-yr)
Kamiokande (SubGeV)	$0.62 \pm 0.06 \pm 0.06$	8.3
Kamiokande (MultiGeV)	$0.57 \pm 0.08 \pm 0.07$	8.2
IMB	$0.54 \pm 0.05 \pm 0.07$	7.7
Soudan II (prelim.)	$0.67 \pm 0.15^{+0.04}_{-0.06}$	2.63
Frejus	$1.00 \pm 0.15 \pm 0.08$	2.0
NUSEX	$0.99 + 0.35 - 0.25$	0.7
SuperK (SubGeV) (prelim)	$0.64 \pm 0.04 \pm 0.06$	12.8
SuperK (MultiGeV) (prelim)	$0.52 \pm 0.09 \pm 0.08$	12.8

Table 4.1: *Summary of the atmospheric neutrino measurements.*

### Introduction and limits on $\bar{\nu}_\mu \rightarrow \bar{\nu}_e$ oscillations

The neutrino experiment KARMEN is situated at the beam stop neutrino source ISIS. It provides  $\nu_\mu$  's,  $\nu_e$  's and  $\bar{\nu}_\mu$  's in equal intensities from the  $\pi^+ \rightarrow \mu^+ \nu_\mu$  decay at rest. The oscillation channels  $\nu_\mu \rightarrow \nu_e$  and  $\bar{\nu}_\mu \rightarrow \bar{\nu}_e$  are investigated with a 56 t liquid scintillation calorimeter at a mean distance of 17.6 m from the  $\nu$ -source.

The most sensitive mode of the KARMEN experiment for the search of  $\nu$ -oscillations is the  $\bar{\nu}_\mu \rightarrow \bar{\nu}_e$  channel.  $\bar{\nu}_e$  's are not produced within the ISIS target apart from a very small contamination of  $\bar{\nu}_e \nu_e < 6 \cdot 10^{-4}$ . The detection of  $\bar{\nu}_e$  's via  $p(\bar{\nu}_e, e^+)n$  would therefore indicate oscillations  $\bar{\nu}_\mu \rightarrow \bar{\nu}_e$  in the appearance channel. The signature for the detection of  $\bar{\nu}_e$  's is a spatially correlated delayed coincidence of positrons from  $p(\bar{\nu}_e, e^+)n$  with energies up to  $E_{e^+} = E_{\bar{\nu}_e} - Q = 52.8 - 1.8 = 51$  MeV and  $\gamma$  emission of either of the two neutron capture processes  $p(n, \gamma)d$  or  $Gd(n, \gamma)Gd$  with  $\gamma$  energies of 2.2 MeV or up to 8 MeV, respectively. The positrons are expected in a time window of 0.5 to 10.5  $\mu$ s after beam-on-target. The neutrons from  $p(\bar{\nu}_e, e^+)n$  are thermalized and captured typically with  $\tau = 120$   $\mu$ s. The neutron detection efficiency for the analyzed data is 28.2%. The data set remaining after applying all cuts in energy, time and spatial correlation consists of 164 sequential events. A prebeam analysis of cosmic ray induced sequences results in an accumulated background level of  $12.2 \pm 0.2$  events per  $\mu$ s in the prompt 10  $\mu$ s-window. The actual rate is  $16.4 \pm 1.3/\mu$ s which corresponds to a beam excess of 2.4  $\sigma$  compared with the prebeam level including  $\nu_e$  -induced CC (9 events) and  $\bar{\nu}_e$  -contamination (1.7 events). Although the secondary part of the sequences shows the typical signature of thermal neutron capture, the prompt time and energy distribution does not follow the expectation from  $\bar{\nu}_\mu \rightarrow \bar{\nu}_e$  oscillation with  $\Delta m^2 = 100$  eV<sup>2</sup>.

To extract a possible small contribution of  $\bar{\nu}_\mu \rightarrow \bar{\nu}_e$ , the data set is scanned with a two-dimensional maximum likelihood analysis on time and energy distribution of the positrons requiring a 2.2  $\mu$ s exponential time constant for the  $e^+$  and a time independent cosmic induced background. The measurement of the  $e^+$  energy with spectroscopic quality is highly sensitive to changes in the energy spectrum due to the dependence of the oscillation probability on the mass term  $\Delta m^2$ . The energy distributions of the positrons used in the likelihood analysis therefore have been tested with spectra for  $\Delta m^2$  in the range from 0.01 to 100 eV<sup>2</sup>.

For most of the investigated parameter range of  $\Delta m^2$  the likelihood analysis results in best fit values compatible with a zero signal within a  $1\sigma$  error band. Only for a parameter region at  $\Delta m^2 = 6.2 \text{ eV}^2$  there is a positive signal  $2.3\sigma$  above zero which is not considered as statistically significant. In addition, this  $\Delta m^2$ -value corresponds to the first theoretical oscillation minimum in the detector with the lowest possible mean energy of the positrons and represents therefore an extremum in the likelihood analysis which should be interpreted with special precaution. On this basis of no evidence for oscillations, 90% *CL* upper limits for oscillation events as well as for the oscillation parameters  $\Delta m^2$  and  $\sin^2(2\Theta)$  are deduced.

Fig. 4.1 shows the KARMEN exclusion curves in the parameter space of  $\Delta m^2$  and  $\sin^2(2\Theta)$  in a two neutrino flavor oscillation calculation for the appearance channels  $\nu_\mu \rightarrow \nu_e$  and  $\bar{\nu}_\mu \rightarrow \bar{\nu}_e$  in comparison with other results of  $\nu$ -oscillation searches at accelerators and reactors. As the sensitivity for  $\bar{\nu}_\mu \rightarrow \bar{\nu}_e$  of the KARMEN experiment is comparable to that of LSND (both experiments expect about 2000 oscillation events for  $\Delta m^2 > 100 \text{ eV}^2$  and  $\sin^2(2\Theta) = 1$  on their data sample until 1995), the KARMEN 90% *CL* exclusion curve cannot exclude the entire parameter space favoured by the positive result of LSND.

**Conclusion:** No evidence for oscillations could be found with KARMEN, resulting in 90% *CL* exclusion limits of  $\sin^2(2\Theta) < 8.5 \cdot 10^{-3}$  ( $\bar{\nu}_\mu \rightarrow \bar{\nu}_e$ ) and  $\sin^2(2\Theta) < 4.0 \cdot 10^{-2}$  ( $\nu_\mu \rightarrow \nu_e$ ) for  $\Delta m^2 > 100 \text{ eV}^2$ .

## The KARMEN Upgrade

Within the near future, only the running KARMEN experiment, with an improved sensitivity, will be able to crosscheck the evidence postulated by LSND. The KARMEN sensitivity in the  $\bar{\nu}_\mu \rightarrow \bar{\nu}_e$  channel can only be substantially increased by the reduction of the small but dominant cosmogenic background. This background is induced by cosmic muons stopping or undergoing deep inelastic scattering in the iron shielding which surrounds the KARMEN detector and veto system. Energetic neutrons emitted in these processes can penetrate deep into the detector without triggering the veto system, thus producing an event sequence of prompt recoil protons followed by the capture of the then thermalized neutrons.

To tag the original muons in the vicinity of the detector, a further active veto layer within the blockhouse has been built in 1996, which consists of 136 plastic scintillator bars (BICRON BC 412) of lengths up to 4 m, 65 cm width and 5 cm thickness, with a total surface of  $300 \text{ m}^2$  covering all sides of the detector (fig. 4.2). There is at least 1 m between the new counter and the existing shield so that energetic neutrons produced by cosmic muons outside the new veto system have to travel a path of more than 4 attenuation lengths in iron ( $\Lambda = 21 \text{ cm}$ ). This reduces cosmogenic neutrons to a negligible fraction of less than 1.5% of the original flux. The new veto system is designed to reduce cosmogenic sequential background by a factor of at least 40. This reduction factor is based on detailed background measurements and extensive GEANT MC simulations of cosmic muons. First preliminary evaluations of cosmic background in a prebeam window indicate the expected reduction factor in the energy region of interest (15-50 MeV) when the information of veto hits is included in the analysis. The number of cosmic induced sequences without veto information (467 events including 123.8 random sequences) can be reduced to 15 events with 2.4 random coincidences including veto information. These data taken with the new detector configuration in a measurement period

of approximately 4 weeks are still preliminary.

**Conclusion:** In 1996, the KARMEN neutrino experiment has been upgraded by an additional veto system. Vetoing of cosmic muons passing the 7000 t massive iron shielding of the detector suppresses energetic neutrons from deep inelastic scattering of muons as well as from  $\mu$ -capture in iron. Up to 1996, these neutrons penetrating into the detector represented the main background for the  $\bar{\nu}_\mu \rightarrow \bar{\nu}_e$  oscillation search. With an expected reduction of the background rate by a factor of 40 the experimental sensitivity for  $\bar{\nu}_\mu \rightarrow \bar{\nu}_e$  will be significantly enhanced towards  $\sin^2(2\Theta) \approx 1 \cdot 10^{-3}$  for large  $\Delta m^2$ .

After two years of measuring time with the new detector configuration, the KARMEN sensitivity for  $\bar{\nu}_\mu \rightarrow \bar{\nu}_e$  is expected to exclude the whole parameter region of evidence suggested by LSND if no oscillation signal will be found (fig. 4.1). In that case, mixing angles with  $\sin^2(2\Theta) > 1 \cdot 10^{-3}$  will be excluded for large  $\Delta m^2$ . The veto upgrade will also increase the signal to background ratio of single prong  $\nu$ -induced events on  $^{12}\text{C}$  and therefore improve the investigation of the published anomaly in this time distribution.

## 4.3 Present and Future $\nu$ Beams at the CERN SPS

Report by Vittorio Palladino<sup>1</sup>, *INFN Naples, Italy and CERN, Switzerland.*

### 4.3.1 Introduction

Significant advances in the operation of the SPS as a  $\nu$  source have been achieved and further progress can be expected in the future. The CERN SPS West Area Neutrino Facility (WANF), largely rebuilt and modernized in 1992-93, has operated at unprecedented proton intensities, thanks to the introduction of multiple extraction per acceleration cycle, the better insight gained in the behavior of the primary target and the record performances of the SPS in 1995 and 1996.

### 4.3.2 Future prospects

The current progress and future prospects for the SPS as a  $\nu$  source has been made possible by the work of many people from PS, SL, ECP and PPE ( CHORUS, NOMAD, NA52/56, ICARUS and NESTOR) Divisions at CERN. The two options presently available for future  $\nu$  physics at CERN are:

---

<sup>1</sup>I would like to thank the large number of people contributing to the present and future of neutrino beams at CERN. Among them, R. Bailey, A. Faugier, G. DeRijk, M. Gyr, M. Jonker, S. Péraire, E. Weisse in the SL Division; J.M.Maugain, A. Ball, V.Falaleev, D. Myers, G. Acquistapace and the ECP Division teams working on the WANF; E. Tsemelis and all the NOMAD  $\nu$  beam team; K. Winter, j. Panman, G. Catanesi and many colleagues in CHORUS; the many people in the ICARUS, NESTOR, ALADIN, SPY and I213 teams that are contributing to the future of  $\nu$  physics at the CERN SPS.

- in the West Area Neutrino Facility (WANF), the location of the present detectors and the direction of flight of  $\nu$ 's towards a possible future medium baseline detector in the Jura;
- in the proposed new neutrino facility (NNF), the direction of flight of  $\nu$ 's towards long baseline detectors at the Gran Sasso Laboratory and the location of a possible near pit for short baseline detectors.

### 4.3.3 The WANF

The West Area Neutrino Facility [36] has been now operating at the SPS for almost 20 years. Limited modifications only were introduced for operation of the CHARM II detector (1985-91) after completion of first generation experiments (BEBC, CDHS, CHARM). A major reconstruction [37] of the WANF line took place in 1992 and 1993 for a new round of  $\nu_\mu$  to  $\nu_\tau$  oscillation experiments (CHORUS and NOMAD).

The SPS presently accelerates protons (p) to 450 GeV with a cycle of 14.4 sec. and extracts them onto the WANF primary target (T9). A resonant extraction of msec duration (fast/slow or F/S) has been chosen since operation with fast (23  $\mu$ sec) one turn extraction (FE) broke the target [38] in 1979. In 1987 a double extraction scheme was introduced to increase the total number of protons delivered to CHARM II. Presently two 6 ms long spills are extracted, separated in time by 2.4 s, one at the start and one at the end of the accelerator flat top.

#### Operation at higher intensities

The physics potential of experiments in  $\nu$  beams depends very strongly on the total amount of protons that can be sustained by the  $\nu$  production target. The mechanical and thermal stress induced in T9 by an intense burst of very high energy p's limits the intensity per spill and is much more severe for short ( $\mu$ sec) spills than for longer (msec) spills. The design [39] of the new target station installed in 1993 incorporated improvements in the three main areas of precision alignment of its rods, cooling with diffused He flow and shielding of the surrounding area. A high intensity test late in 1994 proved that at least  $3.0 \cdot 10^{13}$  protons per cycle can be sustained in two extractions by the new target. Higher and higher average p intensities have been delivered onto T9 during 1995, 1996 and 1997, reaching frequently values close to or above  $2.6$  or  $2.7 \cdot 10^{13}$  protons in 2 spills, hitting occasionally the current safety limit  $3.0 \cdot 10^{13}$  and making the WANF a much more intense  $\nu$  'factory'.

This was made possible by the unprecedented performance of the CERN p acceleration complex from 1995 on. This required a careful tuning of the quality of the high intensity beam provided from the CERN PS to the SPS and a remarkable improvement of the capability of the SPS to capture and accelerate higher intensities. Record cycles with more than  $4.5 \cdot 10^{13}$  accelerated p's have been recorded in 1996. Record intensities became thus possible on T9, while all other SPS experimental targets were still adequately served.

Research on high intensity target technology continues. Graphite [40] may prove a useful alternative to Beryllium as a target material.

## Present understanding of neutrino yields

In experiments using  $\nu$  beams, the knowledge of the beam characteristics is an important and difficult problem. One has to set up an accurate simulation of the beam, correct and refine it until it reproduces well the quantities measurable in the  $\nu$  detectors; one can then trust its predictions for the non-measurable quantities with reasonable confidence. Such accurate simulations are also needed as a tool for the design of modified or completely new beamline configurations.

A MonteCarlo program (GBEAM), based on the GEANT library, was developed [41] by the CHARM II Collaboration and is now used by CHORUS to predict the WANF  $\nu$  fluxes.  $\pi$  and K produced in the hadronic shower induced by a 450 GeV/c p, in the primary interactions in the thin Be target as well as in the secondary interactions, are tracked through the passive material and the active focusing elements of the beam line until they escape, are absorbed or decay.  $\nu$  fluxes at the detectors can thus be predicted.

A similar program (NUBEAM) was later independently developed by NOMAD [42] and a modified version [43] of the simulation was used in the design of the new long baseline facility.

## The SPY measurement

The choice of the generator describing hadronic interactions in the target and other materials has proven very critical. Analysis of data from  $\nu$  interactions in CHARM II in the recent past and now in CHORUS and NOMAD shows that the average  $\nu_\mu$  energy is lower and the  $\bar{\nu}_\mu$  contamination higher than those predicted by calculations based on existing data [44] for production in p-Be collisions of secondaries with momenta above 60 GeV/c and on extrapolations of these data to the region below 60 GeV/c where no data is available.

These discrepancies, as well as new ideas [45, 43] of more systematic exploitation of lower energy  $\nu$  parents have prompted a new measurement of the yield of low energy  $\pi$  and K produced in the primary target. The SPY/NA56 experiment [46] used the existing NA52 524 m long double bend double focusing one particle spectrometer, equipped with excellent particle identification detectors and housed in the H6 beam originating from the T4 target of the SPS North Area. It collected, in the spring of 1996, data on forward production of positive and negative  $\pi$  and K in the 7-40 GeV/c secondary momentum range and at two momenta (67.5 and 135 GeV/c) where comparison with the existing higher momentum data is possible. At 15 and 40 GeV/c data were collected at several production angles.

An old absolute normalization procedure [47] of the monitors of p intensity on T4 was resurrected for the goals of SPY and was extended also to the other North Area target stations T2 and T6.

Preliminary SPY data have already been presented [48, 49]. The SPY sample should soon contribute to a better understanding of  $\nu$  fluxes and energy distributions in present and future  $\nu$  beam configurations. The more precise determination of the K/ $\pi$  ratio will also improve our predictions of the  $\nu_e$  content of the beam.

## The $\nu_\tau$ content of the beam

Two new estimates of the prompt  $\nu_\tau$  content of the WANF, irreducible background for CHORUS, NOMAD and any similar experiment, have been published [50, 51].

The two estimates suggest values of the ratio  $R$  of the number of  $\nu_\tau$  over the number of  $\nu_\mu$  induced charged current interactions much larger than the one (of order  $10^{-7}$ ) quoted in the CHORUS and NOMAD proposals several years ago. The estimate of  $R$  in the CHORUS fiducial volume based on a semi-empirical parametrization [50] of  $D_s$  production is  $3.3 \cdot 10^{-6}$ , while the one obtained from non-perturbative QCD inspired calculation [51] is some 20% larger. They agree reasonably well, within the uncertainties of both approaches.

This level of irreducible background, still well below one event in the lifetime of CHORUS and NOMAD, suggests a reduction of the primary  $p$  energy for future searches sensitive to smaller  $\nu$  mixing.

### 4.3.4 The New Neutrino Facility (NNF)

The basic layout of a new long baseline  $\nu$  beam, designed at CERN [43, 52] for the proposals of ICARUS[53, 54, 55] and other detectors at the Gran Sasso Laboratory, is the following:

Protons are to be extracted onto the  $\nu$  target via the same extraction line serving the TI8 transfer line from the SPS to LHC. The target and focusing element would be housed in a neutrino cave (about 45 m long in the present design). Parent hadrons would decay in a tunnel ( about 1000 m long with 3 m diameter ) or would be absorbed in a iron hadron stop. An experimental pit after about 900 m of iron and earth shielding may be excavated and house a near  $\nu$  detector.

A compact focusing system with target, horn and reflector fitting within 25 m in a short neutrino cave is foreseen there.

Several focusing configurations are in fact considered in [43]. The preferred focusing system is aimed at collection of large angle and low energy parent hadrons. The correspondent  $\nu$  event rate at the Gran Sasso location is calculated to be 473 events/kt/ $10^{19}$  protons, with a low average value of the neutrino energy. of the neutrino events are shown in fig. 9 and 10.

Alternative configuration have also being investigated. The layout studied in the most recent calculation [55], performed, with a different simulation technique, by the ICARUS Collaboration resembles closer to the configuration used in the WANF. A reflector at about 90 m from the target would require a longer neutrino cave ( or maybe a properly excavated alcove housing the reflector ). A harder neutrino spectrum would be produced and an event rate of 1019 events/kt/ $10^{19}$  protons is calculated at the Gran Sasso location.

The choice of the optimal focusing configuration appears as an important subject of careful study.

### 4.3.5 Possible evolution of the WANF

Continued operation of the WANF has also been suggested by a proposal for a medium baseline experiment located on the Jura and by a letter of intent for a new short baseline experiment [56] (I213).

## Short baseline: I213

It is proposed to operate the WANF with 350 GeV protons and to adopt a new SPS supercycle, combining two (or more) acceleration cycles and promising a significant increase of the SPS repetition rate.

Operation at 350 GeV is meant to reduce the prompt  $\nu_\tau$  background. The cross section for production of charm and the acceptance and interaction probability of prompt  $\nu_\tau$ 's are steep functions of the proton energy. The ratio R of the number of  $\nu_\tau$  over the number of  $\nu_\mu$  induced charged current interactions is reduced at 350 GeV by about a factor 2.5, at the expenses of a 25 % loss of  $\nu_\mu$  event rate.

A modified scheme of operation of the SPS has been worked out together with the CERN SL Division aiming at a realistic optimisation of the operation of the WANF and taking into account all presently known operational constraints. It aims to make available to neutrino experiments the maximum possible proton intensity, by increasing the SPS repetition rate.

It was taken into account that

- after the decommissioning of LEP II the SPS repetition rate can be increased.
- a SPS acceleration cycle to 450 GeV will continue to be necessary for SPS fixed target experiments and test beams and these SPS users require a long flat-top, presently 2.4 sec
- time for machine development should be incorporated in the cycle

The proposed SPS supercycle duration is 19.2 sec long, and consists of two sub-cycles. The first one, lasting 13.2 sec with a 3.2 sec flat-top at 450 GeV, is similar to the present one and will serve all targets. A second 6.0 sec long sub-cycle will be introduced with just a bare acceleration cycle to 350 GeV, with no flat top, serving only the neutrino target T9. The duty cycle for the 450 GeV flat-top (3.2 sec every 19.2 sec) is very similar to the present one.

Two fast-slow extractions for neutrino physics (FS/1 and FS/2) would take place at about 350 GeV on the ramp-up of the first sub-cycle, separated by about 100 msec. Another two fast-slow extractions (FS/3 and FS/4), identical to FS/1 and FS/2, would take place in the dedicated neutrino sub-cycle.

The neutrino target could be served with at least  $2.5 \cdot 10^{13}$  protons out of  $4.5 \cdot 10^{13}$  accelerated in the first subcycle, leaving enough protons for the other SPS users. It will certainly be able to withstand at least  $3.9 \cdot 10^{13}$  protons in the second subcycle, for a total of at least  $6.4 \cdot 10^{13}$  protons per supercycle. The overall gain with respect to the present WANF configuration amounts to about a factor of two in terms of protons per unit time. The present target, or possibly a new target made of graphite, could however withstand in the second sub-cycle more or all of the available intensity of  $4.5 \cdot 10^{13}$  protons.

## Medium baseline: ICARUS on the Jura

The significant independent discovery potential of the ICARUS proposal of a medium baseline oscillation search experiment on the Jura is discussed in [54, 55]. It is also argued there



that an exposure on the Jura could gain important information on the long baseline beam as seen at the Gran Sasso. Their study of the asymptotic behaviour of the beam shows that the Jura location should be preferred as location for a near detector ancillary to the long baseline search to a very near (1 Km) position. Of course, the configuration of the WANF and of the NNF have to be made as similar as possible for this aim.

#### 4.3.6 The physics potential of the CERN and of the NuMI facilities

The NuMI Technical Design [57] in 1995 estimated that  $3.7 \cdot 10^{20}$  120 GeV protons could be delivered to the neutrino target per year, assuming  $4.0 \cdot 10^{13}$  protons per cycle of 1.9 sec and 300 days of operation at 2/3 efficiency. Typically 30 times less protons ( $1.2 \cdot 10^{19}$ ) per year have been collected on T9 at the SPS in the recent years, with 150 days of operation at about  $2.0 \cdot 10^{13}$  protons per cycle of 14.4 sec. A clear advantage is evident, although the NuMI factors will deserve careful scrutiny and this advantage will be partly balanced by the higher energy of the SPS.

##### Short baseline stations at WANF and NuMI

In the same NuMI Technical Design an expected event rate of  $2.0 \cdot 10^6$  CC events/Ton/year is quoted. More recently, after the introduction of a third horn in the NuMI Technical Design, a rate of  $3.7 \cdot 10^6$  CC events/Ton/year has been presented, in particular at this Workshop [58]

The number of events than could be collected by I213 in the present WANF short baseline station is  $7.6 \cdot 10^5$  CC events/Ton/year. This is 4.9 times smaller than at COSMOS.

This number follows because the factor 30 quoted above is to be 1) reduced by a factor 3.6 because  $4.3 \cdot 10^{19}$  350 GeV protons could be delivered per year to T9, assuming  $6.4 \cdot 10^{13}$  protons per cycle of 19.2 sec and 200 days of operation at 3/4 efficiency; 2) increased by a factor 1.4 because of the higher production of useful neutrinos per proton at COSMOS ( $2.7 \cdot 10^{-3}$ ) due to the 3 times longer NUMI decay tunnel whose effect is only partially balanced by the higher multiplicity and Lorentz boost of parent hadrons at the SPS; 3) reduced by a factor 2.5 because of the higher interaction cross section of the more energetic SPS neutrinos.

For an experiment searching  $\nu_\mu$  to  $\nu_\tau$  oscillation, however, an additional factor in favour of the SPS comes from suppression of  $\nu_\tau$  interactions at low energy. I213 estimated that its experimental location is only about 1.6 times worse than the COSMOS location. Two times worse appears infact more realistic.

##### Long baseline stations at Gran Sasso and Soudan

About 500 CC events/kt/ $10^{19}$  pots are expected[43] in the Gran Sasso cavern from a 450 GeV proton energy operation of the CERN NNF. The rate of events/kt/pot is therefore 5 times better than what is expected at NUMI [58] which is estimated to be about 3850 CC events/kt/year (or 100 CC events/kt/ $10^{19}$ ).

It should be noted that 77 CC events/kt/ $10^{19}$  are quoted if the SPS would operate at 120 GeV. The two calculation are thus roughly consistent.

The number of protons that can be collected per year on the NNF neutrino production target depends on the extraction scheme adopted and on the number of extractions per acceleration cycle that can be performed. The extraction hardware foreseen to serve the TI8 transfer line and thus the NNF only permits fast extraction. The estimates quoted in the NNF basic design [52] were obtained assuming fast extraction and the current operation of the SPS, with 14.4 sec cycle. Those estimates are less favourable than the ones that appear possible adopting the new SPS supercycle proposed by I213.

It seems thus natural to consider for the NNF the same supercycle. In its first subcycle, when a flat top is operated, only one fast extraction can be performed, at the end of the flat top. In the second subcycle multiple fast extraction could be proven possible. We assume that the target can stand in total  $1.5 \cdot 10^{13}$  protons in case of single FE,  $2.6 \cdot 10^{13}$  in case of double FE and  $3.3 \cdot 10^{13}$  in case of triple FE.

The total number of protons on target per year on target would be

- $3.2 \cdot 10^{19}$  with 1 + 3 FE, ie 2.5 times less rate/kt/year than at Soudan
- $2.8 \cdot 10^{19}$  with 1 + 2 FE, ie 2.9 times less rate/kt/year than at Soudan
- $2.0 \cdot 10^{19}$  with 1 + 1 FE ie 4.0 times less rate/kt/year than at Soudan

Operation with multiple extractions appears very important for a competitive physics program.

#### 4.3.7 Conclusions

The SPS WANF is presently the most copious and reliable source of high energy  $\nu$ , thanks to the long effort of a large number of people from different CERN Divisions and from Collaborating Institutions. It should be made competitive for future  $\nu$  physics.

The option of a new SPS  $\nu$  facility is also being vigorously pursued. It may one day replace (or complement) the WANF, inheriting its strength and thriving on its experience. A number of decisive choices are to be taken soon.

## 4.4 Future Experiments

If the atmospheric neutrino anomaly is the result of neutrino oscillations with a value  $\Delta m^2 \approx 10^{-2} eV^2$ , then these oscillations should manifest themselves as an energy-dependent modulation in the disappearance and appearance rates measured in suitable detectors located at distances of the order of 1000 km from a source of neutrinos with energies of the order of 10 – 20 GeV.

The first long baseline experiment[59] to address this problem will use a wide band neutrino beam from the KEK 12 GeV proton synchrotron in conjunction with the SuperKamiokande detector at a distance of 250 km. Both  $\nu_\mu$  disappearance and  $\nu_e$  appearance will be studied. The project utilizes already existing facilities and the neutrino beam line is well under construction. The experiment will start data taking at the beginning of 1999.

The possibility to aim a neutrino beam from the CERN SPS to the Gran Sasso National Laboratory in Italy at a distance of 732 km is being discussed at CERN as a possible option for a future long baseline neutrino program in Europe. During the workshop, various detector concepts have been discussed. We had reports on ICARUS, NOE and LBL-RICH proposals and also discussed new ideas on the use of emulsion techniques for intermediate and long baselines. The potentialities of a conventional calorimeter have also been discussed.

### 4.4.1 ICARUS

Report by C. Montanari, Dipartimento di Fisica e INFN, Universita di Pavia, Pavia, Italy, and F. Pietropaolo, Dipartimento di Fisica e INFN, Universita di Padova, Padova, Italy, on behalf of the ICARUS-CERN-Milano collaboration (P. Benetti<sup>a</sup>, A. Borio<sup>a</sup>, E. Calligarich<sup>a</sup>, A. Cesana<sup>a</sup>, R. Dolfini<sup>a</sup>, A. Gigli Berzolari<sup>a</sup>, F. Mauri<sup>a</sup>, L. Mazzone<sup>a</sup>, A. Piazzoli<sup>a</sup>, A. Rappoldi<sup>a</sup>, G.L. Raselli<sup>a</sup>, M. Rossella<sup>a</sup>, D. Scannicchio<sup>a</sup>, M. Terrani<sup>a</sup>, P. Torre<sup>a</sup>, C. Vignoli<sup>a</sup>, A. Bettini<sup>b</sup>, C. Carpanese<sup>b</sup>, S. Centro<sup>b</sup>, D. Pascoli<sup>b</sup>, A. Pepato<sup>b</sup>, S. Ventura<sup>b</sup>, F. Arneodo<sup>c</sup>, F. Cavanna<sup>c</sup>, S. Parlati<sup>c</sup>, G. Piano Mortari<sup>c</sup>, C. Rossi<sup>c</sup>, M. Verdecchia<sup>c</sup>, F. Sergiampietri<sup>d</sup>, D. Cavalli<sup>e</sup>, A. Ferrari<sup>e</sup>, M. Paganoni<sup>e</sup>, A. Pullia<sup>e</sup>, S. Ragazzi<sup>e</sup>, N. Redaelli<sup>e</sup>, S. Resconi<sup>e</sup>, P. Sala<sup>e</sup>, T. Tabarelli<sup>e</sup>, F. Terranova<sup>e</sup>, F. Casagrande<sup>g</sup>, G. Mannocchi<sup>g</sup>, P. Picchi<sup>g</sup>, L. Periale<sup>h</sup>, S. Suzuki<sup>h</sup>, P. Cennini<sup>i</sup>, J.P. Revol<sup>i</sup>, A. Rubbia<sup>i</sup>, C. Rubbia<sup>i</sup>, D. Cline<sup>j</sup>, S. Otwinowski<sup>j</sup>, H. Wang<sup>j</sup>, J.Y. Zeng<sup>j</sup>. <sup>a</sup>Dipartimento di Fisica e INFN, Universita di Pavia, Pavia, Italy, <sup>b</sup>Dipartimento di Fisica e INFN, Universita di Padova, Padova, Italy, <sup>c</sup>Dipartimento di Fisica e INFN, Universita dell'Aquila, Coppito(AQ), Italy, <sup>d</sup>Dipartimento di Fisica e INFN, Universita di Pisa, Pisa, Italy, <sup>e</sup>Dipartimento di Fisica e INFN, Universita di Milano, Italy, <sup>f</sup>Laboratori Nazionali di Legnaro dell'INFN, Legnaro(PD) , Italy, <sup>g</sup>Laboratori Nazionali di Frascati dell'INFN, Frascati(Roma) , Italy, <sup>h</sup>Istituto di Cosmo Geofisica del CNR di Torino, Torino, Italy, <sup>i</sup>CERN, Geneva, Switzerland, <sup>j</sup>Department of Physics, UCLA, Los Angeles, CA, USA.)

## Introduction

The realization of a 600 tons liquid argon (LAr) TPC represents the first step of the ICARUS project. The principal aim of this detector, to be run at the Gran Sasso Laboratory, will be a detailed analysis of the atmospheric and solar neutrinos fluxes with very low and well controlled experimental systematics and the search for proton decay into exotic channels. The final goal of the project is to reach, by addition of other 600 tons modules, a sensitive mass of the order of 5000 tons to study the matter stability up to nucleon lifetimes of the order of  $10^{34}$  years and to search for Long BaseLine Neutrinos Oscillations (LBLNO) with a neutrino beam from CERN.

Recently, the collaboration has submitted to the CERN SPSLC committee an updated programme for the LBLNO search[54] based on two exposures of similar ICARUS modules one at the Gran Sasso (730 km from CERN) and the other at Jura (17 km from CERN). We demonstrated[55] that the potentialities of the Long Baseline programme are fully exploited (precise measurement of the mixing parameters) if complemented by the measurement of the unoscillated neutrino spectrum at a near location (Jura location). Moreover, with a detector at the Jura location, the LSND claim of oscillations can be directly tested. Therefore, within a single programme all the present neutrino oscillation signals can be tested unambiguously by means of appearance methods. In case that no oscillation signals are observed, ICARUS can contribute to significantly enlarge the explored region in the mixing parameter space.

## The ICARUS detector: Status Report

The technological grounds of the LAr TPC have been firmly established by the ICARUS collaboration during several years of R&D[60]. The successful completion of all the steps of the R&D program lead to the submission of a proposal[53] to the Gran Sasso scientific committee and to the INFN. Both the scientific program and the detector construction scheme have been formally approved by both committees during 1995.

In July 1996, funded by the INFN, the engineering design of all the detector components officially started. The basic strategy followed by the collaboration foresees a deep involvement of industry during all the realization process and, for some specific items like e.g. for the operation of the cryogenics systems, also during the normal detector operation. The detector will be assembled outside the Gran Sasso Lab, in Pavia, where it will be tested by taking cosmic rays data. It will be then partially dismantled and transported to the Gran Sasso.

The basic engineering of the most important detector components is now completed; the basic scheme described in the proposal has been confirmed to be sound and feasible. Evolution from the R&D program and discussions with experts from the industries involved into the project lead however to a certain number of important additions and modifications:

- 1) simpler chamber geometry without screening/focusing wires in between the sense wires;
- 2) new mechanics for the wires supports: the wires tension will be kept constant by means of spring controlled devices;

- 3) no electronics immersed in LAr for safer detector operation;
- 4) detection of scintillation light in LAr that will give a measurement of the tracks position along the drift coordinate and a trigger system.

An innovative technique for the construction of the main cryostat has been proposed by the industry in charge of the project. It foresees the employment of aluminum honeycomb panels for the LAr container and Nomex honeycomb modules flushed with nitrogen gas for the thermal insulation with several advantages with respect to temperature uniformity of the liquid argon, transportation (lightweight), and ease of installation (modularity of the external insulation). **A  $10m^3$  cryostat realized with the proposed technique, fully equipped with purification and recirculation units in the same scale foreseen for the 600 ton module, is presently under completion. Cryogenic and purification tests will be performed within this summer.**

Full scale prototypes are presently being built of the readout chambers and the other internal detector components. A chamber module will be mechanically tested in the  $10 m^3$  cryostat after the cryogenic and purification tests.

Commissioning of the 600 ton components will start shortly after the completion of the tests (before winter 1997). The 600 tons module will be assembled and tested in Pavia before the end of 1999; the start of data taking in the Gran Sasso Lab is foreseen by mid year 2000.

### The ICARUS neutrino oscillations programme

A description of the complete ICARUS physics programme is beyond the purpose of this workshop; This section is devoted to the long and medium baseline neutrino oscillations programme with neutrino beams from CERN. Refer to the proposals and technical notes for all other details[54, 55, 53].

**The collaboration plans to perform both  $\nu_\mu \rightarrow \nu_e$  and the  $\nu_\mu \rightarrow \nu_\tau$  oscillation searches at both locations (Gran Sasso and Jura) in order to give a complete answer to the atmospheric neutrino problem[27, 61] and to the LSND claim[28] for neutrino oscillations.**

The experimental programme is aimed at searching for neutrino oscillations in the mass difference regions which are today of great interest, namely the  $\Delta m^2 \simeq 10^{-2} eV^2$  and the  $\Delta m^2 \simeq 1.5 eV^2$  regions, and is motivated by the prejudice on the three neutrino oscillation solution as proposed by Acker and Pakvasa[62]. It proposes to find evidence for the predicted  $\nu_\mu \rightarrow \nu_e$  and the  $\nu_\mu \rightarrow \nu_\tau$  oscillations at the proper  $L/E$  distances.

With the Jura exposure acting as a 'near' measurement of the energy spectrum of the  $\nu_\mu$  component of the beam, a  $\nu_\mu \rightarrow \nu_x$  disappearance experiment at the Gran Sasso can also be performed free of many systematics. The oscillation searches will therefore be *disappearance* and *appearance* measurements, starting with an initially pure nm beam converting over its path into the  $\nu_e$  and  $\nu_\tau$  channels.

To compare the  $\nu_\mu$  neutrino energy spectrum at the 'near' and at the 'far' position, a beam line setup which is similar to the current CERN SPS West Area setup (WANF) (see Ref. [55] for more details) was considered. Under these assumptions, at the Gran Sasso location, the expected rates are about 1000 deep inelastic  $\nu_\mu$  neutrino events per  $10^{19}$  protons on target and per kiloton of target; with a reference three ICARUS modules (1800

tons) detector and an integrated proton intensity of  $4 \times 10^{19}$  protons on target (pot), a total of 4890 deep inelastic  $\nu_\mu$  neutrino events are expected. For the Jura location, the rates are quite large, due to the relatively close distance, about 843000 deep inelastic  $\nu_\mu$  events per  $10^{19}$  protons on target and per kiloton of target; with a reference one ICARUS module (600 tons) detector and an integrated proton intensity of  $2 \times 10^{19}$  pot, a total of 674000 deep inelastic  $\nu_\mu$  neutrino events are predicted.

The integrated intensities should be easily achievable in a few years of normal operation of the CERN SPS machine. Shorter machine cycles could also be envisaged in order to achieve the required exposure in a shorter time[43].

The neutrinos energy of the CERN SPS wideband beam is sufficiently high to produce directly a large number of  $\nu_\tau$  charged current events (the kinematic suppression of the charged current cross-section is  $\sigma_\tau/\sigma_\mu = 0.48$  for deep inelastic events and  $\approx 0.9$  for quasi-elastic events).

The expected event rates for deep inelastic neutrino interactions (DIS), for quasi-elastic neutrino interactions (QE) and for neutrino interactions with production of a single baryon resonance (RES) are summarized in Table 1.2 in case of no oscillations. The number of oscillated  $\nu_\mu \rightarrow \nu_e$  events at the Gran Sasso, expected for the parameters  $\Delta m_{2,1}^2 \approx 0.008 eV^2$ ,  $\sin^2 2\theta = 0.9$ , and the  $\nu_\mu \rightarrow \nu_\tau$  oscillated events at the Jura for the parameters  $\Delta m_{3,2}^2 \approx 1.5 eV^2$ ,  $\sin^2 2\theta = 0.06$  are also shown.

At the Gran Sasso Laboratory, the rate of quasi-elastic and resonance processes is rather small and the analysis is based on deep inelastic events. At the Jura location, the rate of the quasi-elastic processes is quite large and those can be used to extract the oscillation signal. If, as expected, evidence for neutrino oscillations at the Gran Sasso at a mass squared difference  $\Delta m^2 \approx 0.008 eV^2$  is found, a change in the beam optics from the wideband ( $\langle E_{\nu_\mu}^2 \rangle^{-1/2} \approx 25 GeV$ ) region to a narrower low energy band ( $\langle E_{\nu_\mu}^2 \rangle^{-1/2} \approx 10 GeV$ ) in order to optimize the rate of neutrinos at low energy to better study the oscillated events is foreseen. Also, it will be very interesting to repeat the study with antineutrinos, by simply changing the polarity of the beam.

The search for oscillations is based on the particle identification capabilities of ICARUS and on the kinematical reconstruction of the events:

- for the  $\nu_\mu \rightarrow \nu_\tau$  disappearance search, we rely on the external muon detector to identify and measure the muon and use the liquid argon to reconstruct the jet energy; the spectrum of events obtained at the 'far' position is compared to that of the 'near' position;
- for the  $\nu_\mu \rightarrow \nu_e$  appearance search, the analysis is based on a rather straightforward identification of the electron in the liquid argon (the development of the shower is completely visible) and the reconstruction of the jet energy; the energy spectrum of events obtained is compared to the one expected from the  $\nu_e$  contamination calculated from the knowledge of the beam. Note that in order to perform the 'event-counting'  $\nu_\mu \rightarrow \nu_e$  appearance test, one must maximize the oscillated signal compared to the intrinsic background which cannot be reduced. It is therefore mandatory to be located at a L/E distance corresponding to the mass difference  $\Delta m^2$  one wishes to test.
- for the  $\nu_\mu \rightarrow \nu_\tau$  appearance search, the analysis is based on the kinematical suppression

	Jura 1 module	Gran Sasso 1 module	Gran Sasso 3 modules
Number of protons (pots)	$2 \times 10^{19}$	$4 \times 10^{19}$	$4 \times 10^{19}$
Distance (km)	17	732	732
Fiducial target mass (tons)	400	400	1200
$\nu_\mu$ CC DIS	674 000	1630	4890
$\nu_\mu$ CC QE	15 200	35	105
$\nu_e$ CC DIS	3790	8.7	26.1
$\nu_e$ CC QE	66	-	-
$\nu_e$ CC RES	116	-	-
$\nu_\mu \rightarrow \nu_e$ CC DIS	-	113	340
$\nu_\mu \rightarrow \nu_\tau$ CC DIS	11 440	-	-
$\nu_\mu \rightarrow \nu_\tau$ CC QE	532	-	-
$\nu_\mu \rightarrow \nu_\tau$ CC RES	931	-	-

Table 4.2: *Expected events at the Jura and at the Gran Sasso locations with the oscillations parameters:  $\Delta m_{1,2}^2 \approx 0.008eV^2$ ,  $\sin^2 2\theta_{1,2} = 0.9$  and  $\Delta m_{2,3}^2 \approx 1.5eV^2$ ,  $\sin^2 2\theta_{2,3} = 0.06$  (DIS = deep inelastic events; QE = quasi-elastic events; RES = baryon resonance production)*

of the background using similar techniques to those of the NOMAD experiment[32]. This requires good energy resolution: the electromagnetic energy resolution in liquid argon is excellent (measured) to be  $\sigma(E)/E \approx 3\%/\sqrt{E(\text{GeV})}$ ; full simulations in argon predict that the energy resolution for hadrons is good  $\sigma(E)/E \approx 15\%/\sqrt{E(\text{GeV})}$ .

A 50 litre LAr TPC prototype has been placed in the CERN neutrino beam to take data during the 1997 run[63] in order to study the reconstruction of neutrino interactions with the Liquid Argon technology.

**Conclusion:** An answer to the present neutrino oscillation problem can be given with two exposures coupled to the CERN SPS wide band neutrino beam of two similar ICARUS detectors: one in the Gran Sasso Laboratory (730 km from CERN) and the other behind the Jura (17 km from CERN). The importance of a measurement in an artificial neutrino beam, free of systematic errors, is stressed.

A proposal[54] for the experimental programme has been submitted to the CERN SPS Committee to request for the construction of the new beam line to the Gran Sasso and to assess the advantages of a continuation of the exploitation of the CERN West Area neutrino beam.

The successful completion of the ICARUS R&D programme has led to the approval of a first 600 ton module. This full-scale module is currently under construction in Italy with a strong industrial involvement. It will be assembled and tested at the University of Pavia during the second half of 1998 and should be installed in Hall C of the Gran Sasso Laboratory in the course of 1999 (beginning 2000).

## 4.4.2 LBL-RICH

**Report by T. Ypsilantis, Collège de France, Paris, France, LBL-RICH, “A Long Baseline RICH with a 27 kton Water Target and Radiator for Detection of Neutrino Oscillations”, (T. Ypsilantis<sup>1</sup>, J. Seguinot<sup>1</sup>, A. Zichichi<sup>2</sup>, <sup>1</sup> Collège de France, Paris, France, <sup>2</sup>University of Bologna, Italy.)**

A 27 kton water volume is investigated as a target for a long baseline neutrino beam from CERN to Gran Sasso. Charged secondaries from the neutrino interactions produce Cerenkov photons in water which are imaged as rings by a spherical mirror.

The photon detector elements are 14400 photomultipliers (PMs) of 127 mm diameter or 3600 HPDs of 250 mm diameter with single photon sensitivity. A coincidence signal of about 300 pixel elements in time with the SPS beam burst starts readout in bins of 1 ns over a period of 128 ns.

Momentum, direction and velocity of hadrons and muons are determined from the width, center and radius of the rings, respectively. Momentum is measured if multiple scattering dominates the ring width, as is the case for most of the particles of interest. Momentum resolutions of 1-10%, mass resolutions of 5-50 MeV and direction resolutions of  $< 1\text{mrad}$  are achievable. Thresholds in water for muons, protons, kaons and protons are 0.12, 0.16, 0.55 and 1.05 GeV/c, respectively.

Electrons and gammas can be measured with energy resolution  $\sigma_E/E \approx 8.5\%/\sqrt{E}(\text{GeV})$  and with direction resolution  $\approx 1\text{mrad}$ .

The detector can be sited inside a Gran Sasso tunnel or above ground because LBL-RICH is directional and the SPS beam is pulsed, thus the rejection of cosmic rays backgrounds is excellent.

The reader is referred to Ref. [64] for further details.

## 4.4.3 NOE

**Report by G.C. Barbarino, Dip. Scienze Fisiche dell' Università di Napoli and INFN Sez. di Napoli - Italy, NOE, “A Scintillating Fiber Calorimeter to Search for Long Baseline Neutrino Oscillations”, (G.C.Barbarino<sup>1</sup>, D.Campana<sup>1</sup>, F.Guarino<sup>1</sup>, G.Osteria<sup>1</sup>, U.Rubizzo<sup>1</sup>, A.Margiotta<sup>2</sup>, M.Spurio<sup>2</sup>, P.Bernardini<sup>3</sup>, G.Mancarella<sup>3</sup>, D.Martello<sup>3</sup>, A.Surdo<sup>3</sup>, S.Bussino<sup>4</sup>, E.Lamanna<sup>4</sup>, M.De Vincenzi<sup>4,5</sup>, A.Di Credico<sup>6</sup>, A.Grillo<sup>6</sup>, C.Gustavino<sup>6</sup>, S.Mikheyev<sup>6,7</sup>, E.Scapparone<sup>6</sup>, <sup>1</sup>Dip. Scienze Fisiche dell' Università di Napoli and INFN Sez. di Napoli - Italy, <sup>2</sup>Dip. Fisica dell' Università di Bologna and INFN Sez. di Bologna - Italy, <sup>3</sup>Dip. Fisica dell' Università di Lecce and INFN Sez. di Lecce - Italy, <sup>4</sup>Dip. Fisica dell' Università di Roma and INFN Sez. di Roma - Italy, <sup>5</sup>Dip. Fisica dell' Università di Roma III - Italy, <sup>6</sup>INFN, Laboratory Nazionali del Gran Sasso, Assergi - Italy, <sup>7</sup>Institute of Nuclear Research, Russian Academy of Science, Moscow, Russia).**

The  $NOE$  detector

The  $NOE$  detector is a fast, massive, fine grain calorimeter based on scintillating



**fiber technology. It consists of a 4 Kton calorimeter and 2 Kton muon detector which completes the experimental apparatus (fig. 4.5).**

A very preliminary detector set up has been described in the letter of intent submitted to Gran Sasso Committee (fig. 4.6). In order to improve the shower axis reconstruction and in general the topology of the event, the ultimate design solution consists of many crossed X,Y fiber layers. Hence, such a layout allows a very fine sampling in two views, making X,Y coordinates completely equivalent. In more detail, very thin iron sheets (2 mm) provide the mechanical support for two planes of fibers embedded into iron ore absorber. The fiber planes are positioned at both sides of the iron sheet,  $90^\circ$  rotated one respect to the other. Each plane consists of adjacent self-supporting extruded iron ore and recycled plastic slabs. The 6.5 mm thin slab is made of two identical profiles which provide the fibers housing. The iron sheet are hung to a supporting mechanical structure.

The extreme modularity of the  $N^{OE}$  design allows to assemble the detector outside the tunnel, greatly improving the construction efficiency. It is worth noting that the intrinsic granularity of the proposed detector is very high: the average distance between the fibers inside the absorber is of the order of 3 mm. In the hypothesis to have in  $13 \times 13 cm^2 \simeq 300$  fibers the energy resolution for electrons and hadrons have been evaluated by means of GEANT Montecarlo simulation. They are, respectively,  $\sigma(E)/E = 0.01 + 0.17/\sqrt{E}$  and  $\sigma(E)/E = 0.08 + 0.42/\sqrt{E}$ . At present such a granularity is limited only by the cost of the read-out electronics.

The experiment wants to address the fiber read-out towards a fine configuration giving a better event topology and tracking information as well. Groups of fibers are coupled to a multinode device. In the detector fiducial volume  $5 cm^2$ , or better, of channel quantization in two views can be achieved in a grid read-out scheme. The shower axis is obtained combining the center of gravity in each calorimetric grid elements (XE,YE) and two X,Y fired channels. The present calculation are performed on the apparatus having crossed fiber channel area of  $6 cm^2$ . The sampling of such a topology is 1 radiation length. The tracking of both the muon and the hadronic shower axis have been determined and their resolution are given by:  $\sigma_\mu(\theta) = 1.27/\sqrt{E_\mu} + 2.27/E_\mu$  and  $\sigma_h(\theta) = 10/\sqrt{E_h} + 20/E_h$ .

A muon detector, implemented by using iron/concrete absorber and streamer tubes, helps to contain the muons when the  $\nu_\mu CC$  interaction occurs in the final part of the calorimeter.

## Event Rates and oscillation searches

**The  $N^{OE}$  experiment privileges the appearance methods. At present, the general design choice is to have a moderate but fully active mass with high granularity, allowing a fine event reconstruction and where all parts contemporarily act as target, tracker, calorimeter, and  $\mu$ -detector.**

The quality of the exclusive measurement need enough granularity to permit the separation between CC interaction events with or without taus in final state when  $\nu_\mu$  in  $\nu_\tau$  oscillation occurs. Such a discrimination is based on the measurement of the missing momentum in transverse plane, due to the two neutrinos coming from tau decay, as well as the angular correlation between lepton, missing momentum and hadronic jet. In  $\nu_\mu \rightarrow \nu_e$  oscillation an excess of e.m. showers will be looked for. Hence, general requirements for adequate detector for such exclusive measurements are the following:

1. good sampling capability to improve the energy resolution.
2. fine topologic read-out to determine both shower axis and electron discrimination by shower profile.
3. Range/dE/dx accurate measurements to make better particle identification.

Having a detector a good energy resolution, oscillation modulation, as a function of L/E (E for defined distance accelerator-detector L), will be achievable. Besides that, inclusive measurement of the ratio NC/CC as a function of L/E (E) complete the exploration of possible neutrino oscillation.

The rate of  $\nu_\mu$ CC unoscillated events expected to be observed at Gran Sasso by the  $N^{OE}$  detector are  $\sim 15000$  in 3 years of operation, given an exposure of  $2 \cdot 10^{19}$  pot and under the hypothesis of the neutrino spectrum of Ref. [43]. In case of oscillation, the  $N^{OE}$  detector should be able to perform  $\nu_\mu$  disappearance measurement by collecting  $\nu_\mu$ CC interaction events as a function of the energy, and a search for excess of  $\nu_e$ CC events and a search for  $\nu_\tau$ CC interactions.

#### $\nu_\mu$ disappearance test

If  $\nu_\mu$  oscillations exist, the rate of  $\nu_\mu$ CC interactions will be depleted independently of the flavour in which the neutrino has oscillated. The residual  $\nu_\mu$ CC interaction spectrum (fig. 4.8) and a survival probability curve as a function of the energy (fig. 4.9) are shown. The effect of the energy resolution (ideal,  $N^{OE}$ , very coarse calorimeter) is clearly visible. The hypothesis of maximal transition rates in  $\nu_e$  and  $\nu_\tau$  are both considered in the following calculations.

#### $\nu_e$ appearance test

Under the exposure defined in the previous section and in case of a predominant mixing  $\nu_\mu \rightarrow \nu_e$ , the oscillating  $\nu_e$ CC and the residual  $\nu_\mu$ CC will be respectively 4051 and 10867 events. The  $\nu_e$  contamination in the beam gives  $\sim 150\nu_e$ CC events rather flatly distributed over the energy, but nevertheless the signal is expected to be very large. Electrons coming from  $\nu_e$ CC can be detected by studying the topology of the electromagnetic shower (maximum charge, depth, shower profile). In addition the capability of  $N^{OE}$  experiment to measure with accuracy the energy loss  $\Delta E$  and the path  $\Delta L$  in each calorimetric element contributes to the electron identification. "Fake" electrons could be produced by the decay of  $\pi^0$ 's generated in the hadronic core. Cuts in event topology, energy and in the  $\Delta E/\Delta L$  versus range correlation can reduce this background to a tolerable level. A simple 1.5 GeV energy cut reduces the  $\pi^0$  contamination to less than 5% of the total number of  $\nu_\mu$ CC. Due to the large oscillation effect, this contamination should not produce large effects in such a calculation.

Finally, the ratio  $\nu_\mu$ CC/ $\nu_e$ CC =  $\mu/e$ , like the parameter used to quote the atmospheric disappearance of  $\nu_\mu$ , can be implemented to point out the existence of long base  $\nu_e$  oscillations. The  $\nu_e$  excess at low energy should be very large.

## $\nu_\tau$ appearance test

Under the considered exposure and a predominant mixing  $\nu_\mu \rightarrow \nu_\tau$ , the total number of  $\tau \rightarrow \mu = \tau \rightarrow e = 300$ . Kinematical identification of the  $\tau$  decay which follows the  $\nu_\tau$ CC interaction requires excellent detector performances: good calorimetric features together with tracking and event topology reconstruction capabilities. *NOE*'s choice to have a high granularity but a relatively moderate mass (6 Kton), compensates the loss of statistics with the ability to perform measurements in the  $\tau$  decay channel. Depending on the examined channel decay, the background is constituted of  $\nu_e$ CC events or  $\nu_\mu$ CC events. In order to separate  $\nu_\tau$  events from the background two basic criteria can be used: 1) the presence of two neutrinos from  $\tau$  decay produces an unbalanced total transverse momentum; 2) the angular correlation between lepton, hadron and missing momentum in the transverse plane. Simulations of  $\nu_\mu$ CC and  $\nu_\tau$ CC events have been performed in order to reconstruct both the unbalanced total transverse momentum and the angular correlation plots  $\phi_{l \rightarrow h}$  versus  $\phi_{pt \rightarrow h}$ .

Preliminary results show that is possible to define cuts allowing to reduce the  $\nu_\mu$ CC background of a factor  $10^{-2}$ . Such a modest rejection factor permits an high  $\tau$  detection efficiency. Taking into account also cuts in fiducial volume, to ensure containment, and in muon energy, to have clear  $\nu_\mu$ CC identification, we obtain 48  $\mu$ 's from  $\tau$  decay and 11 residual  $\mu$ 's from  $\nu_\mu$ CC interactions.

## Conclusion

Experimental hints of atmospheric neutrino oscillations and related theoretical models suggest accurate explorations in the region of the parameter space characterized by large mixing angle and  $\Delta m^2 \simeq 10^{-2} \text{ eV}^2$ . A long-baseline neutrino detector, having in this region a good signal over background ratio, is a very powerful tool of investigation.

The *NOE* apparatus, thanks to a good balance between mass and granularity, should allow to detect a large and clear effect in the energy modulation both in the disappearance  $\nu_\mu \rightarrow \nu_x$  and in the appearance rate  $\nu_\mu \rightarrow \nu_e$  and/or  $\nu_\tau$ . In absence of signal in large mixing region, the sensitivity limits for exclusive and inclusive channels are shown in fig.4.7.

### 4.4.4 OPERA

Report by P. Strolin, *Universita "Federico II" and INFN, Naples, Italy* OPERA, "An emulsion detector for medium and long baseline  $\nu_\mu - \nu_\tau$  oscillation search", (A. Ereditato<sup>1</sup>, K. Niwa<sup>2</sup> and P. Strolin<sup>1</sup>, <sup>1</sup> *Universita "Federico II" and INFN, Naples, Italy*, <sup>2</sup> *University of Nagoya, Japan*).

## Introduction

The nuclear emulsion technique, which finds its first large scale application in the active target of the CHORUS [33] experiment, can be further improved for future  $\nu_\mu - \nu_\tau$  neutrino oscillation experiments [66][67][68][69]. In [70] several ideas for emulsion-based experiments suitable for  $\nu_\mu - \nu_\tau$  oscillation searches were presented. In particular, it was outlined the

conceptual design of a massive detector (OPERA<sup>2</sup>) able to operate on a medium or long baseline location, to explore with high sensitivity the low  $\Delta m^2$  region ( $10^{-2} - 10^{-3} \text{ eV}^2$ ). In OPERA, emulsion are used as high precision trackers, unlike in CHORUS or TOSCA [69] where they compose the active target. The extremely high space resolution of the emulsion copes well with the peculiar signature of the short lived  $\tau$  lepton, produced in the interactions of the  $\nu_\tau$ .

An experiment exploiting such a detector would benefit from the impressive progress in the field of computer controlled microscopes, read-out by CCD cameras, with automatic pattern recognition and track reconstruction. After the pioneering work in Nagoya [71], the Nagoya and Salerno groups in the CHORUS Collaboration have produced second generation automatic systems about 10 times faster [72][73]. Further improvements are expected from the intense R&D programs under way.

### OPERA in a 100 ton configuration

Medium or long baseline experiments can be designed by exploiting the emulsion technique in a form evolved from the so-called Emulsion Cloud Chamber (ECC) [74]. The ECC technique has been used for several (also large scale) applications [75] and recently revised and proposed for neutrino oscillation experiments [76].

The OPERA concept is an evolution of the ECC. We will consider in the following a configuration yielding a 100 ton detector. The iron/emulsion target is subdivided in 92 modules. Each module, whose dimensions orthogonal to the beam direction are about  $3 \times 3 \text{ m}^2$ , consists of a sequence of 30 sandwiches, each made out of a  $500 \mu\text{m}$  thick iron plate followed by an ES, a drift distance of 2 mm, and another ES (Fig. 4.10). An ES is made up of a pair of emulsion layers  $50 \mu\text{m}$  thick, on either side of a  $100 \mu\text{m}$  plastic base. The drift space can be realistically filled with very low density material. We will show in the following that the “empty gap” between the ES allows, on one hand, a substantial background reduction and, on the other hand, the possibility to directly detect the  $\tau$  “kink”, whereas an impact parameter measurement is performed with the conventional ECC.

Along the beam axis, the total thickness of one module is about 10 cm. Each module could be subdivided into elements, e.g. with a  $30 \times 30 \text{ cm}^2$  area, transverse to the beam direction. When neutrinos interact in the iron, primary particles are produced, some of which, in turn, may interact or induce showers in the downstream iron plates, leaving two space-track segments in each ES. If a  $\tau$  is produced, it can be detected by measuring the angle formed by the charged decay daughter of the  $\tau$  with respect to the  $\tau$  direction. This decay “kink” angle is due to the invisible neutrino(s) produced in the  $\tau$  decay. The directions of the primary (and secondary) charged-particle tracks of the event are reconstructed by means of the first pair of ES downstream of the iron plate where the primary vertex occurs.

The emulsion sheets have, obviously, no time resolution. Therefore, electronic detectors are needed to correlate a neutrino event to the target element where the interaction occurs. These electronic trackers, placed behind each 10 cm target module, detect the shower induced

---

<sup>2</sup>OscillationProject with Emulsion-tRacking Apparatus.

by the neutrino interaction and, hence, locate the ES where scanning must start. About 1 cm<sup>2</sup> of this ES is scanned in correspondence of the shower axis and all the track segments found are measured. These are then extrapolated and searched for in the upstream ESs, until the event vertex is reached. The tracking detectors have the additional task of muon identification with good efficiency and angular acceptance. Honeycomb chambers may be envisaged. To increase the detection efficiency and, consequently, the background rejection, muon detectors could also be added around the target.

The momentum of the  $\tau$  decay products is determined by a multiple scattering measurement in the emulsion. The resolution achievable with this method is weakly dependent upon the momentum. It ranges from 10% at 1 GeV/c to 20% at 30 GeV/c. A magnetized-iron muon spectrometer is placed behind the iron/emulsion target with the purpose of measuring the charge of forward muons.

### OPERA in a medium baseline experiment

In the following, we assume to run OPERA to search for  $\nu_\mu - \nu_\tau$  oscillation in the Jura medium baseline location in the CERN Wide Band Beam. In the Jura location the expected number of CC events in OPERA (100 ton) is  $2.5 \times 10^5$  for  $5 \times 10^{19}$  pot (2 year's running time), with 80000 neutral current (NC) interactions. **In this experiment, no kinematical cuts (or very loose ones) are applied to reduce the number of events to be scanned, leading to a high efficiency for the signal.** All the  $\tau$  decay channels are studied. For the hadronic decays, which have the largest branching ratio (64%), an important source of background is potentially given by hadron reinteractions. In this case, one of the primary hadrons of the (NC) event may reinteract in the vertex iron plate, giving products invisible in the emulsion, so faking the decay of the  $\tau$ . Given the average number of hadrons per event, the iron plate thickness and the number of NC events, one can predict the number of background events from hadron reinteractions to be  $\sim 800$ .

**A special feature of the OPERA concept is that this background is removed by requiring that the  $\tau$  decay occurs in the 2 mm drift space between consecutive iron plates or in the plastic base of the upstream ES (Fig. 4.10). Therefore, one rejects those  $\tau$  decays occurring in the iron plate of the primary vertex ("short decays"), which are the only ones affected by the reinteraction background.**

In the whole kinematical domain accessible by OPERA, the detection efficiency  $\times$  branching ratio (BR) of the hadronic channels ranges from  $\sim 40$  to 50%, also accounting for a 95% "kink" finding efficiency. Similar considerations apply to the muon and electron decay of the  $\tau$ . The BR is 18% and an efficiency  $\times$  BR ranging from 10 to 14% (according to the  $\Delta m^2$  domain) is obtained. The requirement that the  $\tau$  decay does not occur in the iron allows, in particular, to reject those CC charm events which may fake a large impact parameter of the muon. We can roughly estimate the potential background induced by  $D^+$  mesons to be of the order of  $\sim 50$  events, and of 110 events the background due to  $D^0$  production and decay.

## Backgrounds and sensitivity

The most relevant background source is given by single charm production by  $\nu_\mu$ , the main component of the beam. If the primary muon is undetected (2% probability), a  $D^+$  meson decaying in one charged particle (plus neutrals) can fake a genuine  $\tau$  event. The reason is that single prongs from  $\tau$  decay are negative, while the (positive) charge of the D daughter is only measured for the muonic decay, with the muon detected by the downstream spectrometer. The high efficiency in detecting the primary muon (98%) is obtained by exploiting, for the small number of candidate events, a detailed analysis of the primary tracks in the emulsion. The muon identification can be very effective just for those low-momentum particle for which the electronic detectors may fail, as described in [77]. We can estimate the above background for the single-hadron decay mode of the  $\tau$  by the following expression

$$N_{bg}(h^-) = 0.03 \times 0.33 \times 0.2 \times 0.8 \times 0.95 \times 0.02 \times 250000 \sim 8 \text{ events}$$

where the factors are, respectively, the probability to produce charm in CC interactions, the  $D^+$  production probability, the BR for 1-prong hadronic  $D^+$  decay (plus neutrals), the probability for the  $D^+$  to decay outside the iron, the “kink” detection efficiency, the probability not to identify the primary muon, and the total number of charged current events. Similar calculations lead to about 4 background events for the muonic and electron channels together. By rejecting low-momentum D-meson daughters ( $< 1.0\text{--}1.5 \text{ GeV}/c$ ), about 30–35% of the D decays are eliminated for a  $\tau$  efficiency of  $\sim 90\%$ . One is left with a total of  $\sim 7$  background events.

The above number of candidates is small enough to allow a full kinematical analysis in the emulsion. In particular, the momentum and the direction of all primary and secondary particles at the vertex will be measured. The electrons will be identified by following their tracks in the ES, and by detecting their electromagnetic interactions [78]. Photon conversions from neutral pions will be searched for in the ES further downstream of the vertex plate. The expected difference in the kinematics of  $\tau$  decays with respect to charm events will be exploited to further reduce the background. A rejection of a factor  $\sim 10$  is achievable, keeping high efficiency for the  $\tau$  decays [33][68][69].

In conclusion, OPERA “medium baseline” should be left with less than one background event with an overall efficiency  $\times$  BR ranging from 55 to 70% (according to  $\Delta m^2$ ). An additional factor 0.9 has to be included to take into account the “vertex kinematics” efficiency described above. The ratio of cross-sections for tau and muon neutrinos is 0.53 for large  $\Delta m^2$ . In the case of no observed candidates, one then obtains the limit of

$$\sin^2 2\theta_{\mu\tau} < (2 \times 2.3) / (N_{CC} \times \epsilon \times BR \times \epsilon_{vert} \times \sigma_\tau / \sigma_\mu) = 5.5 \times 10^{-5} \text{ (90\% CL)}$$

in the mixing parameter for large  $\Delta m^2$ . The sensitivity is thus improved by a factor of about 4 with respect to CHORUS and NOMAD in the limit of large  $\Delta m^2$ , and more important, by about 3 orders of magnitude for  $\Delta m^2 \sim 1 \text{ eV}^2$ . The minimum detectable  $\Delta m^2$  for full mixing is

$$\Delta m^2 \sim 6.5 \times 10^{-3} \text{ eV}^2.$$

The 100 ton target is, therefore, large enough to also make the experiment sensitive to the low  $\Delta m_{\mu\tau}^2$  region, corresponding to the atmospheric neutrino anomaly reported by the Kamiokande experiment (Fig. 4.11).

### OPERA at a long baseline location

The possibility of sending a neutrino beam from the CERN SPS to the Gran Sasso Laboratory (at 731 km distance) is under study [54, 55, 53, 43, 79]. A massive apparatus placed in the Gran Sasso laboratory can be adopted to search for  $\nu_\mu - \nu_\tau$  and  $\nu_\mu - \nu_e$  oscillation in the low  $\Delta m^2$  region. Therefore, the target has to be massive. Again, the OPERA detector may be used in this case. We can conceive to keep the 100 ton target presented for the medium baseline application. We observe that all the experiments proposed so far feature very large target mass (1 kton or more). **The high detection efficiency of OPERA together with its negligible background and the direct observation of the  $\tau$  “kink” allow to limit the target weight (and dimensions), still retaining good sensitivity in the interesting domain of the oscillation parameters.**

We remind that several possibilities can be contemplated for the oscillation scenario. There could be a pure  $\nu_\mu - \nu_\tau$  or  $\nu_\mu - \nu_e$  conversion or a combination of the two. In all cases OPERA allows an *appearance* experiment. Indeed, also prompt electrons (signature of  $\nu_\mu - \nu_e$  oscillation) may be efficiently detected by exploiting the properties of the emulsion [78]. This procedure is feasible due to the small number of events of the experiment.

Neutrinos (mostly  $\nu_\mu$ ) are produced by a 450 GeV proton beam. The mean energy of the  $\nu_\mu$  is  $\sim 37$  GeV, while the mean energy of the  $\nu_e$  contaminating the beam is 50 GeV. The number of CC  $\nu_\mu$  ( $\nu_e$ ) interactions is 1019 (5.4) per kton and per  $10^{19}$  pot. The experiment may run for three years. This period is compatible with the use of a single set of emulsion to be used for the target. **The expected number of events in a three year exposure ( $7.5 \times 10^{19}$  pot) is 750 muon neutrino CC, 240 NC, and  $\sim 5$  events induced by the electron neutrinos. This is valid in case of absence of oscillation and for a 100 ton target.**

OPERA in the medium baseline location would yield less than 10 background events induced by charm production and decay. It is evident that using the same mass detector at a much longer distance from the source the estimated background becomes negligible. Therefore, the further background rejection by the detailed vertex analysis is unnecessary. This allows to increase the detection efficiency with respect to the medium baseline location.

**OPERA at the Gran Sasso Laboratory would be a background-free experiment searching for  $\nu_\mu - \nu_\tau$  oscillation. For a total number of 750 CC events, in the case of no observed candidates, one would obtain a limit of  $\sin^2 2\theta_{\mu\tau} < \sim 1 \times 10^{-2}$  (90% CL) in the mixing parameter for large  $\Delta m^2$ . The corresponding minimum  $\Delta m^2$  for full mixing is  $\Delta m^2 \sim 3 \times 10^{-3} \text{ eV}^2$ . The experiment, therefore, will be sensitive to the low  $\Delta m^2$  region corresponding to the atmospheric muon neutrino deficit in the hypothesis of  $\nu_\mu - \nu_\tau$  conversion. The sensitivity to  $\nu_\mu - \nu_e$  oscillation is under study.**

## Scanning

The number of events to be scanned in OPERA for the medium baseline location amounts to about 350000, a sample comparable to that of the CHORUS experiment. However, the scanning procedure is more complicated and time consuming than for CHORUS and for TOSCA. For each event, several emulsion sheets must be scanned over a larger area. Moreover, some tracks have to be followed upstream to the primary vertex. With the present technology, the time needed for a complete scanning of an event in OPERA can be estimated in 30 minutes. Assuming 15 microscopes to be available and reasonable scanning downtimes, the complete analysis can be performed within 2 years.

The situation for the Gran Sasso experiment is much more favourable. The total number of events to be scanned is about 1000, and therefore the scanning load is very limited. Moreover, given the small rate of events (of the order of 1 per day) the event analysis can be performed quasi-on-line. One can periodically remove those target elements where the event vertex occurs, and perform the emulsion scanning. This scheme allows a fast analysis, with some complication of the detector set-up.

### 4.4.5 A conventional calorimeter for an oscillation search CERN-Gran Sasso

**Report by R. Santacesaria**, Universita La Sapienza and INFN, Rome, Italy, "A conventional calorimeter for an oscillation search CERN-Gran Sasso", (U. Dore<sup>1</sup>, P.F. Loverre<sup>1</sup>, R. Santacesaria<sup>1</sup>, M. Spinetti<sup>2</sup>, <sup>1</sup>Universita La Sapienza and INFN, Rome, Italy, <sup>2</sup>Frascati National Laboratory, Frascati, Italy.)

In the following we shall describe the sensitivities accessible to a conventional detector dedicated to the search for oscillations of muon neutrinos produced at CERN and directed towards the Gran Sasso laboratory. The use of standard, full proof techniques should guarantee the high reliability required to an apparatus which has to be very large and must be running for many years to insure the statistical accuracy of the measurement. The choice of the detectors must necessarily be guided by cost considerations. A detector mass of 10 Kt and an integrated beam intensity of  $4 \times 10^{19}$  PoT corresponding to about three years running are assumed. Two beam optics are considered:

1. a wide band beam (WBB) very similar to the existing CERN-WANF but with a longer decay tunnel (1000 m) (beam WANF in [43] with the rate increased of a factor 3 due to the longer decay tunnel);
2. a narrow band beam (NBB) centered at about 10 GeV ( beam H20 in Ref. [43]).

The total number of  $N_{CC}$  are about 40K and 11K events in the WBB and the NBB cases respectively.

The most sensitive test to detect oscillations is based on the, so called,  $R = NC/CC$  measurement at two detector locations. Experimentally, the  $R' = 0\mu/1\mu$  ratio is measured.



Despite the fact that there can be classification problems ( $\pi/K$  decays, hidden/escaping muons etc.) what really matters is that the two detectors behave in the same way in this respect. **Since no serious simulation of the detector response has been done so far we will assume, very generically, a systematic error of 1% in the ratio  $R'_{far}/R'_{close}$ .**

In fig. 4.12 the behaviour of  $R'$  and the number of oscillated events are shown as a function of  $\Delta m^2$  and for the two beam options. The exclusion plots for  $\nu_\mu \rightarrow \nu_e$  and  $\nu_\mu \rightarrow \nu_\tau$  oscillation with this method are also shown.

$\nu_e$ appearance	WBB	NBB
$N_{CC}^{\nu_\mu}$	40000	10600
$N_{qe}^{\nu_\mu}$	2000	1000
$N_{qe}^{\nu_e}$	20	10
$(N^{\nu_e} + N^{\pi^0}) (E_{first} < 8 \text{ Mev})$	6+6	3+3
Upper limit	8.6	5.8

Table 4.3: The upper limits are calculated assuming a 15% systematic error in the subtraction of the background that can be measured in the close detector.

Other tests are possible using the calorimetric technique. For instance, a low density fine grained calorimeter à la CharmII [80] could access the  $\nu_\mu \rightarrow \nu_e$  appearance with good sensitivity. To keep the  $\pi^0$  background at a reasonable level only quasi-elastics events should be considered.

We recall that CharmII was a 600 t calorimeter of  $1/2 X_0$  sampling frequency (5 cm of glass) and  $1 \times 1 \text{ cm}^2$  streamer tubes planes; a plane every 5th was also equipped with scintillator counters. With this detector, applying vertex activity cuts, the visible q.e. cross section was measured to be about  $0.7 \times 10^{-38} \text{ cm}^2$  for  $\nu_\mu$  and  $0.4 \times 10^{-38} \text{ cm}^2$  for  $\nu_e$  (the difference is due to the efficiency of the algorithms to select pure e.m. showers) while the  $\pi^0$  component was about five times larger than the  $\nu_e$  quasi-elastics. The requirement of having 1 m.i.p. in the first scintillator plane after the vertex ( $E_{first} < 8 \text{ Mev}$ ) gets rid of 90% of the  $\pi^0$ 's with a 60% efficiency on electrons. Assuming a 10Kton detector having the same performance as CharmII we obtain the numbers reported in table 4.3. The  $\nu_e$  contamination is assumed to be 1% for both beams. The discovery potential of this search is shown in fig.

$\nu_\tau$ in emulsion	WBB	NBB
$N_{CC}^{\nu_\mu}$	2000	530
$\sigma_\tau/\sigma_\mu$	0.5	0.3
$N_{\nu_\tau} (\Delta m^2 = 10^{-2} \text{ ev}^2, \sin^2(2\Theta) = 1)$	140	110
$N_{\nu_\tau}^{obs} (\epsilon = 0.5)$	70	55

Table 4.4: Comparison of WBB versus NBB options for  $\nu_\tau$  appearance

4.13a for the WBB case only. The sensitivity expressed by the exclusion plots is shown in fig.4.13b.

A fine grained calorimeter could also allow exclusive searches for  $\nu_\mu \rightarrow \nu_\tau$  oscillations. For instance, the analysis of the events having a single charged pion in the final state can, as done by CharmII [81], reveal q.e.  $\nu_\tau$  interactions and subsequent  $\tau \rightarrow 1\pi^- \nu_\tau$  decay ( $BR = 12.7\%$ ). The efficiency is, in this case, very low but a check of a relevant part of the atmospheric signal can be done at  $3\sigma$  level (see fig.4.13c).

An emulsion detector could be integrated, at a later stage, in the calorimeter to directly search for  $\nu_\mu \rightarrow \nu_\tau$  oscillation. The integration would consist in the use of the tracking part of the calorimeter to identify the region where the vertex should be looked for in the emulsions. The best way to observe  $\nu_\mu \rightarrow \nu_\tau$  oscillation is offered by the emulsion technique. A possible scenario could be to first look at inclusive signature like  $NC/CC$  test and then, if a signal is observed, build a large emulsion-iron sandwich detector. In a  $1k\ ton$  detector and  $2 \times 10^{19} PoT$  a large number of  $\nu_\tau$  ( $> 100$ ) interactions would occur at  $\Delta m^2 = 10^{-2} ev^2$  and  $\sin^2(2\Theta) = 1$ . Using the "impact parameter" technique ([82]) and looking only at events without a muon in the final state, to avoid the muonic charm decays, the background can be kept at the level of  $5 \times 10^{-5}$  and the efficiency to about 50%. In fig. 4.13d the exclusion plots are shown for the two beam options and in table 4.4 the relevant numbers are summarized.

## Conclusion

A "fine grained", "high sampling" calorimeter could be the right choice to explore extensively neutrino oscillations at large distance. Having fixed the total mass and the sampling frequency a calorimeter made of low  $Z$  material as absorber, (like glass or concrete) has the further advantage of requiring a smaller number of detector planes. The inclusion of a muon spectrometer at the end of the calorimeter can be envisaged to better control the beam spectra and components. An emulsion detector could be integrated, at a later stage, in the calorimeter to directly search for  $\nu_\mu \rightarrow \nu_\tau$  oscillation.

### 4.4.6 An "Anti-tagged" $\nu_\mu \rightarrow \nu_e$ Experiment

**Report by Lucio Ludovici**, On leave from INFN, Sezione di Roma "La Sapienza", Rome, Italy, "An "Anti-tagged"  $\nu_\mu \rightarrow \nu_e$  Experiment", (Lucio Ludovici and Piero Zucchelli, CERN, CH-1211 Geneva 23, Switzerland.)

From the point of view of studying the properties of a possible signal (like the oscillation parameter  $\Delta m_{e\mu}^2$ ) a *zero background* experiment offers the advantage of a *clear event by event* identification of the signal, while in presence of background any information about the signal has to be extracted statistically from the candidate events.

An experiment on a beam of  $E_\nu \approx 1\ GeV$ , about  $1\ Km$  away from the neutrino source, would have the maximum sensitivity  $\Delta m_{e\mu}^2 \approx 1\ eV^2$ , thus allowing to probe the LSND claim. At CERN the neutrino beamline of the CPS accelerator could be resurrected and could be possible to collect in three years, 40 times more proton on target respect to the latest CPS oscillation experiment at BEBC[84]. This would allow a high energy, "zero background" experiment to search for  $\nu_\mu \rightarrow \nu_e$  oscillations, fully covering the region where LSND claim

evidence: the *anti-tagged experiment*. [85]

The principle of the anti-tagging consists in a delayed time coincidence between the  $\nu_e$  production time in the meson decay and its interaction time in the neutrino detector. With respect to the existing idea of a *tagged neutrino beam* [86, 87], the flavour identification is restricted to the  $\nu_e$  background events and the neutrino detector can be at any distance from the source because no spatial correlation between the decay and the interaction is required.

Given a neutrino interaction, the information of all tagging modules is recorded in order to look for possible positron signals. It can be shown that, for reasonable detector geometry, the time difference between the tagging of the positron and the neutrino interaction, depends only from the distance between the tagging module and the neutrino interaction vertex. The time resolution  $\delta t$  of the anticoincidence, has to be small enough to minimize the accidental coincidence between an oscillation event and an uncorrelated positron.

Each tagging module operates by detecting the Cherenkov light produced by the positrons in the gas filling the decay tunnel. The Cherenkov photons produced along the positron path are emitted in the forward direction and they all reach the tagging module almost simultaneously, filling a circular area around the positron impact point (*Cherenkov spot*) with a constant *radial* density and within a radius which is about  $2 \div 3$  cm after 3 meters of Helium or Neon radiator. Helium and Neon are natural candidates because at STP because they have a high Cherenkov threshold for hadrons and muons. The Cherenkov light yield is intrinsically small for light gases (0.027 photons/cm in helium) but increases with the bandwidth and then there is a clear advantage in detecting light up to the extended ultraviolet region (EUV). Light noble gases are particularly suitable because of their high ionization potential which determines the upper frequency for the light transmission. Appropriate EUV photon detectors have to face the problem that most materials (in particular all solids) are not transparent. In the optical region the refractive index is essentially constant but in the EUV, close to the allowed dipole transitions, the variation of the refractive index has to be taken into account in evaluating the integrated light yield and the effective Cherenkov threshold. The addition of a proper "Cherenkov quencher", i.e. traces of gas with a lower ionization potential, allows to tune the Cherenkov threshold and the light yield.

We have started an R&D project to develop an EUV photon detector based on the Micro-Gap Chamber (MGC) technology [88]. The goal is a detector with a time resolution of  $1$  ns, a small radiation length and a high rate capability.

In order to keep the tagging rate to an acceptable level, the available proton intensity should be extracted onto the target as slowly as possible. The optimal solution would be the accumulation in a storage ring with a continuous extraction. Without accumulation, the anti-tagging is feasible provided a slow extraction scheme is adopted.

To assess the feasibility of the anti-tagging we have studied by MonteCarlo simulation of the beamline, the issues of tagging rate, efficiency, neutrino flux and backgrounds. The secondary meson beam is focussed and bent by  $15^\circ$  with a magnetic system which transports the positive charge particles into the decay tunnel. The decay tunnel is 80 m long and is instrumented with the tagging detector, which is followed by a conventional dump to absorb all particles except neutrinos.

The tagging detector consists of 25 tagging modules positioned along the tunnel. Each module is a Cherenkov threshold detector consisting of a 3 m long gas radiator followed

by a planar photon detector. The gas radiator is operated slightly above the atmospheric pressure for gas purity considerations. The radiator and the photon detector are contained in a cylindrical vessel of 1 m radius with thin windows on the front and rear side. The rear window is just on the back of the photon detector. We estimate the material of each tagging module being less than  $5 \cdot 10^{-3} X_0$ .

The neutrino detector is located 810 m from the center of the decay region. For acceptance calculations, we assume a detector transverse square section of  $4 \times 4 \text{ m}^2$ . A traditional horn scheme for the focussing system is incompatible with the slow extraction because it has to be operated in short pulses. A magnetic system consisting of quadrupoles and dipoles can both focus and bend the meson beam from the target into the decay tunnel. In addition to the charge selection, the bending removes from the meson beam the  $K^0$  component, which is the main source of  $\nu_e$  background, and the direct photon yield from the target. The momentum acceptance of the focussing system cuts the low momentum part of the secondary beam, strongly suppressing the rate in the tagging detector due to the positrons produced by soft kaon decays and those produced in the target. A main advantage in such a focussing scheme consists in the low  $\nu_e$  background in the neutrino detector. The relative  $\nu_e$  flux is about 0.1% for a corresponding  $\nu_\mu$  yield of  $1.42 \times 10^{-5} \nu_\mu/\text{pot}$  on the neutrino detector.

The meson beam focussing is not a critical issue, because at this energy the neutrino beam divergence is determined by the large neutrino decay angle with respect to the parent meson (24 mrad for  $\pi_{\mu 2}$  and 64 mrad for  $K_{\mu 2}$  on average). The meson beam divergence should be small enough to contain the secondary beam inside the tagging detector.

In our simulation we have a magnetic focussing system with an angular acceptance of  $50 \mu\text{Sr}$ , a momentum selection of  $\Delta P/P = 20\%$  centered around  $P_0 = 8.5 \text{ GeV}/c$  and a meson beam divergence of 3 mrad with a beam width of 10 cm.

The flux of minimum ionizing particles in the central region of a tagging module, where the beam intensity is maximum, is estimated to be  $180 \text{ MHz}/\text{cm}^2$ , including also the secondary particles from decays in the tunnel.

We identify the following sources of  $\nu_e$  background, of which the associated positrons are not detected by the anti-tagging detector (including also neutrinos from muon decays):  $\nu_e$  produced before the bending optics ( $< 0.2 \cdot 10^{-5} \nu_e/\nu_\mu$ , decays in uninstrumented regions of the decay tunnel ( $3.2 \cdot 10^{-5} \nu_e/\nu_\mu$ ) and the tagging modules acceptance ( $2.0 \cdot 10^{-5} \nu_e/\nu_\mu$ ). Then the irreducible background is about  $5 \cdot 10^{-5} \nu_e/\nu_\mu$ , which improves by more than two orders of magnitude the  $\nu_e$ -contamination with respect to conventional neutrino beams.

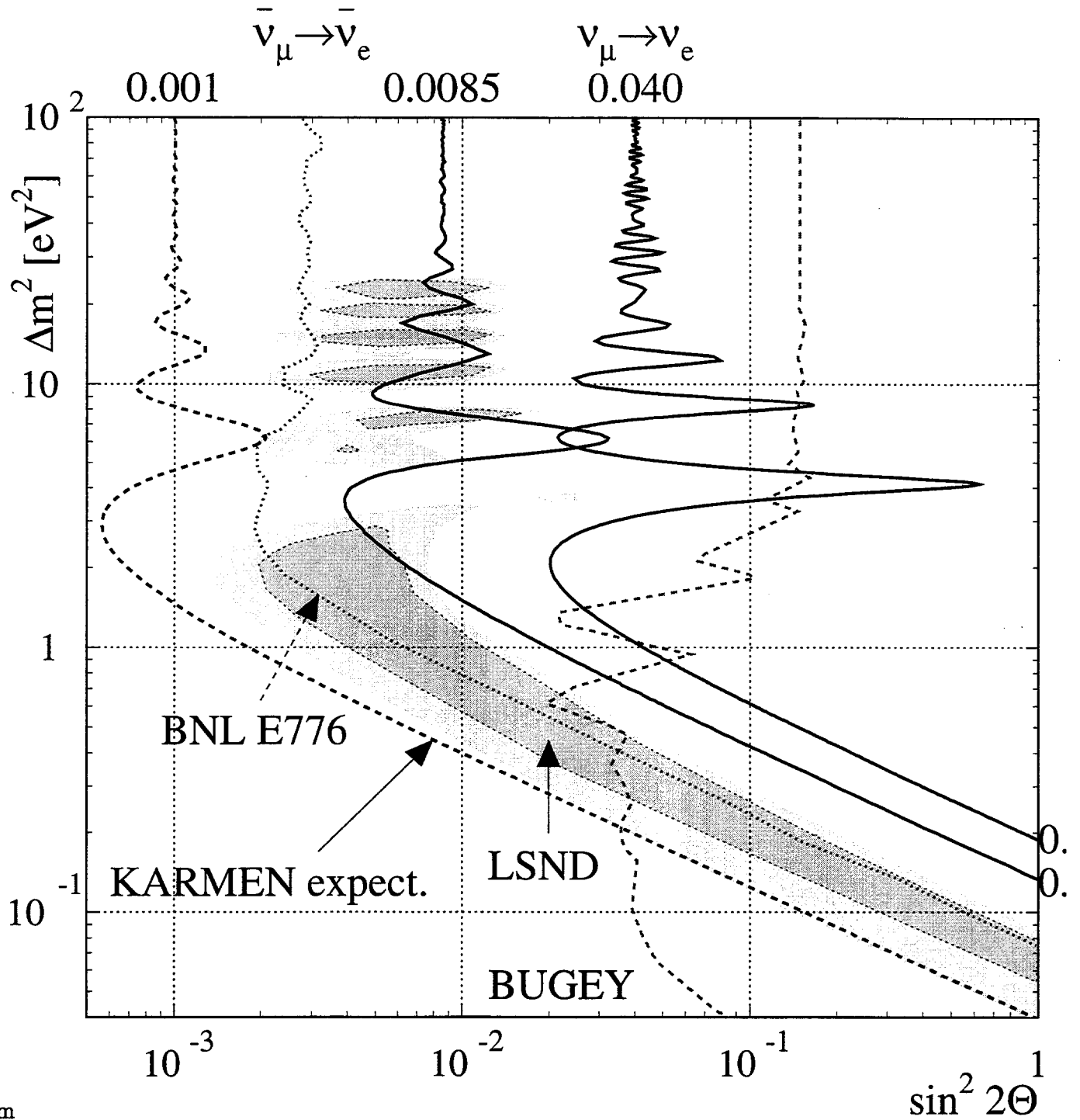
**In two years of data taking the flux onto the neutrino detector is  $1.4 \cdot 10^{15} \nu_\mu$  (in a two years data taking about  $1.0 \cdot 10^{20}$  protons on target could be expected). This corresponds to about 36,500 neutrino interactions (corrected for accidental vetoes) in a 300 t detector. From previous considerations on background, the irreducible contamination due to the beam  $\nu_e$  component is 1.8 events. To evaluate the sensitivity in the oscillation search we restrict the sample to the range  $2 < E_\nu < 5 \text{ GeV}$ , which loosely corresponds to neutrinos produced in the pion decays: in that case 36,200  $\nu_\mu$  events are left, with a background of 1.0  $\nu_e$  events.**

Assuming a separation capability  $e/\pi^0 = 10^{-4} \div 10^{-3}$  of the neutrino detector, the overall  $\pi^0$  contamination can be evaluated in  $0.14 \div 1.4$  events. The exclusion plot resulting from a negative search is shown in figure 4.14.

**If the LSND hypothesis on  $\nu_\mu \rightarrow \nu_e$  oscillation is correct, the expected signal**

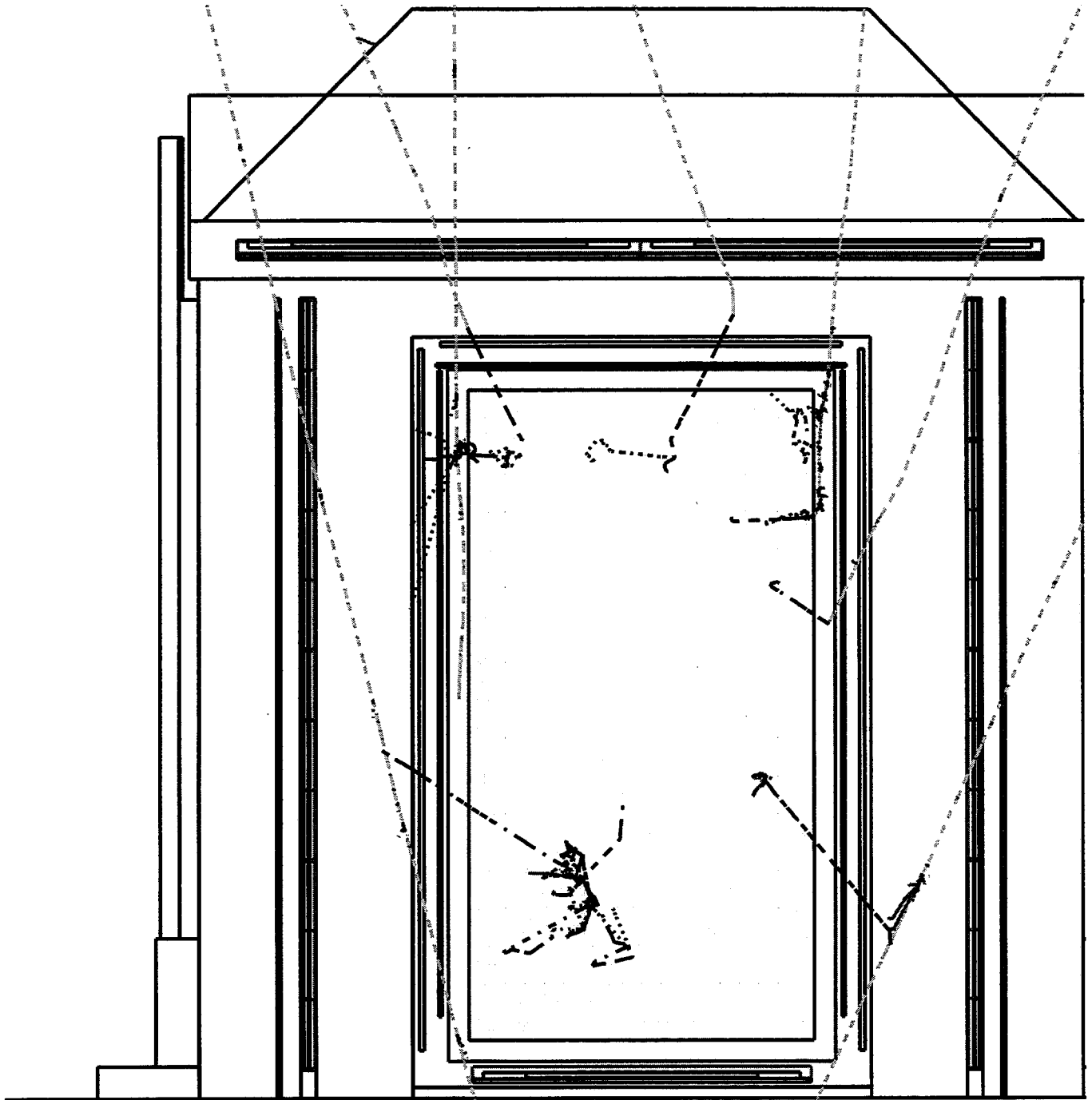
after two years run is  $112 \pm 40$  events, with a background of  $1.1 \div 2.4$  events. We can profit from the small uncertainty on the neutrino flight path ( $\Delta L/L \approx 3\%$  *RMS*) to measure  $\Delta m_{e\mu}^2$  from the energy distribution of the oscillation events. In figure 4.15 are reported the energy distributions of the candidates for different values of  $\Delta m_{e\mu}^2$ , in the hypothesis of a detector resolution  $\Delta E/E = 5\%/\sqrt{E(\text{GeV})}$ . In the figure are shown 224 oscillation events that could be collected in four years running.

Independently from  $\sin^2 2\theta_{e\mu}$ ,  $\Delta m_{e\mu}^2$  can be measured below a few  $eV^2$ , while a lower limit on  $\Delta m_{e\mu}^2$  is set for higher values. In the last case, an extension run with a higher meson momentum selection or a close smaller detector could increase the region where the  $\Delta m_{e\mu}^2$  modulation is measurable.



10.0cm

Figure 4.1: 90% *CL* exclusion curves and limits for  $\Delta m^2 = 100 \text{ eV}^2$ ,  $\sin^2(2\Theta) = 1$  from KARMEN for  $\nu_\mu \rightarrow \nu_e$  and  $\bar{\nu}_\mu \rightarrow \bar{\nu}_e$  as well as the expected sensitivity for  $\bar{\nu}_\mu \rightarrow \bar{\nu}_e$  after the upgrade; oscillation limits from BNL E776 and Bugey; LSND evidence is shown as shaded areas (90% *CL* and 99% *CL* areas respectively).



10.0cm

Figure 4.2: Cross section of the KARMEN central detector with surrounding shield counters and massive iron blockhouse, now including the additional veto system. Cosmic muons passing or stopping in the iron which produce energetic neutrons can now be tagged by the new veto scintillators.

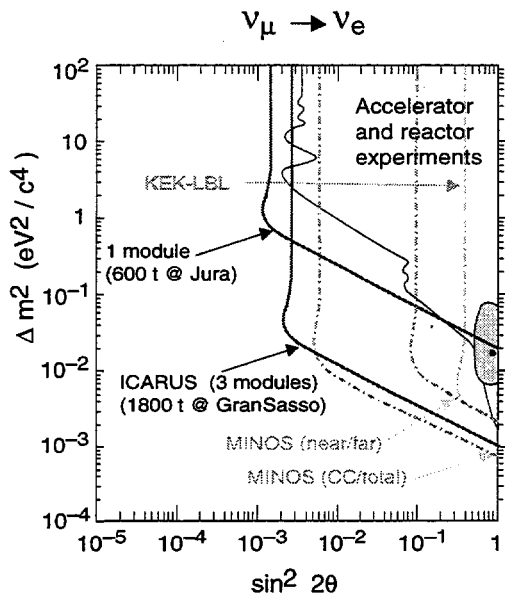


Figure 4.3: Two flavor neutrino oscillation sensitivity regions (90% C.L.) for  $\nu_\mu \rightarrow \nu_e$  oscillations.

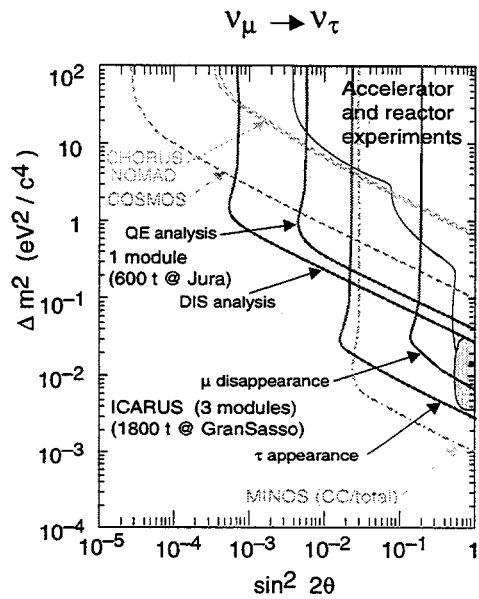


Figure 4.4: Two flavor neutrino oscillation sensitivity regions (90% C.L.) for  $\nu_\mu \rightarrow \nu_\tau$  oscillations.

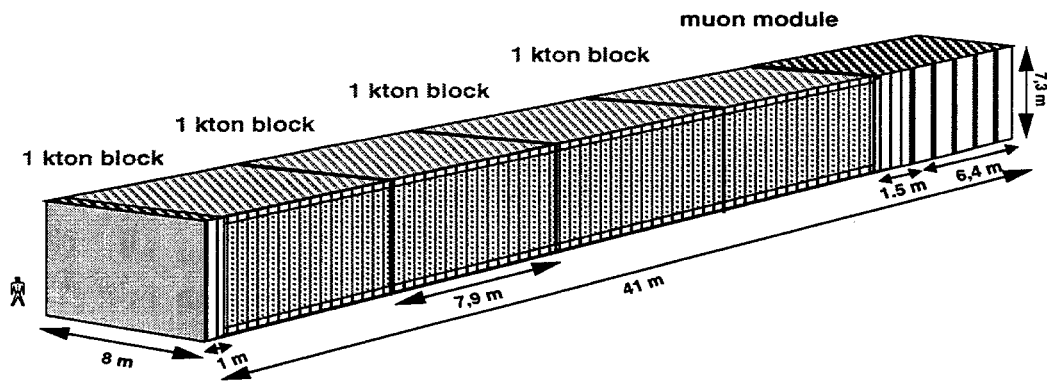


Figure 4.5: The general view of the NOE detector



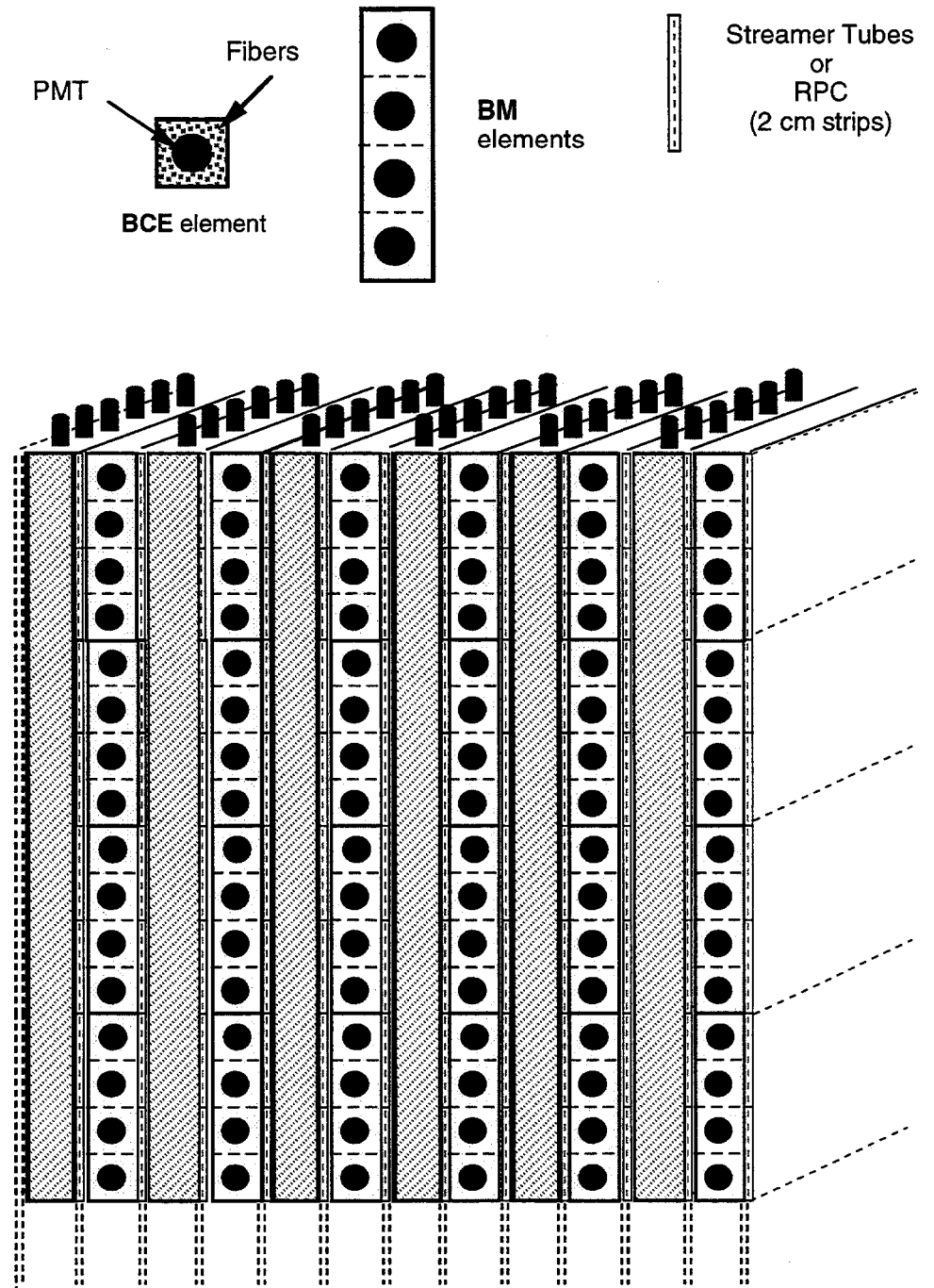


Figure 4.6: *The NOE side view.*

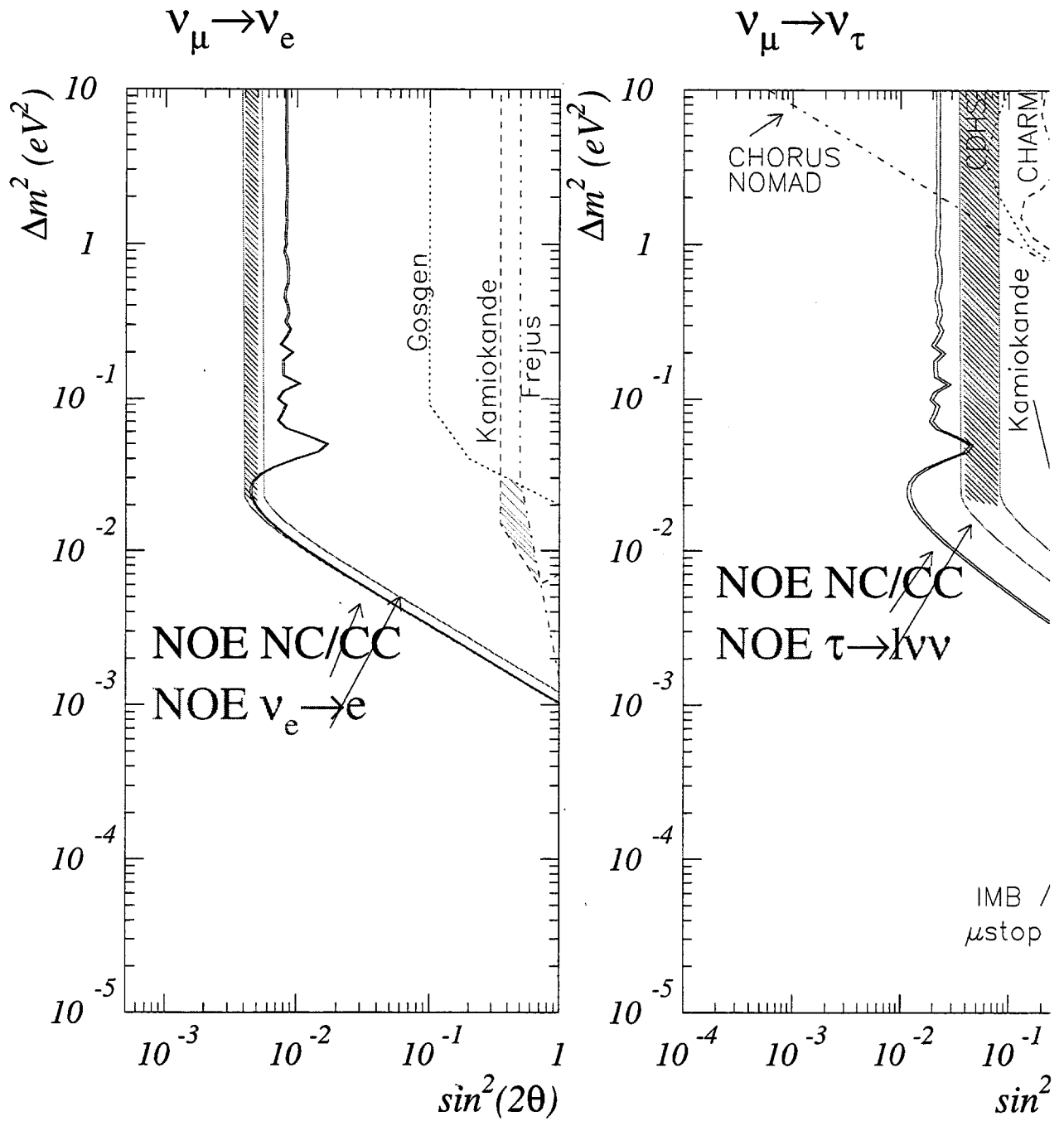


Figure 4.7: The NOE sensitivity to long baseline  $\nu$  oscillations.

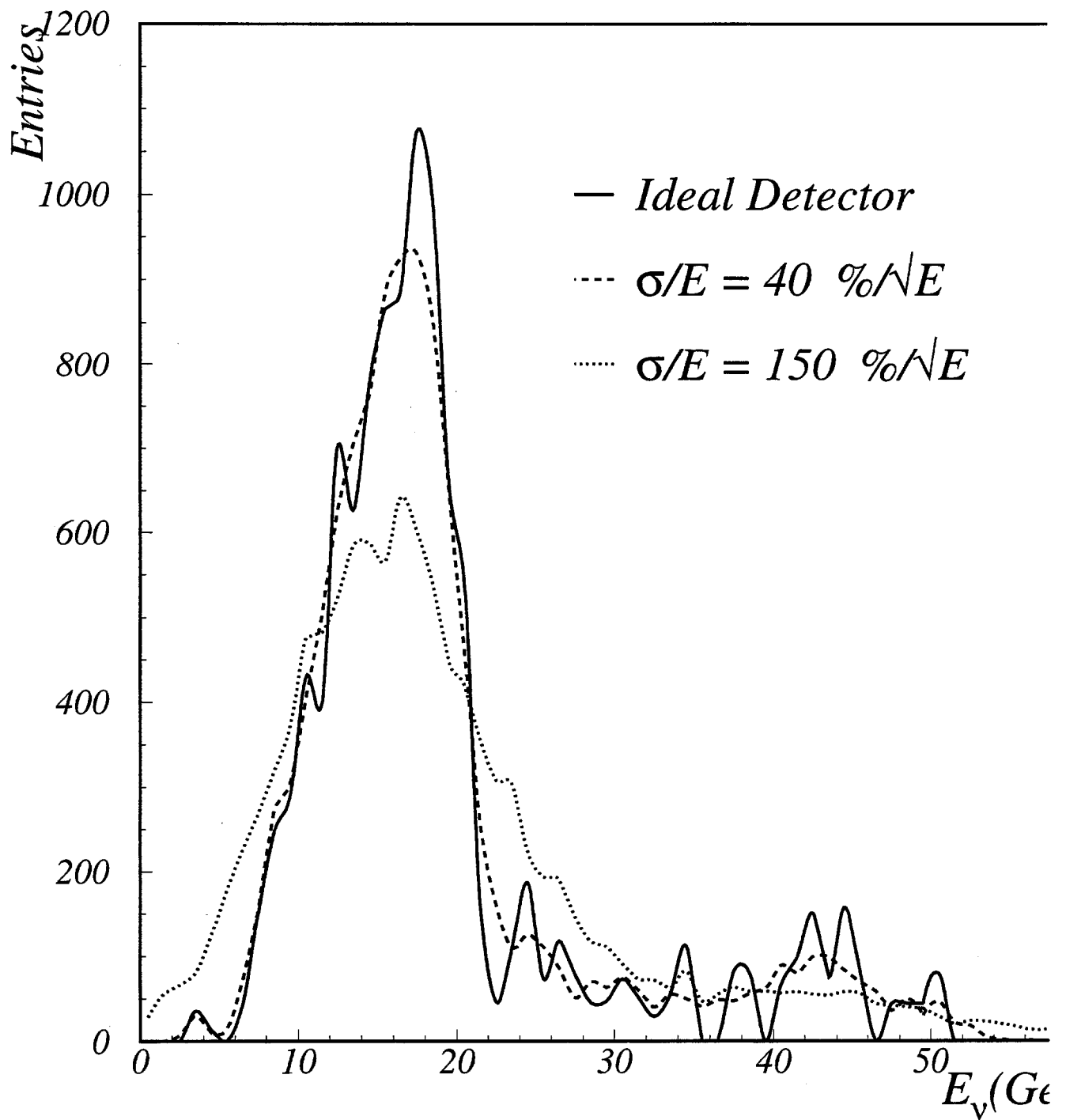


Figure 4.8: *The residual  $\nu_\mu CC$  interaction spectrum.*

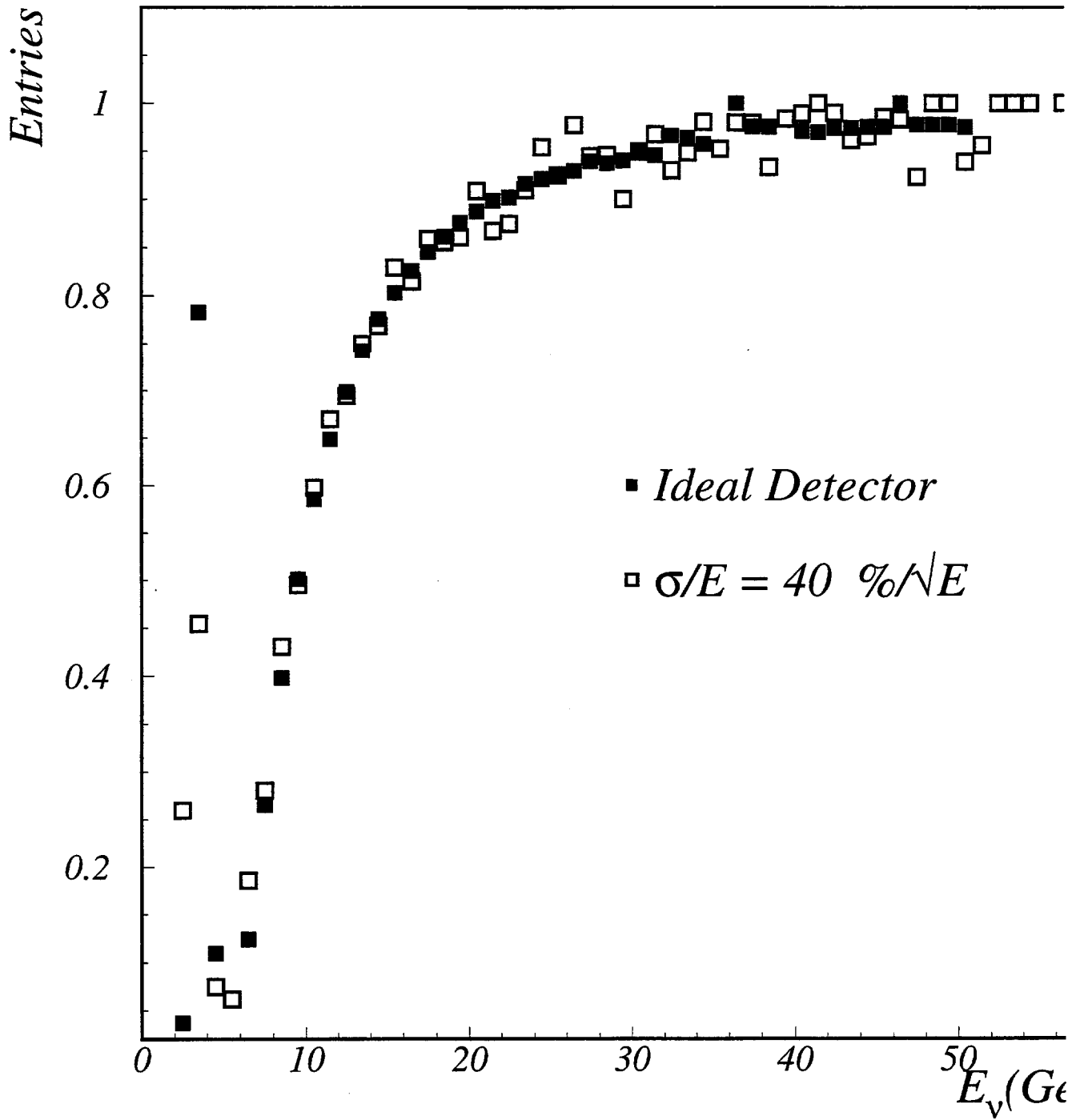


Figure 4.9: The  $\nu_\mu$  survival probability.

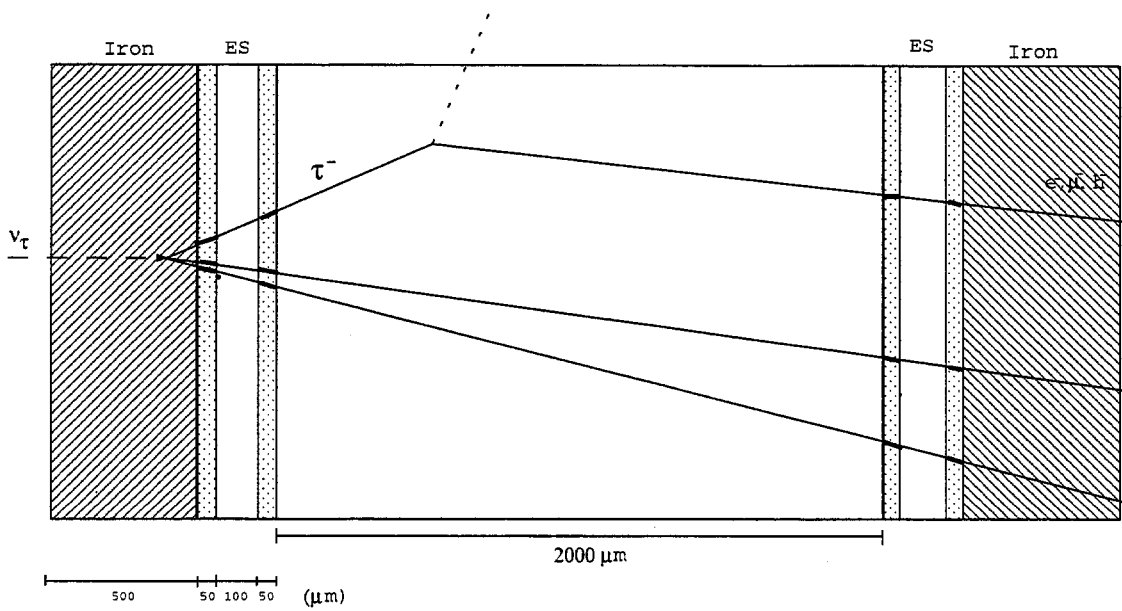


Figure 4.10: Schematic structure of the OPERA target.

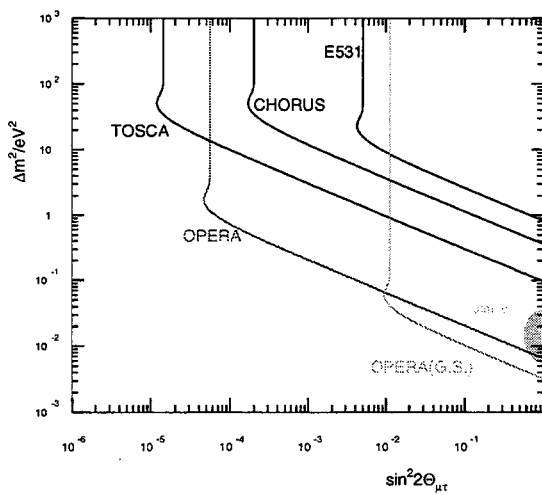


Figure 4.11: Sensitivity of OPERA in the medium and long baseline location as compared to other experiments.

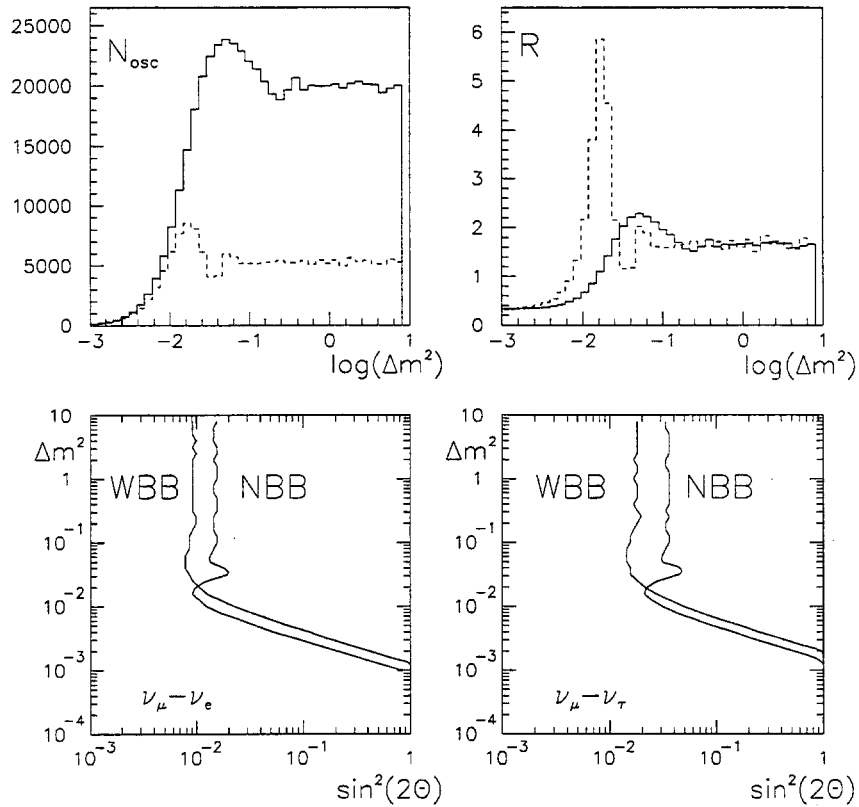


Figure 4.12: The number of oscillated events (top left) and the measured value of  $R'$  (top-right) for maximum mixing as a function of  $\Delta m^2$ : the full line is for WBB while the dashed line represents NBB case. Exclusion plots with the R method for  $\nu_\mu \rightarrow \nu_e$  (bottom-left) and  $\nu_\mu \rightarrow \nu_\tau$  (bottom-right).

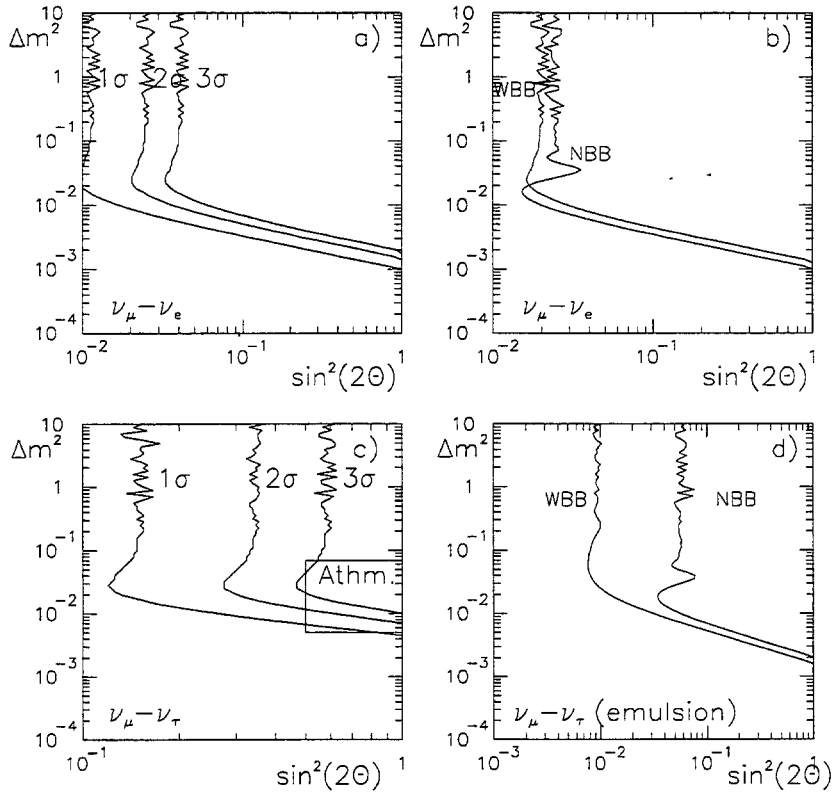


Figure 4.13: Discovery potential of  $\nu_\mu \rightarrow \nu_e$  (a) and exclusion plot (b).  $\nu_\mu \rightarrow \nu_\tau$ : discovery potential via the single pion search in the calorimeter (c); the sensitivity of an emulsion detector (d)

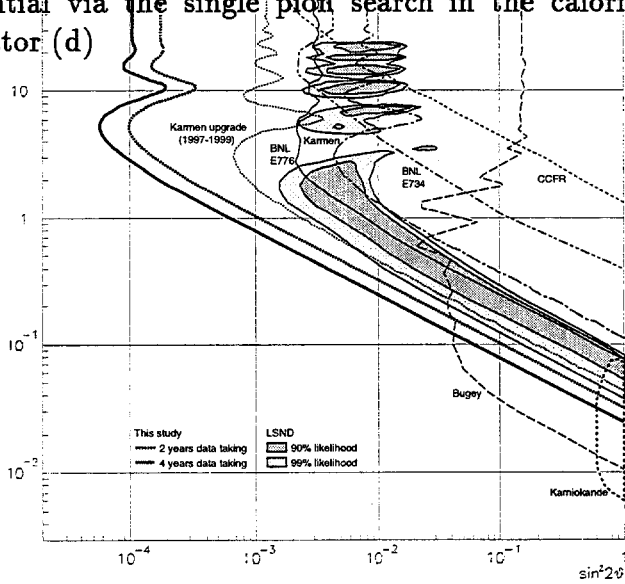


Figure 4.14: Exclusion plot.

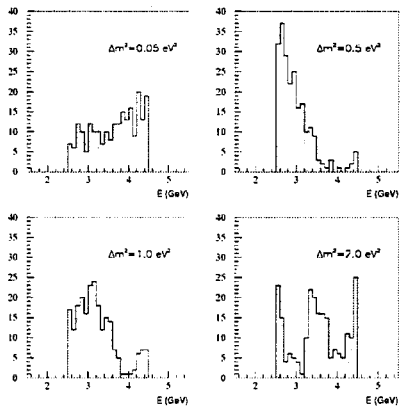


Figure 4.15: Spectra of oscillation events for some  $\Delta m_{e\mu}^2$ .



# Chapter 5

## Summary of the Conventional (Non-oscillation) Physics Working Group

Reported by P. Spentzouris, Columbia Univ. and J. G. Morfin, Fermilab

### 5.1 Introduction

We discussed possibilities for exploring non-oscillation neutrino physics based on the following principles:

- The physics is interesting.
- The integrated physics program could be executed using a single experimental apparatus.
- The detector possibilities that were examined were:
  1. The use of an existing (in the NuMI grant scheme) detector (COSMOS, near MINOS), with the possibility of extensions that do not interfere with the oscillation program.
  2. To propose a new detector (which could be used as the MINOS beam monitoring to justify its cost).

The physics prospects examined were Inclusive Structure Function measurements, Polarization of the strange component of the nucleon's sea, Charm Physics, and Electroweak Measurements.

### 5.2 Polarized intrinsic nucleon strangeness and elastic neutrino scattering on nucleon

A.M.Rozhdestvensky and M.G.Sapozhnikov

The possible strange quark content of the nucleon is currently of considerable experimental and theoretical interest. Results from experiments on  $\pi N$  scattering demonstrate

that the contribution of strange quarks to the nucleon mass could be as high as 20 % [2]). Other evidence comes from the polarized DIS measurements [3] that indicate that the strange quarks in the nucleon may be polarized opposite to the proton spin:  $\Delta s \equiv \int_0^1 dx [q_\uparrow(x) - q_\downarrow(x) + \bar{q}_\uparrow(x) - \bar{q}_\downarrow(x)] = -0.10 \pm 0.02$ . Also, the observation of strong violation of the OZI-rule seen recently at LEAR experiments in  $\phi$  and  $f'_2(1525)$  production [4] could be interpreted by postulating the presence of long-lived  $s\bar{s}$  pairs in the nucleon's wave function [5], [6].

The elastic neutrino scattering off nucleons is a very good tool to obtain information about the possible polarization of the strange quarks in the nucleon. The last measurement of the  $\nu p$  elastic scattering was done 10 years ago [7], and the re-analysis of this data [8] was inconclusive in determining the size of  $\Delta s$ .

An analysis was presented trying to determine to what extent the measurement of elastic neutrino scattering at the MI could be improved, in order to obtain information about the polarization of strange quarks in the nucleon [1]. In this analysis, the formalism of [8], Solution II, was used, where the cross-section is parameterized in terms of the nucleon weak current axial, charge and magnetic form factors  $G_1, F_1$  and  $F_2$ , which have contributions from  $u, d$  and  $s$  quarks. The strange quark contribution to the vector form factors was ignored, since current experiments at TJNAF, MAMI and Bates will very likely measure this contribution.

A simulation using the near MINOS detector [9] and the neutrino beam parameters for the NuMI Wide Band Beam (WBB) [9] was presented. The results indicate that even order 1k events are enough to determine  $\Delta$  in terms of statistics. Unfortunately, a systematic error of order 10 %, which is expected from the previous experience with this kind of measurement, complicates the situation. The possibility to reduce the systematic by using the ratio R elastic to quasi-elastic  $\nu_\mu n \rightarrow \mu^- p$  cross-section was also examined, but the results were not improved.

The systematic uncertainty effects were examined, in order to find possible solutions:

The kinematics of elastic scattering dictate some conditions for the detector. The proton momentum spectrum peaks at 0.5 GeV/c and it is concentrated below 2 GeV/c. If we could measure protons with momentum starting from 100 MeV/c we could obtain  $Q^2$  up to  $10^{-3}$  GeV/c<sup>2</sup>. The correlation between  $Q^2$  and the angle of recoiled proton is more essential. To reach  $Q^2 = 10^{-1}$  (GeV/c)<sup>2</sup> we need to measure tracks with angles about 70-80 degrees. These features fix the possible parameters of a detector suitable for this measurement. Good identification of low energy protons with high efficiency is the most important issue. Large transverse dimensions are also essential, in order to obtain enough points on a particle track with opening angle 70 degrees. It is clear that a liquid scintillator detector is most suitable from the point of view of identification of elastic scattering events. A liquid scintillator detector with 6 meter length could obtain the same statistics as the expected statistics for the MINOS beam monitor detector described in the proposal [9].

## 5.3 Structure Function Measurements

Jorge G. Morfín and Panagiotis Spentzouris

The MI intense neutrino beam provides the event rates of the previous generation neutrino beam lines but at much lower energies. The kinematic region covered is comparable to that of the kinematic region of the SLAC experiments (moderate and high- $x$  with  $Q^2$  in the pQCD regime, low- $x$  with low  $Q^2$ ). With this kinematic coverage we could study the transition from the pQCD region to the resonance region, and obtain very interesting measurements on the following subjects:

### High- $x$ Structure Functions and Parton Distribution Functions (PDF).

Recent investigations of the behavior of parton distributions within the nucleon have emphasized the very high energy reach of the collider data by concentrating on the very low  $x$  region. Interestingly enough, we now have much more data exploring the low ( $< 0.1$ ) to ultra-low ( $< 0.001$ )  $x$  region than we do the high  $x$  ( $> 0.5$ ) region. Whereas we need high energies to reach the high  $x$  necessary to study the low- $x$  region we need high statistics on a nucleon target to study the high- $x$  region with low statistical and systematic errors.

Our ignorance of the high- $x$  Bj region is not limited to the "higher twist" and nuclear effects expected (but hardly studied) in this region, but extends even to the behavior of simple quarks at  $x > 0.5$ ! The ratio of the d-quark to u-quark -  $d(x)/u(x)$  - is expected to approach 1/5 in the framework of pQCD (Farrar and Jackson), however current fits are just as consistent with this ratio approaching 0 as the expected 0.2.

A recent project of some members of the CTEQ collaboration emphasized the limited knowledge of this region when constructing a toy model which could simultaneously explain the high- $q$ , high- $x$  anomalous ZEUS events at HERA and the high- $p_t$  events of CDF at the collider. It was found that an additional quark contribution, equal to around 1 % of the integrated d-quark contribution, could be added at  $x$  near 1.0 and  $q = 2$  GeV without seriously contradicting any data. This could, for example, be an intrinsic heavy quark contribution. Through normal  $q$ -evolution of the parton distributions these evolve down to the  $x$  of the ZEUS events at the proper  $q$ . This exercise indicated that we can adjust high  $x$  parton distributions with relative impunity with respect to the very limited and imprecise data currently available.

**Higher Twist Effects.** Although twist-2 phenomena is expected to follow  $Q^{-2}$  behavior, the  $x$  dependence of the matrix element is unknown. This has made a careful study of this phenomena difficult since one needs a high statistics data set with small systematic errors over a wide range in both  $q$  and  $x$ .

Currently there are studies of twist-4 phenomena in electro-production experiments which combine SLAC e-p data with BCDMS mu-p data. This study indicates that the twist-4 contribution is large and positive. On the other hand, the only studies using neutrino DIS are based on low-statistics, heavy-target Gargamelle and BEBC bubble chamber experiments. These indicate that the twist-4 contribution is relatively small and negative! This is not completely surprising since the early work of Vainstein and Shuryak indicated that the twist-4 effects from the two processes might very well be different. Current global fits of DIS results indicate no real need for a higher-twist contribution when fitting both electro-production and neutrino production data together.

The extremely high data rate available with the NuMI wide band beam (roughly  $4 \times 10^3$  events per kg per year) insures adequate event rates using even low-A targets.

**Nuclear effects.** There is very little known experimentally about Structure Function nuclear effects in neutrino DIS. The only existing data are from low statistics bubble chamber experiments *citenucs*. On the other hand, nuclear corrections are needed in order to extract the nucleon's PDFs from the high precision neutrino Structure function data, which are obtained using nuclear targets. The corrections applied are determined from charged lepton DIS on nuclear targets. Furthermore, nuclear effects in  $F_3$  have never been measured, and the difference (if any) between nuclear effects in  $F_2$  and  $F_3$  would allow to differentiate between the behaviour of valence and sea quarks in a nuclear environment. Such differences could be used to differentiate between parton-parton and nucleon-nucleon correlation effects.

Structure Function Nuclear effects could be categorized according to the  $x$  region examined [11]:

1. Shadowing effect ( $x < 0.1$ ),  $\sigma_A < \sigma_D$ . There are 2 types of models that try to explain this effect: parton recombination and vector meson dominance models. In the second case, if the effect is due to virtual boson fluctuations to mesons, a difference is expected between neutrino and charged lepton scattering (axial component of W). This difference is maximized at low- $Q^2$ .
2. EMC effect  $0.3 < x < 0.6$ ,  $\sigma_A < \sigma_D$ . This effect is explained using nucleon-nucleon correlation arguments.
3.  $0.1 < x < 0.2$ ,  $\sigma_A > \sigma_D$ , the transition region. No real explanation.
4. Fermi motion region,  $x \geq 1$ .

It is interesting that there is no single model that explains all 4 regions in a unified way.

With the MI neutrino beam we could measure the EMC effect region in the pQCD regime, and the shadowing region in both the pQCD (higher  $x$ ) and the lower  $Q^2$  regions (for event rates as a function of the kinematic variables see [12]). Because of the high event rates ( $4 \times 10^3$  events per kg per year), the size of the nuclear targets could be kept small ( $\sim 1$ ton). The addition of a nuclear target system to any of the planned detectors should be trivial (in front of the MINOS near detector, as part of the COSMOS veto system), more study is needed in order to decide an optimal configuration in terms of acceptance.

For the structure function measurements we need good acceptance for low energy muons, so low mass detectors are preferable. In order to reconstruct the event kinematics, a measurement of the total hadronic energy is required, so a hadronic calorimeter is needed or else an inclusive measurement of all the final state particles (tracking+electromagnetic calorimeter). Also, in order to take full advantage of the neutrino DIS we need to also run in  $\bar{\nu}$  mode.

## 5.4 Charm Physics

Tim Bolton, Douglas Morrison, J. K. Woo and I. Bigi

The rates for charm production are high (0.5-5 % of the total neutrino-nucleon cross-section), and the events are characterized by relative low multiplicities and of course energies (and decay lengths). There is a unique opportunity to study charm production inclusively, using a low mass detector with complete event reconstruction and emulsion quality vertexing. All the studies and ideas presented were focused on the use of the COSMOS detector, which appears to be adequate for this kind of physics [12]

The measurements that could be performed include:

- Measurement of the differential cross-section from inclusive charm production, study of its threshold behaviour near the charm mass, and extraction of the value of the charm mass ( $m_c$ ),  $V_{cd}$  and the strange PDF. Over an order of magnitude reduction in the error on  $m_c$  is possible. If the measurement is totally inclusive, then the accuracy on the  $V_{cd}$  determination could allow a unitarity test of the CKM matrix.
- Form factor measurements from exclusive  $\Lambda_c$  production
- $D - \bar{D}$  mixing from same sign di-muon events, with the second muon from a detached vertex. Sensitivity could be improved by 2 orders of magnitude ( $\sim 10^{-4}$ )
- Charm sea measurements from events with 2 charm vertices ( $\sim 100$  events)
- Flavor changing neutral currents from events with a single charm vertex in an event with no primary muon (sensitivity  $\sim 10^{-6}$ )
- Branching fraction for  $D^0$ ,  $D^+$ ,  $D_s^+$ ,  $\Lambda_c^+$  to 10%
- Diffractive  $D^*$ ,  $D_s^*$  production and tests of vector meson dominance.

## 5.5 Parton propagation in nuclear matter

Elena Vataga

The question of parton propagation in dense nuclear matter is a rather new one and is not very accurately studied. The issue is that secondary hadrons produced at the interaction point would undergo strong rescattering when traversing the nuclear matter on their way out of nucleus. However, the hadrons or hadron constituents may not be created at the interaction point and the produced object could pass some distance in nuclear matter before gaining the normal ability for interaction. This distance is referred to as formation length. There are two extreme cases: formation length of parton corresponds to the time after which the first constituent of the hadron has been formed (constituent length); and formation length of newly-formed hadrons, after which all hadron constituents have met to form a hadron ('yo-yo' length). The last one was studied in a number of experiments and manifests in the absence of intra-nuclear cascading of the high-energy hadrons. The first one is more subtle

and so far very few works on this subject have been published [13]. The Nucleus is a unique tool for studying the properties of the state which propagates in it and a nuclear target is particularly attractive in the case of a lepton beam, where the parton structure of nucleon is clearly manifest and the direction of the jet is easy to reconstruct. In this case, by studying the evolution of pure parton jet one could learn more about the confinement mechanism, color transparency, both kinds of formation length. Important by itself, this information is also relevant for the issue of quark-gluon plasma formation in heavy-ion collisions.

As it was showed on the workshop, study of this effects can be done by comparing data from different nucleus target to data from nucleon target, as well as using nuclear targets alone and comparing hadrons produced in nucleus collisions with cascade and in interactions without cascade [14]

The MI intense neutrino beam provides a good opportunity to study this subject with high statistic and at low energy. According to previous studies the effects of the "yo-yo" formation length can be seen only with energy transfer  $\nu$  (virtual boson energy) up to 70 GeV [15] or even less - about 20 GeV. For formation length measurements we need nuclear target, full reconstruction of event kinematics and good acceptance for the fastest hadrons.

## 5.6 Electroweak measurements and detector development

Donna Naples and R. Schwiehorst

The following possibilities for improved Electroweak measurements were examined:

- trident production (scattering off the Coulomb field of the nucleus, measurement of distractive W and Z diagram interference): COSMOS could improve the existing results (CCFR, CHARM II) by using the emulsion to reduce backgrounds (low energy dimuon production from charm, coherent single pion production).
- inverse muon decay cross section,  $\sin^2\theta_w$  from neutrino electron scattering differential cross-section, neutrino magnetic moment from the y dependence of the neutrino electron differential cross-section at low y.
- These measurements need good angular resolution, ability to reject backgrounds and the last two also ability to identify electrons. In order to improve the existing results also large mass is needed (statistics). The possibility to use a liquid scintillator detector, segmented in small cells, with a multi-pixel photo-detector readout was examined. In addition, this type of detector could be used for the strange form factor measurement, and could serve as part of the MINOS beam monitoring apparatus. It could be used in front of any of the 2 detectors (COSMOS, near MINOS) -need of a muon spectrometer, or in a more advanced and independent version it could be placed inside a magnet and become an independent system.

# Chapter 6

## Summary of the Neutral Kaon Working Group

Reported by K. Arisaka (UCLA) and R. Ray (Fermilab)

### 6.1 Introduction

After over 30 years of hard work, the source of CP violation is still unknown. All observations are currently consistent with a Standard Model formulation with a single complex phase in the CKM matrix as well as Superweak interactions which lie entirely outside the Standard Model. There continues to be a great deal of activity in experimental kaon physics at CERN, BNL, KEK, DAPHNE and Fermilab. The present round of activities at these facilities promises to shed a great deal more light on this 30+ year old question. One method for probing this issue lies in collecting large quantities of neutral K decays to charged and neutral  $2\pi$  final states and extracting the quantity  $\text{Re}(\epsilon'/\epsilon)$  from the well known double ratio. Experiments are currently underway at CERN and Fermilab to carry out this measurement with unprecedented precision. Another window on this and other interesting physics lies in rare kaon decays, a number of which are expected to have significant direct CP violating amplitudes. In order to reach sensitivities which will allow sensitive tests of the standard model, large fluxes of kaons will be required. The Main Injector at Fermilab will provide a significant flux of high energy neutral kaons. How to make the best use of this new facility using the existing KTeV detector with strategic upgrades over time will be the focus of the Neutral Kaon Working group.

### 6.2 Theoretical Motivation

The ongoing neutral kaon program at Fermilab has always had, at its core, significant theoretical motivation. The current KTeV run consists of two physics programs which address the most important issues currently accessible to the neutral kaon sector: a precise measurement of the direct CP violation parameter  $\epsilon'/\epsilon$  (E832), and a study of CP violating and other rare kaon decays (E799-II). The importance of extending this program into the Main Injector era was supported in presentations by Buchalla and Donoghue in the working group and by Wolfenstein in a plenary session.

Buchalla presented his current thinking on the importance of measuring both  $K_L \rightarrow \pi^0 \nu \bar{\nu}$

AND  $K^+ \rightarrow \pi^+ \nu \bar{\nu}$ , reinforcing much of his work which has appeared in the literature [89] [90]. The decay  $K_L \rightarrow \pi^0 \nu \bar{\nu}$  is virtually pure direct CP violating. Observation of this mode would allow the cleanest determination of the height of the unitarity triangle, the parameter in the Standard Model which determines the size of all CP violating observables [91][92]. The decay  $K^+ \rightarrow \pi^+ \nu \bar{\nu}$  together with its neutral counterpart completely constrain the unitarity triangle. Measurement of both of these modes should allow one to accurately extract the CKM parameters  $|V_{td}|$ ,  $\eta$  and  $\sin 2\beta$ . There are very few observables of this type, and all of them are needed. Similar clean observables exist in the B system in decays to  $\psi K_S$  ( $\sin 2\beta$ ) and  $\pi\pi$  ( $\sin 2\alpha$ ). By using information from the cleanest K and B decays, unprecedented precision can be achieved for all of the basic CKM parameters. If values of  $\rho$  and  $\eta$  derived from the K and B systems disagree, it would be a definite signal of new physics beyond the Standard Model.

Donoghue reminded us of the importance of measuring the decay  $K_L \rightarrow \pi^0 e^+ e^-$ . He also mentioned some related decay modes which may be backgrounds to  $\pi^0 e^+ e^-$  and which are interesting in their own right.

The decay  $K_L \rightarrow \pi^0 e^+ e^-$  has a CP conserving component, an indirect CP violating component and a direct CP violating component. The direct CP violating component is of primary interest and could be the largest of the three [93]. The branching ratio for this decay is predicted to be on the order of  $10^{-12}$  and the current best limits on the decay are at the  $10^{-9}$  level [94]. Once detected, untangling the various contributions to the decay, particularly in the presence of the attendant background from the radiative Dalitz decay of the kaon,  $K_L \rightarrow e^+ e^- \gamma \gamma$ , is a significant experimental challenge. Donoghue pointed out that there could be a significant electron asymmetry present, of the form

$$A = \frac{N(E_+ > E_-) - N(E_+ < E_-)}{N(E_+ > E_-) + N(E_+ < E_-)} \quad (6.1)$$

which would signal the interference of the CP violating and CP conserving amplitudes. The importance of measuring the branching ratio of the decay  $K_S \rightarrow \pi^0 e^+ e^-$  as a means of understanding the indirect CP violating component of  $K_L \rightarrow \pi^0 e^+ e^-$  was also pointed out.

Donoghue also called our attention to a new decay,  $K_L \rightarrow \pi^0 \gamma e^+ e^-$ , which might serve as an additional background to  $K_L \rightarrow \pi^0 e^+ e^-$ . The radiative decay  $K_L \rightarrow \pi^0 \gamma e^+ e^-$  is a power of  $\alpha$  larger than the nonradiative decay  $K_L \rightarrow \pi^0 e^+ e^-$  and is interesting in its own right in connection to chiral perturbation theory through its relationship to  $K_L \rightarrow \gamma \gamma$ .

### 6.3 Current Status of KTeV

The KTeV Beam line and detector, which represent significant improvements over what had been available for previous experiments, were both newly constructed for the 1996-1997 fixed target run. Both the beam line and detector were commissioned during the Summer of 1996 and physics quality data was being collected by the Fall of 1996. A schematic picture of the KTeV detector (E832 configuration) is shown in Figure 6.1.

A review of the current status of KTeV, as of the date of this Workshop, follows in the sections below. The KTeV detector, with appropriate upgrades over time, will evolve into



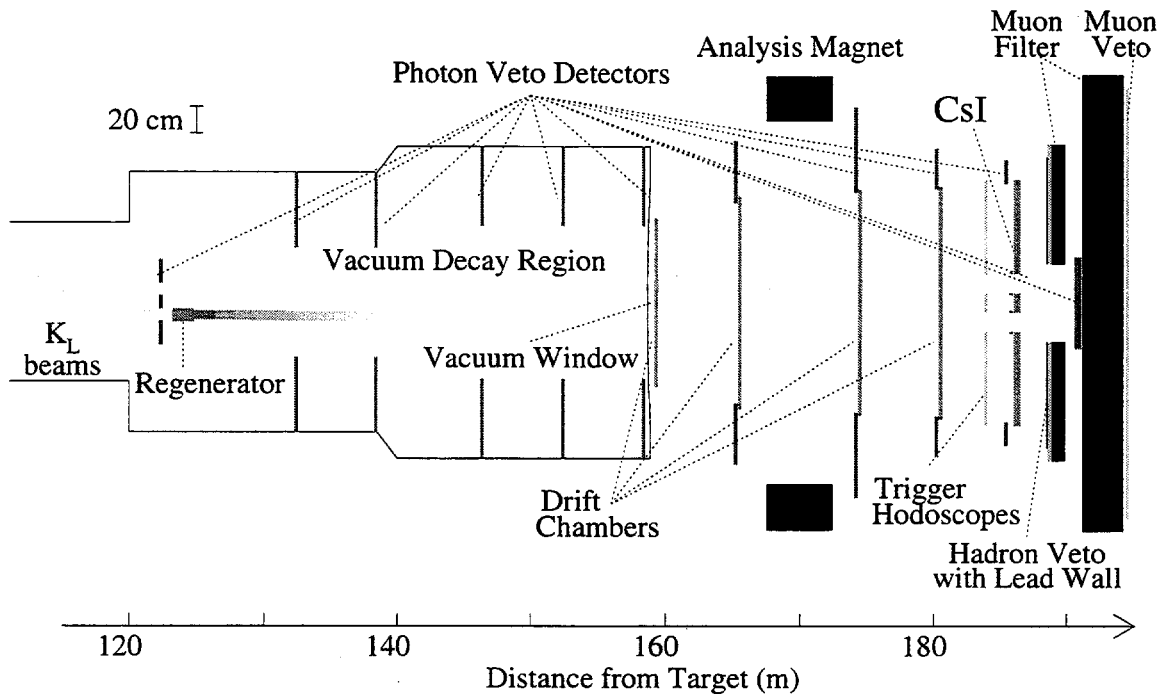


Figure 6.1: Plan view of KTeV detector (E832 configuration) The horizontal scale has been highly compressed relative to the vertical scale.

the KAMI detector. The status and eventual degree of success of KTeV is a good baseline from which to project to the ultimate degree of success of the KAMI project.

### 6.3.1 Measurement of $\epsilon'/\epsilon$ - E832

E731's measurement of  $\text{Re}(\epsilon'/\epsilon)$  gave a result of  $(7.4 \pm 5.2 \pm 2.9) \times 10^{-4}$  [95], for an overall uncertainty of about  $7 \times 10^{-4}$  dominated by the statistical error of  $5.2 \times 10^{-4}$ . The original goal of KTeV is to reach an overall accuracy (statistical + systematic) of  $1.0 \times 10^{-4}$ . This requires many millions of reconstructed decays with exceptionally good control of systematics.

Data for E832 has been collected at a rate which is more than 10 times faster than E731. On the average, 0.25 million  $K_L \rightarrow 2\pi^0$  events are collected, after offline cuts, for each good week's worth of running (about 130 hours of useful beam). We expect to collect about 5 million  $K_L \rightarrow 2\pi^0$  events, our statistically limiting decay mode, during the 1996-97 run. This will result in a statistical uncertainty of about  $1.2 \times 10^{-4}$ .

Since the data has not yet been fully analyzed the systematic error can only be guessed at. The goal is to reduce the systematic error to about half of the statistical error. This may require a few years of concerted effort.

Besides the  $\epsilon'/\epsilon$  measurement, the current E832 data will result in significantly improved measurements of the the regeneration phase,  $\Delta m$ ,  $\Delta\phi$ ,  $\phi_{+-}$ ,  $K_L \rightarrow \pi^+\pi^-\gamma$ ,  $K_L \rightarrow \pi^0\gamma\gamma$ , the  $K_{e3}$  charge asymmetry, as well as some rare  $K_S$  decay searches.

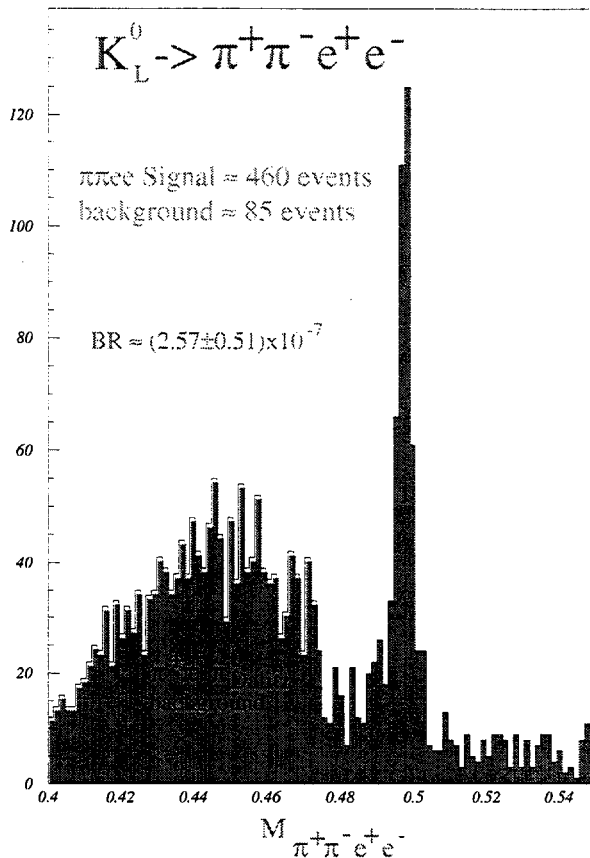


Figure 6.2: Mass peak from the first observation of  $K_L \rightarrow \pi^+\pi^-e^+e^-$ .

### 6.3.2 Rare Kaon Decays - E799

As an example of what can be expected from E799-II, we summarize in Table 6.1 the expected SES, the 90% confidence limit on branching ratios, the measured branching ratios or the number of events expected for some major decay modes. The last column of the table includes the data KTeV expects to collect during an anticipated run in 1999. It is worth noting that a single day of data for the decay mode  $K_L \rightarrow \pi^0 e^+ e^-$  in KTeV is equivalent to half of the entire E799 phase I run during 1992.

In the present run of KTeV, the previously undetected decay  $K_L \rightarrow \pi^+\pi^-e^+e^-$  has been definitively observed [105]. We show in Fig. 6.2 the mass peak from approximately 3 weeks of running. Approximately 460 events are observed in the peak over a background of 85 events for this data sample. A preliminary branching ratio of  $(2.57 \pm 0.51) \times 10^{-7}$  has been measured based on one day of data taking.

We expect to accumulate  $\approx 7500$  additional  $K_L^0 \rightarrow \pi^+\pi^-e^+e^-$  during a KTeV run in 1999. Thus, the indirect CP violation asymmetry will be measured with a statistical error of  $\approx 1\%$  using the total data from the 1997 and 1999 runs ( $\approx$  one half the expected statistical error of the 1997 run).

Moreover, the factor of three increase in statistics afforded by a 1999 run will allow the study of the asymmetry (and other features of the  $\pi\pi e e$  decay) as a function of the various kinematic variables of the decays such as  $M_{ee}$ ,  $M_{\pi\pi}$  and  $\sin\phi\cos\phi$ .

Decay Mode	Previous Experiments	Previous Exp. Results	KTeV97	KTeV97 + KTeV99
$K_L \rightarrow \pi^0 e^+ e^-$ SES 90% CL	E799-I [94]	$1.8 \times 10^{-9}$ $< 4.3 \times 10^{-9}$	$5.0 \times 10^{-11}$ $< 2.5 \times 10^{-10}$	$1.3 \times 10^{-11}$ $< 8.5 \times 10^{-11}$
$K_L \rightarrow \pi^0 \mu^+ \mu^-$ SES 90% CL	E799-I [96]	$2.2 \times 10^{-9}$ $< 5.1 \times 10^{-9}$	$7.0 \times 10^{-11}$ $< 1.6 \times 10^{-10}$	$1.8 \times 10^{-11}$ $< 4.0 \times 10^{-11}$
$K_L \rightarrow \pi^0 \nu \bar{\nu}$ SES ( $\pi^0 \rightarrow e^+ e^- \gamma$ ) 90% CL	E799-I [97]	$2.5 \times 10^{-5}$ $< 5.8 \times 10^{-5}$	$7.5 \times 10^{-8}$ $< 1.7 \times 10^{-7}$	$1.6 \times 10^{-8}$ $< 3.8 \times 10^{-8}$
$K_L \rightarrow \pi^0 \nu \bar{\nu}$ SES ( $\pi^0 \rightarrow \gamma \gamma$ ) 90% CL	None	- -	$4.4 \times 10^{-7}$ $< 1.8 \times 10^{-6}$	$1.1 \times 10^{-9}$ $< 2.5 \times 10^{-9}$
$K_L \rightarrow \pi^+ \pi^- e^+ e^-$ $\delta\phi_{asym}$	None	- -	2000 events 2.2%	8000 events 1.1%
$K_L \rightarrow e^+ e^- e^+ e^-$	E799-I [98]	29 events $(4.0 \pm 0.8) \times 10^{-8}$	260 events	1000 events
$K_L \rightarrow e^+ e^- \mu^+ \mu^-$	E799-I [99]	1 event $(2.9_{-2.4}^{+6.7}) \times 10^{-9}$	35 events	140 events
$\pi^0 \rightarrow e^+ e^- e^+ e^-$	BNL [100]	146 events $(3.2 \pm 0.3) \times 10^{-5}$	20000 events	80000 events
$K_L \rightarrow e^+ e^- \gamma$	BNL [101] CERN [102]	1k events $(9.2 \pm 0.5) \times 10^{-6}$	120k events	480k events
$K_L \rightarrow e^+ e^- \gamma \gamma$	E799-I [103]	58 events $(6.5 \pm 1.3) \times 10^{-7}$	3000 events	12000 events
$K_L \rightarrow \mu^+ \mu^- \gamma$	E799-I [104]	207 events $(3.2 \pm 0.3) \times 10^{-7}$	9000 events	36000 events

Table 6.1: Expected single event sensitivity (SES), 90% CL on the branching ratio, the measured branching ratio or the number of events for various decay modes to be studied in KTeV.

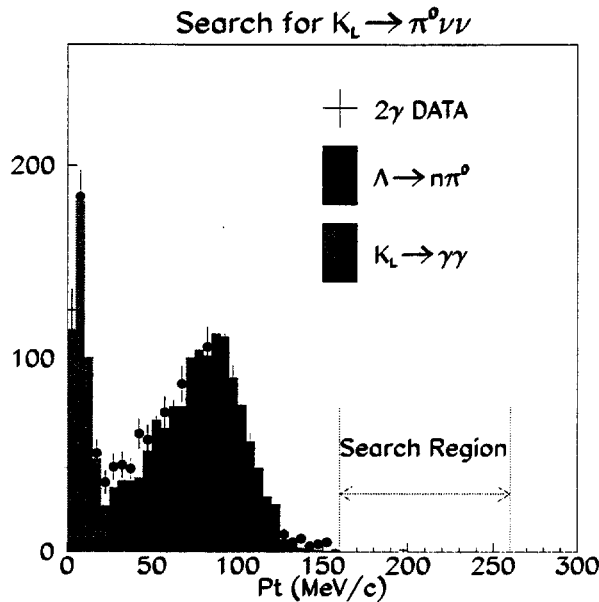


Figure 6.3:  $P_t$  distribution of  $K_L \rightarrow \pi^0 \nu \bar{\nu}$  candidate events using the  $2\gamma$  decay mode of the  $\pi^0$  during a special 1 day run in December of 1996.

$$K_L \rightarrow \pi^0 \nu \bar{\nu}$$

Although the best limit for this mode from KTeV in the 1997 run will come from the full analysis of the  $\pi^0$  Dalitz mode ( $\pi^0 \rightarrow e^+ e^- \gamma$ ), we are also investigating the  $2\gamma$  decay mode. The  $2\gamma$  mode provides us with more than two orders of magnitude higher sensitivity per unit time, but at the cost of increased background due to fewer kinematical constraints. This study is important input to the design of the KAMI detector whose ultimate goal is the detection of this signal.

To understand the type and level of backgrounds we will ultimately be confronted with, a special half-day of data was taken in December 1996. During this special run, one beam was further collimated down to 4 cm x 4 cm (at the CsI). The second beam was completely closed off. This beam configuration was used in order to accurately measure the transverse momentum ( $P_t$ ) of the  $\pi^0$ , which is the only observable kinematical variable from the  $\pi^0 \rightarrow 2\gamma$  decay. The beam size must be carefully selected to balance the increased rate from a big beam versus the improved  $P_t$  resolution and the subsequent reduction in backgrounds from a small beam. From a preliminary analysis, we have obtained an upper limit on the branching ratio of  $1.8 \times 10^{-6}$  at a 90% CL [108]. This represents a factor of 30 improvement over the best existing limit, obtained by E799-I using the Dalitz decay mode of the  $\pi^0$  [97].

Figure 6.3 shows the  $P_t$  distribution of candidate events after the final cuts. As is shown here, the observed  $P_t$  distribution can be well reproduced by  $K_L \rightarrow 2\gamma$  and  $\Lambda \rightarrow n\pi^0$ . For  $P_t$  values above 160 MeV/ $c^2$ , one event still remains. We are currently investigating this remaining event.

KTeV intends to extend this measurement even farther during an anticipated run in

1999. With the addition of some photon veto counters we expect to achieve a sensitivity of  $1.0 \times 10^{-9}$  in 4 weeks of dedicated running using the same beam configuration as in 1996.

## 6.4 Kaon Physics at the Main Injector

The central issue for this working group was the evolution of the existing KTeV program into the future Main Injector program known as KAMI (Kaons At the Main Injector). The concept of using the Main Injector as a source of high-intensity kaons predates the KTeV program [109]. KTeV was designed with this eventual evolution in mind.

The Main Injector makes it possible to carry out a whole new generation of neutral kaon experiments with sensitivities not previously attainable. Although the energy of the Main Injector is not as high as the Tevatron, it is still quite high relative to other kaon facilities around the world. Additionally, the the proton intensity of the Main Injector is two orders of magnitude greater than the Tevatron. This high flux of protons allows for the construction of well-defined, high-intensity neutral kaon beams. This combination of high energy and high intensity will make it possible to probe with ever greater precision and sensitivity the fundamental questions of CP violation and rare decays.

In Table 6.2 the essential beam parameters are listed for KTeV and two KAMI scenarios; KAMI-far and KAMI-near. The KAMI-far scenario brings Main Injector Beam onto the existing KTeV target which is 186 m upstream of the CsI calorimeter. In the KAMI-near scenario, a new target station is built in the KTeV detector hall, downstream of the existing target. In both scenarios, the existing KTeV detector is squeezed to account for the lower momentum kaons. The target position defines the origin of the coordinate system (0,0,0).

KAMI will likely begin with a 24 mrad targeting angle in order to minimize the number of neutrons into the Back Anti, the veto counter which sits in the beam hole downstream of the CsI. It is possible that KAMI will eventually move to an 8 mrad targeting angle, resulting in a significantly higher rate of kaon decays as well as significantly more neutrons. The steeper targeting angle also results in higher energy gamma rays incident on the photon veto detectors, which increases the efficiency for detection.

## 6.5 $K_L \rightarrow \pi^0 \nu \bar{\nu}$ at KAMI

Once a precise measurement of  $\text{Re}(\epsilon'/\epsilon)$  has been completed, it seems clear that the most important remaining issues in kaon physics become the measurement of the branching ratio of  $K_L \rightarrow \pi^0 \nu \bar{\nu}$  and  $K^+ \rightarrow \pi^+ \nu \bar{\nu}$ . The theoretical case for these measurements was made at this workshop by both Wolfenstein and Buchalla. The main focus of this working group is to determine how to detect the neutral decay and measure its branching ratio.

### 6.5.1 Detector Requirements for $K_L \rightarrow \pi^0 \nu \bar{\nu}$

In order to understand the level of detector performance required in order to perform the  $\pi^0 \nu \bar{\nu}$  measurement at KAMI, an extensive Monte Carlo simulation is required. Arisaka reported on the status of these studies.

	KTeV	KAMI-Far	KAMI-Near
Proton Energy	800 GeV	120 GeV	120 GeV
Intensity per pulse	3-5E12	1-3E13	1-3E13
Repetition cycle	60 sec	2.9 sec	2.9 sec
Flat top	20 sec	1.0 sec	1.0 sec
Targeting angle	4.2 mrad	24 mrad	8 mrad
Beam x width	0.54 mrad	0.54 mrad	1.8 mrad
Beam y width	0.54 mrad	0.54 mrad	1.8 mrad
No. of beams	2	1	1
Beam solid angle	0.54 $\mu$ str	0.29 $\mu$ str	3.2 $\mu$ str
CsI position	186 m	186 m	54 m
Decay Volume	90-160 m	153-173 m	20-40 m
$K_L$ decays	0.7 MHz	1.2 MHz	36 MHz
Average Kaon momentum	70 GeV	15 GeV	26 GeV
Neutron flux	55 MHz	25-140 MHz	2600-15000 MHz

Table 6.2: Beam parameters for the KTeV and KAMI beams. KAMI-near and KAMI-far are defined in the text.

With a reasonable beam size (0.29  $\mu$ str - KAMI-Far) a single event sensitivity of  $10^{-13}$  per year appears possible. This would result in 20-30 events per year, based on Standard Model predictions for the branching ratio. The real challenge is to accurately predict the background levels and understand how to minimize them.

The Monte Carlo study thus far has been focused on the background from  $K_L \rightarrow 2\pi^0$ . The branching ratio of this mode is rather low ( $9 \times 10^{-4}$ ), however, the maximum possible  $P_i$  is quite high (209 MeV). Thus, if two photons out of the four are missed, this decay is indistinguishable from the signal. The two photons which miss the CsI are correlated to one another. The most serious case is where one of the missing photons has a large energy ( $>1$  GeV) in the forward direction and the second photon has a low energy ( $<20$  MeV) and a large opening angle. In this case, at least one of the missing photons must be detected by either the Back Anti (BA) or the photon veto system. The level of performance required from various detector elements in order to achieve a Signal/Noise ratio of unity are listed in Table 6.3.

Detector	Energy Range	Inefficiency
Photon Veto	2-20 MeV	$<0.2$
Photon Veto	1-3 GeV	$<10^{-5}$
CsI Calorimeter	3-10 GeV	$<10^{-5}$
Beam Hole Veto (Back Anti)	$>10$ GeV	$<10^{-2}$

Table 6.3: Inefficiency requirements for various KAMI detector components.

This study does not include any additional kinematical constraints such as time-of-flight or the direction of the photons. These kinematical measurements may be helpful in relaxing the inefficiency requirements listed above. These studies are continuing.

A program of R & D to understand the feasibility of building detectors with sufficient efficiency in the appropriate energy regions is essential in order for this program to move forward. Constructing detectors using conventional, inexpensive and reliable technology is of the highest priority.

### 6.5.2 $K_L \rightarrow \pi^0 \nu \bar{\nu}$ at KEK

The current status of an experiment at KEK utilizing the existing 12 GeV proton machine to measure  $K_L \rightarrow \pi^0 \nu \bar{\nu}$  was presented by Inagaki. During the first phase of this experiment it is expected that a sensitivity of  $10^{-10}$  will be achieved by 1999. The KEK experiment is very similar to KAMI conceptually in that extremely good photon veto efficiency is required. The ultimate goal is to perform this measurement with a new 50 GeV high-intensity machine, JHP, which is expected to be operational in 2003.

### 6.5.3 $K_L \rightarrow \pi^0 \nu \bar{\nu}$ at Brookhaven

At BNL, a new proposal for measuring  $K_L \rightarrow \pi^0 \nu \bar{\nu}$  was submitted last year. This experiment proposes to use a micro-bunched proton beam with a 45 degree targeting angle to produce a kaon beam with a mean momentum of 700 MeV/c. The low kaon momentum allows for a time-of-flight measurement. Sufficient kinematical constraints are available in order to reconstruct all four-vectors, including those of the missing neutrinos. The kaon production rate at such a large targeting angle has never before been studied. The primary focus of this group over the next year will be to measure this flux.

### 6.5.4 Future Prospects for $K_L \rightarrow \pi^0 \nu \bar{\nu}$

The Fermilab, KEK and BNL groups all appear to be making reasonable progress. No show-stoppers were reported at this workshop though it is clear that much more work is needed on many fronts. Since all three groups need to develop inexpensive, large area photon veto detectors it was suggested by Inagaki that an international collaboration of detector R & D be organized to make use of the tagged photon test beam channel at INS in Japan.

## 6.6 Other Physics Opportunities at KAMI

### 6.6.1 $\epsilon'/\epsilon$ at KAMI

The final results from the current round of  $\epsilon'/\epsilon$  measurements at Fermilab and CERN will determine whether additional work on this measurement is desirable at the Main Injector. Winstein reported that a statistical accuracy of  $3E-5$  is feasible at the Main Injector in 1 year of running (50% beam efficiency) based on the order of magnitude increase in decay rate.

It was also noted that the regeneration amplitude for the lower energy kaons provided by the Main Injector is seven times higher than the current amplitude in KTeV. Backgrounds

from the regenerator will also likely increase. One way to deal with the additional backgrounds would be to imbed all or part of the regenerator in a magnetic field. This option would require a significant Monte Carlo study to determine its feasibility.

### 6.6.2 $K_L \rightarrow \pi^0 e^+ e^-$ at KAMI

The physics motivation for the decay  $K_L \rightarrow \pi^0 e^+ e^-$  has been stated in the literature many times and was reiterated once again at this workshop by Donoghue.

A Monte Carlo study of this decay mode as well as the background decay  $K_L \rightarrow e^+ e^- \gamma \gamma$  has been performed under three different scenarios in order to understand the magnitude of this experimental challenge in the near future at Fermilab. The three scenarios defined in Table 6.4 below are KTeV, KAMI-far and KAMI-near. These are identical to the scenarios defined earlier, except that in all cases two beams are used, doubling the rates for KAMI-near and KAMI-far.

	Proton Momentum	Protons per Spill	Targ. Angle	Decay Volume	CsI Position	Decay Rate (Mhz)
1. KTeV	800 GeV/c	$4 \times 10^{12}$	4.2 mr	90-160 m	186 m	0.7
2. KAMI-far	120 GeV/c	$1 \times 10^{13}$	24 mr	153-173 m	186 m	2.4
3. KAMI-near	120 GeV/c	$3 \times 10^{13}$	8 mr	20-40 m	54 m	72.

Table 6.4: Definition of the various running scenarios considered for the study of the decay  $K_L \rightarrow \pi^0 e^+ e^-$ . Two beams are used, doubling the rates for KAMI-near and KAMI-far listed in Table 6.2.

In all cases the target is at 0 m. The detector geometry has been squeezed longitudinally in scenarios 2 and 3 to account for the softer kaon spectrum resulting from the less energetic protons and the steeper targeting angles. The squeezed detector configuration studied thus far is shown in Figure 6.4. The rate of kaon decays in the appropriate decay volume has been calculated using a  $K_L$  spectrum which results from the Malensek parameterization [110] with a beam size defined to be 9.3 cm x 9.3 cm at the distance of the CsI calorimeter. The resulting decay rates are calculated on-spill and the duty factor in all cases is 1/3.

The KTeV Monte Carlo has evolved over several generations of neutral kaon experiments. It includes a full detector and trigger simulation. A uniform phase space generator is used to produce  $\pi^0 e^+ e^-$  events.  $e^+ e^- \gamma \gamma$  events are generated using the matrix elements which result from evaluation of the Feynman diagrams for  $K_L \rightarrow e^+ e^- \gamma$  with radiative corrections leading to  $K_L \rightarrow e^+ e^- \gamma \gamma$ . An infrared cutoff of 5 MeV is used for evaluation of the branching ratio.

Aside from  $K_L \rightarrow e^+ e^- \gamma \gamma$ , there are a number of other potential backgrounds which were studied extensively in preparation for KTeV. Using the set of cuts described in reference [94], these other backgrounds are all suppressed to tolerable levels [111]. An additional cut of  $\pm 2$  MeV around the  $\pi^0$  mass is imposed to reduce the background from  $e^+ e^- \gamma \gamma$ . The product of



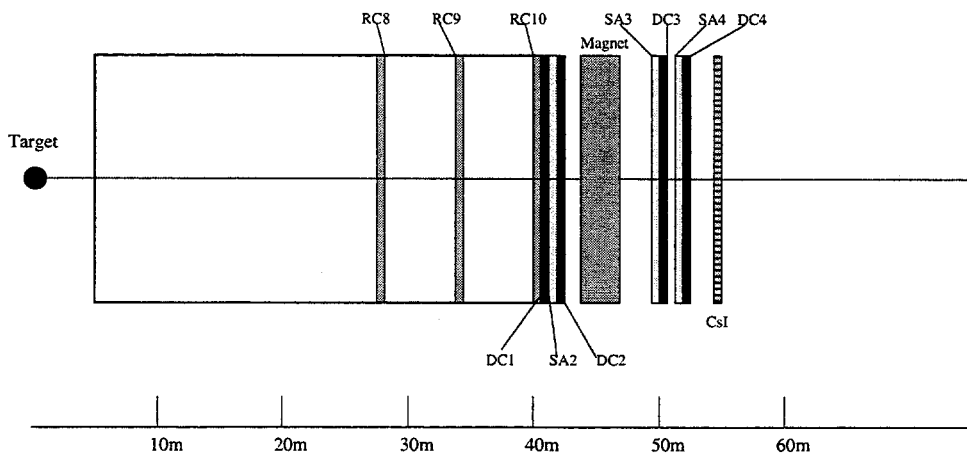


Figure 6.4: The KAMI “Squeezed” Geometry Detector.

detector acceptance and cut efficiencies are listed in Table 6.5 below for the various scenarios considered.

	$\pi^0 e^+ e^-$ Efficiency	$e^+ e^- \gamma \gamma$ Efficiency
KTeV	0.030	$1.2 \times 10^{-4}$
KAMI-far	0.020	$9.9 \times 10^{-5}$
KAMI-near	0.016	$5.9 \times 10^{-5}$

Table 6.5: Efficiencies for  $K_L \rightarrow \pi^0 e^+ e^-$  and  $e^+ e^- \gamma \gamma$  for the various beam scenarios. Efficiency in this case is the product of detector acceptance and analysis cuts.

Further reductions in the background from  $K_L \rightarrow e^+ e^- \gamma \gamma$  require the use of additional phase-space fiducial cuts which differentiate between the signal and background. This procedure is described in detail in reference [112] where, for a given signal efficiency  $\epsilon_{\pi^0 ee}$  the background efficiency  $\epsilon_{ee\gamma\gamma}$  is made as small as possible. The phase-space cuts which maximize the signal-to-background correspond to efficiencies for  $K_L \rightarrow \pi^0 e^+ e^-$  and  $K_L \rightarrow e^+ e^- \gamma \gamma$  of 0.40 and 0.0039, respectively [113]. Using the measurement of  $\text{BR}(K_L \rightarrow e^+ e^- \gamma \gamma, E_\gamma^* \geq 5 \text{ MeV}) = 6.5 \times 10^{-7}$  [113], the phase-space cut efficiency and the acceptance and analysis efficiencies, we arrive at the single event sensitivities and the number of  $e^+ e^- \gamma \gamma$  background events reported in Table 6.6.

The predicted background level depends, through the matrix elements mentioned above, on the  $e^+ e^- \gamma \gamma$  form factor. The need for a better measurement of this form factor is clear. If  $K_L \rightarrow \pi^0 e^+ e^-$  occurs at about the predicted branching ratio, it is unlikely that there will ever be a measurement of the decay with negligible background. It is clear that the decay can be detected as a peak at the  $\pi^0$  mass on top of a broad  $M_{\gamma\gamma}$  background distribution. In the case of KAMI-near, a  $3\sigma$  measurement is obtained for a  $K_L \rightarrow \pi^0 e^+ e^-$  branching ratio

	Running Time	$K_L$ decays ( $\times 10^{12}$ )	SES for $\pi^0 e^+ e^-$	Background Events From $e^+ e^- \gamma \gamma$
KTeV	15 weeks	1.16	$7.2 \times 10^{-11}$	0.34
KAMI-far	1 year	8.8	$1.4 \times 10^{-11}$	1.3
KAMI-near	1 year	540	$2.9 \times 10^{-13}$	134.

Table 6.6: Single event sensitivities and the number of  $e^+ e^- \gamma \gamma$  background events from the study of  $K_L \rightarrow \pi^0 e^+ e^-$ .

of  $10^{-11}$ . Untangling the various CP conserving and CP violating components of the decay in the presence of this background will be a complex and difficult task, however. Only at a facility such as the Main Injector, where large kaon fluxes are possible, can one even begin to contemplate such a task.

A new potential background,  $K_L \rightarrow \pi^0 \gamma e^+ e^-$ , has recently been identified by Donoghue and Gabbiani [114] with a predicted branching ratio of  $2.3 \times 10^{-8}$ . How this decay contributes as a background for  $K_L \rightarrow \pi^0 e^+ e^-$  ultimately depends on the spectrum of the radiative photon and the mass spectrum of the  $e^+ e^-$  pair. This decay mode is currently under study in KTeV.

### 6.6.3 $\pi^+ \pi^- e^+ e^-$ at KAMI

One of the strong interests in the just recently observed decay  $K_L^0 \rightarrow \pi^+ \pi^- e^+ e^-$  mode is the prospect for observing CP violation effects as predicted in Ref. [106]. This decay can proceed via the four processes shown in Fig. 6.5. The interference of the *indirect* CP violation Bremsstrahlung process (Fig. 6.5a) with the CP conserving M1 emission of a virtual photon (Fig. 6.5b) is expected to generate an asymmetry in the angle  $\phi$  between the normals to the decay planes of the  $e^+ e^-$  and the  $\pi^+ \pi^-$  in the  $K_L^0$  center of mass. In addition, *direct* CP violation effects, albeit small, can occur in this mode via the interference of the weak process of Fig. 6.5c with the other three amplitudes and be manifested in asymmetries in the functions of the angle  $\theta$ .

We show in Fig. 6.6 the angles in which the indirect and direct CP violation asymmetries are expected to be observed. The angular distribution as a function of  $\phi$  and  $\theta$ , where  $\theta$  is the angle of the positron with respect to the direction of the  $M_{\pi\pi}$  cms in the  $M_{ee}$  cms, is given by

$$\frac{d\Gamma}{d\cos\theta d\phi} = K_1 + K_2 \cos 2\theta + K_3 \sin^2 \theta \cos 2\phi + K_4 \sin 2\theta \cos 2\phi + K_5 \sin \theta \cos \phi \\ + K_6 \cos \theta + K_7 \sin \theta \cos \phi + K_8 \sin 2\theta \sin \phi + K_9 \sin 2\theta \sin 2\phi.$$

The  $K_4$ ,  $K_7$  and  $K_9$  terms are the ones in which CP violation is expected to appear. The  $K_7$  term is where direct CP violation would occur. Ignoring small terms and integrating over  $\theta$ , the  $\phi$  angular distribution is obtained:

# The Physics of $K \rightarrow \pi\pi ee$

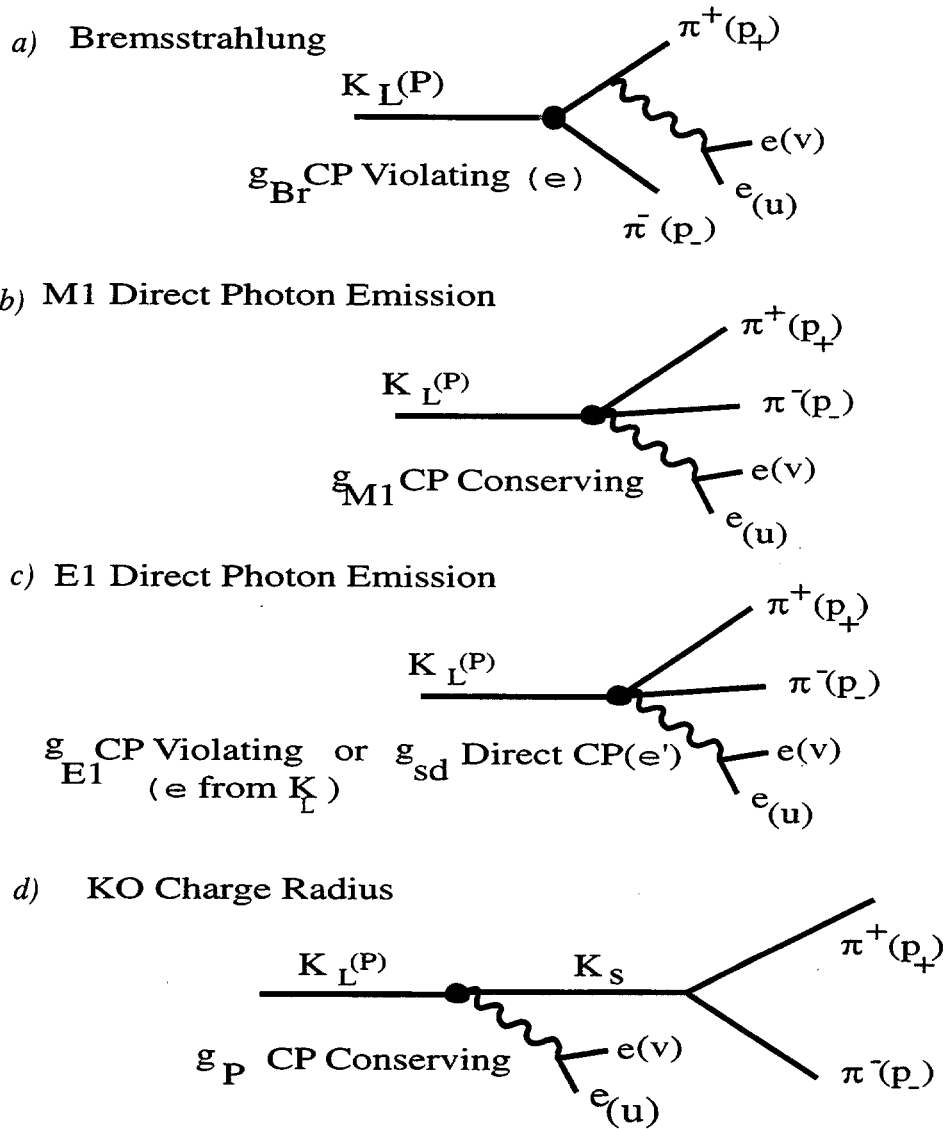
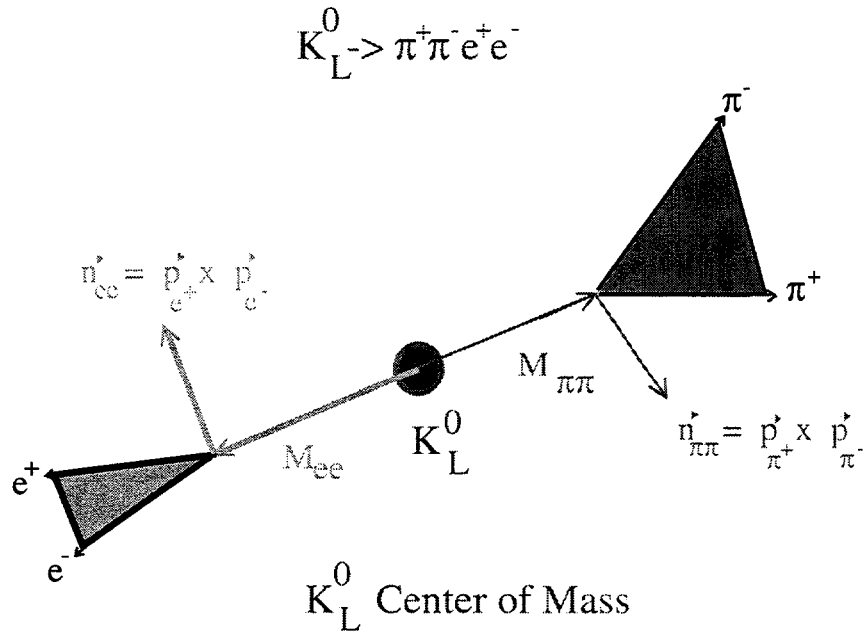


Figure 6.5: Contributing Diagrams for the decay  $K_L^0 \rightarrow \pi^+\pi^-e^+e^-$ .



= angle between the normals to the  $ee$  and  $\pi\pi$  planes

This angle lies in the plane perpendicular to the  $M_{ee}$  and  $M_{\pi\pi}$  vectors

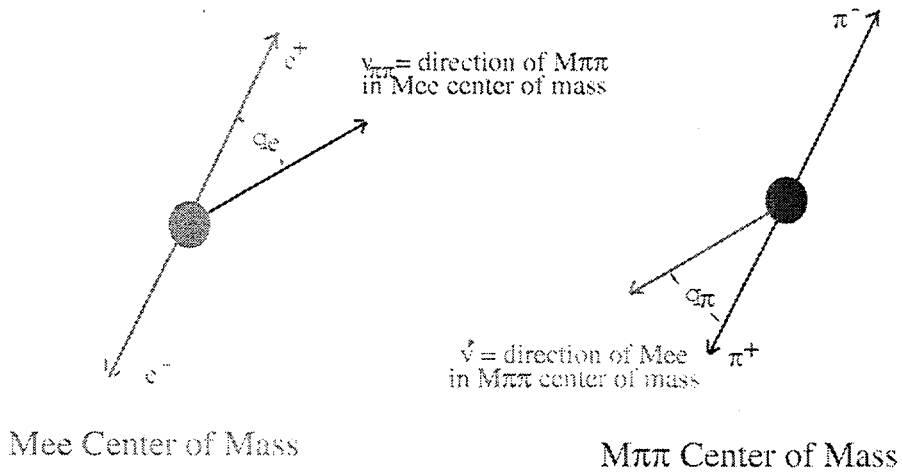


Figure 6.6: Angles in which indirect and direct CP violation asymmetries may be seen.

$$\frac{d\Gamma}{d\phi} = \Gamma_1 \cos^2 \phi + \Gamma_2 \sin^2 \phi + \Gamma_3 \sin \phi \cos \phi.$$

An asymmetry in the  $\sin\phi\cos\phi$  distribution will signal the presence of indirect CP violation. This would be the *fourth* evidence for indirect CP violation observed in 35 years and the *first* manifestation of CP violation in a dynamic variable. The expected  $\sin\phi\cos\phi$  angular distribution calculated using the various parameters of the CP violating  $K_L^0 \rightarrow \pi^+\pi^-$  decay and the branching ratio [116] for  $K_L^0 \rightarrow \pi^+\pi^-\gamma$  (which sets the strength of the M1 photon emission) is shown in Fig. 6.7a for a 50,000 event MC sample. An asymmetry of 13.1% is expected between  $\sin\phi\cos\phi \geq 0$  and  $\sin\phi\cos\phi \leq 0$  for events which fall within the detector acceptance.

The ultimate study of asymmetries in  $K_L^0 \rightarrow \pi^+\pi^-e^+e^-$  will take place in KAMI in the Main Injector era. The extremes of proton and  $K_L^0$  beam targeting configurations and the required “squeezed” KTeV spectrometer under study are briefly described below.

The acceptance of the KAMI “squeezed” spectrometer configuration has been determined from MC simulations to be 7.4% for  $K_L^0 \rightarrow \pi^+\pi^-e^+e^-$ . Assuming the reconstruction efficiency of the KAMI spectrometer to be similar to that of the present KTeV spectrometer (20.6%), the yields of  $K_L^0 \rightarrow \pi^+\pi^-e^+e^-$  for the various levels of trigger and analysis for the “far” and “near” configurations are as shown in Table 6.6.3 below. This assumes a 70% Main Injector efficiency and 200 days of operation per year.

Targeting Configuration	“far”	“near”
$K_L^0/\text{yr}$ in fiducial region	$9 \times 10^{12}$	$2.9 \times 10^{14}$
$K_L^0 \rightarrow \pi^+\pi^-e^+e^-/\text{yr}$ in fid. region	$2.5 \times 10^6$	$7.5 \times 10^7$
$K_L^0 \rightarrow \pi^+\pi^-e^+e^-/\text{yr}$ through L2	$1.8 \times 10^5$	$5.5 \times 10^6$
$K_L^0 \rightarrow \pi^+\pi^-e^+e^-/\text{yr}$ reconstructed	$3.7 \times 10^4$	$1.1 \times 10^6$

Table 6.7: Yields of  $K_L^0 \rightarrow \pi^+\pi^-e^+e^-$  in KAMI

We show in Fig. 6.8 the expected precision with which an indirect CP violation asymmetry of a given magnitude in  $\sin\phi\cos\phi$  can be measured in KTeV97, KAMI “far” and KAMI “near” configurations. As one can see, the best that one can do at the theoretical expectation of  $\approx 12\%$  is 2% using the present 2,500 KTeV97 events as compared to 0.4% and 0.08% using the 37,000 and 1,100,000 KAMI “far” and KAMI “near” event yields, respectively. In addition, the ability to study variations of asymmetries with kinematic variables such as  $M_{\pi\pi}$  and  $M_{ee}$  which can be studied well only with increased statistics will be greatly enhanced in the KAMI experiment.

KAMI will greatly increase the sensitivity for studies of the indirect CP violation effects expected in the  $K_L^0 \rightarrow \pi^+\pi^-e^+e^-$  mode. In addition, although direct CP violation effects in due to Standard Model CKM phase in  $K_L^0 \rightarrow \pi^+\pi^-e^+e^-$  decay are expected to be small, the increased statistics from the KAMI over a period of years will allow much more sensitive

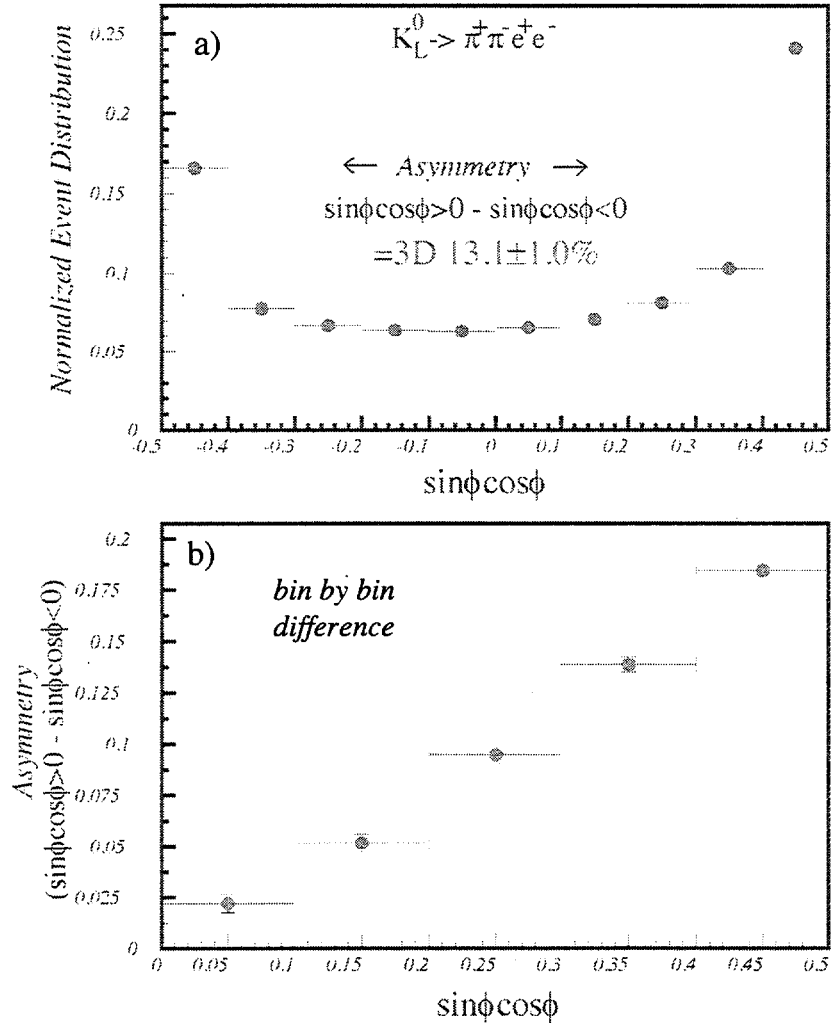


Figure 6.7: (a) The  $\sin\phi\cos\phi$  angular distribution, (b) bin by bin asymmetry between  $\sin\phi\cos\phi \geq 0$  and  $\sin\phi\cos\phi \leq 0$ .

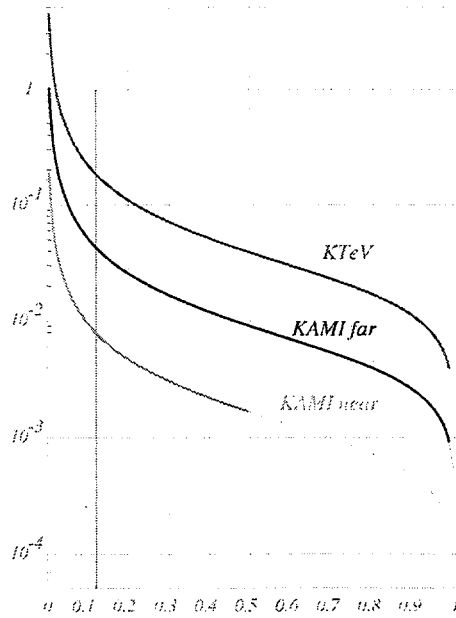


Figure 6.8: The asymmetry vs the percent error in asymmetry for the KTeV, KAMI-far and KAMI-near scenarios.

studies of the more complex, joint  $\theta, \phi$  correlations in which the direct CP violation asymmetries are expected to be manifested. Sensitivity of searches for more exotic, non standard CP violation sources will also be greatly increased.

## 6.7 KAMI Detector

While the decay mode  $K_L \rightarrow \pi^0 \nu \bar{\nu}$  will be the highest priority of the KAMI program, there is a wide array of other decay modes which will be accessible and which offer important and interesting insights into the question of CP violation and provide tests of the Standard Model. In order to measure  $K_L \rightarrow \pi^0 \nu \bar{\nu}$  a high-efficiency, hermetic photon veto system is required along with the existing high-resolution CsI calorimeter. A charged particle spectrometer using the existing KTeV analysis magnet and upgraded tracking detectors is required for all other modes, as well as for calibrating the CsI. Particle ID is also required for some modes.

The afternoon session of the Workshop's second day was devoted to detector technology to cover the latest developments in this area. This was a joint session with the charged kaon group and the detector group.

### 6.7.1 CsI Calorimeter

The KTeV CsI calorimeter is the most advanced, high-precision electromagnetic calorimeter currently in use. The calorimeter consists of 3100 pure CsI crystals which come in two sizes:  $2.5 \times 2.5 \times 50 \text{ cm}^3$  and  $5.0 \times 5.0 \times 50 \text{ cm}^3$ . The 50 cm length corresponds to 27 radiation lengths. Each crystal has an individually optimized wrapping in order to produce a uniform

response longitudinally along the crystal. The crystals are read out using photomultiplier tubes and the signals are digitized at the PMT base in 19 ns time slices, in synch with the RF structure of the beam. The digitizer is a multi-ranging device with 16 bits of dynamic range in the form of an 8-bit mantissa and a 3-bit exponent. The noise per channel is about 8 fC which corresponds to about 0.8 MeV. The digitized signals flow through a digital pipeline to the data acquisition system. The energy resolution of the calorimeter is reported by Roodman to be better than 1% over the energy region of 5 - 100 GeV. Resolution at this level is necessary in order to reject backgrounds to decays such as  $K_L \rightarrow \pi^0 \nu \bar{\nu}$  and  $K_L \rightarrow \pi^0 e^+ e^-$ . Because the KAMI beam will likely be debunched with no real RF structure, the digitization scheme for the readout electronics will have to be modified. No additional modifications should be needed.

### 6.7.2 Photon Veto System

One of the most challenging detector issues facing KAMI is the efficient detection of all photons produced by background events along the approximately 20 m long vacuum decay region. Complete hermeticity and efficient photon detection down to energies as low as 5 MeV are required. A photon veto detector for KAMI will likely be based on the existing KTeV veto design. However, in order to improve detection efficiency for low energy photons, both finer sampling and more scintillation light is required. Tilting the lead sheets by 45 degrees to account for the wide incidence angle of the photons which hit the detector should also help. The cost of such a detector is of primary concern and a good deal of effort has gone into designing a low-cost device.

Progress was reported on an inexpensive polystyrene based scintillator, currently under development by the MINOS collaboration. Both injection molded and extruded polystyrene based scintillator appears to be very promising. The expected material cost is about \$6/kg, an order of magnitude less than the standard plastic scintillator manufactured by conventional means. We plan to develop and test the first prototype during the KTeV 99 run.

The inefficiency of the photon veto counters, particularly for low energy photons, is of critical importance. The inefficiency is dominated by sampling effects, where a significant fraction of the shower electrons are absorbed in the lead, and photonuclear absorption. In the latter case, it is possible for a photon to experience a photonuclear absorption interaction before it begins to shower. If all of the secondary products in the interaction are neutrons, the interaction may escape detection. Photonuclear absorption has been studied extensively in the past in various energy regions [115].

A GEANT simulation of a possible photon veto design shows that with 1 mm lead sheets and 4-5 mm thick scintillator tiles, better than 80% detection efficiency for photons with energies between 2-20 MeV can be achieved. Photonuclear absorption effects still need to be taken into account. More detailed study still appears to be necessary.

### 6.7.3 Fiber tracking

The KAMI fiber tracking system would consist of about 70K channels of 0.5 - 0.8 mm scintillating fibers with a VLPC readout; about the same size as the DO fiber tracker. The



latest developments on this front were shown by Choi from the D0 group. With double layers of 830 micron fibers, about 10 pe per MIP are observed, resulting in a doublet position resolution of 92 micron. The detection efficiency in the presence of a 40 MHz background is >98%. This system would work nicely for KAMI.

## 6.8 Concluding Remarks

This workshop has succeeded in bringing together a large group of people including theorists; experimenters from Fermilab, Brookhaven and KEK; and detector experts. Based on the discussions which took place over several days, we are optimistic that KAMI, like KTeV before it, will be at the frontier of neutral kaon experiments. Excellent physics motivation exists for carrying out this physics program, many key detector components already exist and are currently working well, and the detector technology required for the missing pieces are available at Fermilab. Combined with high-intensity, year-round 120 GeV beam from the Main Injector the result should be an extremely bright future for kaon physics at Fermilab.

## Thursday, May 1

(Morning - Plenary session)

### < Introduction >

2:00 - 2:15	G. Bock	Introduction
2:15 - 2:35	R. Coleman	Main Injector Neutral kaon beam

### < Theory talks - joint session with $K^+$ group >

2:40 - 3:10	G. Buchalla	$K \rightarrow \pi\nu\bar{\nu}$
3:10 - 3:40	J. Donoghue	The radiative complex of rare $K_L$ decays
3:40 - 4:10	A. Kostelecky	CPT tests with neutral-meson systems
4:10 - 4:30	coffee break	

### < Special Interest Talks - Open to the lab-wide Community >

4:30 - 5:00	S. Somalwar	E832 status
5:00 - 5:30	V. O'Dell	E799 status and new results
6:00	Reception	

## Friday, May 2

### < $\pi^0\nu\bar{\nu}$ >

9:30 - 9:50	T. Nakaya	$\pi^0\nu\bar{\nu}$ at KTeV
9:50 - 10:30	K. Arisaka	$\pi^0\nu\bar{\nu}$ at KAMI
10:30 - 11:00	coffee break	
11:00 - 11:30	T. Inagaki	$\pi^0\nu\bar{\nu}$ at KEK
11:30 - 11:45	L. Littenberg	$\pi^0\nu\bar{\nu}$ at BNL
11:45 - 12:30	(Discussion)	
12:30 - 1:30	lunch	

### < Detectors - Joint session with $K^+$ and detector groups >

1:30 - 1:50	A. Roodman	CsI calorimeter at KTeV
1:50 - 2:05	R. Tschirhart	CsI calorimeter readout at KAMI
2:05 - 2:25	B. Hsiung	Photon veto at KTeV
2:25 - 2:45	T. Inagaki	Photon veto at KEK $\pi^0\nu\bar{\nu}$
2:45 - 3:05	S. Choi	D0 upgrade central fiber tracker
3:05 - 3:30	K. Arisaka	Photon veto and fiber tracking at KAMI
3:30 - 4:00	coffee break	
4:00 - 5:00	wine and cheese	

## Saturday, May 3

### < Other physics >

9:00 - 9:30	R. Ray	$\pi^0e^+e^-$ at KAMI
9:30 - 10:00	B. Winstein	Thoughts on further $\epsilon'$ measurements at the Main Injector
10:00 - 10:30	B. Cox	$\pi^+\pi^-e^+e^-$ at KAMI
10:30 - 11:00	coffee break	
11:20 - 12:30	Discussion	
12:30 - 1:30	lunch	
1:30 - 3:30	Discussion	

# Chapter 7

## Summary of the CPT Tests with Kaons Working Group

Reported by G. Thomson, Rutgers and H. White, Fermilab

The "CPT Tests with Kaons" working group at the Main Injector Fixed Target Workshop consisted of a group of physicists interested in developing the concept of an experiment to study tests of CPT symmetry conservation that will be sensitive at the Planck scale, measurements of CP violation parameters for  $K_S$  decays that have never been measured, improved measurements of CP violation parameters in  $K_L$  decays, tests of the  $\Delta S = \Delta Q$  rule, and searches for rare  $K_S$  decays. This experiment has been described previously in a Letter of Intent to Fermilab, and has been designated P894. The physicists in the P894 collaboration come from Fermilab, Rutgers University, TRIUMF, and the University of Wisconsin. Gordon Thomson and Herman White were the co-organizers of the working group.

The  $K_L/K_S$  system forms a finely balanced interferometer that can be effected by small perturbations like CP violation or CPT violation (if it exists). The experiment is designed to maximize this interference to best search for these effects. It consists of an RF-separated  $K^+$  beam that strikes a target at the entrance of a magnetized collimator (called a hyperon magnet) which defines a short neutral beam coming from that target. The  $K^+$ 's make  $K^0$ 's copiously by charge exchange, with only a very small component of  $\bar{K}^0$ 's. This is the situation that maximizes the interference between the  $K_S$  and  $K_L$  decays of the  $K^0$  mesons in the beam. The detector consists of a Vee spectrometer, a lead glass electromagnetic calorimeter, and a muon detector.

The working group focused on the physics of the experiment, the experimental setup, plans for the RF-separated  $K^+$  beam, possible sites for the experiment in the Meson Lab, and on apparatus and magnets that we could borrow.

The CPT theorem is based on the assumptions of locality, Lorentz invariance, the spin-statistics theorem, and the assumption of asymptotically free wave functions. All quantum field theories (including the standard model of the elementary particles) obey CPT symmetry invariance. But there is a theoretical hint of the level at which CPT symmetry might be violated. This comes from the fact that gravity can't be included in a quantum field theory. Many physicists think that there must be a more general theory that has quantum field theory embedded in it. In this more general theory CPT symmetry may be violated.

In fact, one process exists, Hawking radiation, that might violate CPT invariance. Hawking radiation is virtual pair production near the event horizon of a black hole, where one member of the pair escapes from the black hole, the other is retained, and one can't predict which one. So one can prepare the black hole to have carefully controlled net baryon and lepton numbers, but after Hawking radiation occurs one can't predict its state. This violates the quantum mechanical idea of causality, and the conditions for the proof of the CPT theorem are not valid. Stephen Hawking thinks that CPT is violated in Hawking radiation, but Roger Penrose thinks that one can conserve CPT in this process. But the CPT theorem is definitely invalid here.

One expects to see effects of quantum gravity at what is called the Planck scale: at energies of  $M_{Planck}c^2 = \sqrt{\hbar c^5/G} = 1.2 \times 10^{19}$  GeV, or at distances of the order of  $10^{-33}$  cm. Since it is hard to see such effects in ordinary processes, one would look in a place where quantum field theories predict a null effect, then if something is observed it could be ascribed to quantum gravity. Therefore, it would be very interesting to test CPT symmetry conservation at the Planck scale.

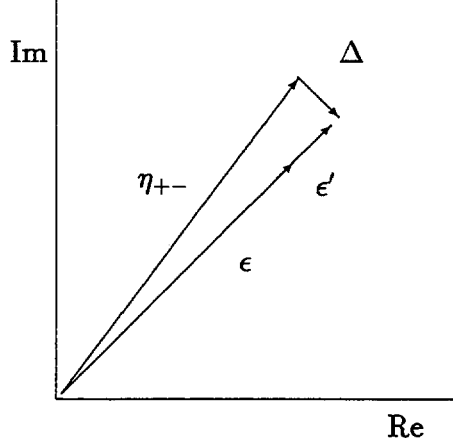
In  $K^0$  physics, one can observe CPT violating effects through mixing or decays (called indirect or direct CPT violation). In mixing, one introduces a parameter  $\Delta$  which is both CP and CPT violating:

$$\begin{cases} K_S = K_1 + (\epsilon + \Delta)K_2 \\ K_L = K_2 + (\epsilon - \Delta)K_1 \end{cases} \quad (7.1)$$

All CP violation seen to date has been through the  $(\epsilon - \Delta)$  term of the  $K_L$ . One can also have direct CPT violation, for example in semileptonic decays, where an amplitude  $y_l$  is introduced that is CPT violating

$$\begin{cases} \langle \pi^- l^+ \nu | T | K^0 \rangle = F_l(1 - y_l) \\ \langle \pi^+ l^- \bar{\nu} | T | \bar{K}^0 \rangle = F_l^*(1 + y_l^*) \end{cases} \quad (7.2)$$

There are several measurements that would signify CPT violation: a difference between the phase of  $\epsilon$  and the phase of  $\eta_{+-}$ , a difference between the phases of  $\eta_{+-}$  and  $\eta_{00}$ , certain interference terms between  $K_L$  and  $K_S$  in semileptonic decays, or evidence for a non-zero  $\Delta$  in the Bell-Steinberger relation. Here we will concentrate on the first method, measuring the phase of  $\eta_{+-}$  and comparing it to the calculated value of the phase of  $\epsilon$ , and comment on the other methods.



The figure above shows the relationships between  $\epsilon$ ,  $\epsilon'$ ,  $\Delta$ , and  $\eta_{+-}$ .  $\epsilon'$  and  $\Delta$  are shown greatly enlarged for clarity. The size of  $|\epsilon'/\epsilon|$  is of order  $10^{-4}$ , and the phase of  $\epsilon'$  is very close to that of  $\epsilon$ , so the phase of the vector  $\epsilon + \epsilon'$  is the same, to good accuracy, to the phase of  $\epsilon$ . We can see from the figure that the component of  $\Delta$  perpendicular to  $\epsilon$ ,  $\Delta_{\perp}$ , is

$$\Delta_{\perp} = |\eta_{+-}|(\phi_{+-} - \phi_{\epsilon}) \quad (7.3)$$

where  $\phi_{+-}$  ( $\phi_{\epsilon}$ ) is the phase of  $\eta_{+-}$  ( $\epsilon$ ). In general, in terms of the elements of the kaon decay matrix  $\Gamma$  and mass matrix  $M$ ,  $\Delta$  is given by:

$$\Delta = \frac{(\Gamma_{11} - \Gamma_{22}) + i(M_{11} - M_{22})}{(\Gamma_S - \Gamma_L) + 2i(M_L - M_S)} \quad (7.4)$$

The mass term has a phase perpendicular to  $\epsilon$  and the decay term is parallel to  $\epsilon$ . We can solve Eqns. 7.3 and 7.4 for  $M_{11} - M_{22}$ , which is the mass difference between the  $K^0$  and  $\bar{K}^0$  mesons:

$$\frac{|M_{K^0} - M_{\bar{K}^0}|}{M_{K^0}} = \frac{2(M_L - M_S)}{M_{K^0}} \frac{|\eta_{+-}|}{\sin \phi_{SW}} |\phi_{+-} - \phi_{\epsilon}| \quad (7.5)$$

where  $\tan \phi_{SW} = 2(M_L - M_S)/(\Gamma_S - \Gamma_L)$ .

In Eqn. 7.5,  $(M_L - M_S)$  is  $10^{-6}$  eV, and when one divides by  $M_{K^0}$  the ratio is of order  $10^{-15}$ .  $|\eta_{+-}|$  is of order  $10^{-3}$ . **These factors let us approach the Planck scale at current accelerator energies.**

The best experimental limit on CPT violation came from Fermilab experiment E773. This limit is (at 90% confidence level),

$$\frac{|M_{K^0} - M_{\bar{K}^0}|}{M_{K^0}} < 1.3 \times 10^{-18} \quad (7.6)$$

By the Planck scale we mean

$$\frac{|M_{K^0} - M_{\bar{K}^0}|}{M_{K^0}} = \frac{M_{K^0}}{M_{Planck}} = 4.1 \times 10^{-20} \quad (7.7)$$

so the E773 result stands at 31 times the Planck scale.

In the KTeV experiment we expect to make an improvement of a factor of 3 to 5. But the interference term from which  $\phi_{+-}$  is measured,  $2|\eta_{+-}||\rho| \cos(\Delta mt + \phi_\rho - \phi_{+-}) \exp(-t/2\tau_s)$ , is reduced by the regeneration amplitude  $|\rho| \simeq 0.03$ , and  $\phi_{+-}$  and  $\phi_\rho$  are hard to disentangle. Using the regeneration method will be difficult beyond the KTeV level.

After the KTeV experiment we expect to stand a factor of 6 to 10 above the Planck scale. To close that gap we will want to do an interference experiment near the kaon production target. The interference term is then  $2D|\eta_{+-}| \cos(\Delta mt - \phi_{+-}) \exp(-t/2\tau_s)$ . Here  $\phi_{+-}$  appears alone, and  $|\rho|$  is replaced with the dilution factor,  $D = (K^0 - \bar{K}^0)/(K^0 + \bar{K}^0)$  at the target. To maximize D and hence the interference, we choose to make our  $K^0$  beam from a  $K^+$  beam by charge exchange. Then at medium to high Feynman x,  $D \simeq 1$ . The charge exchange cross section is large, about 20% of the total cross section. To maximize the flux of  $K^+$  made from the 120 GeV/c protons from the Fermilab Main Injector we choose a  $K^+$  momentum of 25 GeV/c. We would use a hyperon magnet to define the  $K^0$  beam, similar to the one in the Proton Center beam line. In the calculations described below we will assume the use of a vee spectrometer and a lead glass electromagnetic calorimeter.

In E773 we measured  $\phi_{+-}$  to 1 degree accuracy. To reach the Planck scale we must achieve 0.03 degree accuracy.

We have calculated the statistical sensitivity of the experiment making the following assumptions:

- A beam of  $2 \times 10^8 K^+$  per spill, striking a 10 cm tungsten target at 9 mrad, for  $1 \times 10^7$  seconds, with the spill structure of the Fermilab Main Injector.
- The measured charge exchange cross sections.
- A solid angle of  $36 \mu\text{ster}$  for the  $K^0$  beam, the same as in beams described in the KAMI Design Report.
- A hyperon magnet 1.3 meters thick.
- A decay region 13.7 meters long, followed by a vee spectrometer and lead glass electromagnetic calorimeter.

We calculated the acceptance using a Monte Carlo program. We calculated the distribution of events in momentum and proper time for the resulting 15 billion events. We fit this distribution using MINUIT. The fitting parameters were  $|\eta_{+-}|$ ,  $\phi_{+-}$ ,  $D$ , and three parameters describing the normalization and shape of the kaon momentum spectrum. The uncertainty in  $\phi_{+-}$  was 0.02 degrees. This is 50% better than what is needed to place a 90% confidence limit on CPT symmetry violation at the Planck scale.

In this experiment we measure  $\phi_{+-}$ , but we must calculate  $\phi_\epsilon$ . Here we describe some corrections to this calculation.

Assuming CPT invariance, the phase of  $\epsilon'$  is known to be  $(48 \pm 4)$  degrees. Its magnitude is unknown, but if we assume it to be the central value from E731 we find that the maximum possible change of  $\phi_\epsilon$  from this source is 0.003 degrees, an order of magnitude smaller than the contribution of CPT violation at the Planck scale.

The full formula for  $\phi_\epsilon$  is

$$\tan \phi_\epsilon = \frac{2\Delta m}{\Gamma_S - \Gamma_L} \cos \xi + \frac{\delta}{\delta} \quad (7.8)$$

where  $\xi = \arg(\Gamma_{12}A_0\bar{A}_0^*)$  and  $\delta = 2Re(\epsilon)$ . Here  $A_0$  is the isospin 0 part of the  $\pi^+\pi^-$  decay amplitude. In the Wu-Yang phase convention,  $A_0$  is real, and  $\Gamma_{12}$  gives contributions from two sources: semileptonic decays through  $Im(x)$ , the  $\Delta S = \Delta Q$  violation parameter, and  $3\pi$  decays through  $Im(\eta_{+-0})$  and  $Im(\eta_{000})$ .

In the standard model we expect  $x \simeq 10^{-7}$ , which is much smaller than we need worry about, but  $Im(x)$  is known experimentally only to an accuracy of  $\pm 0.026$ . This results in an uncertainty in  $\phi_\epsilon$  of 1.7 degrees. To prove that an observed difference between  $\phi_{+-}$  and  $\phi_\epsilon$  were due to CPT violation one would have to measure  $Im(x)$  about 50 times more accurately than today's level. The way to do this is described below.

The contribution to  $\phi_\epsilon$  from the  $3\pi$  modes in the standard model is 0.017 degrees, which is about 1/2 of the contribution of CPT violation at the Planck scale. But if one takes into account the current world's knowledge, the uncertainty these decay modes contribute is 2.2 degrees. So they have to be measured better also.

The experimental approach to measuring these three quantities,  $x$ ,  $\eta_{+-0}$ , and  $\eta_{000}$ , is the same. One would choose an experiment with high dilution factor and observe interference between  $K_L$  and  $K_S$  close to the target; i.e. the experiment described here. So these measurements should be thought of as being an important part of this experiment. We have performed calculation of the sensitivity of this experiment for these quantities, and we estimate that we can reach at least the required sensitivity. We conclude that we can calculate  $\phi_\epsilon$  to the required accuracy.

The session on the RF-separated  $K^+$  beam was sponsored jointly by the CPT tests with kaons, the  $K^+$ , and the beams working groups. It was attended by all of the physicists who want to use that beam (members of the CPT and CKM collaborations), by the organizers of the beams working group, and by some of the physicists who would actually have to build the beam. There were three talks in the session, on the optics of the beam (by Gordon Thomson), on building superconducting RF cavities (by Al Moretti), and on the possibility of modulating the Main Injector proton beam at a subharmonic of the RF frequency used in the  $K^+$  beam (by Phil Martin and Chandra Bhat).

The designer of the RF-separated  $K^+$  beam, Jaap Doornbos of TRIUMF, was working at KEK and was not available for the workshop, so Gordon Thomson had several E-mail and telephone sessions with him to bring himself up to date on the design, and present it at the workshop. The goals of the beam design are as follows:

- Flux of  $2 \times 10^8$   $K^+$ /spill, with  $5 \times 5$  mm<sup>2</sup> spot size (for the CPT experiment).
- Flux of  $3 \times 10^7$   $K^+$ /spill, with 50 - 100  $\mu$ rad divergence in x and y (for the CKM experiment).
- Impurity  $\leq 10\%$ .
- Simple change-over between the two experiments.

- 25 GeV/c for CPT and 22.8 GeV/c for CKM.

The beam design that was presented accomplished all these goals. The first section of the design consists of quads to collect the beam made by the 120 GeV/c protons striking a 1 interaction length target at 0 mrad, bending magnets for momentum analysis, and more quads to make a focus on the first RF cavity. The quadrupoles also deform the beam phase space to reduce the divergence in  $y$  (the coordinate in which the RF cavities operate) to make the RF separation more efficient. The two RF cavities work in the C-band, at a frequency of 5.79 GHz, and are separated by 75.1 m. In this situation protons arrive at the second RF cavity exactly 360 degrees behind pions, and kaons are 90 degrees behind the pions. The cavities are run with a relative phase such that their effects cancel for pions and protons but not for kaons. The second cavity is followed by a quad string that rotates the phase space to turn the angular difference between pions and kaons into a position difference, and a beam stopper wipes out the pions and protons and allows about 60 % of the kaons to pass. Now the  $K^+$  beam is cleaned up and focused (for the CPT experiment) or made parallel (for the CKM experiment).

There is one bending magnet after the beam stopper whose polarity is switched to send the  $K^+$  beam to the other experiment. In addition slit openings have to be changed, some magnet currents adjusted, the stopper changed (from 1.5 cm thickness for CPT to 0.5cm for CKM), and two magnets have to be moved by about a foot. The whole changeover should take about a shift.

Al Moretti of Fermilab made a very interesting presentation on building the RF cavities we need for the experiment. RF-separated  $K^+$  beams have been built before by ANL, BNL, SLAC, and CERN. All but the CERN beam used room temperature copper RF separators which needed high power but had a low duty cycle (they were used to send beams to bubble chambers). The CERN beam used superconducting RF cavities running at the C-band frequency. These cavities were CW, and required only 10's of Watts to operate. While they seems similar to our needs, they were built in 1977 and achieved only 1.3 MV/m, where we need approximately 10 MV/m. The state of the art has advanced considerably since then, and this higher field should be easily achieved. The  $\pi/2$  deflecting TM11 mode would be used for our cavities.

The first step in building the RF cavities would be an R & D phase that would take about a year and cost about \$750k. The construction of the cavities would take about an additional 1 1/2 years and cost about \$1,800k. This time scale is not poorly matched to that of the Main Injector era, and the costs are not beyond what might be expected to be available to build a beam that would be used for two experiments, and for others in the future. This beam could be tuned for antiprotons, for example.

One way to improve the separation of kaons from pions and protons would be to have the protons arrive already bunched at the target where the secondary beam is made. Phil Martin and Chandra Bhat looked into the possibility of bunching the Main Injector protons, and concluded that it was a difficult and expensive undertaking. Their scheme was to debunch the Main Injector beam once it had reached flat-top energy, and rebunch at the first subharmonic of the C-band frequency used in the  $K^+$  beam. Using the full C-band frequency would require RF cavities to be introduced into the Main Injector whose apertures would be too small for that accelerator. One of their conclusions was that this rebunching would require 0.8 sec.



This would lengthen the cycle time of the accelerator in an unacceptable way. Even if there were no other problems, this makes the scheme unworkable.

Roger Tokarek has been looking into the beam lines of the Meson Lab to see where our beam and experiment would fit, and he spoke about his progress. He thinks that two beam lines are best: Meson West and Meson East. For Meson West a target pile exists in the Meson Detector Building, and the experimental hall could be an extension of the Wonder Building structures using existing parts. For the Meson East option, there is a target hall located in about the right place, which is currently empty, and the Meson East target pile could be mined for all the necessary parts. The magnet that switches the  $K^+$  beam from the CPT to the CKM experiment would be located just before the Detector Building, and the two experiments could fit into the eastern part of the Detector Building, with the CPT experiment to the west and the CKM experiment to the east.

In summary, there were several things we accomplished in the Workshop. We presented our ideas for the experiment to the general high energy community. Our experiment will confront several exciting physics topics, and we hope that we communicated that excitement to the workshop participants. We have concluded that the experiment and beam are feasible, and are working hard on a Proposal. There are challenges including the R & D work needed for building our RF cavities, and in building the cavities in a reasonable time frame. The Workshop has provided the environment for progress in the experimental design, the hyperon magnet design, and the beam design.

# Chapter 8

## Summary of the Experiments with Charged Kaons Working Group

Reported by P. S. Cooper, Fermilab and J. Ritchie Univ. of Texas at Austin

Members of the Working Group: G. Buchalla, SLAC; M. Diwan, BNL; J. Engelfried, Fermilab; V. Kubarovski, IHEP Serpukhov; L. Littenberg, BNL, H. Ma, BNL; C. Milstene, Tel Aviv; M. Moinester, Tel Aviv; E. Ramberg, Fermilab; T. Shinkawa, KEK; R. Tschirhart, Fermilab

### 8.1 Introduction

The working group focused on the opportunities for high sensitivity experiments using charged kaon beams. We looked in detail at the options for precision measurements and rare decay searches using the charge kaon decay in flight technique; particularly the CKM letter of intent. The initial concept for the CKM experiment was a non magnetic decay in flight spectrometer with the capability to run with at least 3MHz of kaon decays. It is based upon phototube ring imaging Cerenkov counters. The major goal of CKM is the measurement of the branching ratio of  $K^+ \rightarrow \pi^+ \nu \bar{\nu}$ .

The interest in an in-flight measurement of  $K^+ \rightarrow \pi^+ \nu \bar{\nu}$  at the Main Injector is motivated by the high kaon fluxes potentially available combined with the opportunity for long fixed-target runs in parallel with Collider running. The Brookhaven experiment focusing on this mode, E787, is currently limited by kaon flux and running time. That experiment has a good chance to observe  $K^+ \rightarrow \pi^+ \nu \bar{\nu}$  for the first time, but in the best case scenario its measurement of the branching ratio is likely to be based on a handful of events. A Main Injector experiment should not be statistics limited. A sample of 100 events appears to be a plausible goal, permitting a 10% measurement of the branching ratio and a determination of the magnitude of the CKM matrix element  $V_{td}$  at a level where experimental and theoretical uncertainties are of similar size. The main challenge in such an experiment will be to reject backgrounds to the necessary level.

## 8.2 Working Group Talks

The working group heard talks from its own members and held joint sessions with several other groups. These included:

1. Experiments with Charged Kaons Working Group Session
  - P. Cooper Overview of the CKM experiment
  - L. Littenberg BNL E787 Results and Lessons
  - M. Diwan T-violation in Km3 at BNL
  - C. Milstene Radiative Km2 with the CKM apparatus
  - J. Engelfried Selex Rich Design and Performance
  - Freewheeling Discussions
2. Joint session with the  $K^0$  group (Theory)
  - G. Buchalla Direct CP violation in Kaons
  - J. Donoghue Radiative Complex of Rare  $K_L$  Decays
3. Joint meeting with CPT working group ( $K^+$  beams)
  - G. Thomson Design for an RF separated  $K^+$  beam
4. Joint meeting with Beams working group
  - P. Cooper CKM requirements for debunched beams
5. Joint session with  $K$  and detector groups (detectors)
  - A. Roodman CsI Calorimeter at KTeV
  - R. Tschirhart CsI Calorimeter readout at KAMI
  - R. Littenberg Photon veto at BNL787/BNL  $\pi^0\nu\bar{\nu}$
  - T. Inagaki Photon veto at KEK  $\pi^0\nu\bar{\nu}$
  - J. Jennings Photon veto at KTeV
  - K. Arisaka Photon veto at KAMI
  - A. Bross Fiber tracking

The discussions of the theory of CP violation by Wolfenstein in the plenary session and Buchalla and Donoghue in the parallel sessions all emphasized the importance of measuring the branching ratios of charged and neutral kaons to the  $\pi\nu\bar{\nu}$  final state. These two decay modes are theoretically clean. A measurement of the charged mode to 10% would determine the magnitude of the CKM matrix element  $V_{td}$  to about 5%, with the theory error being of similar magnitude. A measurement of the neutral mode directly measures the Wolfenstein parameter  $\eta$ , upon which Standard Model CP violation depends. This class of measurement is complimentary to measurements of decay rate asymmetries in the  $\psi K_S$  and  $\pi^+\pi^-$  decay

modes of the B meson which are the primary aims of the B factories and major goals of the upcoming Fermilab collider experiments. Ultimately the combination of measurements with K's and B's will provide a stringent test of the Standard Model; either all CP violation comes from the imaginary parts of  $V_{td}$  and  $V_{bu}$  or there is clear evidence for a non-Standard Model CP violating interaction. The values of  $V_{td}$  measured in the kaon and B sectors must not only have imaginary parts - they must be the same complex number for the Standard Model to adequately describe the violation of CP. Such agreement between the kaon and B sectors would be compelling confirmation of both the Standard Model as the sole source of CP violation and of the validity of the measurements.

According to Buchalla, the predicted Standard Model branching ratio of the  $K^+ \rightarrow \pi^+ \nu \bar{\nu}$  decay mode is  $[0.9 \pm 0.3] \times 10^{-10}$  where the uncertainty is mainly a reflection of the uncertainties in our knowledge of other standard model parameters which enter the calculation. The decay is dominated by diagrams involving top quark loops. The largest theoretical error in extracting the magnitude of  $V_{td}$  from the  $K^+ \rightarrow \pi^+ \nu \bar{\nu}$  branching ratio comes from the uncertainty in the small contribution from charm quark loops, owing to the uncertain charm quark mass. The cost of this theoretical "purity" is an experiment of extraordinary difficulty.

This kaon decay mode has di-neutrinos in the final state which make the best conceivable measurement kinematically under-constrained. A successful experiment must eliminate or control all background processes to well below the  $10^{-11}$  level in branching ratio in order to demonstrate a convincing signal. The most promising region of decay phase space for controlling backgrounds is the range of center-of-mass momenta between the peaks from the  $K_{\pi 2}$  and  $K_{\mu 2}$  decays. All efforts thus far have been focused on a measurement of  $K^+ \rightarrow \pi^+ \nu \bar{\nu}$  in this region.

Experimental progress to date in the search for the  $K^+ \rightarrow \pi^+ \nu \bar{\nu}$  decay mode has been exclusively via the stopped kaon technique. This work has spanned more than 30 years. For the last half of this period the flagship experiment was and is E787 at BNL. The status and plans for this experiment were reviewed by Laurie Littenberg. E787 published in 1995 an upper limit of  $2.4 \times 10^{-9}$  at 90% CL for this decay mode based upon data taken before 1991. The experiment has had a major upgrade and has taken new data. They hope that with data in hand plus significant running in the next two years they should be able to make a first observation of this decay. Under optimal circumstances E787 may achieve a single event sensitivity of about  $2 \times 10^{-11}$ , permitting the observation of about 5 events.

Littenberg reported that they have pushed the sensitivity of BNL787 up to a useful  $K^+$  stopping rate above 1 MHz. The experiment features an active scintillating fiber target surrounded by hermetic photon vetos, high precision tracking with redundant measurements of energy, momentum and range for the  $p^+$ . Identification of the  $\pi^+$  is accomplished by observing the  $\pi \rightarrow \mu \rightarrow e$  decay chain. The beam is a separated, high purity, low energy,  $K^+$  beam with  $\frac{K^+}{\pi^+} \approx 3$  driven with  $2-3 \times 10^{13}$  protons/spill. The experiment represents an investment of more than 10 years and 20M\$ with a team of physicists who are now the world experts in this type of physics.

The experiment's acceptance after all necessary cuts is  $\approx 0.2\%$ . This is nearly an order of magnitude below design goals. This loss came about in a traditional way; a large number of factors of 0.8-0.9 relative to the design. The major backgrounds which they needed to control are  $K^+ \rightarrow \pi^+ \pi^0$  [ $K_{\pi 2}$ ] with the  $\pi^0$  unrecognized due to photon veto inefficiencies and  $K^+ \rightarrow \mu^+ \nu$  [ $K_{\mu 2}$ ] with the  $\mu^+$  mis-identified as a  $\pi^+$ . The limitations of the present

experiment are available kaon flux and running time. The experiment is statistically limited and has pushed the stopped kaon technique to such a level that it will be a very hard act to follow.

In another talk Milind Diwan described the recently approved BNL E923 experiment to improve the measurement of the T violating component of the muon polarization in  $K_{\mu 3}$  decay. The goal is to improve the limit on the out of plane component of the muon polarization to the  $1.5 \times 10^{-4}$  level; 30 times better than the previous measurements. There are model predictions at the  $1 \times 10^{-3}$  level, an order of magnitude higher than the proposed sensitivity. The experiment is done by decay in flight in a high intensity ( $2 \times 10^7 K^+$  / spill) 2 GeV/c separated charged kaon beam. The decay muons are stopped in a precision polarimeter based upon the muon spin precession technique. This appears to be a promising and elegant experiment which approaches the questions of CP violation in the Standard Model from a rather different observable.

### 8.3 The CKM Experiment

The rationale for a decay in flight experiment at the Fermilab Main Injector is to lift the flux (statistics) limitations. The separated  $K^+$  beam discussed in this workshop would provide 15 MHz of  $K^+$ , 3 MHz of decays and  $\approx 100 K^+ \rightarrow \pi^+ \nu \bar{\nu}$  events detected in 2 years of running. The required input of protons to drive this beamline is  $2 \times 10^{12}$  / spill; less than 10% of the MI design intensity. The ability to run in parallel with the Fermilab collider program should allow adequate running time. The goals set forth in the CKM expression of interest which was submitted to Fermilab in April 1996 are:

1. To be able to observe  $\approx 100 K^+ \rightarrow \pi^+ \nu \bar{\nu}$  events for a  $1 \times 10^{-10}$  branching ratio in two years of running with the Main Injector
2. To reduce all background to the level of a few events
3. To limit capital cost to less than 10M\$.

The detector described in the CKM EOI consists of two phototube ring imaging Cerenkov counters separated by a vacuum decay volume with a surrounding photon veto system. The beam envisioned in the EOI was an unseparated 300MHz beam which yielded 3MHz of  $K^+$  decays in the decay volume. The two RICHs are each velocity spectrometers which measure the vector velocity of the kaon and pion respectively from the center and radius of each observed ring. Both counters can be blinded to the Cerenkov light from beam pions by not instrumenting the small region illuminated by beam pion rings. The intrinsic fast time response of photomultipliers gives this design very high rate capabilities. In a simple simulation the proposed CKM detector was able to maintain  $\approx 2\%$  acceptance while controlling the background from the  $K_{\pi 2}$  mode to the level of a few events.

The choice of phototube RICHs was based upon the experience with this technique in the Selex(E781) experiment. Jurgen Engelfried presented a detailed report of the design, performance and experience with the present Selex RICH. The Selex RICH appears to have met its major design criteria. Detailed offline alignment and calibrations have not yet been done because data taking is still underway in Selex and the present performance is more

than good enough for the preliminary charm analyses now underway. The Selex RICH has a readout with a 160 nsec time gate. The intrinsic time resolution of phototube RICHs is unexplored and the random noise level is much higher in the Selex RICH than is proposed for CKM.

The most valuable portions of the workshop were the unstructured (freewheeling) discussions. The experience in kaon rare decay experiments of the working group members sitting around the table approached 100 years. Particular areas of concern were various scattering and interaction processes which could corrupt events and the lack of redundant measurements. Milind Diwan raised the possibility of a background source from  $K^+$  charge exchange scattering in the kaon RICH gas followed by a  $K^+ \rightarrow \pi^+ \nu e$  decay with the electron unobserved. Stan Wojcicki expressed concern about all the bad things which can happen in 3% of a radiation length of Nitrogen. He also questioned how the experiment could be triggered. Thus far little thinking has gone into triggering CKM so no satisfying answer to this question was given. There was consensus that too much rejection was being required of the RICH velocity spectrometers. This is consistent with the view that  $\pi^0$  rejection needs to be improved over what was assumed in the CKM EOI. The requirements on the muon veto system seems to be a rejection of about  $10^{-3}$ .

There was discussion on other physics measurements which might be possible in the CKM apparatus. It was felt that a program broader than just one measurement was important for the health and sociology of a CKM collaboration. This is particularly important for students and younger member of the collaboration. The list identified includes:

1. High statistics studies

- $K^+ \rightarrow \mu^+ \nu \gamma$ - Kaon structure dependent form factors
- $K^+ \rightarrow \pi^+ \mu^+ \mu^-$ ,  $\pi^+ e^+ e^-$ ,  $\pi^+ \gamma \gamma$

2. Precision measurements

- $K_{e3}^+$  and  $K_{\mu 3}^+$  -  $V_{us}$  to  $\approx 0.1$

3. Lepton flavor violation

- $K^+ \rightarrow \pi^+ \mu^+ e^-$

Caroline Milstene reported on the possibilities to measure the Kaon structure dependent form factors in the kaon radiative decay  $K^+ \rightarrow \mu^+ \nu$ . In a dedicated one week run with a small high precision photon calorimeter  $10^7$  events are accepted. This should yield  $\approx 10^5$  events in the region of the Dalitz plot sensitive to the  $F_v + F_a$  and  $F_v - F_a$  form factors. The present best measurement is as yet unpublished from BNL787. Laurie Littenberg showed, privately, a measurement of  $\text{abs}(F_v + F_a)$  from 2500  $K_{\mu 3}$  events obtained in a one week dedicated run of BNL787.

## 8.4 Beam Issues

An important improvement in the prospects for a rare kaon decay in flight experiment has been provided by Gordon Thomson and co-workers. They have designed an RF separated

$K^+$  beam. The impetus for this work has been the CPT experiment, described elsewhere in these proceedings. However, such a beam is needed for CKM as well. The present design accommodates both CPT and CKM. This beam can provide 30 MHz of  $K^+$  with a contamination of less than 10%  $\pi^+$  in a beam with less than 100 mrad divergence and a 1% momentum bite to the CKM experiment for about  $5 \times 10^{12}$  protons per spill incident on the kaon production target.

The availability of such a beam will make it practical for CKM to place tracking detectors in the beam. Several indications point to this as a requirement. The previously discussed need to determine the decay angle free of multiple scattering in the RICH gas is one. Also, chromatic dispersion in nitrogen, which is planned for the beam RICH, probably degrades the ring resolution to the point where this measurement alone is insufficient to determine the beam momenta. Finally, beam kaons which decay upstream of the beam RICH will produce pions and muons at lower than beam energies which can fake a kaon at the beam energy. These last two effects point to a need for a magnetic determination of beam particle energy, which of course requires tracking in the beam."

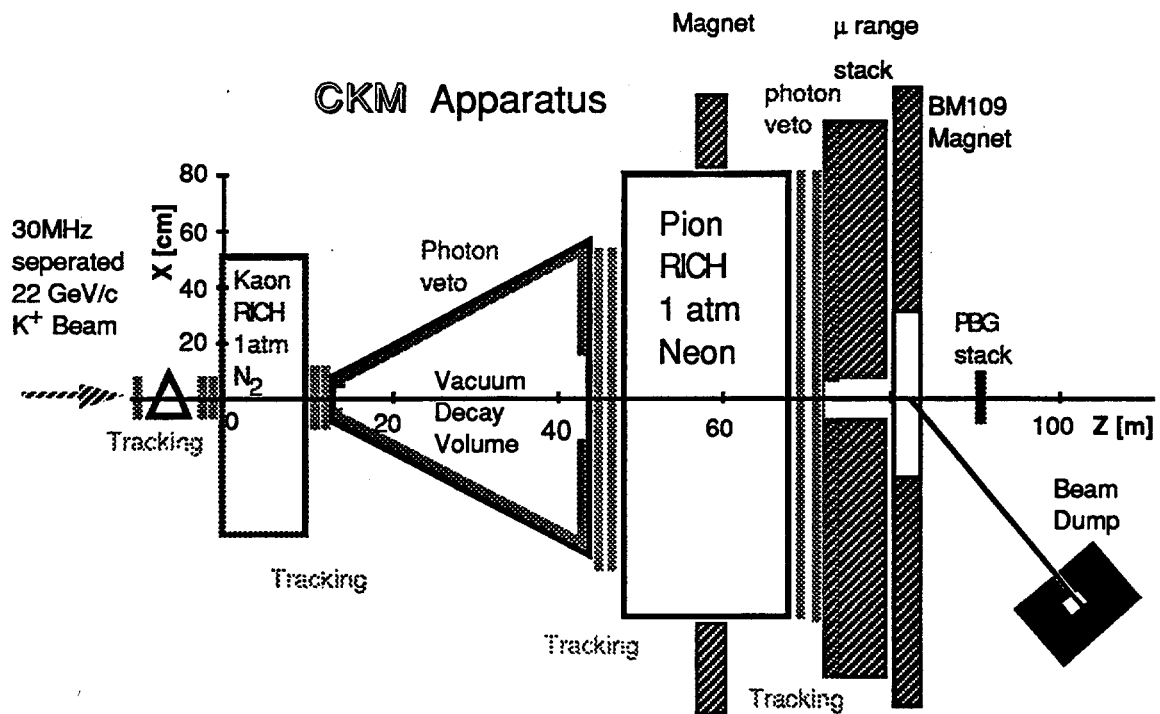
Another beam issue is the spill structure. In 300 MHz unseparated beam the idea was to request debunched protons with enough 53 MHz RF ripple remaining to allow the Beams Division to control the beam. The question was raised by Milind Diwan whether a debunched beam is really advantageous. In a 30 MHz separated kaon beam there may be significant advantages to having zero rate in a 18.8 nsec window around a particular kaon. There is some loss if RF buckets with more than one beam particle are rejected. The RF bucket occupancy will be recorded and can be analyzed after the fact to keep as much beam as possibly consistent with the requirements of controlling the background levels. This issue requires further study.

## 8.5 Conclusions

By the last meeting of the working group on Saturday afternoon a revised CKM apparatus was written on the blackboard by Cooper. This figure (Fig. 8.1) is reproduced below. It contains charged particle tracking around each element of the original CKM apparatus plus tracking upstream in the beamline to give an independent magnetic measurement of the kaon momentum. The "straw man" proposal for these tracking stations were two multi view (xyuv) strawtube chambers spaced by 2m for a total of 8 planes. This suggestion is based upon similar chambers which were used in BNL871. The angular resolution would be  $\approx 100$  mrad. The material introduced into the beam would be about  $2 \times 10^{-3}$  radiation lengths per station. There was also a magnet with  $\approx 100$  MeV/c pt kick and  $\approx 1$ m length added in the middle of the pion RICH. This will produce two rings for each decay pion. The angular separation of the two rings is an independent measure of the momentum of the pion. The field also provides charge determination. This option needs careful study, since it will probably make it harder to veto photons which convert inside the pion RICH.

This revised detector considerably increases CKM's redundancy and addresses some of the known problems with the initial version of CKM. For instance, the measurements of the tracks just before and after the vacuum decay volume decouples the decay reconstruction and background rejection from scattering in the radiator gas in either RICH.

Several members of the working group expressed interest in doing real work in the near future in order to bring the CKM ideas to the level of a real proposal. The next step is to simulate the revised apparatus and start to address the background issues at a level appropriate for a proposal. The revised CKM apparatus addresses the issues of redundant measurements and control of scattering at the conceptual level. The question now is how much these additions improve the background rejections at the level of serious simulations. While observing 100  $K^+ \rightarrow \pi^+ \nu \bar{\nu}$  decays with low background is a daunting task, we believe it is a very exciting prospect. It would be a strong addition to the Main Injector fixed-target physics program.





# Chapter 9

## Summary of the Strong Interactions Working Group

Reported by C. Brown, Fermilab and D. Geesaman, Argonne National Lab.

### 9.1 Introduction

The SU(3) color segment is an integral component of the standard model but it is perhaps the most difficult to quantitatively test, except in the perturbative regime. The strong interactions working group could not possibly attempt a complete coverage of the issues in strong interaction physics that are best studied at the Main Injector. The list is simply too long. Instead it naturally focused on issues with a core constituency of interested parties that could develop into proposals for the Main Injector in short order. Since the physics topics are disparate, it was also not appropriate to seek a consensus on the 'best' experiments to do.

In the standard model of the strong interaction, the only sensitivity to quark flavor occurs in the quark mass dependence. Experiments which test the quark mass dependence are one path to find physics beyond the standard model. Another is to study the anomaly structure of QCD. At the same time, accurate strong and electroweak predictions often depend on nonperturbative QCD features, such as parton distributions and form factors, which must be determined by experiment. Finally, the richness of QCD leads to many surprising many body phenomena of interest to diverse segments of the strong interaction community.

The presentations to the strong interactions working group were:

### 9.2 Inclusive hadron cross sections

**Raja Rajendran (FNAL)** - An experiment to measure with large acceptance the inclusive hadron yields and correlations at MI energies. These measurements would test a scaling law which appears to describe many of the correlations in the particle distributions. These measurements would provide a quite comprehensive characterization of the secondary hadron beams which is needed to understand the neutrino flux for the MI neutrino experiments.

### 9.3 Antiproton energy deposition in Nuclei

**Kris Kwiatkowski (Indiana)** - Antiproton beams are perhaps the most efficient way to transfer excitation energy to atomic nuclei. This results in high-temperature, relatively low density, nuclear systems which vaporize in a liquid-gas nuclear phase transition. The first evidence for this type of transition was obtained at FNAL a decade ago in proton-nucleus collisions, but 10-20 GeV antiproton beams are clearly the tool of choice to definitively establish this behavior. The detectors for these experiments exist if the beams are available.

### 9.4 Hadronic Atoms

**Yuri Ivanov (Petersburg NPI)** - Stopping mesons and hyperons produced in MI production targets form mesic and hyperonic atoms. The exquisite sensitivity and resolution of the X-ray detectors makes detecting the atomic transitions of these atoms the most accurate measurements of a number of masses and spin-orbit couplings. Significant results would have impact in a number of physics areas including the limit on the muon neutrino mass.

### 9.5 Drell-Yan with 50-120 GeV hadrons and mesons

**Don Geesaman (ANL)** - The MI is an optimum environment for Drell-Yan dimuon production at high fractional parton momenta. Several experiments were described that are only possible with the lower energy and higher flux of the MI. These include precise measurements of  $u(x)$ - $d(x)$  and  $u\bar{u}$ - $d\bar{d}$  at high  $x$  on the proton, nuclear dependences, and Kaon structure functions.

### 9.6 Polarized Drell-Yan

**Joel Moss (LANL)** - If the MI proton beam were polarized, definitive measurements of the sea antiquark and gluon polarizations would be possible with a polarized target.

### 9.7 Single Spin Asymmetries in D-Y

**Vassilios Papavassiliou (NMSU)** - Features of the NLO Drell-Yan dimuon production with an unpolarized beam and polarized target were examined for sensitivity to the the sea antiquark and gluon polarizations. Several kinematic regions were identified as promising for further study.

### 9.8 Theory/Experiment Seminar

**Mark Strikman (Penn State)** - This Joint Theory/Experimental Friday Seminar emphasized the need to measure and study non-perturbative QCD, particularly at MI energies. It focused on coherent phenomena where the interactions with multiple partons are important.

In the past few years there have been significant strides in identifying which such processes are calculable and lead to firm predictions for hadron and nuclear reactions.

## 9.9 Exclusive Reactions at high $P_T$

**Mark Strikman (Penn State)** - Exclusive reactions provide another regime where perturbative QCD techniques should be applicable to coherent phenomena. Many of the features of QCD in these reactions are intimately related to the phenomenon of color transparency, the reduction of the interaction cross sections for the small color singlet objects that are expected to dominate the exclusive reaction mechanisms.

## 9.10 Low energy hadron-hadron cross sections

**Mark Strikman (Penn State) for Misha Zhalov** - The operation of a hydrogen streamer chamber with an electronic readout has now been demonstrated. This could be an ideal detector for low energy hadron-nucleon scattering including such topics as the pion-nucleon sigma term and threshold proton-antiproton elastic scattering.

## 9.11 Conclusion

It was clear that the Main Injector presented many valuable new opportunities in studying the strong interactions. It appears likely that proposals to the FNAL PAC would result from the first four topics as viable collaborations are formed. A letter of intent was submitted in 1995 for Polarized Drell-Yan measurements. It appears likely that the unpolarized Drell-Yan and single and double spin polarized Drell-Yan measurements could use a common apparatus in a coherent program. Many of the other ideas are important to our understanding of the strong interactions and indicate future possible opportunities for the FNAL experimental program.

# Chapter 10

## Summary of the Experiments with Low Energy Antiprotons Working Group

Reported by M. Macri, INFN Genoa and S. Pordes, Fermilab

The first question addressed was the availability of antiprotons for dedicated experiments during Collider running. An analysis by Gerry Jackson suggested, to our surprise, that given a working Recycler, the antiproton source could devote as much as 1/3 of its time to providing antiprotons for non-collider use. The Recycler has added a degree of freedom to the antiproton production system whose impact has yet to be fully exploited.

From the side of physics experiments, the three experiments which have run in the antiproton source showed that they had by no means exhausted their topics. The antiproton lifetime experiment (Geer et al.) is planning an experiment sensitive to lifetimes of less than  $10^7$  years - this is a factor 10 improvement in sensitivity over their current results. They are considering running either on the antiproton accumulator or on the Recycler in the Main Injector era. The antihydrogen experiment of Munger et al. is submitting a proposal to measure the Lamb-shift in antihydrogen using a technique based on the Stark effect induced as the  $\bar{H}$  passes through magnetic fields. The charmonium experiment of Cester et al. will not finish its program this run and one could envisage an apparatus with better sensitivity to low energy photons to complete the study of charmonium states that decay to two photons.

While the  $\bar{H}$  experiment could probably survive in the pbar source with antiproton accumulation for the colliders, any successor to the charmonium experiment would require extensive shielding since it lies along the injection line to the debuncher. The antiproton lifetime experiment just needs time with beam circulating and no stacking.

The other use of antiprotons for very low energy physics was presented by Tom Phillips who mentioned the basic ("New York Times") type of experiments such as whether anti-matter falls up or down. The provision of very low energy antiprotons would require a new ring to decelerate the antiprotons and Gerry Jackson listed 9 alternatives. The only point we would make at this stage is that the Fermilab source produces antiprotons at more than 20 times the rate at CERN.

# Chapter 11

## Summary of the Booster Neutrino Physics Working Group

Reported by J. M. Conrad, Columbia Univ. and G. B. Mills, Los Alamos

The purpose of this working group[17] was to develop ideas for a Booster-based neutrino oscillation experiment. This experiment is motivated by the LSND observation, which has been interpreted as  $\bar{\nu}_\mu \rightarrow \bar{\nu}_e$ , and by the atmospheric neutrino deficit which may result from  $\nu_\mu$  oscillations. The BooNE (Booster Neutrino Experiment) program will have two phases. The first phase, MiniBooNE, is a single detector experiment designed to:

- Obtain  $\sim 400$  events per Snowmass-year ( $1 \times 10^7$  s) if the LSND signal is due to  $\nu_\mu \rightarrow \nu_e$  oscillations.
- Extend the search for  $\nu_\mu \rightarrow \nu_e$  oscillations approximately one order of magnitude in  $\Delta m^2$  beyond what has been studied previously if no signal is observed.
- Search for  $\nu_\mu$  disappearance, to address the atmospheric neutrino deficit, through the suppression of the expected 50,000  $\nu_\mu C \rightarrow \mu + X$  events per Snowmass-year.
- Test CP-violation in the lepton sector if oscillations are observed by running with separate  $\nu_\mu$  and  $\bar{\nu}_\mu$  beams.

The second phase of the experiment introduces a second detector, with the goals of:

- Accurately measuring the  $\Delta m^2$  and  $22\theta$  parameters of observed oscillations.
- Determining the CP violation parameters in the lepton sector.

The MiniBooNE experiment (phase 1) would begin taking data in 2001. By using phototubes and electronics from the LSND experiment, the MiniBooNE Detector is relatively inexpensive, \$1.6 M, and able to be constructed on a short time scale. The detector would consist of a double-wall cylindrical tank which is 11 m in diameter and 11 m high. The inner tank would be covered on the inside by 1220 8-inch phototubes (10% coverage) and filled with 600 t of mineral oil, resulting in a 400 t fiducial volume. The volume between the tanks would be filled with scintillator oil to serve as a veto shield for identifying particles both

entering and leaving the detector. The detector would be situated 1000 m from a neutrino source.

The neutrino beam constructed using the 8 GeV proton Booster at FNAL would service both phases of the experiment. The neutrino beam line would consist of a target followed by a focusing system and a  $\sim 30$  m long pion decay volume. The low energy, high intensity and 1  $\mu$ s time-structure of a neutrino beam produced from the booster beam are ideal for this experiment. This Booster experiment is compatible with the Fermilab collider or the fixed-target MI programs. The FNAL Booster is capable of running at 15 Hz ( $5 \times 10^{12}$  protons per pulse), or 30 Booster batches per 2 s Main Injector Cycle. The antiproton stacking requires only 6 Booster batches at the start of the Main Injector cycle. In principle, this means the BooNE beam line could receive 12 Hz, well above the expectation on which our sensitivities are based.

The BooNE experiments represent an opportunity to resolve two outstanding neutrino oscillation questions on a short-time scale. Within the upcoming five years, no existing or approved experiments will be able to address conclusively the LSND signal region. Also, there are no accelerator-based experiments within this time scale that can prove conclusively that oscillations are the source of the atmospheric neutrino deficit. Thus BooNE represents an important and unique addition to the Fermilab program.

A Letter of Intent for this experiment has been submitted to the Fermilab Physics Advisory Committee for consideration at the June 1997 Meeting. A formal proposal for this experiment will be submitted in the autumn of 1997.

## 11.1 Neutrino Oscillation Formalism

If neutrinos have mass, it is likely that the interaction responsible for mass will have eigenstates which are different from the weak eigenstates that are associated with weak decays. In this model, the weak eigenstates are mixtures of the mass eigenstates and lepton number is not strictly conserved. A pure flavor (weak) eigenstate born through a weak decay will oscillate into other flavors as the state propagates in space. This oscillation is due to the fact that each of the mass eigenstate components propagates with a different phase if the masses are different,  $\Delta m^2 = |m_2^2 - m_1^2| > 0$ . The general form for 3-component oscillations

$$\begin{pmatrix} \nu_e \\ \nu_\mu \\ \nu_\tau \end{pmatrix} = \begin{pmatrix} U_{e1} & U_{e2} & U_{e3} \\ U_{\mu1} & U_{\mu2} & U_{\mu3} \\ U_{\tau1} & U_{\tau2} & U_{\tau3} \end{pmatrix} \begin{pmatrix} \nu_1 \\ \nu_2 \\ \nu_3 \end{pmatrix}$$

This formalism is analogous to the quark sector, where strong and weak eigenstates are not identical and the resultant mixing is described conventionally by a unitary mixing matrix. The oscillation probability is then:

$$\text{Prob}(\nu_\alpha \rightarrow \nu_\beta) = \delta_{\alpha\beta} - 4 \sum_{j>i} U_{\alpha i} U_{\beta i} U_{\alpha j}^* U_{\beta j}^* 2 \left( \frac{1.27 \Delta m_{ij}^2 (\text{eV}^2) L (\text{km})}{E_\nu (\text{GeV})} \right) \quad (11.1)$$

where  $\Delta m_{ij}^2 = |m_i^2 - m_j^2|$ . Note that there are three different  $\Delta m^2$  (although only two are independent) and three different mixing angles. The oscillation probability also depends upon the length, L, from the source and neutrino energy,  $E_\nu$ .

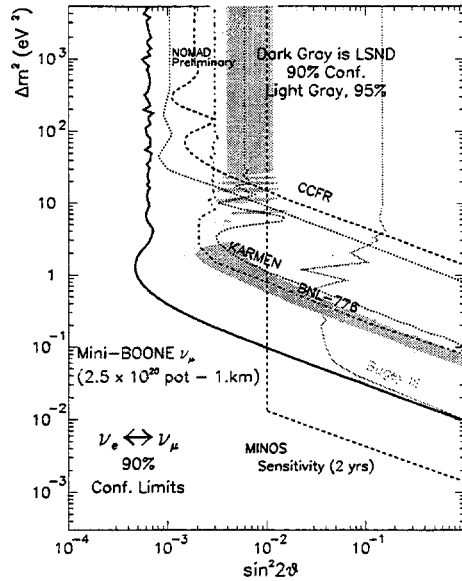


Figure 11.1: 90% C.L. limit expected for MiniBooNE for  $\nu_\mu \rightarrow \nu_e$  appearance after one year of running, including 10% systematic error, if LSND signal is not observed. Summary of results from past experiments and expectations for the future MINOS experiment are also shown.

Although in general there will be mixing among all three flavors of neutrinos, two-generation mixing is often assumed for simplicity. If the the mass scales are quite different ( $m_3 \gg m_2 \gg m_1$  for example), then the oscillation phenomena tend to decouple and the two-generation mixing model is a good approximation in limited regions. In this case, each transition can be described by a two-generation mixing equation:

$$P = 22\theta^2 \sin^2(1.27\Delta m^2 L/E_\nu) \quad (11.2)$$

where  $\theta$  is the mixing angle. However, it is possible that experimental results interpreted within the two-generation mixing formalism may indicate very different  $\Delta m^2$  scales with quite different apparent strengths for the same oscillation. This is because, as is evident from equation 11.1, multiple terms involving different mixing strengths and  $\Delta m^2$  values contribute to the transition probability for  $\nu_\alpha \rightarrow \nu_\beta$ .

## 11.2 Experimental Motivation

The BooNE experiment is motivated by two important pieces of evidence for neutrino oscillations. The first is the observation of events by the LSND collaboration that are consistent with  $\bar{\nu}_\mu \rightarrow \bar{\nu}_e$  oscillations. The second is the observed deficit of atmospheric neutrinos which may be attributed to  $\nu_\mu$  disappearance through oscillations. Here we briefly review these results and the expectation for what MiniBooNE can contribute.

The LSND experiment at Los Alamos has reported evidence[18] for  $\bar{\nu}_\mu \rightarrow \bar{\nu}_e$  oscillations with an oscillation probability of  $\sim 0.3\%$ . The allowed values of  $\Delta m^2$  and  $22\theta$  corresponding to this oscillation probability are indicated in Fig. 11.1 by the grey region. Previous oscillation searches have not seen oscillations in the LSND allowed region for  $\Delta m^2 > 4 \text{ eV}^2$ , as

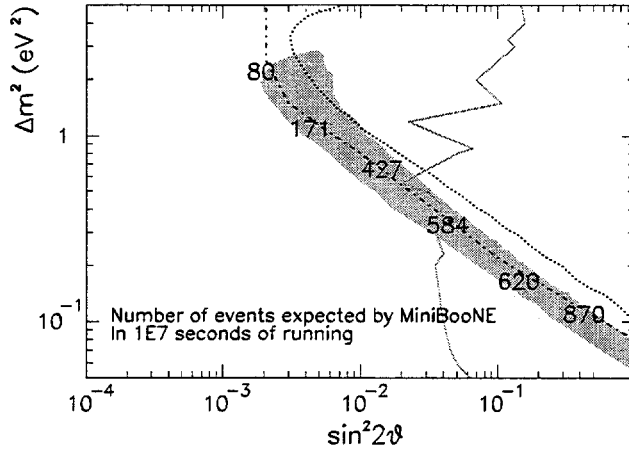


Figure 11.2: If LSND signal is observed, this plot shows the number of events expected in 1 Snowmass-year of running for MiniBooNE for the low  $\Delta m^2$  favored region for LSND (shaded). Lines indicate regions excluded by past experiments (see figure 2).

shown in Fig. 11.1. This isolates the most favored region at low  $\Delta m^2$ . LSND also is able to search for  $\nu_\mu \rightarrow \nu_e$  oscillations using  $\pi^+$  that decay in flight in the beam stop. This decay-in-flight oscillation search[19] has different backgrounds and systematics than the decay-at-rest search, and the presence of an excess that is consistent with the decay-at-rest search provides additional evidence that the LSND results are due to neutrino oscillations.

If the LSND signal is due to neutrino oscillations, MiniBooNE expects between 100 and 400 events per Snowmass-year, depending on the  $\Delta m^2$  and  $22\theta$  of the oscillation, outside of the regions ruled out by previous experiments. The expectations are shown in Fig. 11.2. The MiniBooNE systematics are significantly different from the LSND systematics. Thus MiniBooNE will be able to verify or disprove the LSND result. The full BooNE two-detector system will then accurately measure the oscillation parameters.

If the LSND signal is not observed by MiniBooNE, then the expected sensitivity is shown in Fig. 11.1. This experiment extends approximately an order of magnitude in  $\Delta m^2$  beyond previous limits.

The second important hint for neutrino oscillations comes from experiments which indicate a deficit of muon neutrinos from cosmic ray production in the atmosphere. The Kamioka and IMB experiments[20, 21] determined the ratio of  $\nu_\mu/\nu_e$  to be only about 60% of the theoretically expected ratio for neutrino energies below  $\sim 1$  GeV, independent of the visible energy of the charged lepton and the projected zenith angle of the atmospheric neutrinos. Interpreting the shortfall as arising from oscillation of muon neutrinos requires a large mixing angle ( $22\theta \sim 0.5$ ) and a  $\Delta m^2 > 10^{-3}$  eV<sup>2</sup>. The atmospheric problem can be attributed to either  $\nu_\mu \rightarrow \nu_e$  or  $\nu_\mu \rightarrow \nu_\tau$  oscillations. Because the Bugey result, shown in Fig. 11.1, excludes the atmospheric neutrino deficit region,  $\nu_\mu \rightarrow \nu_\tau$  oscillations are considered to be the likely candidate.

Upper limits on the possible  $\Delta m^2$  range come from previous accelerator-based experiments and the zenith angle dependence of the atmospheric neutrino deficit. The CDHS search for  $\nu_\mu$  disappearance indicates  $\Delta m^2 < 0.4$  eV<sup>2</sup>. The Kamioka group has observed a zenith angle dependence of the high energy (greater than 1 GeV) atmospheric neutrino sample[22] which indicates that  $\Delta m^2 \ll 0.5$  eV<sup>2</sup> (Kamioka prefers a  $\Delta m^2 \sim 10^{-2}$  eV<sup>2</sup>), although



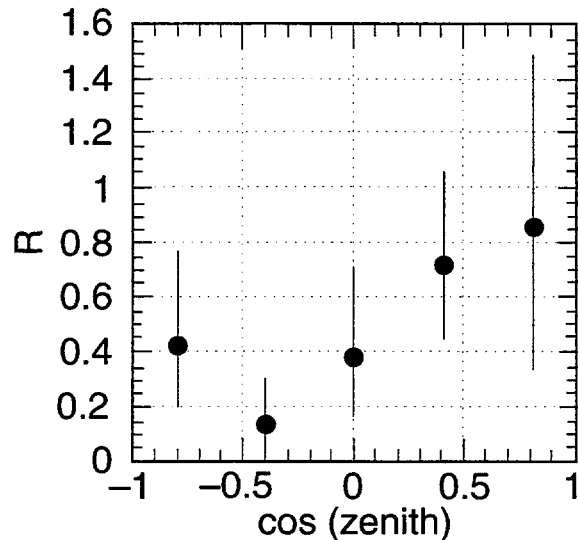


Figure 11.3: The Super Kamioka preliminary zenith angle distribution for the multi-GeV contained events.

the uncertainties are large. However a recent publication from the IMB collaboration[23] reports no zenith angle dependence. Also, preliminary data from the Super Kamiokanda collaboration shows a zenith angle distribution that is consistent with being flat and, in any case, with less angular dependence (see Fig. 11.3).

Figure 11.4 shows an overview of past experiments (narrow dashed and dotted lines) and expectations for future approved experiments (wide dashed lines) for  $\nu_\mu \rightarrow \nu_\tau$  searches. In light of the changing situation concerning the zenith angle dependence, Fig. 11.4 shows the allowed region if there is a zenith angle dependence (solid) and if there is no dependence (hatched). In the higher  $\Delta m^2$  scenario, MiniBooNE (solid line) can address the atmospheric neutrino oscillation question by searching for  $\nu_\mu$  disappearance. MiniBooNE is sensitive to variations in the flux with energy that are consistent with oscillations. Statistical and 10% systematic errors were included in this determination.

The case where the  $\Delta m^2$  values from atmospheric neutrino experiments are compatible with LSND provides a useful example of three-generation mixing models with two of the masses being “almost degenerate,” with large mixing between the degenerate partners. In this case,  $m_1 \approx m_2 \ll m_3$  leads to two  $\Delta m^2$  scales given by a small  $\Delta m_{12}^2$  and a larger  $\Delta m_{13}^2 \approx \Delta m_{23}^2$ . In this model, each oscillation channel ( $\nu_\alpha \rightarrow \nu_\beta$ ) can be treated using the two-generation formalism with  $22\theta \approx 4|U_{\alpha 3}|^2|U_{\beta 3}|^2$  and the appropriate  $\Delta m^2$ . With effectively only two mass scales, it would seem hard to explain the three  $\Delta m^2$  scales associated with solar ( $\Delta m^2 \approx 10^{-5}$  eV<sup>2</sup>), atmospheric ( $\Delta m^2 \approx 10^{-2}$  eV<sup>2</sup>), and LSND ( $\Delta m^2 \approx 10^{-1}$  eV<sup>2</sup>) experiments, unless, as Cardall and Fuller[24] have suggested, the atmospheric and LSND  $\Delta m^2$  values could be similar. This is possible if one discounts the zenith angle dependence. The common value would be in the range  $0.1 < \Delta m_{LSND,atmos}^2 < 0.5$  eV<sup>2</sup>. The solar oscillation signal is accommodated by having  $\Delta m_{12}^2 \approx 10^{-5}$  eV<sup>2</sup>. Thus, the solar, atmospheric and LSND data can all be explained by oscillations through the various mass eigenstates:

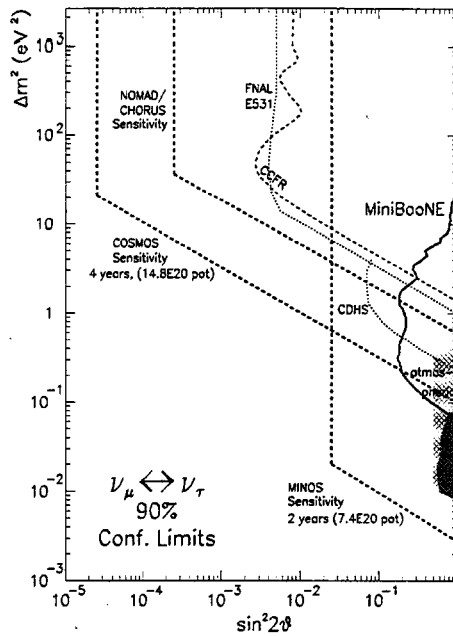


Figure 11.4: Summary of results from past experiments (narrow, dashed and dotted), future approved experiments (wide, dashed) and 90% C.L. limit expected for MiniBooNE (solid) for  $\nu_\mu$  disappearance after one year of running at 1 km. Solid region indicates the favored region for the atmospheric neutrino deficit from the Kamioka experiment. A result from Kamiokanda indicating no zenith angle dependence extends the favored region to higher  $\Delta m^2$  as indicated by the hatched region.

$$\begin{array}{l}
 \text{LSND :} \quad \nu_\mu \rightarrow \begin{pmatrix} \nu_1 \\ \nu_3 \end{pmatrix} \text{ or } \begin{pmatrix} \nu_2 \\ \nu_3 \end{pmatrix} \rightarrow \nu_e \quad \begin{array}{l} \Delta m^2 \approx 0.1 - 0.5 eV^2 \\ 22\theta \approx 5 \times 10^{-3} \end{array} \\
 \text{Atmospheric :} \quad \nu_\mu \rightarrow \begin{pmatrix} \nu_2 \\ \nu_3 \end{pmatrix} \rightarrow \nu_\tau \quad \begin{array}{l} \Delta m^2 \approx 0.1 - 0.5 eV^2 \\ 22\theta \approx 1 \end{array} \\
 \text{Solar :} \quad \nu_e \rightarrow \begin{pmatrix} \nu_1 \\ \nu_2 \end{pmatrix} \rightarrow \nu_\mu \quad \begin{array}{l} \Delta m^2 \approx 10^{-5} eV^2 \\ 22\theta \approx 3 \times 10^{-3} \end{array}
 \end{array}$$

The MiniBooNE experiment has the sensitivity to test for both  $\nu_\mu \rightarrow \nu_e$  and  $\nu_\mu \rightarrow \nu_\tau$  oscillations in the  $\Delta m^2 = 0.1 - 0.5 \text{ eV}^2$  mass region at the above mixing levels and, thus, offers an opportunity to explore this possible inclusive scenario.

### 11.3 Overview of Beam and Detector

Discussion with FNAL staff and management indicate that the Booster is capable of providing an additional 5 pulses per second at  $\sim 5 \times 10^{12}$  protons per  $1 \mu$  sec pulse at 8 GeV beyond the requirements for antiproton stacking. As 2 GeV pion production is copious from an 8 GeV beam, we propose building a focusing system capable of producing a parallel beam of pions with momentum spectrum centered on 2 GeV/c. Presently, a horn-beam design is planned, although other possibilities are under consideration. This beam has a relatively short decay length of 30 m, so that the fraction of  $\nu_e$  in the beam from the  $\pi \rightarrow \mu \rightarrow e$  decay chain is kept at a low level, as these  $\nu_e$  are a basic background for the appearance measurement. The focusing system will be capable of operation in either positive or negative polarity. The positive polarity yields a higher neutrino flux, although the  $\nu_e$  background

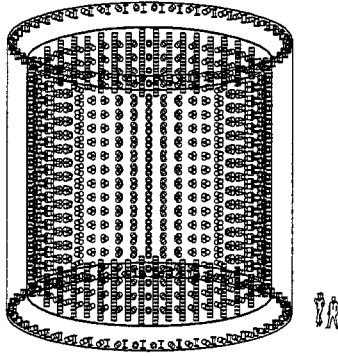


Figure 11.5: Schematic of the proposed detector.

Table 11.1: The characteristics of the BooNE detector.

	Detector	Veto
Volume	695 m <sup>3</sup>	400 m <sup>3</sup>
Mass	591 t	340 t
PMTs	1220(10%)	292
Fiducial Volume	449 m <sup>3</sup>	
Fiducial Mass	382 t	

from kaon decays is lower for the negative polarity. The duty factor of the Booster beam with single turn extraction makes cosmic ray background manageable and makes the data acquisition problem much simpler than for LSND. The decay region is designed to reduce the  $\nu_e$  contribution from kaon and muon decays. Particle production in the beam line is monitored using similar systems to those in the NuTeV experiment.

We propose building a 400 ton fiducial volume detector located at 1000 m from the neutrino source. The detector will consist of two concentric tanks. The inner (main detector) volume is a right cylinder, 9.6 m in height and 9.6 m in diameter, while the outer tank is 11 m in height and 11 m in diameter. The main detector will be filled with pure mineral oil or dilute scintillator oil. This detector has 1220 eight-inch photomultiplier tubes, taken from the LSND apparatus. The detector will be capable of measuring the  $\nu_e$  and  $\nu_\mu$  energy spectra through quasi elastic scattering, and the event energy distribution in the detector will allow the determination of the neutrino oscillation parameters. The region between the inner and outer tanks will be filled with high-light-output liquid scintillator oil to provide the veto. This veto surrounds the main detector on all sides. Characteristics of the MiniBooNE detector are shown in Table 11.1. A schematic of the detector is shown in Fig. 11.5. The detector is very similar to that in the LSND experiment, allowing transfer of analysis expertise, particularly in the area of particle identification. The trigger and DAQ for the MiniBooNE detector will re-use electronics from the LSND experiment, requiring only minor software modifications. The detector will be placed partially below ground level, with a dirt-embankment forming a hill over the tank to provide cosmic-ray shielding for the above-ground-level portion of the

detector.

## 11.4 MiniBooNE Capabilities and Issues

As discussed above, there is a need for experiments to probe  $\nu_\mu \rightarrow \nu_e$  oscillations in the  $0.01 - 1.0 \text{ eV}^2$  mass region with mixings down to  $22\theta \approx 10^{-3} - 10^{-2}$ . For  $\Delta m^2 = 0.1 \text{ eV}^2$ , an experiment needs an  $L/E$  value between 2 to 4. Since the rate from a neutrino source falls as  $1/L^2$ , the most cost effective way to probe this region is with the smallest  $L$  for the available  $E_\nu$  value. A neutrino beam from the 8 GeV Fermilab Booster is almost optimal for this region using an  $L$  value of  $\sim 1 \text{ km}$  combined with  $0.15 < E_\nu < 1.0 \text{ GeV}$ . In addition, a sensitive search for  $\nu_\mu \rightarrow \nu_e$  oscillations requires low intrinsic  $\nu_e$  background in the beam. A Booster  $\nu$  beam would have low  $\nu_e$  background event rate ( $\nu_e/\nu_\mu \approx 10^{-3}$ ) since the  $K$  production source is reduced with the low primary proton energy and a short decay pipe can be used, thus, minimizing the  $\mu$  decay source.

A low-energy Fermilab  $\nu$  experiment is possible due to the very high proton fluxes available from the Booster. Combining the high proton flux with a high efficiency horn focused secondary beam will provide over 100,000  $\nu_\mu$  events/kt-yr at 1 km from the source. The high intensity and rapid cycling of the Booster does make important requirements for the beam design. There will need to be significant shielding to meet radiation safety requirements. The beam elements including the high-current horn will need to be reliable at cycle rates of  $\approx 5 \text{ Hz}$ . A new underground enclosure must be constructed to house and provide access to the beam, the 30 m decay pipe and the dump. The neutrino beam will be directed horizontally at 7 m below the ground level, thereby minimizing any surface radiation. In order to make the experimental costs low, the enclosure needs to be made using conventional construction techniques and existing shielding materials where possible.

The proposed experiment would start with a single detector with the goal of probing the LSND mass region and establishing definitive indications of neutrino oscillations. If a positive signal is observed, this first stage would be followed up using a two detector experiment in the same neutrino beam. For the initial single detector experiment, MiniBooNE, accurate  $\nu$  flux and background calculations will be needed. Modern simulation tools can accurately model beam transport and scraping but need to be augmented and checked using direct measurements. A primary ingredient for the simulation is the particle production spectrum from the 8 GeV proton interactions in the thick production target. Data does exist from Argonne and KEK but will need to be supplemented by measurements taken with the actual neutrino beam. Position and profile monitors similar to those used by NuTeV and BNL 776 in the primary beam, decay pipe, and post-dump region will provide important constraints on the beam simulation. It is also possible to measure the momentum spectrum by allowing a tiny part of the secondary beam to pass through the dump into a small spectrometer. Analysis methods have been developed in previous neutrino experiments to use the measured neutrino spectrum in the detector to determine the secondary particle fractions. For example, this technique has been successfully used to fix the charged  $\pi/K$  fraction in the NuTeV experiment and, thus, fix the  $\nu_e$  background from  $K^+/K^-$  decay.

The MiniBooNE experiment needs a detector with a large fiducial mass and good particle identification for neutrino events in the  $0.15 < E_\nu < 2.0 \text{ GeV}$  energy region. At these

low energies, a totally active detector is necessary. A detector based on a large volume of dilute, mineral-oil-based scintillator is both cost effective and very powerful for particle identification using the techniques developed for the LSND experiment. Mineral oil has several advantages over distilled water as a detection medium: a) more Čerenkov light, b) no purification requirements, c) shorter radiation length, d) less  $\mu^-$  capture probability, and e) the ability to form a dilute scintillator mixture for better particle identification. Many of the critical detector components are available from the LSND experiment including the 1220 eight-inch photomultiplier tubes (PMTs) with readout and data acquisition system. The dilute scintillator will be contained in a double wall tank 11 m in diameter by 11 m high leading to a fiducial volume corresponding to  $\sim 400$  tons. The 70 cm region between the two tanks will be filled with regular liquid scintillator and instrumented with PMTs as a veto. In order to minimize costs, the tank will use standard commercial oil/water tank technology and safety standards and be partially buried.

Particle mis-identification is an important limitation for the  $\nu_\mu \rightarrow \nu_e$  oscillation measurement. Using the techniques developed and tested in the LSND experiment, the mis-identification of  $\nu_\mu$  events as  $\nu_e$  events can be reduced to the  $\approx 2 \times 10^{-3}$  level while keeping the  $\nu_e$  and  $\nu_\mu$  efficiency above 50%. The identification techniques are based on the spatial and time correlation of the detected Čerenkov and scintillation light by the PMTs lining the walls of the detector. A further strength of the experiment is the ability to measure these backgrounds from the preponderance of events which are identified correctly. Muon neutrino events are identified by observing an exiting  $\mu$  or a decay electron with the correct time and position correlation with the  $\mu$  track. For  $\nu_\mu$  events, about 8% of the outgoing  $\mu^-$ s are captured before decay and must be identified by the spatial and time signature of the Čerenkov and scintillation light. In this type of detector, a  $\mu$  has a more focused Čerenkov ring and relatively more scintillation light than an  $e$  or  $\gamma$  interaction. (Scintillation light can be isolated due to its much broader time distribution.) The signature for a  $\nu_e$  event is a diffuse Čerenkov ring with relatively low scintillation light. This signature can also be satisfied by  $\nu_\mu N \rightarrow \nu_\mu \pi^0 X$  events where the  $\gamma$ s from the  $\pi^0$  decay are identified as electrons. The cross section and  $E_\nu$  threshold for the  $\pi^0$  production reduces the rate substantially for this process with respect to  $\nu_\mu N \rightarrow \mu X$  scattering but a rejection factor of 100 is still needed to reduce this background to the  $10^{-3}$  level. This rejection is available for the MiniBooNE detector by detecting the second  $\gamma$  or by detecting late scintillation light from an energetic recoil proton or outgoing muon. Further reductions are also possible by minimizing the high energy component of the  $\nu_\mu$  beam where  $\pi^0$  production is largest. The high energy component can be reduced by moving the detector off the beam axis and by adding dispersion in the beam optics.

The 8 GeV Booster  $\nu$  beam using a focusing horn system and a 30 m decay pipe will provide  $\sim 50,000$  (10,000) identified  $\nu_\mu(\bar{\nu}_\mu)$  events/yr in the 400 ton MiniBooNE detector. For the  $\nu_\mu \rightarrow \nu_e$  oscillation measurement, the beam-related and mis-identification backgrounds can be held to less than  $\sim 0.5\%$  and be known with a systematic uncertainty of 10%. If oscillations exist at the LSND level, MiniBooNE should see several hundred anomalous  $\nu_e$  events over a beam-related (mis-identification) background of 100 (150) events, establishing the signal at the  $> 5 \sigma$  level. If no oscillation signal is observed, the experiment will exclude  $\nu_\mu \rightarrow \nu_e$  oscillations with  $22\theta > 6 \times 10^{-4}$  for large  $\Delta m^2$  and  $\Delta m^2 > 0.01 \text{ eV}^2$  for  $22\theta = 1$  as shown in Fig. 11.1.

### 11.4.1 Non-oscillation Neutrino Physics with MiniBooNE

With the MiniBooNE detector and FNAL booster neutrino source, a plethora of nuclear and particle physics using the neutrino as a probe could be investigated. These topics include the role of strangeness in the proton, the behavior of the axial vector mass and coupling constant in nuclear matter, the helicity structure of the weak neutral current, and the neutrino magnetic moment. The copious flux of intermediate energy (100 MeV - 2 GeV) neutrinos from the FNAL booster source would provide a new opportunity to pursue this physics. The following is a partial list of ideas presented at the workshop:

- Neutrino-Nucleon Elastic Scattering and a Measurement of  $G_s$ .
- Neutrino Charged-Current Scattering.
- Neutral-Current  $\pi^0$  Production.
- Neutrino-Electron Neutral-Current Scattering.

## 11.5 BooNE: A Future Upgrade to Two Detectors

Given that an oscillation signal is observed in MiniBooNE, then a natural upgrade to the MiniBooNE experiment is to add a second detector, allowing us:

- to determine the oscillation parameters from both  $\nu_\mu \rightarrow \nu_e$  and  $\nu_\mu$  disappearance. We estimate that, for the oscillation parameters above,  $\Delta m^2$  can be determined with an uncertainty of  $< 0.1 \text{ eV}^2$  and  $22\theta$  with an uncertainty of  $< 25\%$ .
- to search for CP violation in the Lepton Sector.

The energy dependence of the ratio of neutrino events in the two detectors determines the oscillation parameters. Comparison of results from running in neutrino mode to antineutrino mode investigates CP violation.

The second detector will be a double-wall cylindrical tank of the same design as the MiniBooNE detector. This new, near detector will be placed approximately 500 meters from the neutrino source. The MiniBooNE detector would be used as the far detector, located at 1000 meters from the beam line target. These distances are chosen to provide the optimum comparison between the rate of events in the near and far detector. The MiniBooNE beam line will be used to provide the neutrino and antineutrino beams for both detectors.

For the estimation of event rates we make the following assumptions. First, we assume that the Booster operates at an energy of 8 GeV and at an average rate of 5 Hz ( $2.5 \times 10^{13}$  protons/s) for 3 years of operation ( $3 \times 10^7$  s) at each focusing polarity. Also, we assume that the fiducial volume of the detector is 382 t ( $1.7 \times 10^{31}$   $CH_2$  molecules) and that the total electron and muon efficiencies, including PID, are 50%. The resulting numbers of quasi elastic events are shown in Table 11.2 for both neutrino and antineutrino scattering and for both the near (500 m) and far (1000 m) detectors. The muon-neutrino quasi elastic scattering estimates assume no oscillations, while the electron-neutrino quasi elastic scattering estimates assume 100%  $\nu_\mu \rightarrow \nu_e$  transmutation.

Table 11.2: The estimated numbers of quasi elastic events for both neutrino and antineutrino scattering and for both the near (500 m) and far (1000 m) detectors (see text for explanation).

Reaction	Near Detector	Far Detector
$\nu_\mu C \rightarrow \mu^- X$	609,600	152,400
$\bar{\nu}_\mu C \rightarrow \mu^+ X$	114,000	28,500
$\nu_e C \rightarrow e^- X$	630,000	157,500
$\bar{\nu}_e C \rightarrow e^+ X$	115,200	28,800

## 11.6 Conclusions

We have considered the design for a detector system and broad band neutrino beam generated from the Fermilab Booster that has the capability of observing and measuring  $\nu_\mu \rightarrow \nu_e$  and  $\bar{\nu}_\mu \rightarrow \bar{\nu}_e$  oscillations over a wide range of  $\Delta m^2$ . The motivation for this experiment stems from the LSND neutrino oscillation result [18] and the atmospheric neutrino problem. In addition, this detector can be used to make a sensitive search for CP violation in the lepton sector, to search for  $\nu_\mu$  disappearance, and to measure all observed neutrino oscillation parameters from the event energy distributions.

# Chapter 12

## Summary of the Detector Technology Working Group

Reported by A. Bross, Fermilab and N. Solomey, Univ. of Chicago

### 12.1 Introduction

The detector technology sessions at the Workshop on physics at the Main Injector were of two types, one session dedicated to new developments and advances in detectors and two sessions in parallel with the Kaon and Neutrino groups, where the emphases was more on the specific needs of future experiments. However, almost every working group had some discussion on detector issues, since detector capabilities are a key factor in any experiment planning. Advances in detector technologies will clearly improve many of the experiments under consideration; how to best do this was hence an important issue.

In summarizing the detector technology sessions, three distinct items can be brought up for the attention of all the attendees of the workshop. These items are:

1. Highlight major achievements in detector technology development that are in currently running experiments or that have just been successfully tested.
2. Bring to attention major new achievements in detector technologies that might be of use to future experiments in the near term.
3. Offer some words of caution and constructive criticisms of ideas in detector technology that are under consideration in order to help guide experimenters in their evaluation of these new technologies.

### 12.2 Recent Achievements of Detector Technology in Experiments or Tests

Discussion on all of the experiments or tests that produced exciting results is far beyond the scope of this summary, but three specific achievements come to mind. First, experiments with emulsions are still providing useful physics results and emulsion experiments are still viable options being considered for the next round of neutrino experiments. This older technology is still viable only because of the advancement in our ability to scan the emulsions.



This scanning technology equipment (helped by tracking and triggering detectors in the experiment) has advanced several order of magnitudes to be able to keep up the very large selected event samples that will exist in future experiments. Hence, combining the older technology of emulsions (with its superior ability to determine a vertex and track length at the decay region) with the more modern fast electronic detectors of today provides a powerful physics tool. Second, events from the test liquid time projection chamber for the ICARUS experiment demonstrate, shown here in Figure 12.1, the superior tracking capabilities of a bubble chamber image without the well known limitations of bubble chambers. The ICARUS TPC also showed that the fine sampling of the liquid has a phenomenal particle identification ability by combining both  $dE/dx$  ionization loss with particle range in the liquid. This detector technology has the potential to make significant contributions to neutrino physics. The ICARUS collaboration is currently building a large module that will permit it to perform one or possibly two neutrino oscillation experiments. Experiments showed how their various detectors are performing and many of them, as expected, are producing wonderful results. They are far too numerous to present them all, but one, the electromagnetic calorimeter of KTeV, is particularly noteworthy. They have a large array of 3000 CsI crystals with fast pipelined read out electronics. This high rate electromagnetic calorimeter is performing with better than 1% total energy resolution above 2 GeV (see figure 12.2a), and is providing more than 300:1 electron-pion rejection by using  $E/p$  (see figure 12.2b).

### 12.3 New Detector Technology Developments

The session on new detector technology had six talks centered around new developments that could be of general interest for experiments in the next round of fixed target experiments at the main injector. These new developments aim at either achieving a better performance, or a good performance at a lower cost. The talks were:

1. New plastic scintillator, Anna Pla.
2. Development of a 5 inch Hybrid Photon Detector, Tom Ypsilantis.
3. Development of the KTeV TRD system, Greg Graham.
4. Development of a Gas Electron Multiplier, Dave Anderson (for Fabio Sauli).
5. Silicon Microstrip Detectors, Lenny Spelial.
6. Pixel Detector R&D at Fermilab, Dave Christian.

The other detector technology sessions held jointly with kaon decay experiments and the neutrino oscillation sessions had new detector technology presentations. Contributions included:

1. Development of the D0 Fiber Tracker, Suyong Choi.
2. A Long Baseline RICH, Tom Ypsilantis.

### 3. Icarus Liquid TPC Detector, C. Montanari and F. Pietropaolo.

The goal of making large amounts of inexpensive fast scintillator is of general interest to all experiments, but most to the neutrino oscillation experiments under consideration. This new technology uses commercial polystyrene for the base polymer and then infuses scintillation dyes into the polystyrene pellets that can then be extruded into various shapes. This technique is both faster and far less expensive than the standard processes for fabricating plastic scintillator plate. These scintillators have slightly less light output than standard scintillator and their optical properties are poorer, however, these features appear to be acceptable given tremendous (up to a factor of 10) savings they can provide. The development of the D0 Scintillating fiber central tracking (shown schematically in Figure 12.3), was presented for possible consideration at the Main Injector fixed target experiments. It has the advantage of fast light output so that experiments with high rates such as the proposed next round of neutral kaon experiments at KAMI will be able to operate at extremely high particle flux rates for the purpose of improving the limits on rare kaon decays. The scintillating fiber tracking system with its VLPC readout was described. Questions regarding position resolution, double-track separation and time after a hit before the second hit can be recorded in the same fiber were items of discussion. The development of a Hybrid Photon Detector where a large photocathode of pure CsI in a thin layer was reviewed. The main components can be seen in figure 12.4. Electrons liberated by a photon of light are then accelerated by a high voltage potential and impact on a multichannel silicon detector. The silicon detector can be of the users geometry optimized for the physics needs of the experiment. The beauty of such a system is its ability to be custom made for an experiments specific needs.

Gaseous wire chambers are still an active part of any experiment currently running and those planned. However wire chambers have a known limitation in the amount of charge per wire they can take. How to overcome this problem has been a concern for experimentalists for some time. A recent invention of Fabio Sauli may have a way to reduce the amplification needed near the wires. His invention, called the Gas Electron Multiplier (GEM), uses a thin film of kapton plated on both sides with a layer of copper. If the copper is removed in an array pattern of holes on both sides, and the kapton is dissolved to give a pattern of holes where ionization can drift through, when a voltage is applied across this kapton plate, a high field region is created in the kapton gap, see figure 12.5, where electrons can be multiplied by a factor of 100 to 300. This has the nice feature that it can be used with a wire chamber, a MSGD, or several GEM detectors that are then put together to give the amplification enhancement needed. It is a stable system of gas amplification that may provide the solution to the MSGD gain limitation problem or in other systems.

Other gaseous detectors were discussed in many of the parallel working sessions of the conference. One talk presented the performance of the large TRD system of KTeV, which currently has better than 200:1 electron-pion rejection in a high rate environment. The detector was very versatile and its use is in active consideration for a neutrino oscillation experiment. Other large area wire chamber systems are currently in use at Fermilab's fixed target experiments and will remain an important part of all future experiments. How to improve on the wire chamber, especially to reduce its cost, was a theme in the neutrino oscillation working group. Other concerns were to make them faster as well as more radiation hard for  $K^+$  decay or CPT experiments.

Silicon strip and pixel array detectors were presented in two presentations. Both of these presentations discussed the problems with making connections to small patterns as well as the radiation damage problem of this type of detector and the associated readout electronics. Pixel array detectors present a formidable packaging (detector to readout electronics) problem and a number of bump-bond techniques were described. The radiation hardness issue with regard to the readout electronics is possibly the most severe technical problem to overcome in high-rate environments. A radiation-hard process developed by the French military looks like a good candidate to try for silicon detector electronics and this process is now commercially available in Europe.

## 12.4 Concluding Words of Caution

From the many detector limitations discussed by the physics working groups, it was obvious that several developments are needed. Detector issues of most importance include higher rate tracking, high-resolution tracking, hermetic photon veto capability, and affordable extremely-large-volume detectors for neutrino experiments. Every new detector development should be approached with some skepticism, however. In order to make a new detector technology available to a wide range of experimental work, this new technology must first be fully understood and, second, its performance limitations must be evaluated for operation in differing experimental conditions. New detector technology developments may have hidden limitations that need to be thoroughly understood, such as radiation damage with silicon detectors or new plastics. So care and prudence should be exhibited in applying these new ideas. Developing a new technology into a real research tool will take time and money, but future experiments can greatly benefit from this effort. It is certainly true that if we do not attempt new detector developments this will likely limit our opportunities to do even better experiments.

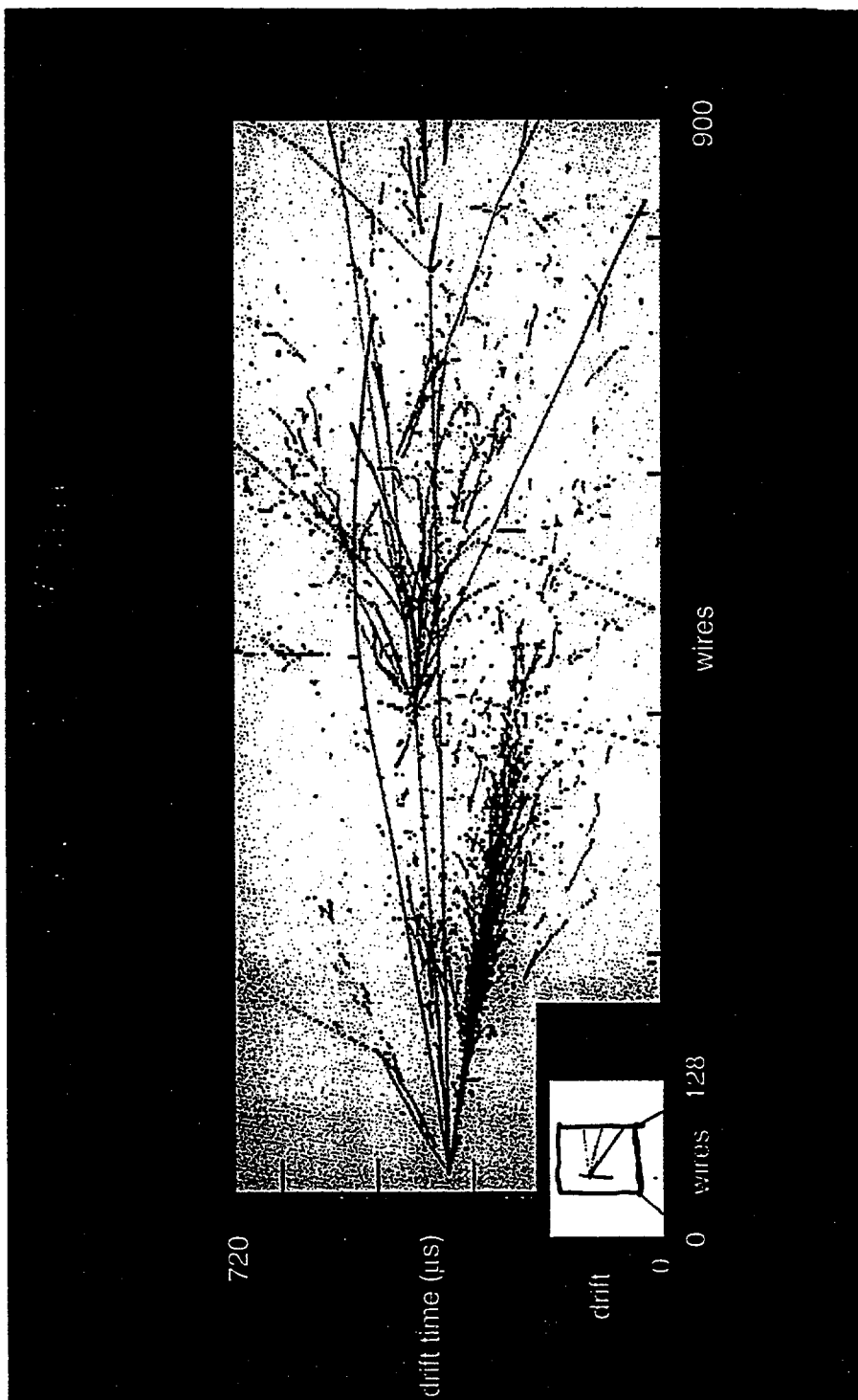
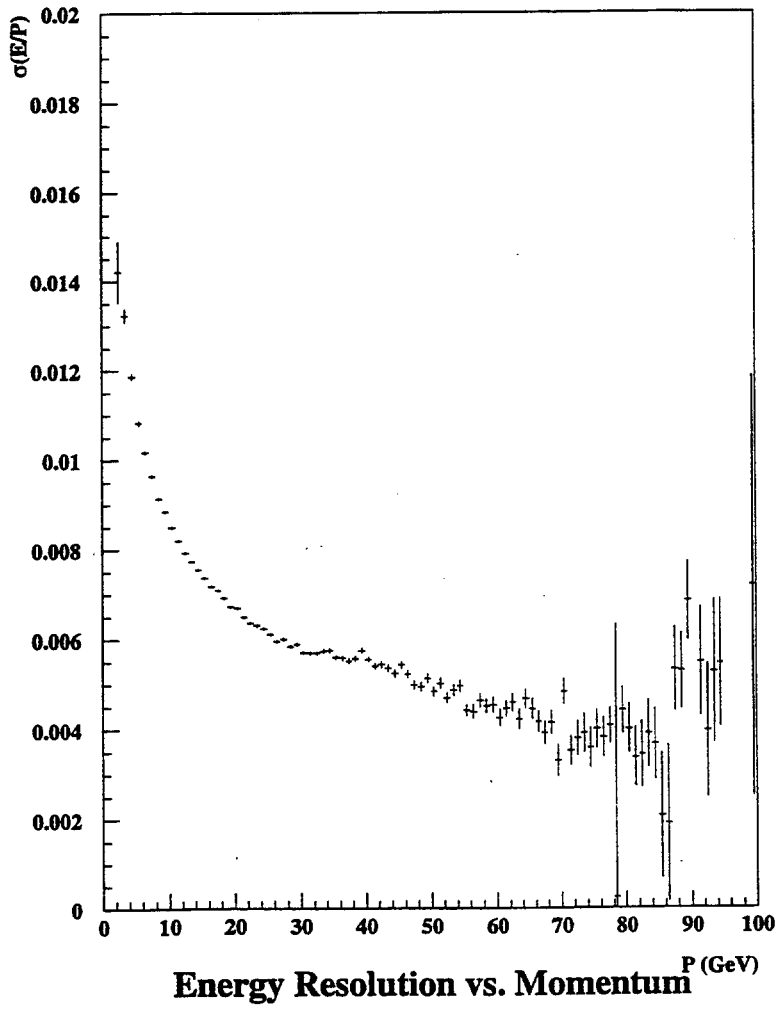


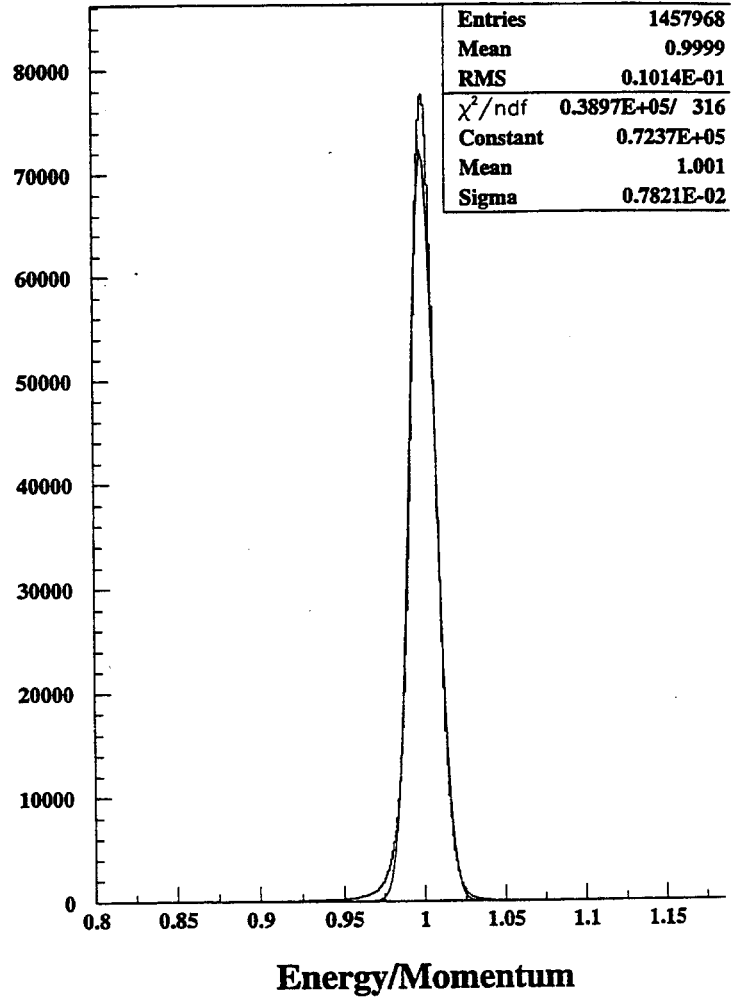
Figure 1. Simulated event in the ICARUS liquid TPC

Electrons from  $K \rightarrow \pi e \nu$



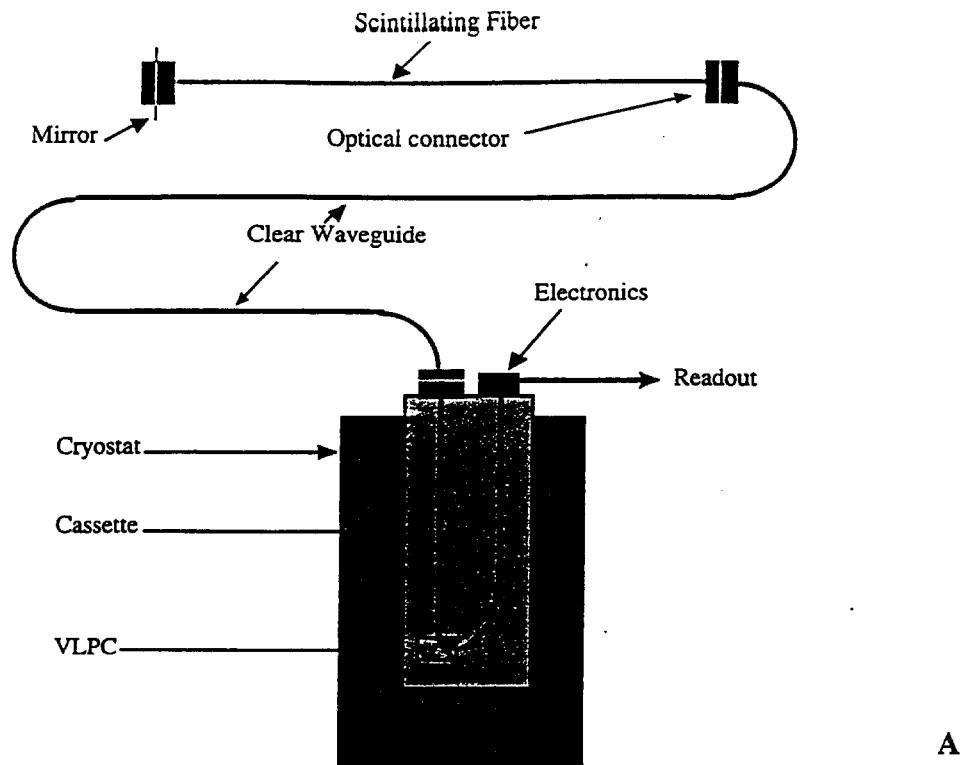
A

Electrons from  $K \rightarrow \pi e \nu$

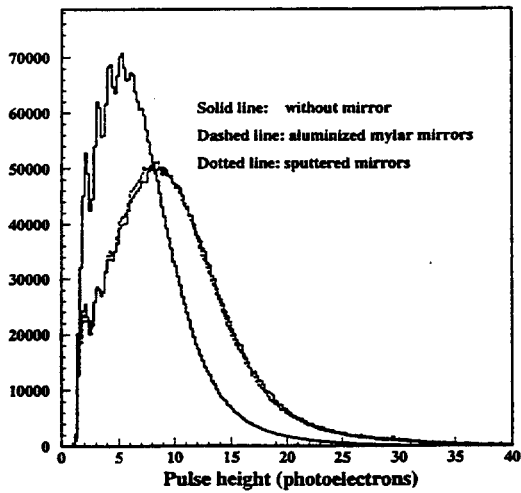


B

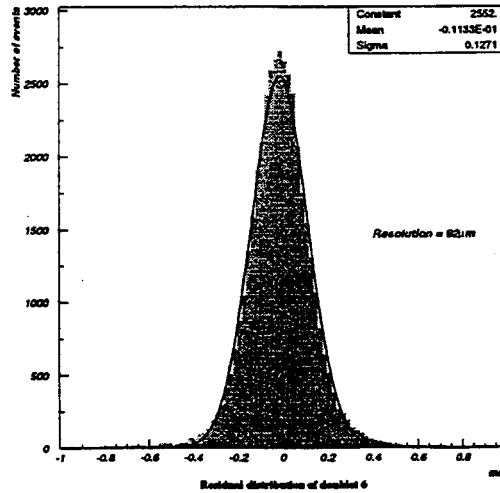
Figure 2. A) Energy resolution of KTeV CsI calorimeter. B) Electron E/P resolution



- ▲ Sci. fiber: 1.6-2.5m
- ▲ Clear fiber: 8-11m
- ▲ Readout from one end



B



C

Figure 3. A) Schematic of scintillating fiber tracker and readout. B) Light yield for MIPs in photoelectrons. C) Doublet resolution of 92  $\mu$ m.

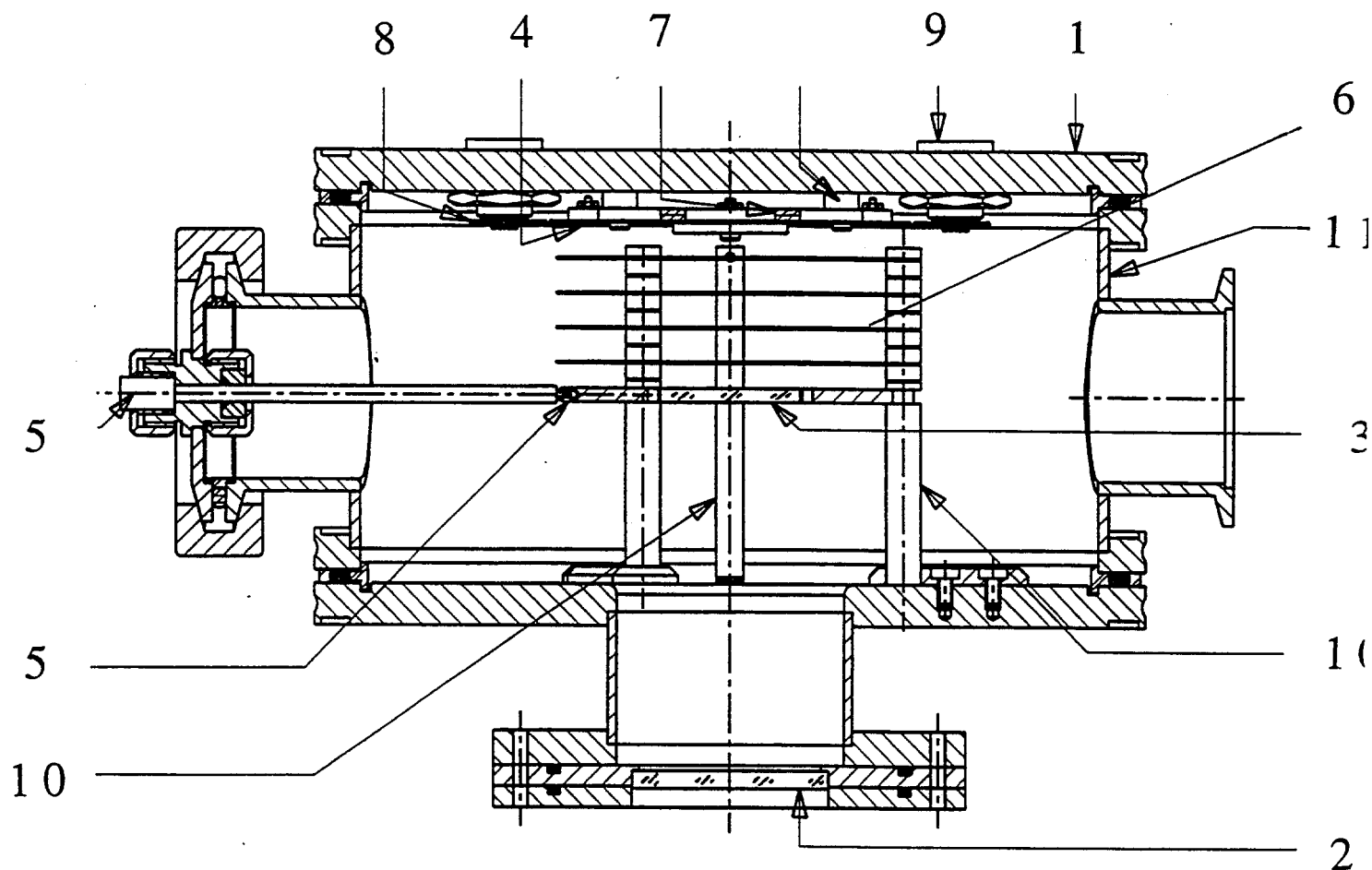
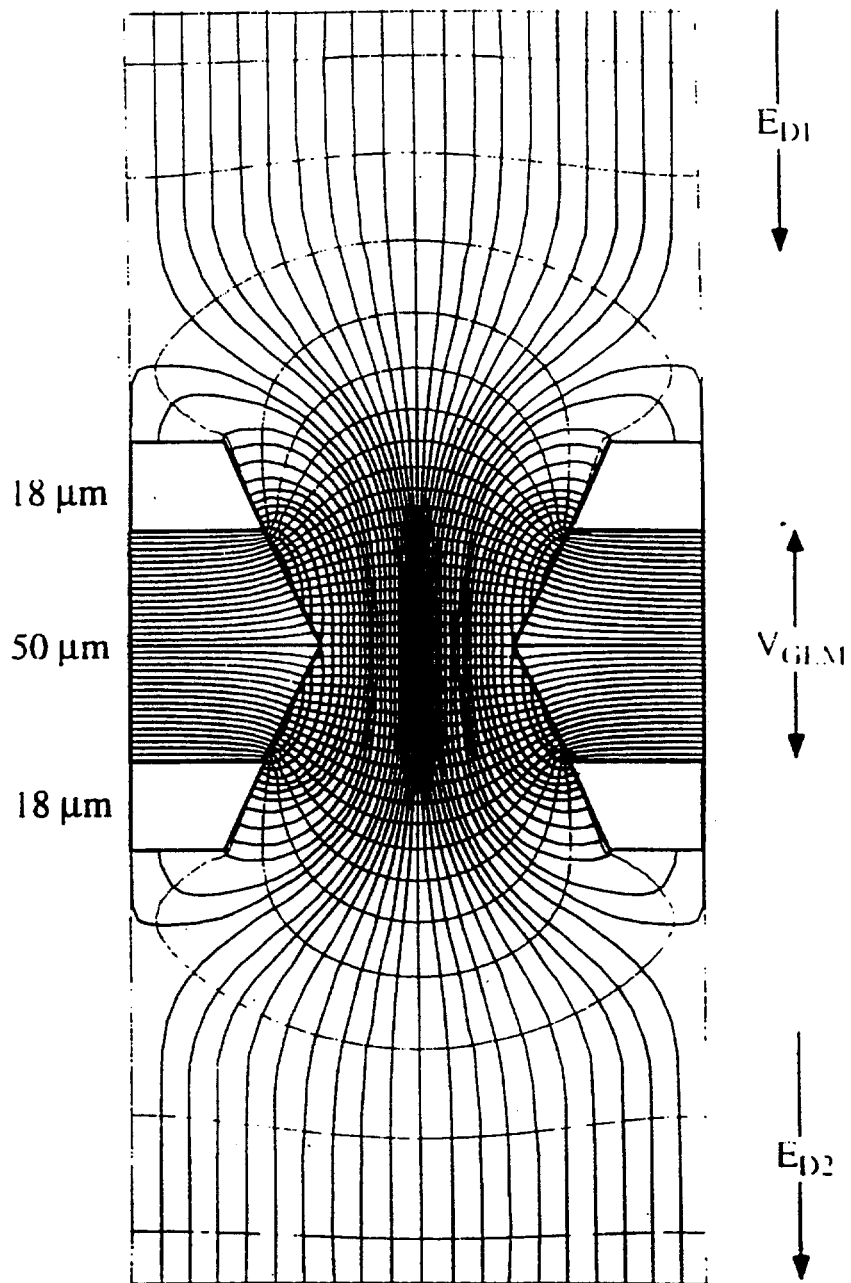


**Figure 4.** Cross section of the HPD test module: (#1) the support flange for the Si detector; (#2) the  $\text{CaF}_2$  window; (#3) the  $\text{CaF}_2$  crystal on which is deposited the semi-transparent CsI photocathode; (#4) the Si photodetector; (#5) the HV connector for the acceleration potential; (#6) the focusing electrodes; (#7) ceramic support for the Si detector. (#8) ceramic support for the VA2 chips.



$V_{GEM} = 360 \text{ V}$      $E_{D1} = E_{D2} = 3 \text{ kV/cm}$

**Figure 5. Typical field distribution within the hole in a GEM.**



# Chapter 13

## Summary of the Main Injector and Beams Working Group

Reported by R. Coleman, P. Martin and T. Murphy, Fermilab

Contributing members: C. Bhat, P. Lucas, M. Martens, and A. Russell

This group presented to the users options available in the year 2000 for 120 GeV extracted beams into the Switchyard and met with experimenters to discuss their needs during that era. Problems of proton economics were discussed, and the issue of whether it is feasible to extract to both NUMI and Switchyard on the same Main Injector cycle was explored.

Fig. 13.1 shows the beams that are planned to be available in the year 2000 and beyond. The capability of extracting 800 GeV to the Proton Area and the KTeV/Kami beamline will be maintained, but of course will not run during Collider operations. However, simultaneously with Collider operations, 120 beam will be slow-extracted from the Main Injector and transported in the remnant Main Ring (F-sector) to the Transfer Hall, where it will be bent out of the Main Ring and rejoin the existing Switchyard between the Proton Area electrostatic septa (PSEP) and Lambertson magnets (PLAM). It can then be split between Meson and the KAMI experiment.

For tuneup purposes, the beam can be switched to the Switchyard dump. In Meson, it is planned to maintain the three-way split (FSEP) as shown in Fig. 13.1. The existing cryogenic Left Bend to Meson will be replaced with conventional EPB dipoles running at a rather modest current. There are no plans to get the 120 GeV beam to Proton or to any other part of Neutrino except KAMI.

The present goals call for making all the revisions necessary in the Transfer Hall through Enclosure B (see Fig. 13.1) during the Sept. '97 - Oct. '98 shutdown. Conceptual design of these changes and additions is nearly complete. The design and schedule for improvements necessary in Enclosure C and beyond are not clear yet. However, a small working group in the Beams Division is actively studying the optics of the entire Switchyard to ascertain what changes are necessary to fit the beams - expected to be 2.6 times bigger than at 800 GeV - through the critical apertures in Switchyard. Because of manpower limitations during the above shutdown, the Left Bends might not be replaced until 1999.

The above goal allows us to take a phased approach. During the 800 GeV fixed target extension of Nov. '98 - May '99 we would use any opportunity to actually extract 120 GeV

beam into the Switchyard and learn about the optics with real beam. This could be done whenever the Tevatron is down, or even during the 40 seconds of Tevatron ramping, if the controls problem of ramping up and down between 800 GeV and 120 GeV in Switchyard is not too challenging. This exercise would help us decide on what further improvements are genuinely needed in Enclosure C and beyond. These final changes would be made during the changeover and Tevatron recommissioning period (May '99 - Oct. '99). The Tevatron recommissioning time is another opportunity to make beam tests.

Some of the changes to Enclosure C and beyond which are being studied and may be necessary are as follows. The electrostatic septa (MSEP, FSEP) may need to have their gaps increased from 2 cm to 4 cm to accommodate the bigger beams. Alternately, quadrupoles may need to be added to the Meson and KAMI lines to make the beams smaller at critical apertures. It is known that the Meson line did have more quadrupoles during the 200 GeV era. The existing FSEP might have to be moved downstream in order to make room for such quadrupoles. Finally, it might be desirable to remove (and in some cases recycle) beam elements that are no longer needed or which are unnecessary apertures.

The important overall goal is to have the 120 beams tested and ready for use during the Collider run of 2000.

The group had discussions with individuals and other groups about their beams needs. In particular, we met with:

- Gordon Thomson (CPT experiment) and Peter Cooper (CKM) and their groups
- Rick Coleman (KAMI)
- Jim Hylen (NUMI)
- Janet Conrad (BooNE) and that entire group.

The discussion with the CPT and CKM groups centered on the RF separated  $K^+$  beam which they have proposed, with a focus on the 2.45 GHz RF systems which they need. A preliminary cost estimate for these systems was made by Al Moretti and is about 2M\$. The required proton intensity during a 2 second spill is  $5 \times 10^{12}$  / spill for CPT and  $1 \times 10^{12}$  for CKM. CKM has a further requirement of a 0.05 to 0.10 mrad beam divergence. They inquired what it would take to bunch the beam to less than 50 ps in the Main Injector itself, which would eliminate the need for one of their RF cavities. Following a talk by Chandra Bhat, the consensus in our group was that it was much too expensive.

The meeting with the BooNE group featured a talk by Dave Herrup on Booster expectations which was informative to them. KAMI, represented by Rick Coleman, indicated that KAMI was planning a staged approach. Initial running would be with the existing KTeV target station which is located 140 m from the start of the decay region. Later running would be with a new target station located 20 m from the start of the decay region. The intensity needs would also follow a staged approach ultimately reaching  $3 \times 10^{13}$ . Debunched Main Injector may be desirable to lower the instantaneous rates in the detector.

Jim Hylen (NUMI) pointed out that they are designing for  $4 \times 10^{13}$  protons per spill, and even if they got "most" of that, just the increased cycle time implied by the presence of slow spill would seriously impact the protons per year that they could expect. They have

been advertising that they hoped to receive  $3.7 \times 10^{20}$  protons/year. This led members of our group to explore various scenarios for "mixed" and "interleaved" cycles (see below). We also learned that they are rather fixed on taking 1 msec spill in the wide band beam (the horns cannot run longer than that).

Weiren Chou gave a talk for our group on factors which limited the MI intensity to  $3 \times 10^{13}$  and how these factors might be overcome. His studies give some hope that the intensity might be increased to  $6 \times 10^{13}$  over the course of several years without major investments in new hardware.

Members of the group then explored various scenarios for "mixed" and "interleaved" MI cycles and the impact of each scenario on the protons/hr delivered to antiproton production (AP), fast spill, and slow spill. The result of this study led to Table I, which requires some detailed explanation. The assumptions common to every line of this table are that the total intensity of the MI is  $3 \times 10^{13}$  / cycle, and that  $5 \times 10^{12}$  protons/cycle are delivered to AP during those "modes" in which AP is listed.

Column 1 of this table lists the "mode" and column 2, the MI cycle time for that mode. The remaining columns list the protons/hr delivered to AP, fast spill, and slow spill in that mode. The first three lines show what the minimum cycle times are for dedicated running of AP, fast spill, or slow spill with a 1 sec flattop (FT). A 2 sec FT is possible, but puts the MI at its cooling limit.

The next two lines show "mixed modes" in which, for instance, beam is sent both to AP and to fast spill for NUMI on the same cycle. The cycle time rises another 0.13 sec owing to additional necessary manipulations.

The next line mixes all three extraction processes on the same cycle, which might be quite pleasing to slow spill users: the "duty factor" is  $1 \text{ sec}/3.4 \text{ sec} = 29\%$  down by more than a factor two from the expectations of NUMI. "Interleaved" cycles is a way to restore some of the flux to NUMI, but at the expense of the duty factor for slow spill.

In the next line, cycles alternate between AP+fast and AP+slow. The protons/hr to fast spill have increased from  $1.3$  to  $1.8 \times 10^{16}$  / hr in the arbitrary 50/50 split between slow and fast spill. The duty factor for slow spill is reduced to 20

Another way to increase the integrated flux to NUMI is to interleave cycles in an unequal way between the two modes, as shown in the last two lines. In the last line, for instance, there are 12 successive AP+fast cycles followed by 1 AP+slow cycle, but with a 4 sec flattop (the MI can do that in this instance since it has the next 16 seconds to cool down). The slow spill duty factor is 13% fast spill would take 1.2 years without counting down time.

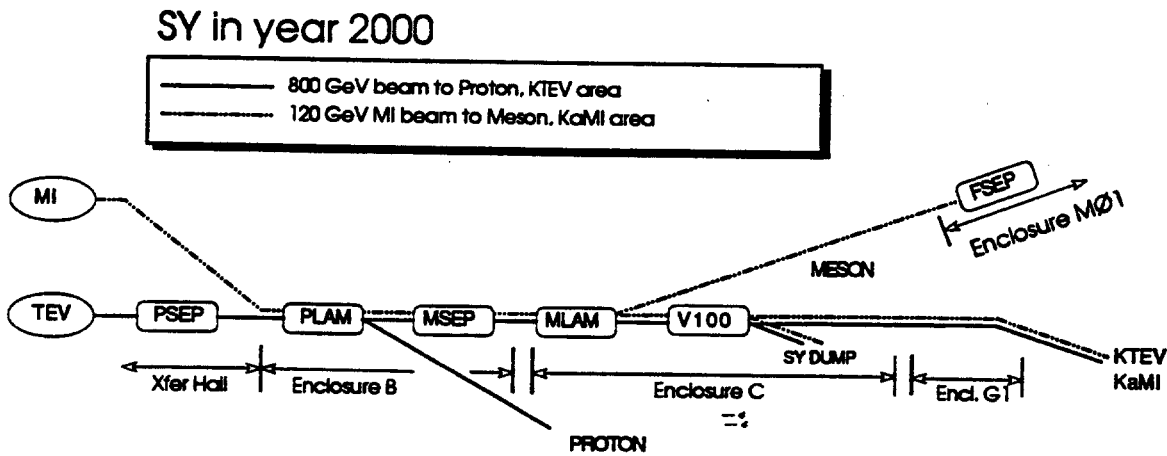
The interleaved schemes are also more favorable to AP than the three-way mixed scheme, reduced to only 67% line 1. Furthermore, as modeled by Gerry Jackson, even if the AP stacking rate were twice as slow as the maximum, and stores had to be doubled in duration, the decrease in the integrated luminosity would go down by only 15 to 20%.

One conclusion of this group is that raising the intensity of the MI to  $5$  or  $6 \times 10^{13}$  per cycle is a very worthwhile goal. 1

Table 13.1: Protons Per Hour Under Various Modes of Operation

Mode	Cycle Time	AP Target	Fast Spill	Slow Spill
Antiproton Production	1.466 sec	$1.2 \times 10^{16}$ (p/hr)	-	-
Fast Spill	1.866	-	$5.8 \times 10^{16}$	-
Slow Spill	2.866	-	-	$3.8 \times 10^{16}$
Mixed - AP + Fast Spill	2.000	$0.9 \times 10^{16}$	$4.5 \times 10^{16}$	-
Mixed - AP + Slow Spill	3.000	$0.6 \times 10^{16}$	-	$3.0 \times 10^{16}$
AP + Fast + Slow <sup>1</sup>	3.400	$0.5 \times 10^{16}$	$2.1 \times 10^{16}$ to $1.3 \times 10^{16}$	$0.5 \times 10^{16}$ to $1.3 \times 10^{16}$
Interleaved Cycles	2+3	$0.7 \times 10^{16}$	$1.8 \times 10^{16}$	$1.8 \times 10^{16}$
Interleave 8 F + S w/ 2s FT <sup>2</sup>	16+4	$0.81 \times 10^{16}$	$3.6 \times 10^{16}$	$0.45 \times 10^{16}$
Interleave 12 F + S w/ 4s FT	24+6	$0.78 \times 10^{16}$	$3.6 \times 10^{16}$	$0.30 \times 10^{16}$

Fig. 1



<sup>1</sup>Assumptions:  $6 \times 10^{10}$  protons per bunch, and additional time is required for bunch manipulations and turning off magnetic switch at F17 in mixed modes.

<sup>2</sup>Without large intensity increases, can support NUMI along with low rep rate slow spill. Interleaved cycles have  $3 \times 10^{13}$  with  $5 \times 10^{12}$  being targeted for antiproton production on each cycle, and the remainder going to one area or the other.

# Bibliography

- [1] A.M.Rozhdestvensky, M.G.Sapozhnikov, "Polarized intrinsic nucleon strangeness and elastic neutrino scattering on nucleon", write-up available from the web page of our working group
- [2] R.Jaffe, Proc. Adriatico Research Conf., Trends in Collider Spin Physics, ICTP, Trieste, Italy, 1995.
- [3] The EMC Collaboration, J. Ashman et al., Phys.Lett.B206 (1988) 364; Nucl.Phys.B328 (1989) 1.  
The NMC Collaboration, P. Amaudruz et al., Phys.Lett.B295 (1992) 159.  
The SMC Collaboration, B. Adeva et al., Phys.Lett.B302 (1993) 533.  
D.Adams et al., CERN preprint PPE/97-22, 1997.  
The E142 Collaboration, P.L. Anthony et al., Phys.Rev.Lett.71 (1993) 959.  
The E143 Collaboration, K. Abe et al., SLAC-PUB-6508.
- [4] M.G.Sapozhnikov, JINR preprint E15-95-544, Dubna, 1995.  
Lecture at the XXIX St.Petersburg Winter School on Nuclear Physics and Elementary Particles, Zelenogorsk, 1995, p.252.
- [5] J. Ellis, E. Gabathuler, M. Karliner, Phys.Lett., B217 (1989) 173.
- [6] J. Ellis et al, Phys.Lett. B353 (1995) 319
- [7] Ahrens L.A. et al., Phys.Rev. D35 (1987) 785
- [8] Garvey G.T. et al., Phys. Rev., C48 (1993) 761.
- [9] P875: A Long-baseline Neutrino Oscillation Experiment at Fermilab (MINOS proposal), February 1995.
- [10] P. Alport et al, Phys. Lett. B232 (1989) 417
- [11] D. Geesaman, K. Saito, A.W. Thomas, Ann. Rev. Nucl. Part. Sci., 45 (1995) 337.
- [12] Tim Bolton, "E803 Physics", linked to our web page.
- [13] EMC, Z. Phys. C52, 1 (1991); BEBC WA21/WA59, Z. Phys. C70, 47 (1996))
- [14] "Separation of intranuclear cascade effects" Elena Vataga for E632, talk presented at the workshop.

- [15] Nucl.Phys. B246, 381 (1984)
- [16] Z. Phys. C70, 47 (1996) and E632 results
- [17] Participants: M. Binkley, J. Conrad, L. DeBarbaro, K. Eitel, R. Drucker, Z. Greenwood, D. Herrup, G. Jackson, R. Imlay, H. Kim, W. Louis, P. Martin, G. Mills, C. Moore, S. O'Day, L. Sawyer, M. Shaevitz, I. Stancu, E. Stern, D. Strom, R. Tayloe, H. White, J. Yu
- [18] C. Athanassopoulos *et al.*, Phys. Rev. Lett. **75**, 2650 (1995); C. Athanassopoulos *et al.*, Phys. Rev. Lett. **77**, 3082 (1996); C. Athanassopoulos *et al.*, Phys. Rev. C **54**, 2685 (1996).
- [19] C. Athanassopoulos *et al.*, submitted to Phys. Rev. C.
- [20] K. S. Hirata *et al.*, Phys. Lett. B**280**, 146 (1992).
- [21] R. Becker-Szendy *et al.*, Phys. Rev. D**46**, 3720 (1992).
- [22] Y. Hirata *et al.*, Phys. Lett. B**335**, 237 (1994).
- [23] R. Clark *et al.*, submitted to Phys. Rev. Lett.
- [24] C. Cardall and G. M. Fuller, Phys. Rev. D **53**, 3532(1996); G. L. Fogli, E. Lisi, and G. Scioscia, hep-ph/9702298.
- [25] R. Davis et al., Proc. 21st Int. Cosmic Rays Conf., Univ. of Adelaide, ed. R.J. Protheroe, Vol 12 (1990) 143; P. Anselmann et al., Phys. Lett. B 285 (1992) 376; loc. cit. 390; B 314 (1993) 445; A.I. Abazov, Phys. Rev. Lett. 67 (1991) 3332; K.S. Hirata et al., Phys. Rev. Lett. 65 (1990) 1297; 66 (1991) 9; Phys. Rev. D44 (1991) 2241.
- [26] L. Wolfenstein, Phys. Rev. D17 (1978) 2369; D20 (1979) 2634; S.P. Mikeyev, A.Yu. Smirnov, Nuovo Cim. 9C (1986) 17.
- [27] K.S. Hirata et al., Phys. Lett. B205 (1988) 416; B280 (1992) 146; Y. Fukuda et al., Phys. Lett. B335 (1994) 237; P.J. Litchfield, Proc. Int. Europ hysics. Conf. on High Energy Physics (Marseille 1993), ed. J. Carr and M. Perrottet (Edition Frontieres, Gif-sur-Yvette) 447; R. Becker-Szendy et al., Phys Rev D46 (1992) 37 20; D. Casper et al., Phys. Rev. Lett. 66 (1992) 2561.
- [28] A. Athanassopoulos et al., LSND Collab., Phys. Rev. Lett. 77 (199 6) 3082; Phys. Rev. C 54 (1996) 2685; Phys. Rev. Lett. 75 (1995) 2650.
- [29] See talk of A. Mann at this workshop.
- [30] See talk of E. Kearns at this workshop.
- [31] See talk of W. Louis at this workshop.

- [32] P. Astier et al., NOMAD Collab., CERN/SPSLC-91/21; CERN/SPSLC- 91/48; CERN/SPSLC-91/53.
- [33] CHORUS Coll., M. de Jong et al., A new search for  $\nu_\mu - \nu_\tau$  oscillation, CERN-PPE/93-131.
- [34] Y. Declais et al., "Search for Neutrino Oscillations at a Distance of 1 km from Two Power Reactors at CHOOZ", Letter of Intent 1992; see also talks of R. Steinberg and J. Steele at this workshop.
- [35] See talk of G. Gratta at this workshop.
- [36] E. Heijne, CERN Yellow Report 83-06, Jul 83
- [37] G. Acquistapace et al., CERN Internal Note, CERN-ECP 95-14, Jul 95
- [38] P. Sievers et al., SPS/ABT/TA/Ps/80-103, 1980
- [39] S. Peraire et al., CERN Internal Note, CERN-SL 95-22, Nov 95
- [40] E. Weisse, Private communication
- [41] C. Foos et al., CHARM II Internal Note, Nov 1989
- [42] E. Tsesmelis et al., NOMAD Internal Note, Dec 1995
- [43] A. Ball et al., 'Design studies for a long base-line neutrino beam', CERN/ECP-95-013.
- [44] H. Atherton et al., CERN Yellow Report 80-06, Aug 1980
- [45] M. Bonesini et al., 'Aladino' proposal, CERN/SPSLC 95/37, Mar 1995
- [46] G. Ambrosini et al., CERN-SPSLC/96-01, Jan 1996
- [47] A. Chapman-Hatchett et al., SPS/ABT/Int 79-1, 1979
- [48] See talk of V. Palladino at this workshop.
- [49] S. Ragazzi, SPY report to SPSC , Mar 97
- [50] B. Van de Vyver et al., CERN-PPE/96-113, Aug 96
- [51] M.C. Gonzales Garcia et al., CERN-TH/96-220, Aug 96
- [52] E. Weisse, Report to Gran Sasso Workshop, Nov 95
- [53] ICARUS Collaboration, LNGS Int. Note, LNGS - 94/99; LNGS 95 /10.
- [54] ICARUS - CERN - Milano Coll., CERN/SPSLC 96-58 (SPSLC/P 304 ) (1996).
- [55] J. P. Revol et al., ICARUS-TM-97/01, 5 March 1997.
- [56] A.S. Ayan et al., CERN-SPSC/I213 , Mar 97

- [57] NuMI Technical Design Fermilab, Jul 1995
- [58] See talk of J. Hylen at this workshop.
- [59] See talk of C.K. Jung at this workshop.
- [60] P. Benetti et al., NIM A327 (1993) 173; NIM A332 (1993) 395; P. Cennini et al., NIM A333 (1993) 567; NIM A345 (1994) 230; NIM A355 (1995) 660.
- [61] P.F. Harrison, D.H. Perkins, W.G. Scott, Phys. Lett. B 349 (19 95) 137.
- [62] A. Acker and S. Pakvasa, 'Three Neutrino Flavors are Enough', hep-ph/9611423.
- [63] S. Ragazzi et al., 'Request for a test of liquid argon TPC on the neutrino beam', CERN SPSLC 96P57 (SPSLC/M 594).
- [64] T. Ypsilantis et al., NIM A371 (1996) 330.; T. Ypsilantis et al., CERN-LAA/96/13 (1996); CERN-LAA/94-17 (1994).
- [65] G. Barbarino, "A possible experiment to search for atmospheric neutrino and long baseline neutrino oscillations", presented at the Gran-Sasso Meeting on Long Baseline Neutrino Experiments, Gran Sasso, Dec. 1994; M. Ambrosio et al., LNGS/Note 94-112 (1994) ; G.Barbarino et al., *Nucl. Phys. B*, **48**, pp. 204-206, (1996).
- [66] K. Niwa, contribution to "Snowmass '94" Conference on "Particle and Nuclear Astrophysics and Cosmology in the Next Millennium", June 29-July 14, 1994, Snowmass, Colorado.
- [67] J. Panman, contribution to the CHORUS Neutrino Oscillation Workshop, Chouilly, 24 Jan. 1995.
- [68] A. Ereditato, G. Romano and P. Strolin, CERN-PPE/96-106, Proc. of "San Miniato '96", to be published on Nucl. Instr. and Meth.
- [69] A. S. Ayan et al., CERN-SPSC/97-5, SPSC/I 213, March 14, 1997.
- [70] A. Ereditato, K. Niwa and P. Strolin, INFN/AE-97/06 and Nagoya DPNU-97-07, 27 January 1997.
- [71] S. Aoki et al., Nucl. Instr. and Meth. B 51, 446 (1990).
- [72] T. Nakano, Ph. D. Thesis, University of Nagoya (1997).
- [73] G. Rosa et al., Prep. Univ. Salerno DSF US 97/1 (1997), submitted to Nucl. Instr. and Meth.
- [74] J. Nishimura, Handbuch der Physik, Springer-Verlag, Vol. 46/2, 1-114 (1967).
- [75] S. G. Bayburina et al., Nucl. Phys. B 191, 1-25 (1981).



- [76] K. Niwa, in "Physics and Astrophysics of Neutrinos" editors M. Fukugita and A. Suzuki, Springer-Verlag, 520-540 (1994).
- [77] C. F. Powell et al., The study of elementary particles by the photographic method, Pergamon Press (1959).
- [78] N. Hotta et al., Phys. Rev. D 22, 1-12 (1980).
- [79] F. Cavanna, CERN-PPE/95-133 (1995).
- [80] Nuclear Instruments and Methods A325 (1993)92, Physics Letters B 335 (1994)246
- [81] Phys. Lett. B 309 (1993)463
- [82] See talks of A. Para and M. Nakamura at this workshop.
- [83] K. Eitel et al. Proc. of the 8th Rencontres de Blois: Neutrinos, Dark Matter and the Universe, June 1996. To be published.
- [84] C. Angelini et al. Phys. Lett. B, 179:307, 1986.
- [85] L. Ludovici and P. Zucchelli. CERN-PPE/96-181, HEP-EX/9701007. Subm. to Nucl. Instr. and Meth.
- [86] V. V. Ammonosov et al. Proposal SERP-E-152.
- [87] R. H. Bernstein et al. Fermilab P-788.
- [88] F. Angelini et al. Nucl. Instr. and Meth., 335:69, October 1993.
- [89] G. Buchalla and A. J. Buras, Nucl. Phys. **B400**, 225 (1993).
- [90] G. Buchalla and A.J. Buras, Phys. Rev. **D54**, 6782 (1996).
- [91] A. J. Buras, hep-ph/9609324, September 1996 (to appear in "Workshop on K-Physics", Orsay, May 1996).
- [92] A. J. Buras and R. Fleischer, hep-ph/9704376, April 1997 (To appear in "Heavy Flavors II", World Scientific, 1997).
- [93] J.F. Donoghue, R. Holstein, and G. Valencia, Phys. Rev. D **35**, 2769 (1987).
- [94] D.A. Harris *et al.*, Phys. Rev. Lett. **71**, 3918, (1993).
- [95] L. K. Gibbons *et al.*, FNAL E731 collaboration, Phys. Rev. Lett. **70**, 1203 (1993).
- [96] D. A. Harris *et al.* (E799-I), Phys. Rev. Lett. **71**, 3914 (1993).
- [97] M. Weaver *et al.*, Phys. Rev. Lett. **72**, 3758 (1994).
- [98] P. Gu, *et al.* (E799-I), Phys. Rev. Lett. **72**, 3758 (1993).

- [99] P. Gu, *et al.* (E799-I), Phys. Rev. Lett. **76**, 4312 (1996).
- [100] N. Samios, Phys. Phys. Rev. **126**, 1844 (1962).
- [101] BNL E845, Phys. Rev. Lett. **65**, 1407 (1990).
- [102] CERN NA31, Phys. Lett. **B240**, 283 (1990).
- [103] T. Nakaya, *et al.* (E799-I), Phys. Rev. Lett. **73**, 2169 (1994).
- [104] M. Spencer, *et al.* (E799-I), Phys. Rev. Lett. **74**, 3323 (1994).
- [105] V. O'Dell, KTeV Collaboration, "Status and New Results of the KTeV Rare Kaon Program" , MIST Workshop Fermilab,(May,1997) to be published.
- [106] L. M. Seghal and M. Wanninger, Phys. Rev. **D46**, 1035(1992); P. Heiliger and L.M. Seghal, Phys. Rev. **D48**, 4146(1993).
- [107] E. J. Ramberg, E731 Collaboration, Fermilab-Conf-91/258, (1991); E. J. Ramberg, *et al.*, Phys. Rev. Lett. **70**, 2529 (1993).
- [108] T. Nakaya, Flavor Changing Neutral Current Conference, Santa Monica, CA (1997).
- [109] K. Arisaka *et al.*, Kaons At the Main Injector Conceptual Design Report (1991).
- [110] A. J. Malensek, FERMILAB-FN-0341, 1981.
- [111] K. Arisaka *et al.*, KTeV Design Report, 36, (1992).
- [112] H.B. Greenlee, Phys. Rev. D **42**, 3724 (1990).
- [113] T. Nakaya, Ph.D. Thesis, Osaka University, 1995.
- [114] J.F. Donoghue and F. Gabbiani, UMHEP-436, 1997.
- [115] W.R. Nelson, H. Hirayama and D.W.O. Rogers, SLAC Report 265 (1985).
- [116] E.J. Ramberg, E731 Collaboration, Fermilab-Conf-91/258, (1991).



## Workshop Participants

Carl H.	Albright	Fermi National Accelerator Lab. - albright@fnal.gov
Theodoroa	Alexopoulos	University of Wisconsin - theoalex@fnal.gov
Shigeki	Aoki	Kobe University - aoki@kekux1.kek.jp
Katsushi	Arisaka	U. of California, Los Angeles - arisaka@physics.ucla.edu
Suzanne	Averitte	Fermi National Accelerator Lab. - averitte@fnal.gov
David	Ayres	Argonne National Laboratory - ayres@hep.anl.gov
Jon	Bakken	Fermi National Accelerator Lab. - bakken@fnal.gov
Milla	Baldo Ceolin	University of Padov - baldoceolin@padova.infn.it
Giancarlo	Barbarino	INFN - barbarino@axpna1.na.infn.it
John	Belz	Fermi National Accelerator Lab. - belz@fnal.gov
Ram	Ben-David	Fermi National Accelerator Lab. - rbd@fnal.gov
Douglas	Bergman	Rutgers University - bergman@hepmail.physics.yale.edu
Diego	Bettoni	INFN - Sezione di Ferrara - bettoni@fnal.gov
Chandrashekhara Bhat		Fermi National Accelerator Lab. - cbhat@fnal.gov
Morris	Binkley	Fermi National Accelerator Lab. - binkley@fnal.gov
W. Robert	Binns	Washington University
Glenn	Blanford	Fermi National Accelerator Lab. - blanford@fnal.gov
Edward	Blucher	University of Chicago - blucher@hep.uchicago.edu
Greg	Bock	Fermi National Accelerator Lab. - bock@fnal.gov
David	Boehnlein	Fermi National Accelerator Lab. - dave_b@fnal.gov
Tim	Bolton	Kansas State University - bolton@phys.ksu.edu
Alan	Bross	Fermi National Accelerator Lab. - bross@fnal.gov
Bruce C.	Brown	Fermi National Accelerator Lab. - bcbrown@fnal.gov
Charles	Brown	Fermi National Accelerator Lab. - chuckb@fnal.gov
Gerhard	Buchalla	SLAC - buchalla@slac.stanford.edu
Ray	Burnstein	Illinois Institute of Technology - burnstein@fnal.gov
Leslie	Camilleri	CERN - leslie.camilleri@cern.ch
Elliott	Cheu	University of Arizona - echeu@fnal.gov
Sam	Childress	Fermi National Accelerator Lab. - childress@fnal.gov
David	Christian	Fermi National Accelerator Lab. - dcc@fnal.gov
Rick	Coleman	Fermi National Accelerator Lab. - coleman@fnal.gov
Janet	Conrad	Fermi National Accelerator Lab. - conrad@nevis1.nevis.columb
Peter	Cooper	Fermi National Accelerator Lab. - pcooper@fnal.gov
Marjorie	Corcoran	Rice University - corcoran@physics.rice.edu
Robert	Cousins	U. of California, Los Angeles - cousins@physics.ucla.edu
Lucyna	De Barbaro	Northwestern University - lucyna@miranda.fnal.gov
Dmitri	Denisov	Fermi National Accelerator Lab. - denisovd@fnal.gov
Alessandra	Di Credico	Lab. Naz. Gran Sasso - dicredico@lngs.infn.it
Milind	Diwan	Brookhaven National Laboratory - diwan@bnl.gov
John	Donoghue	University of Massachusetts - donoghue@phast.umass.edu
Robert	Drucker	Fermi National Accelerator Lab. - drucker@fnal.fnal.gov
Klaus	Eitel	FZ Karlsruhe - klaus@ik1.fzk.de
Jurgen	Engelfried	Fermi National Accelerator Lab. - jurgen@fnal.gov
Antonio	Ereditato	Argonne National Laboratory - antonio.ereditato@cern.ch
Albert	Erwin	University of Wisconsin - erwin@wishpa.physics.wisc.edu
Carlos	Escobar	University of Sao Paulo - escobar@fnal.gov
Valeri	Falaleev	CERN
Gary	Feldman	Harvard University - feldman@physics.harvard.edu
Gian Luigi	Fogli	University of Bari - gianluigi.fogli@ba.infn.it
Rick	Ford	Fermi National Accelerator Lab. - rickford@fnal.gov
Valeri	Garkusha	Institute for High Energy Physics
Gabriele	Garzoglio	Fermi National Accelerator Lab. - garzoglio@fnal.gov
Stephen	Geer	Fermi National Accelerator Lab. - sgeer@fnal.gov
Donald	Geesaman	Argonne National Laboratory - geesaman@anl.gov
Juan-Jose	Gomez	CERN - gomez@axnd02.cern.ch
Maurycy	Goodman	Argonne National Laboratory - mcg@hep.anl.gov
Iouri	Gornouchkine	Fermi National Accelerator Lab. - gornushk@fnal.gov
Greg	Graham	University of Chicago - greg@hep.uchicago.edu
Giorgio	Gratta	Stanford University - gratta@hep.stanford.edu
Zeno	Greenwood	Louisiana Tech University - greenw@phys.latech.edu
Fausto	Guarino	INFN - guarino@axpna1.na.infn.it

Eva	Halkiadakis	Rutgers University - evah@fnal.gov
Kazu	Hanagaki	Fermi National Accelerator Lab. - kazu@fnal.gov
Robert W.	Hatcher	Indiana University - hatcher@astro.indiana.edu
Jose-Angel	Hernando	CERN - hernando@axmd02.cern.ch
Satoshi	Hidaka	Fermi National Accelerator Lab. -hidaka@fnal.gov
Stephen	Holmes	Fermi National Accelerator Lab. -holmes@fnal.gov
Yee Bob	Hsiung	Fermi National Accelerator Lab. -hsiung@fnal.gov
James	Hylen	Fermi National Accelerator Lab. -hylen@fnal.gov
Richard	Imlay	Louisiana State University -phimla@lsuvax.sncc.lsu.edu
Takao	Inagaki	KEK - inagaki@kekvax.kek.jp
Yuri	Ivanov	Petersburg Nuclear Physics Institute - yumi@hep486.pnpi.spb.
Gerald P.	Jackson	Fermi National Accelerator Lab. - gpj@fnal.gov
Catherine	James	Fermi National Accelerator Lab. - cjames@fnal.gov
Douglas	Jensen	Fermi National Accelerator Lab. - djensen@fnal.gov
David	Johnson	Fermi National Accelerator Lab. - dej@fnal.fnal.gov
Tomas	Kafka	Tufts University - kafka@tuhep3.phy.tufts.edu
Erotokritos	Katsavounidis	California Institute of Technology - katsvnds@vaxgs2.lngs.
Edward	Kearns	Boston University - kearns@budoe.bu.edu
Rick	Kessler	University of Chicago - rkessler@fnal.gov
Yuri	Khodyrev	Institute for High Energy Physics
Hong Joo	Kim	Louisiana State University - hjkim@phzeus.phys.lsu.edu
Hwi	Kim	U. of California, Los Angeles - hwi.kim@cern.ch
Jasper	Kirkby	CERN - Jasper.Kirkby@cern.ch
Takeshi	Komatsubara	Brookhaven National Laboratory - koma@bnlku2.phy.bnl.gov
Alan	Kostelecky	Indiana University - kostelec@indiana.edu
Yoshitaka	Kuno	KEK - kuno@kekvax.kek.jp
Kris	Kwiatkowski	Indiana University - kwiat@iucf.indiana.edu
Karol	Lang	University of Texas, Austin - lang@jep.utexas.edu
William	Leeson	Argonne National Laboratory - leeson@hep.anl.gov
Laurence	Littenberg	Brookhaven National Laboratory - littenbe@bnl.gov
William	Louis	Los Alamos National Laboratory - louis@lanl.gov
Peter	Lucas	Fermi National Accelerator Lab. - lucas@fnal.gov
Lucio	Ludovici	CERN - ludovici@cern.ch
Hong	Ma	Brookhaven National Laboratory - hma@bnl.gov
Peter	Maas	Fermi National Accelerator Lab. - maas@fnal.gov
Mario	Macri	CERN - mario.macri@cern.ch
W. Anthony	Mann	Tufts University - mann@tuhep3.phy.tufts.edu
Mauro	Marinelli	INFN, Genova - marinelli@infn.ge.infn.it
Philip	Martin	Fermi National Accelerator Lab. - pmartin@fnal.gov
Patrick	McGaughey	Fermi National Accelerator Lab. - plm@lanl.gov
Shawn	McKee	University of Michigan - smckee@umich.edu
Scott	Menary	Fermi National Accelerator Lab. - menary@fnal.gov
Douglas	Michael	California Institute of Technology - michael@cithex.caltech.
Geoffrey B.	Mills	Los Alamos National Laboratory - mills@lanl.gov
Sanjib	Mishra	Harvard University - mishra@physics.harvard.edu
Emmanuel	Monnier	University of Chicago - monniere@fnal.gov
Claudio	Montanari	Universita' degli Studi di Pavia - cmontana@cern.ch
Jorge	Morfin	Fermi National Accelerator Lab. - jorge@fnal.gov
Douglas	Morrison	CERN - douglas.morrison@cern.ch
Joel	Moss	Los Alamos National Laboratory - imm@lanl.gov
Maria-Teresa	Muciaccia	University of Bari - maria_teresa.muciaccia@cern.ch
Charles	Munger	Stanford Linear Accelerator Center - charles@mailbox.slac.st
Thornton	Murphy	Fermi National Accelerator Lab. - thornton@fnal.gov
Roberto	Mussa	Fermi National Accelerator Lab. - musa@fnpx19.fnal.gov
Mitsuhiro	Nakamura	Nagoya University
Tsuyoshi	Nakaya	University of Chicago - nakaya@fnal.gov
Jeffrey	Nelson	University of Minnesota - jkn@mnhepw.hep.umn.edu
David	Neuffer	Fermi National Accelerator Lab. - neuffer@fnal.gov
Vivian	O'Dell	Fermi National Accelerator Lab. - odell@fnal.gov
Sandip	Pakvasa	University of Hawaii - pakvasa@uhhep.phys.hawaii.edu
Vittorio	Palladino	INFN, Naples/CERN - vittorio.palladino@cern.ch

Vassili Papavassiliou New Mexico State University - pvs@nmsu.edu  
Adam Para Fermi National Accelerator Lab. - para@fnal.gov  
Jen-Chieh Peng Los Alamos National Laboratory - peng@lanl.gov  
Thomas Phillips Duke University - Phillips@phy.duke.edu  
Francesco Pietropaolo INFN - fpp@vxcern.cern.ch  
Stephen Pordes Fermi National Accelerator Lab. - stephen@fnal.gov  
Chang Ging Qiao University of Chicago - qiao@hep.uchicago.edu  
Rajendran Raja Fermi National Accelerator Lab. - raja@fnal.gov  
Erik Ramberg Fermi National Accelerator Lab. - ramberg@fnal.gov  
Regina Rameika Fermi National Accelerator Lab.  
Ron Ray Fermi National Accelerator Lab. - rray@fnal.gov  
Lincoln Read Fermi National Accelerator Lab. - alr@fnal.gov  
Bill Reay Kansas State University - reay@phys.ksu.edu  
Jean Rhoades Fermi National Accelerator Lab. - jrhoades@fnal.gov  
Stefania Ricciardi CERN - ricciars@mail.cern.ch  
Jack Ritchie University of Texas, Austin - ritchie@hep.utexas.edu  
Andre Rubbia CERN - andre.rubbia@cern.ch  
Allison Russell Fermi National Accelerator Lab. - russell@fnal.gov  
Masayoshi Sadamoto Fermi National Accelerator Lab. - sada@fnal.gov  
Roberta Santacesaria CERN - roberta.santacesaria@cern.ch  
Mikhail Sapozhnikov JINR, Dubna - sapozhnikov@axnua.jinr.dubna.su  
Steve Schnetzer Rutgers University - steves@physics.rutgers.edu  
Paul Schoessow Argonne National Laboratory - pvs@hep.anl.gov  
Reinhard Schwienhorst University of Minnesota - schwier@physics.spa.umn.edu  
Katsumi Senyo Fermi National Accelerator Lab. - senyo@fnal.gov  
Kamal Seth Northwestern University - kseth@nwu.edu  
Michael Shaevitz Columbia University - shaevitz@nevis.nevis.columbia.edu  
Takao Shinkawa KEK - takao.shinkawa@kek.jp  
Ron Sidwell Kansas State University  
William Slater U. of California, Los Angeles - slater@physics.ucla.edu  
Wesley M. Smart Fermi National Accelerator Lab. - smart@fnal.gov  
Nickolas Solomey University of Chicago - solomey@uchep.uchicago.edu  
Sunil Somalwar Rutgers University - sunil@ruthep.rutgers.edu  
Al Sondgeroth Fermi National Accelerator Lab. - sondgeroth@fnal.gov  
James Sowinski Indiana University - sowinski@iucf.indiana.edu  
Panagiotis Spentzouris Columbia University - spentz@hecate.fnal.gov  
Jeff Steele Drexel University - steele@cheesesteak.physics.drexel.edu  
Ray Stefanski Fermi National Accelerator Lab. - stefanski@fnal.gov  
Richard Steinberg Drexel University - steinberg@duphy4.physics.drexel.edu  
Jon Streets Fermi National Accelerator Lab. - streets@fnal.gov  
Mark Strikman Pennsylvania State University - strikman@phys.psu.edu  
Paolo Strolin University of Naples/CERN - paolo.strolin@cern.ch  
John Strologas University of Illinois at Urbana-Champaign - strolog@uihep1.  
David Strom University of Oregon - strom@bovine  
Earl C. Swallow Elmhurst College/U. of Chicago - earls@elmhurst.edu  
Gianni Tassotto Fermi National Accelerator Lab. - tassotto@fnal.gov  
Rex Tayloe Los Alamos National Laboratory - rex@lanl.gov  
Murray Thompson University of Wisconsin - thompson@wishpa.physics.wisc.edu  
Gordon Thomson Rutgers University - thomson@ruthep.rutgers.edu  
Jonathan Thron Argonne National Laboratory - jlt@hep.anl.gov  
Rudolf Thun University of Michigan - rthun@umich.edu  
Robert Tribble Texas A&M University - tribble@comp.tamu.edu  
Robert Tschirhart Fermi National Accelerator Lab. - tsch@fnal.gov  
George Tzanakos University of Athens - tzanakos@atlas.uoa.gr  
Elena Vataga Moscow State University - vataga@viola.npi.msu.su, vataga@fna  
Steven E. Vigdor Indiana University - vigdor@iucf.indiana.edu  
Vic Viola Indiana University - vicv@iucf.indiana.edu  
Yau W. Wah University of Chicago - wah@uchep.uchicago.edu  
Alan Wehmann Fermi National Accelerator Lab. - wehmann@fnal.gov  
Herман White Fermi National Accelerator Lab. - hwhite@fnal.gov  
Hywel White Los Alamos National Laboratory - white@lanl.gov

Bruce	Winstein	University of Chicago - bruce@uchep.uchicago.edu
Stanley	Wojcicki	Stanford Linear Accelerator Center - sweg@slac.stanford.edu
Lincoln	Wolfenstein	Carnegie Mellon University - lincoln@defoe.phys.cmu.edu
Jong-Kwan	Woo	U. of California, Los Angeles - woo@physics.ucla.edu
Taku	Yamanaka	Osaka University - taku@fnal.gov
Thomas	Ypsilantis	CERN - thomas.ypsilantis@cern.ch
J. C.	Yun	Fermi National Accelerator Lab. - yun@fnal.gov
Victor	Zarucheisky	Institute for High Energy Physics
George	Zioulas	Fermi National Accelerator Lab. - giorgos@fnal.gov
Renata	Zukanovich	Funchal University of Sao Paolo - zukanov@fn781a.fnal.gov

